A Review: Water pollution by heavy metal and organic pollutants: Brief review of sources, effects and progress on remediation with aquatic plants

Isiuku Beniah Obinnaa and Enyoh Christian Ebere[a,*]

[a,*] *Department of Chemistry, Imo State University, Imo State, Nigeria*

ABSTRACT

Heavy metals and organic pollutants are ubiquitous environmental pollutants affecting the quality of soil, water and air. Over the past 5 decades, a lot of strategies have been being developed for treatment of polluted water. Strategies involving aquatic plant use are preferable to conventional methods. In this study, an attempt was made to provide a profound and brief review on latest and newest progresses in research and practical applications of phytoremediation for water resources with the following objectives: (1) to discuss the toxicity of chemicals pollution in water to plant, animals, and human health (2) to summarise the physicochemical factors affecting removal of toxic chemicals such as heavy metals and organic contaminants in aqueous solutions by aquatic plants; (3) to summarise and compare the removal rates of heavy metals and organic contaminants in aqueous solutions by diverse aquatic plants; and (4) to summarise chemometric models for testing aquatic plant performance. More than 20 aquatic plants specie have been used extensively while duckweed (*L. minor*), water hyacinth (*Eichhornia crassipes*), water lettuce (*P. stratiotes*) are the most common. Overall, chemometrics for performance assessment reported include: Growth rate (GR), Growth rate inhibition (% Inhibition), Metal uptake (MU), translocation/ transfer factor (TF), bioconcentration factor (BCF), Percent metal uptake (% MU), Removal capacity (RC) and Tolerance index (TI) while absorption rate have been studied using the sorption kinetics and isotherms models such as pseudo-first-order (PFO), pseudo-second-order (PSO), Freundlich, Langmuir and Temkin. Using modeling and interpretation of adsorption isotherms for performance assessment is particularly good and increases level of accuracy obtained from adsorption processes of contaminant on plant. Conclusion was drawn by emphasizing the gap in knowledge and suggesting very important future areas of research for scientists and policymakers.

1. Introduction

One precious natural resource is water, which is relied on for agricultural sustainability and mankind civilization. Water covers over 70 % of the earth crust and majority of the water have been subjected to maximum exploitation and severely degraded or polluted because of anthropogenic activities. Often times, water resources (including surface water and groundwater) even though they are interrelated and connected, are sperately managed and studied [1]. Surface water seeps through the soil and becomes groundwater and vice versa. Therefore, both surface and groundwater sources maybe contaiminated by similar pollution sources. Pollution sources may include point (from a single, identifiable source) and non-point (many sources) sources. Irrespective of the contamination source, damaging effects are still made to the ecosystem; especially those sources that add heavy metals or organic pollutants to waters because they are persistent in the environment and have been associated with mutagenic, teratogenic and carcinogenic effects. These pollutants cannot be easily destroyed biologically but are often

transformed from one oxidation state or organic complex to another [2-3], thus remaining in the environment for a very longtime. Therefore, toxic chemical pollution of water poses a great threat to the ecosystem. Many technologies that are easy to use have been developed as part of the continuous efforts to make water free from contamination, be of good quality, sustainable and economically feasible. Approaches involving chemical extraction, chemical isolation and containment, thermal method, chemical redox process, and electrokinetics have been widely used, especially at a small scale while difficult to use at large scale due to high costs and side effects [4]. Therefore, the search for an alternative clean and cheap technique for water cleaning became important. Plants use in treating contaminatedwater was proposed about 300 years ago, as an emerging cheaper technology [5]. Over the years, the concept has gained increasing attention and has been adopted by scientist, governmental and non-governmental organizations. Many studies regarding plant use for environment clean-up has focused on contaminated soils while regarding water medium have been less studied. Many aquatic plant species have been identified and tested for removing heavy metals and organic pollutants in water [4]. Mechanisms of uptake by whole plant as well as remediation performance studied using chemometrics have been done. There are progresses made over the years using hydroponics or field experiment. They were reviewed and reported in this paper.

2. Methodology

This research was carried out through a collection of data and information from scientific articles regarding the potential of some aquatic plants for phytoremediation of toxic chemicals such as heavy metals (specifically: As, Cu, Cr, Hg, Cd, Ni, Pb and Zn) and organic pollutants. The scientific articles were sought majorly from Google scholar and back searches through references. For an article to be included, it must be published in year 2000 and above, in order to ensure that current information was provided. However, few selected articles prior to 2000 included were due to their importance in the initial set of empirical studies.

3. Water pollution

All life forms on earth depend on water for their presence in the ecosystem. According to [6], water is the second most important element required by human for survival after the air we breathe. The quality of water globally has been affected negatively due to man-made activities including unskilled utilization of natural water resources. Even though, the United Nations recognizes the availability of good drinking water for humans as a human right, considerable numbers of people worldwide are still suffering with the absence of clean and new drinking water. Over 900 million people out of the 7.7 billion people currently in the world, lack access to enhanced drinking water. A value which present a significance decrease from around 2.6 billion peoples in 1990 and approximately 600 billion people expected in 2015 if the United Nations' Millennium Development Goal was achieved having access to enhanced drinking water [7,8]. Furthermore, World Water Council estimated that around 3.9 billion people by 2030 will be living in water scare areas [9]. In Nigeria, irrespective of the total replenishable water resource estimated at 319 billion cubic meters, only 58% and 39% of the inhabitants in urban and rural areas have access to potable water supply respectively [10]. Whilst there is an increase in urbanization, industrialization and population, the demand for water assets is expanding daily and thereby leading to serious contamination of surface and ground water. The chief sources of water pollution are presented in Table 1 and 5. Marine pollution and nutrient pollution are the two types of surface water pollution. The former involves introduction of toxic substances (such as toxic metals, pharmaceuticals, pesticides, dyes, and surfactants) while the later refers to contamination by excessive inputs of nutrients, which is primarily responsible for eutrophication of surface waters. It is considerable that 70–80% of all well-known problems in developing countries are identified

with water pollution, especially for children. The toxic pollutants released in wastewaters can be detrimental to aquatic organisms which also cause the regular waters to be unfit as consumable water sources [11-14]. Studies have implicated water pollution as the leading cause of death and diseases worldwide [15-16]. In 2015, water pollution caused the deaths of 1.8 million people [17]. Thereby, making water pollution a global concern, which requires continous assessment and revision of water resource policy at all levels (international down to individual aquifers and wells).

3.1. Heavy metals

Metals with high density (≥ 5 g/cm^{-3}) are often regarded as heavy metals. They are ubiquitous in nature and adversely affect the environment and living organisms [18]. The levels and compositions of heavy metal are often determined and controlled/ influenced by local activities [19-21] while those ones suspended in air is monitored by the metal properties and various environmental factors [22] such as precipitation, rainfall and wind etc. Water (surface and ground) pollution by heavy metals is a global issue. Many surface and ground water in many countries (if not all) of the world have been affected by heavy metal pollution, but the severity of pollution vary enormously and controlled mainly by local activities. Many areas in Europe have been reported to be greatly affected by heavy metals [23] while in the USA, government statistics revealed that more than 19000 km of US streams and rivers have been contaminated by heavy metals from coal mine and acid mine drainage [24,25]. In Asia, some countries such as India, Pakistan and Bangladesh are experiencing severe pollution of surface water due to untreated effluents being poured in surface drains by small industrial units and from the use of raw sewage in producing vegetables near big cities, which ends in surface water by runoff and groundwater by leaching processes [25]. Generally, heavy metals identified in the polluted rivers in Asia include As, Cu, Cd, Pb, Cr, Ni, Hg and Zn. In different parts of Africa including North, East, South and West Africa, there are reports on heavy metal

(notably Pb, Cd, Hg, Cu, Co, Zn, Cr, Ni, Mn, Fe, As and V) concentrations in surface water exceeding recommended limits, thereby polluting the surface waters in the region [26]. In Nigeria alone out of inland freshwater system estimated to be about 283,293.47 hectares, only about 84,988.041 is still useful due to pollution [21]. In West Africa, najor pollution source is peteroleum-related activities including frequent acts of sabotage to oil facilities [21,26]. In Northern Africa, the contribution of agricultural activities (use of phosphate fertilizers and pesticides), East Africa include indiscriminate dumping of waste while in Southern Africa, mining activities are the major sources of environmental pollution [26]. Literatures reveal that natural rock weathering or geogenic sources and anthropogenic sources (man-made based from emission or effluent from the use of products containing heavy metals or capable of absorbing metals) are two broad sources for heavy metals introduction into the environment [20, 27-29]. The summary of sources of various heavy metals is listed in Table 1 while the consumption related emissions are presented in Table 2. The intensity of pollution is ontrolled by local activities; high anthropogenic activities may cause high heavy metal pollution. Generally urban waterbodies have higher heavy metals' concentrations in comparison with less urbanized areas. However, in Europe the emission of some metals is decreasing perhaps due to increase in use of clean(er) technologies, improvements in emission controls and phasing out of leaded petrol, following the 1998 Heavy Metals Protocol enforced by 29 December 2003. The trend of emission of selected heavy metals between the years 1990 to 2016 is presented in Figure 1. The emissions of Cd, Hg and Pb have declined by approximately 35 %, 30 % and 10 % respectively since 1990 [30]. Furthermore, other priority heavy metals emissions such as As, Cu, Ni and Zn is simultaneously reduced by 57%, 53%, 65% and 29%, respectively [31].

3.1.1. Effects of heavy metals pollution of water

Many previous studies have extensively reviewed the adverse effects of heavy metals to human

Table 1. Different sources of some heavy metals

Heavy metals (HM)	Sources
As	Semiconductors, petroleum refining, wood preservatives, animal feed additives, coal power plants, herbicides, volcanoes, mining and smelting
Cd	Geogenic sources, anthropogenic activities, metal smelting and refining, fossil fuel burning, application of phosphate fertilizers, sewage sludge
Cr	Electroplating industry, sludge, solid waste, tanneries
Cu	Electroplating industry, smelting and refining, mining, biosolids
Hg	Volcano eruptions, forest fire, emissions from industries producing caustic soda, coal, peat and wood burning
Ni	Volcanic eruptions, land fill, forest fire, bubble bursting and gas exchange in ocean, weathering of soils and geological materials
Pb	Mining and smelting of metalliferous ores, burning of leaded gasoline, municipal sewage, industrial wastes enriched in Pb, paints
Zn	Electroplating industry, smelting and refining, mining, biosolids

Source: [25].

Table 2. Consumption-related emissions factors (ppm) of heavy metals

HM	Metallic use[a]	Plating and coating[b]	Paint pigments[c]	Electron tubes and batteries[d]	Other electrical equipment[e]	Chemical uses, not embodied[f]	Chemical uses, embodied[g]	Agricultural uses[h]	Non-agricultural uses[i]	Medical and dental[j]	Misc. NEC
As	0.001	0	0.5	0.01	NA	NA	0.05	0.50	0.8	0.8	0.15
Cd	0.001	0.15	0.5	0.02	NA	1	0.15	NA	NA	NA	0.15
Cr	0.001	0.02	0.5	NA	NA	1	0.05	NA	1	0.8	0.15
Cu	0.005	0	1.0	NA	0.10	1	0.05	0.05	1	NA	0.15
Hg	0.050	0.05	0.8	0.20	NA	1	NA	0.80	0.9	0.2	0.50
Pb	0.005	0	0.5	0.01	NA	1	0.75	0.05	0.1	NA	0.15
Zn	0.001	0.02	0.5	0.01	NA	1	0.15	0.05	0.1	0.8	0.15

NA- Not available

a. As alloys or analgams (in the case of Hg) not used in plating, electrical equipment, catalysts or dental work. Losses can be assumed to be due primarily to wear and corrosion, except for mercury which volatilizes.

b. Protective surfaces deposited by dip coating (e.g. galvanizing, electroplating vacuum deposition, or chemical bath (e.g. chromic acid).Losses in use are mainly due to wear and abrasion (e.g. silverplate), or flaking (decorative chrome trim). In the case of mercury-tin "silver" for mirrors, losses were largely due to volatilization.

c. Paints and pigments are lost primarily by weathering (e.g. for metal-protecting paints), by wear, or by disposal of painted dyes or pigmented objects, such as magazines. Copper- and mercury-based paints slowly volatilize over time. A factor of 0.5 is rather arbitrarily assumed for all other paints and pigments.

d. Includes all metals and chemicals (e.g. phosphorus) in tubes and primary and secondary batteries, but excludes copper wire. Losses in manufacturing may be significant. Mercury in mercury vapour lamps can escape to the air when tubes are broken. In all other cases it is assumed that discarded equipment goes mainly to landfills. Minor amounts are volatilized in fires or incinerators or lost by corrosion; lead-acid batteries are recycled.

e. Includes solders, contacts, semiconductors and other special materials (but not copper wire) used in electrical equipment control devices and instruments, etc. Losses to the environment are primarily via discard of obsolete equipment to landfills. Mercury used in instruments is lost via breakage and volatilization or spillage.

f. Chemical uses not embodied in final products include catalysts, solvents, reagents, bleaches, etc. In some cases a chemical is basically embodied but there are some losses in processing. Losses in chemical manufacturing per se are included here. Major examples include copper and mercury catalysts (especially in chloride mfg); copper, zinc and chromium as mordants for dyes; mercury losses in felt manufacturing; chromium losses in tanning; lead in desulphurization of gasoline; zinc in rayon spinning, etc. In some cases virtually all of the material is actually dissipated. We include detonators such as mercury fulminate and lead azide (and explosives) in this category.

g. Chemical uses embodied in final products other than paints or batteries include fuel additives (e.g. TEL). anti-corrosion agents (e.g. zinc dithiophosphate), initiators and plasticizers for plastics (e.g. zinc oxide), etc. Also included are wood preservatives and chromium salts embodied in leather. Losses to the environment occur when the embodying productivity is utilized, for example gasoline containing TEL is burned and largely dispersed into the atmosphere. However, copper, chromium, and arsenic are used as wood preservatives and dispersed only if the wood is later burned or incinerated.

h. Agricultural pesticides, herbicides, and fungicides. Uses are dissipative but heavy metals are largely immobilized by soil. Arsenic and mercury are exceptions because of their volatility.

i. Non-agricultural biocides are the same compounds, used in industrial, commercial, or residential applications. Loss rates are high in some cases.

j. Medical/dental uses are primarily pharmaceutical (including cosmetics) germicides, also dental filling material. Most are dissipated to the environment via waste water. Silver and mercury dental fillings are likely to be buried with the dead body
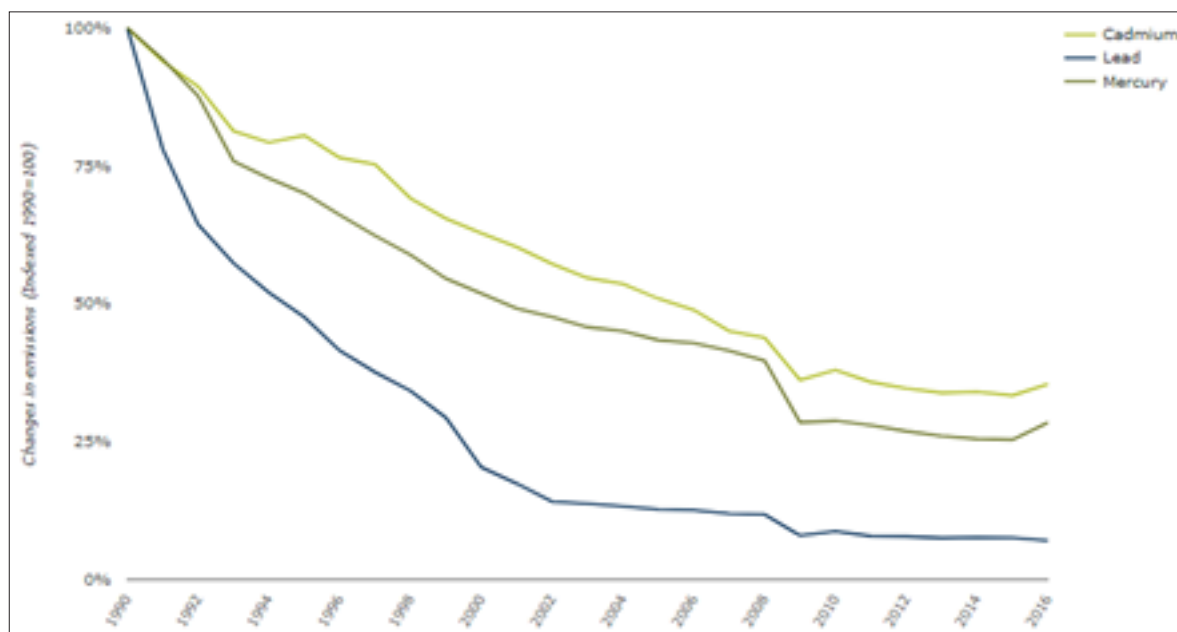
Source: [32]

Fig. 1. Trends in emissions of heavy metals from 1990 to 2016 (Source: [30])

and ecological system [14, 18, 33-36]. Increased levels of heavy metal contaminants in water affect negatively the ecological function of water including recycling and primary production of nutrients. Also affected is the health of wildlife and humans through bioaccumulation in the food chain with the lasting impact of metal tolerance development among certain organisms. Furthermore, harmful ecological impacts of metals may include info-disruption, that impact intra and interspecies interaction among freshwater organisms and microbes [21]. However, the effects of heavy metal pollution in water shall be discussed under the following; plants, aquatic animals and humans. The toxicity of heavy metals to aquatic plant, animal and human is depended on the solubility and bioavailability of the metals, organism tolerance, pH, and presence of other ions that interfere with bioavailability, among other issues that may interfere with the result of contact with the element [37].

3.1.1.1. Plant
Some heavy metals are needed for upkeep and growth by aquatic plants. However, when the concentrations become excessive, the plant may be at risks of heavy metal toxicity both directly and indirectly. High concentrations of heavy

metals in plant may interfere with metabolic functions, including physiological and biochemical processes such as oxidative stress from production of reactive oxygen species (ROS), inhibition of photosynthesis, and respiration and degeneration of main cell organelles, even leading to death of plants [2, 38-39]. Other specific effects include growth reduction (especially the origin and main part of system is more affected), chlorosis and leaf necrosis followed by traces of senescence and abscission, which changes lead to lower nutrient uptake and interfere with the biomass acquired [40]. A visual symptom of metal toxicity to plant is presented in Figure 2.

The effect of heavy metal toxicity on the aquatic plants varies according to the particular heavy metal involved in the process, multi-metal interaction in the water and the plant itself. In terms of particular heavy metal, exposure of Water hyacinth *(Eichhornia crassipes)* to excess arsenic (As) concentration of 6 mg/L over $\geq$ 8 days lead to the death of the plant while the plant became unhealthy after 3 days of exposure [42]. At the same concentration of 6 mg/L and a different concentration of 2.5 mg/L, *Eichhornia crassipes* was able to withstand zinc (II) and cadmium (II) sorption respectively in water [43]. Furthermore, in
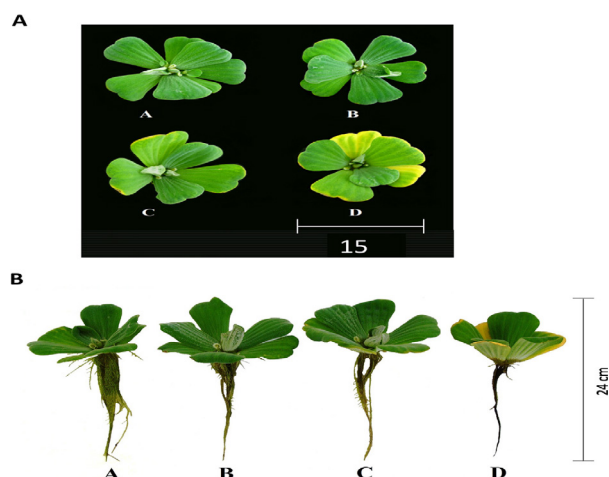
Fig. 2. Visual symptoms of arsenic toxicity in leaves (A) and roots (B) of *Pistia stratiotes* exposed to three As^{III} concentrations after four days (reprinted from [41]).

terms of plant, Brake fern (*Pteris vita*) accumulated As up to concentration of 7500 mg/kg without showing symptom of toxicity [44] while Water hyacinth *(Eichhornia crassipes*) survives at that concentration. Literature reveals that adverse effects have been observed in aquatic plants for Pb, Cd, Hg, and As at very low concentration in the growth medium. Also, effects maybe enhanced or reduced by the combination or presence of many metals in the media. Wiafe [45] observed that the level of uptake of metals (As, Hg, Cd and Pb) by *Typha capensis* was inhibited when either two of the heavy metals existed in the solution. Some plants tolerate or counteract the damages of heavy metals while some at certain concentration increase in nutrient and size. For example, when *E. camaldulensis* species was exposed to 45 µmol/L Cd, an increase of carotenoids (related to the tolerance to oxidative stress), epidermis and root endoderm thickness was obseverd [37, 51]. The tolerance could be due to some phyto-compounds such as anthocyanins, thiols, and antioxidant scavenging enzymes [52]. Furthermore, at 50 mg/kg of Co, there was an increase in nutrient content of tomato plants [53] and increase in plant growth, nutrient content, biochemical content, and antioxidant enzyme activities (catalase) in radish and mung bean [54, 55]. Over 14 days exposure of *Ipomonea aquatica* (water spinach) to high Cr^{3+} (10 mg L^{-1}) in contaminated water (in hydroponic

system), the root of the plant increased in size (becoming fatter) rather than longer [50]. Some aquatic plants have the tendency to recover within days after exposure to high concentration of heavy metals. For instance, Drost et al., [56] observed that after high exposure to copper, nickel and cadmium toxicity, Duckweed recovered within days. It is safe to state where plant survives a high level of exposure to a toxicant or stress, there is a potential for full recovery [57].

3.1.1.2. Aquatic animals
One major biomarker of heavy metal toxicity in aquatic environment is fish. Although, they are of great importance economically, they are greatlty affected by heavy metals. Exposure of fish species to heavy metals may be from contact directly or from food web or chain indirectly. Long term exposure can cause death to juvenile fish and reduced breeding potential of adults fish as indicated in many reports [58-61]. The toxicity may cause structural changes in the organs at microscopic cellular, DNA, chronic stress and organ level leads to alterations of the function systems and eventual growth inhibition [62]. In fish system, highest concentration of heavy metals was reported to be in the kidney and liver [63]. Creatures in benthic environment, such as worms, crustaceans and insects are greatly by contaminated sediment by heavy metals, affecting their feeding habit and eventual death and reducing the food availability for larger animals such as fish [64].

3.1.1.3. Human health
In water, metals are present as complex mixtures of discrete mineral phases. However, bioavailability of metals (determined through metal speciations) determines the impacts on human health. Several studies have explored routes of exposure from water which include dermal contact and the most direct exposure pathway including oral ingestion [6,10,13,27-28,65-66]. Adverse health impacts to human health are mainly controlled by concentrations (amount) ingested and individuals (with compromised metabolism and poor clearance

Table 3. Effect of heavy metal toxicity on some aquatic plants

Metal	Aquatic Plant	Toxic effect	References
Al	Duckweed (*Lemna minor* L.)	Decline in enzymatic activity, reduced efficiency of photosynthetic energy conversion	[46]
As	Water hyacinth (*Eichhornia crassipes*)	Stunted growth, chlorosis, wilting, death	[42]
	Water lettuce (*Pistia stratiotes* L.)	Sharp reduction in the root volume, chlorosis, organ also became darker, cell membrane damage, reduction in relative growth rate; reduced photosynthetic O_2 evolution activity, high enzyme activitysuch as superoxide dismutase (SOD), catalase (CAT), peroxidase (POX) and ascorbate peroxidase (APX)	[41]
	Brake fern (*Pteris* vita)	Decline in enzymatic activity, reduced efficiency of photosynthetic energy conversion	[44]
Cd	Duckweed (*Lemna minor* L.)	Reduced shoot growth; inhibition of root growth	[47]
	Iridaceae (*Gladiolous*), Isoetaceae (*Isoetes taiwaneneses* D.) and Amazon sword plant or burhead (*Echinodorus Amazonicus*)	Reduced shoot growth; inhibition of root growth	[48]
	Water hyacinth (*Eichhornia crassipes*)	Stunted growth, plant height and root length decreased, chlorosis	[49]
	Water lettuce (*Pistia stratiotes* L.)	Stunted growth, plant height and root length decreased, chlorosis	[49]
Cr	Water spinach (*Ipomonea aquatica*)	Increased in root size, root length decreased	[50]
Zn	Duckweed (*Lemna minor* L.)	Decline in enzymatic activity, reduced efficiency of photosynthetic energy conversion, decrease in chlorophyll	[46]
	Water hyacinth (*Eichhornia crassipes*)	Stunted growth, plant height and root length decreased, chlorosis	[49]
	Water lettuce (*Pistia stratiotes* L.)	Stunted growth, plant height and root length decreased, chlorosis	[49]

mechanisms) [28,66]. Generally, assessment of health risk of potentially toxic metals involves the quantitative assessment of the possibility of the deleterious impacts occurring in a given set of conditions [66]. Summary of selected heavy metal impacts on human health nand major biomarkers of importance is presented in Table 4.

3.2. Organic pollutants

Organic pollutants are pollutants that are organic in nature i.e basically containing carbon covalently bonded with other compounds. They are known to be toxic or carcinogenic in nature. Their presence in water in large quantity causes considerable and widespread concern. Rivers serves as hotspot for organic pollutant loading, particularly those in lowland regions [74].

Organic water pollutants generally include: detergents, disinfection by-products (having "down-the-drain" applications [221]), food processing waste, insecticides and herbicides, petroleum hydrocarbons and lubricants, and fuel combustion byproducts (from storm water runoff) [75], volatile organic compounds, chlorinated solvents, perchlorate (from personal care products), drug pollution (involving pharmaceutical drugs and their metabolites). Some of these organic water pollutants contain compounds that are persistent in nature and elicited most concern from the international community regarded as persistent organic pollutants (POPs). POPs are heterogeneous set of man-made compounds that

Table 4. Human health effects of some heavy metals

Metal	Effects	Most common Biomarkers of Exposure	References
Cd	Increased risk of osteoporosis, renal tubular, glomerular and lung damage, by affecting cardiovascular, developmental, digestive, nervous, urinary, reproductive, and respiratory (From the nose to the lungs) systems.	Blood, urine, feces, liver, Kidney and Bone.	[67]
Cr	Causes allergic dermatitis, low birth weight and also affecting immune, urinary, respiratory and cardiovascular systems.	Blood or urine	[68]
Co	Nausea and vomiting Dermatitis.	Urine and Blood.	[69]
Cu	Liver and kidney damage, immunotoxic, and death.	Blood, urine, hair, and nails.	[70]
Ni	Dermatitis, allergicreaction and chronic bronchitis.	Blood, bone, and urine.	[71]
Pb	Affects the central nervous system, impair neurodevelopment in children, metabolic processes, renal, gastrointestinal, ocular and musculoskeletal systems, thereby causing nausea ,anorexia, severe abdominal cramps, colic, weight loss, renal tubular dysfunction, abortion, muscle and joint pains and strong biochemical effect behavioral disorders, low intelligence, strokes.	Blood, bone, and urine.	[72]
Zn	Attacks digestive, haematological, and respiratory system and causing anemia, pancreas damage, and decrease high density lipoprotein (HDL) cholesterol.	Serum zinc level. High levels of zinc in feces or urine are indicative of recent exposure	[73]

are easily transported from their source and easily reconcentrated in the new environment to potential toxic or hazardous levels. Concern regarding the toxicities of these pollutants brought about a global treaty which is known as the Stockholm Convention, launched in 2001 to reduce drastically or eliminate POP release to the environment [76]. Many evidences exist regarding waterbodies pollution by organic pollutants. In drinking water, concentration rarely exceeds 20 mg/L^{-1} [74]. Some organic pollutants including polychlorinated dibenzo-*p*-dioxins and polychlorinated dibenzofurans (PCDD/Fs), antibiotics, herbicides and bisphenol A (BPA), have drawn significant attention by environmental researchers [77, 227]. However, other organic pollutants considered low priority pollutants may be inform of nutrient or dissolved materials including phosphates, nitrate, sulphate, ammonium nitrate, nitrite etc. Major sources of specific classes of pollutant in water are summarized in Table 5.

3.2.1 Adverse effects of Organic pollutants in water

Although microorganisms can degrade organic pollutant load in water through a self-purification process involving using of sufficient oxygen, dilution, sedimentation and sunlight. The adverse effect of organic pollutants in water sources shall be discussed briefly under the following headings; plant, aquatic animal and human.

3.2.1.1. Plant

Exposure of aquatic plants to organic pollutants is generally through uptake from roots influenced by their low volatility and through plant leaves by contact from air, often a consequence of agricultural spraying with organochemicals. After uptake by plants, organic pollutants are translocated to different parts of the plants, where toxicity may occur. Transport pathways in higher plants generally involves; short distance transport (intracellular and intercellular) and long distance transport (conducting tissue transport) [78]. However, some chemical based on their chemistry (e.g water-hating organic chemicals) are only limited in phloem [78-79]. Aquatic plant tolerance to uptake of organic pollutants seems to correlate with the ability to deposit large quantities of

Table 5. Major sources of organic pollutants in water

Chemical class	Sources
Aliphatic and aromatic hydrocarbons (including benzenes, phenols and petroleum hydrocarbons)	Petrochemical industry wastes, Heavy/fine chemicals industry wastes, Industrial solvent wastes, Plastics, resins, synthetic fibres, rubbers and paints production, Coke oven and coal gasification plant effluents, Urban run-off, Disposal of oil and lubricating wastes
Polynuclear aromatic hydrocarbons (PAHs)	Urban run-off, Petrochemical industry wastes, Various high temperature pyrolytic processes, Bitumen production, Electrolytic aluminium smelting, Coal-tar coated distribution pipes
Halogenated aliphatic and aromatic hydrocarbons	Disinfection of water and waste water, Heavy/fine chemicals industry wastes, Industrial solvent wastes and dry cleaning wastes, Plastics, resins, synthetic fibres, rubbers and paints production, Heat-transfer agents, Aerosol propellants, Fumigants
Organochlorine pesticides	Agricultural run-off, Domestic usage, Pesticide production, Carpet mothproofing, Timber treatment
Polychlorinated biphenyls	Capacitor and transformer manufacture, Disposal of hydraulic fluids and lubricants, Waste carbonless copy paper recycling, Heat transfer fluids, Investment casting industries PCB production
Phthalate esters	Plastics, resins, synthetic fibres, rubbers and paints production, Heavy/fine chemicals industry wastes, Synthetic polymer distribution pipes

Source: [74]

pollutant metabolites in the 'bound' residue fraction of plant cell walls compared to the vacuole, where enzymatic and metabolic activities may occur [80]. However, toxicity of organic pollutants may be based on plant part viz root and leave. To the leave cell, toxic effects may include cell ultrastructure, biosynthesis, membrane stability and DNA while to the root cell, toxic effects include inordinate mitotic division [81]. Other effects may be on plant physiological and biochemical responses. Some recent studies [82-85], found that the system of defense and growth of *Chara vulgaris L.*, *Lemna minor L.*, *H. dubia* (Bl.) *Backer* and *Potamogeton perfoliatus L* respectively are affected by Linear Alkylbenzene Sulphonate, (LAS). Furthermore, our re-intepetation of their data reveals that the effects are varied among the different aquatic plant species. Similarly, [86] reported that at concentration of 840 mg/L of ammonium nitrate in water, the growth rate, carbon contents, carbon-nitrogen ratio, photochemical cells and induced reactive oxygen stress (ROS) of *Lemna minor L* (Duckweed) was reduced, resulting in cell mortality of the aquatic plant. A simple indicator of aquatic plants exposure to organic pollutant is seen by the increased ROS production, leading to plants inability to do its

regular ecological function of regulating nutrients in aquatic environment [57]. Information regarding the toxic effects of organic pollutants especially POPs on aquatic plant species or macrophyte is very scarce. Therefore, more studies are required to fill this knowledge gap.

3.2.1.2. Aquatic animals
Available oxygen in water is reduced organic pollutants. This affects water organisms by causing reduced fitness or death from asphyxiation. Effects also include increased turbidity (especially by petroleum-related wastes) of the water, which reduces the available light for photosynthetic organisms and potentially leading to its death. It can also settle on the benthic and alters the characteristics. Organic pollutants have been detected in marine organisms, including the green mussel, *Perna viridis* [87-90], barnacles [91], odontocete species [92] and fish species [58-61, 93].

3.2.1.3. Human health
Environmental xenobiotic compounds have the potential to induce adverse effects on human health [94]. A common example is hydrophobic

contaminant like POPs are known to be a potential endocrine disruptor compounds. Although, impact of organic pollutants to human health is yet to be fully examined [95-99], evidences still exists which correlates development and manifestation of some chronic diseases to exposure of certain organic chemicals. Particular, cancer cases has been greatly linked [74]. Other toxic effects could be on ovarian function in women [100], reproductive disorders in both male and female [101], female breast cancer [102], blood poisoning, eyes and skin irritation (by exogenous pollutant e.g. LAS) [103].

4. Decontamination strategy: Phytoremediation

According to United Nations Environment Programme [104], the efficient use of plants for removing, detoxifing, or immobilising environmental contaminants is regarded as phytoremediation. The strategy is eco-friendly and cheap. The concept of phytoremediation of contaminated medium has been extensively discussed in many scientific, governmental and non-governmental studies [41, 104-115]. The overall objective of any treatment method is to create a final solution that is protective of human health and the environment [29]. Whilst there are many studies on remediation of contaminated soil by plant, aquatic medium by aquatic plants have generally been less studied and reviewed. Aquatic plants are extremely important components of an aquatic ecosystem for primary productivity and nutrient cycling [116-118] and providing refuge, habitat and food for some aquatic organisms. Aquatic phytoremediation involves the use of plants for the removal of contaminants from aqueous solutions. Generally, members of Cyperaceae, Potamogetonaceae, Ranunculaceae, Typhaceae, Haloragaceae, Hydrocharitaceae, Najadaceae, Juncaceae, Pontederiaceae, Zosterophyllaceae, Lemnaceae, mainly represent aquatic plants [4]. These plants are either emergent (i.e their roots are attached to the substrate at the bottom of water bodies while the leaves grow to or above the surface of the water), submerged (their root system is attached to the substrate but their leaves do not reach the surface of the water), or free floating (i.e exclusively found on the surface of water bodies, usually found in standing or slow moving waters) [115]. The overview of phytoremediation techniques or mechanism for the different pollutants is presented in Figure 3. For heavy metals removal mechanism include phytoextraction, phytostabilzation, phytoaccumulation, phytofilteration (rhizofilteration/ blastofiltration) while for organic pollutants mechanism include phytodegradation, phytostimulation, phytotransformation, phytovolatilization, phytodetoxication, phytoassimilation, phytoevaporation. Phytoextraction and phytoaccumulation technique is based on hyper-accumulation, contaminant extraction and capture by plant; phytofilteration is based on the use of plant roots (rhizofiltration) or seedlings (blastofiltration) to accumulate, extract and
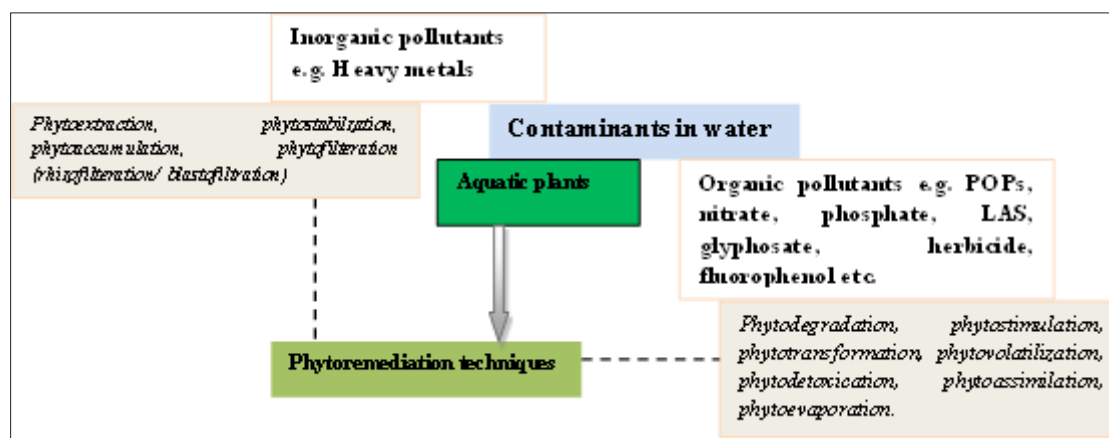

Fig. 3. Overview of phytoremediation techniques by aquatic plant for both organic and inorganic contaminants removal in water

capture contaminants; phytostabilization is based on complexation and/or contaminant destruction; phytodegradation is based on contaminant destruction; phytovolatilization is based on volatilisation by leaves, contaminants extraction from media and release into air; phytoassimilation is based on contaminant transport and metabolism in plant chloroplast [119-120].

Research status of aforementioned phytoremediation techniques is either at laboratory (involving use of hydroponics), pilot or field applications stages (involving use of constructed wetlands) [106, 107, 121] (see Figure 4). Phytoextraction and phytoaccumulation is at laboratory, pilot and field applications stages, phytofilteration is at laboratory and pilot scale stages, phytostabilization, phytodegradation (including rhizodegradation) is at field demonstration and application stage, phytovolatilization is at laboratory and field application stages while phytoassimilation, phytoevaporation, phytodetoxication, phytostimulation and phytotransformation is at laboratory or field demonstration stages. In any approach, at the end of the exercise, plant biomass is often harvested, dried and ashed for disposal or extracted using appropriate solvent before analysis. Aquatic plants which operate by rhizofiltration are preferable in aquatic phytoremediation than those plants that efficiently transfer the contaminants (translocators) from root to shoot. The reason is that translocators can potentially pollute above ground biomass, which increases the cost of processing, as well as the risk of exposing the ecosystem to the contaminated plants [4]. The analyses for heavy metals and organic pollutants concentrations in plant biomass are often done by spectroscopic and chromatographic techniques following extraction processes. Extraction technique for heavy metals is commonly by acid digestion while organic pollutants include liquid–liquid extraction (LLE), solid-phase extraction (SPE) and matrix solid-phase dispersion (MSPD). Common techniques for analysis after extraction include atomic absorption spectroscopy (for heavy metals) [6, 24], ultraviolet-visible spectroscopy (for dyes), high performance liquid chromatography (HPLC), liquid chromatography/tandem mass spectrometry (LC-MS/MS) or gas chromatography/mass spectrometry (GCMS) (for agricultural chemicals and
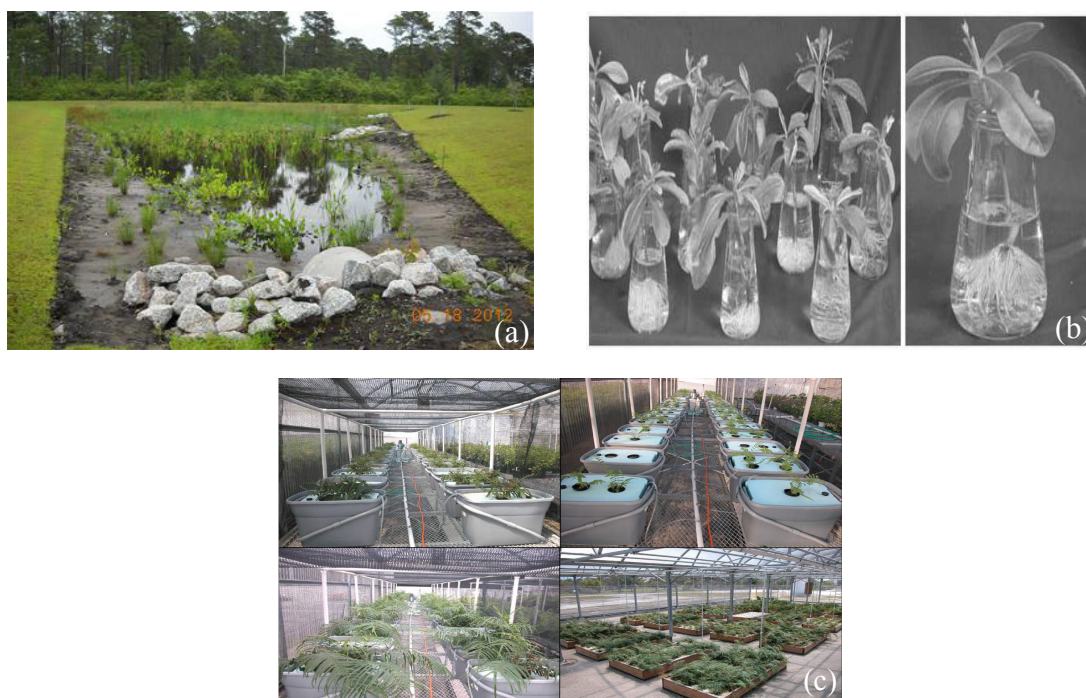

Fig. 4. Experimental system for aquatic phytoremediation. (a) Field experiment showing a constructed wetland [122], (b) Pilot scale setup using *Pteris vittata* for removal of As from contaminated water [80] (c) Hydroponic system developed for rhizofiltration of environmental contaminants by *Talinum cuneifolium* (Portulacaceae) [4].

petroleum hydrocarbons).

4.1. Physicochemical factors affecting phytoremediation
Cellular mechanism for detoxification and tolerance has been discussed recently [112]. In general, the efficiency of removal by aquatic plants depends on water and contaminant physico-chemistry as well as physiology and genotype of the plant [4, 123-124]. However, in this study emphasis was placed on the physiochemistry summarized in Table 6. These parameters can be manipulated or modified in water to enhance phytoremediation.

Currently, studies modifying water physico-chemistry for phytoremediation of toxic chemicals is at infancy. There is therefore, need for more efforts for their effective use in the future. For metals,

Table 6. Physical and chemical factors known to affect the pollutants uptake, accumulation, and toxicity

Parameter	Effects
Heavy metal	
Temperature	More uptake/toxicity at higher temperatures
Light	Uptake is light dependent in some cases
pH	Lower pH generally increases the uptake/capacity
Salinity Monovalent Cations (K, Na)	Lower salinity increases the content/toxicity
Divalent Cations Ca, Mg, Mn, Fe	Increasing monovalent cations reduces the uptake
Anions	Increasing divalent cations reduces the uptake
Organic Acids	Reduces uptake and toxicity
Sediment Fraction	Binds metals, reduces uptake/toxicity
Heavy Metals	Reduces uptake/toxicity by binding metals Complex metals, reduces uptake/toxicity Zn/Cd, Ni, Cu combinations are antagonistic. Fe can stimulate Cu accumulation
Suspended solids	Complex metals, reduces uptake/toxicity
Sulphate	Insignificant but reduces uptake slightly
Nitrate(N)	Significantly reduces toxicity
Polypeptides	Reduces uptake/toxicity by complexation
Polysachharides	Chelate metals, reduces uptake/toxicity
Sulphur (amino acids)	Reduces uptake and toxicity indirectly
Extracellular Products	Reduces toxicity
Source: [125]	
Organic pollutants	
Solubility and concentration of organic pollutants	Increases uptake
pH	Lower pH generally increases the uptake
Light intensity	Uptake is light dependent in some cases
Nitrates	Significantly reduces removal
co-occurring ions	Increasing dissolved ions reduces the uptake
Partition coefficients	High partition coefficient between octanol and water (K_{OW}), and low partition coefficient between octanol and air (K_{OA}) increases uptake/absorption from water and air respectively
Molecular mass of pollutants	Generally, mass < 1000 increases uptake
Lipid content	High lipid contents increases uptake/toxicity
Temperature	Higher temperature coefficient for diffusion processes of organic pollutants can accelerate passive absorption by the plant. On the other hand, temperature rise stimulated transpiration stream rate and enzyme activity of plants
Transpiration stream concentration factor (TSCF)	The TSCF can show the capacity of organic pollutant translocation from roots to aboveground parts.

Sources: [80] ,[81], [113], [126-132].

phytoextraction capabilities of many plant species can be enhance by reducing the concentration of organic acids in the water, since organic acids are known to form complexes with metals [6, 13, 65, 125]. Reducing organic acid will thereby increase the concentration of free metal ions readily available for uptake. In addition, the bioavailability of metals can also be enhanced by aquatic plant roots exuding acidifying protons in water. The lowering of water pH increases the adsorption of heavy metals and reduces their concentrations in the aqueous solution [6, 65, 125, 133-134]. Also, the salt contents in terms of salinity, when in high concentrations reduces uptake of metals in water. For organic pollutant uptake and translocation by plants, parameter such as molecular mass and hydrophobicity with partition coefficients (between octanol and water (K_{OW}) /air (K_{OA})) plays crucial roles. Many reports have shown that high K_{OW} and low K_{AO} values of organic pollutants correlated positively to easy (high) uptake of organic pollutants in water and absorption from air by aquatic plants [80,127-130]. Succinctly, when log K_{ow} is less than 1, the organic pollutant becomes more soluble in water and mainly absorb on the plant roots at a rate surpassing passive influx into the transpiration stream (measured as TSCF) while at log Kow > 3.5, due to high sorption on the roots, aquatic plants may not or very slowly passed the contaminants into the transpiration stream and further to the stems and leaves [80, 127]. Log K_{ow} values of some frequently found organic contaminants in the environment have been reviewed [80]. Lipid content has the strongest influence on the uptake of organic pollutants, since most of the organic pollutants are hydrophobic organic contaminants (HOCs). Other factors which impact uptake of by influencing the adsorption of organic pollutants on sediments or chelates formation; include metal type in the solution, dissolved organic carbon (DOC) concentration, pH, organic matter content, light intensity and presence of nitrate. High intensity of light and presence of nitrate was reported to negatively affect perchlorate removal by *Pistia sp*. [131] and willow trees grown in hydroponic solution [135]. These results suggest that

for successful phytoremediation of metal/organic polluted water, a strategy should be developed to combine a rapid screening of aquatic plant species possessing hyperacumulating tendency with practices focusing on physicochemical factors listed in Table 6.

4.2. Phytoremediation of heavy metal polluted water

Literature reviewed reveals that many aquatic species have been identified and tested for the phytoremediation of selected heavy metals (As, Cu, Cr, Hg, Cd, Ni, Pb and Zn) from the polluted water (Table 7). These include sharp dock (*Polygonum amphibium* L.), duck weed (*Lemna minor* L.), water hyacinth (*Eichhornia crassipes*), water lettuce (*P. stratiotes*), water dropwort (*Oenathe javanica* (BL) DC), calamus (*Lepironia articulate*), pennywort (*Hydrocotyle umbellate* L.), Water fern (*Azolla filiculoides*), Poaceae (*Phragmites communis* Trin), spiny water nymph, spiny naiad and holly-leaved naiad (*Najas marina*), Water lilies (*Nymphaea spontanea*), Poaceae (*Phragmites australis* Cav.), Se a clubrush, cosmopolitan bulrush, alkali bulrush, saltmarsh bulrush, and bayonet grass (*Bolboschoenus maritimus* L.), water-starwort (*Callitriche cophocarpa* Sendtn), umbrella palm (*Cyperus alternifolius*), Salviniaceae (*Salvinia herzogii*), Water Mint (*Mentha aquatica* L.), Water Mint (*Mentha sylvestris* L.), Canna (*Canna × generalis*), Cannaceae (*Canna indica L.*), giant baby tears (*Micranthemum umbrosum*), aquatic moss (*Warnstorfia fluitans*), hippo grass (*Vossia cuspidate*), blue moon (*Iris sibirica*), marigold (*Tagetes erecta*), yellow bur head (*Limnocharis flava*), willow (*Salix matsudana*), Alpine pennycress (*Noccaea caerulescens*), Mint (*Elsholtzia argyi*) and Mint (*Elsholtzi splendens*) (Table 7). The summary of concentrations, period, experimental framework, removable rate of different aquatic plants reported in literature for heavy metals phytoremediation is presented in Table 7.

Some plants are considered hyper-accumulator due to their well-developed fibrous root system and large biomass e.g Azolla species, water hyancinth,

duckweed etc. Removal rates by the water hyancinth in hydroponic solution for Cd, and Zn was 50-90 % for both metals [142] while for Ni removal was 68 % in field experiment [150] and 19.84 % in hydroponics after 10 d exposure to 15 mg/L of Ni [177]. Furthermore, strong removal was also observed for Cd removal (> 90 %) conducted in a pot [25]. Also using water hyancinth, Lu et. al., [142] demonstrated the potential for the removal of Cd and Zn. In their study, the plant was exposed to concentrations of 0.5, 1, 2 and 4 mg/L of Cd and 5, 10, 20, and 40 mg/L of Zn, and harvested separately after days 0, 4, 8 and 12. They observed fast removal in the first 4 days with overall removal rates of 50-90 %. They concluded that the plant was a moderate accumulator of Cd and Zn at low concentrations. Abbas et al [173] assessed the effectiveness of

water hyacinth for the phytoremediation of landfill leachate for the period of 15 days. The authors used fifteen plastic containers in experimental setup and the plant was fitted as a floating bed with the help of thermopole sheet. Results from their study showed that the removal rates of heavy metals like Zn, Pb, Cu and Ni from landfill leachate gradually increased from day 3 to day 15 of the experiment. The maximum removal rate for heavy metals such as for Zn (80–90%), Pb (76–84%), Cu (72-87%) and Ni (68-81%) was attained by the plants. Low values (< 1) of BCF and translocation factor, indicating low transport of heavy metals from roots to the above-ground parts of the plants. Therefore, from their results, they suggested that the plant is suitable for the removal of pollution load from landfill leachate. Priyanka et al [162] tested water

Table 7. Summary of selected heavy metals in aqueous medium associated with aquatic plants remediation

Metal	Concentration	Exposure duration	Experimental framework	Plant specie	Removal rate (%)	References
As	0.5	21d	Field	Duckweed (*L. minor*)	5	[136]
	96 µg/L	3 d	Field	Duckweed (*L. minor*)	7070	[137]
	0-100 µM	192 h	Hydroponic	*Warnstorfia fluitans*	82	[138]
	16.31ppb	25 d		Duckweed (*L. minor*)	90.95	[139]
	20	24 h	Field	Water lettuce (*Pistia stratiotes*)	77	[41]
Cd	1-8	12 d	Hydroponics	Duckweed (*Wolffia globosa*)	50-90	[140]
	17.20-26.25 µg/L	Inconsistent	Field	Poaceae (*Phragmites communis Trin*)	45.6-80	[141]
	17.20-26.25 µg/L	Inconsistent	Field	spiny water nymph, spiny naiad and holly-leaved naiad (*Najas marina*)	45.6-80	[141]
	0.5-4	12 d	Hydroponic	Water hyacinth (*Eichhornia crassipes*)	50-90	[142]
	0.003-10⁻⁷ M	28	Field	Duckweed (*L. minor*)	95	[143]
	0.5-3.0	22	Field	Duckweed (*L. minor*)	42-78	[144]
			Hydroponic	*Veronica anagallis*	50-90	[145]
			Hydroponic	*Epilobium laxum*	50-90	[145]
	0.018	7 d	Field	Duckweed (*L. minor*)	78	[146]
	0.01-10	48 h	Field	Duckweed (*L. minor*)	97.32	[147]
	0-12.39	28 d	Field	Duckweed (*L. minor*)	72-91	[148]
	10 µM	7 d	Field	Duckweed (*L. minor*)	38	[149]
	0-12.39	28	Field	Water fern (*Azolla filiculoides*)	72-91	[148]
	1.47 ppb	25 d	Hydroponic	Duckweed (*L. minor*)	97.79	[139]
	Variable concentrations	10 d	Field	umbrella palm (*Cyperus alternifolius*)	3	[150]
	Variable concentrations	10 d	Field	Water hyacinth (*Eichhornia crassipes*)	20	[150]

Table 7. (Continue)

Metal	Concentration	Exposure duration	Experimental framework	Plant specie	Removal rate (%)	References
Cr	1-8	12 d	Hydroponics	Duckweed (*Wolffia globosa*)	50-90	[140]
	<0-2.20 µg/L	Inconsistent	Field	Poaceae (*Phragmites communis Trin*)	45.6-80	[141]
	<0-2.20 µg/L	Inconsistent	Field	spiny water nymph, spiny naiad and holly-leaved naiad (*Najas marina*)	45.6-80	[141]
	1.0–2.0	24 h	Field	Salviniaceae (*Salvinia herzogii*)	70–83	[151]
	0.1-1.0	12 d	Hydroponic	Water fern (*Azolla caroliniana*)	100	[152] [a]
	0.1-1.0	12 d	Hydroponic	Water fern (*Azolla caroliniana*)	74	[152][b]
	1	15 d		Duckweed (*L. minor*)	96.94	[153]
	1.0–2.0	24 h	Hydroponic	Water lettuce (*Pistia stratiotes*)	58–80	[151]
	1-10	9 w	Hydroponic	Water lilies (*Nymphaea spontanea*)	31.6	[154]
	< 0 – 0.51	Inconsistent	Field	Poaceae (*Phragmites australis Cav.*)	50–80	[155]
	< 0 – 0.51	Inconsistent	Field	Sea clubrush, cosmopolitan bulrush, alkali bulrush, saltmarsh bulrush, and bayonet grass (*Bolboschoenus maritimus* L.)	50–80	[155]
	0.04-98	60 d		Duckweed (*L. minor*)	25-77.42	[156]
	10	3 w	Hydroponic	water-starwort (*Callitriche cophocarpa* Sendtn)	50-80	[157][a]
	0.25–5.0	14 d	Pilot with continuous flow	Duckweed (*L. minor*)	76.4–20.0	[134][a]
	10.946	7 d		Duckweed (*L. minor*)	99.97	[158]
	10.4	7 d	Hydroponic	Duckweed (*L. minor*)	75	[159]
	0.776	7 d	Field	Duckweed (*L. minor*)	63	[146]
	0-0.20 mM	16 d		Duckweed (*L. minor*)	27.6	[160]
				Phalari arundinacea		[161]
	2	15 d	Field	Water hyacinth (*Eichhornia crassipes*)	99.9	[162][a]
	67.33 ppb	25 d		Duckweed (*L. minor*)	90.25	[139]
	0-12.39	28 d	Field	Duckweed (*L. minor*)	72-91	[148]
	0-12.39	28 d	Field	Water fern (*Azolla filiculoides*)	90	[148]
Cu	1.95-4.20 µg/L	Inconsistent	Field	Poaceae (*Phragmites communis Trin*)	45.6-80	[141]
	1.95-4.20 µg/L	Inconsistent	Field	spiny water nymph, spiny naiad and holly-leaved naiad (*Najas marina*)	45.6-80	[141]
	1-7	4 d	Hydroponic	Duckweed (*L. minor*)	77.78	[163]
	1	15 d	Hydroponic	Duckweed (*L. minor*)	96.94	[153]
	1-7	15 d	Hydroponic	Mint (*Elsholtzia argyi*)	50-90	[164]
	1-7	15 d	Hydroponic	Mint (*Elsholtzi splendens*)	45-80	[164]
	1.23 – 1.75	Inconsistent	Field	Poaceae (*Phragmites australis Cav.*)	50–80	[155]
	1.23 – 1.75	Inconsistent	Field	Sea clubrush, cosmopolitan bulrush, alkali bulrush, saltmarsh bulrush, and bayonet grass (*Bolboschoenus maritimus* L.)	50–80	[155]

Table 7. (Continue)

Metal	Concentration	Exposure duration	Experimental framework	Plant specie	Removal rate (%)	References
	0.003-10⁻⁷ M	7 d		Duckweed (*L. minor*)	86.5	[143]
	0.46	20 d		Duckweed (*L. minor*)	71.4	[165]
	4.359	7 d		Duckweed (*L. minor*)	99.97	[158]
	3	7 d	Hydroponic	Duckweed (*L. minor*)	40	[159]
	1.432	7 d	Field	Duckweed (*L. minor*)	86	[146]
	67 μg/L	3 d		Duckweed (*L. minor*)	87	[137]
	0.5 and 0.25	7 d		Duckweed (*L. minor*)	0	[166]
	1-5	4 w		Duckweed (*L. minor*)	90	[167]
	200 μM	3 d		Duckweed (*L. minor*)	20.2	[168]
				Vossia cuspidata		[169][170]
	2	2 w		Duckweed (*L. minor*)	54.2	[171]
	0.05-1.2	5 d		Duckweed (*L. minor*)	83.3	[172]
	0-12.39	28 d	Field	Duckweed (*L. minor*)	72-91	[148]
	23.84 ppb	25 d		Duckweed (*L. minor*)	98.46	[139]
	0-12.39	28 d	Field	Water fern (*Azolla filiculoides*)	80	[148]
	0.09-0.73	15 d	Field	Water hyacinth (*Eichhornia crassipes*)	36.98-87.09	[173]
	0.08-0.46	15 d	Field	Water lettuce (*Pistia stratiotes*)	39.72-72.58	[173]
Hg	0.1-1.0	12 d	Hydroponic	Water fern (*Azolla caroliniana*)	75-93	[152]
	0.04-98	60 d	Field	Duckweed (*L. minor*)	25-77.42	[156]
	0.23	20 d	Hydroponic	Duckweed (*L. minor*)	66.5	[165]
	0.5 and 0.25	7 d	Hydroponic	Duckweed (*L. minor*)	0	[166]
			Hydroponic	*Salix matsudana*		[160]
	200 μM	3 d	Hydroponic	Duckweed (*L. minor*)	20.2	[168]
	0-30 μM	6 d	Hydroponic	Duckweed (*L. minor*)	58.3	[81]
			Field	*Limnocharis flava*		[174]
	0.36 ppb	25 d	Hydroponic	Duckweed (*L. minor*)	82.84	[139]
Ni	1-8	14 d	Hydroponic	Water Mint (*Mentha aquatica* L.)	22.3	[175]
	1-8	14 d	Hydroponic	Water Mint (*Mentha sylvestris* L.)	17.9	[175]
	0.0-10.0	24 h	Batch	Duckweed (*L. minor*)	82	[176]
	1.90-17.30 μg/L	Inconsistent	Field	Poaceae (*Phragmites communis Trin*)	45.6-80	[141]
	1.90-17.30 μg/L	Inconsistent	Field	spiny water nymph, spiny naiad and holly-leaved naiad (*Najas marina*)	45.6-80	[141]
	1.98 – 4.51	Inconsistent	Field	Poaceae (*Phragmites australis* Cav.)	50–80	[155]
	1.98 – 4.51	Inconsistent	Field	Sea clubrush, cosmopolitan bulrush, alkali bulrush, saltmarsh bulrush, and bayonet grass (*Bolboschoenus maritimus* L.)	50–80	[155]
	0.04-98	60 d	Field	Duckweed (*L. minor*)	25-77.42	[156]
	15	10 d	Hydroponic	Water hyacinth (*Eichhornia crassipes*)	19.54	[177]
			Hydroponic	*Tagetes erecta*		[178]

Table 7. (Continue)

Metal	Concentration	Exposure duration	Experimental framework	Plant specie	Removal rate (%)	References
	0-12.39	28	Field	Duckweed (*L. minor*)	72-91	[148]
	0-12.39	28	Field	Water fern (*Azolla filiculoides*)	72-91	[148]
	346.81 ppb	25 d		Duckweed (*L. minor*)	98.08	[139]
	Variable concentrations	10 d	Field	Umbrella palm (*Cyperus alternifolius*),	66	[150]
	Variable concentrations	10 d	Field	Canna (Canna × generalis)	31	[150]
	0.07-1.83	15 d	Field	Water hyacinth (*Eichhornia crassipes*)	25.68-81.56	[173]
	0.03-1.36	15 d	Field	Water lettuce (*Pistia stratiotes*)	28.96-68.79	[173]
	Variable concentrations	10 d	Field	Water hyacinth (*Eichhornia crassipes*)	68	[150]
Pb	0.0-10.0	24 h	Batch	Duckweed (*L. minor*)	76	[176]
	1	15 d		Duckweed (*L. minor*)	98.55	[153]
	0.70-4.45 µg/L	Inconsistent	Field	Poaceae (*Phragmites communis Trin*)	45.6-80	[141]
	0.70-4.45 µg/L	Inconsistent	Field	spiny water nymph, spiny naiad and holly-leaved naiad (*Najas marina*)	45.6-80	[141]
	0.1-10.0	24 h	Hydroponic	Duckweed (*L. minor*)	58-79	[133]
	0.04-98	60 d	Field	Duckweed (*L. minor*)	25-77.42	[156]
	$0.003\text{-}10^{-7}$ M	7 d	Hydroponic	Duckweed (*L. minor*)	93	[143]
	0.875	7 d	Hydroponic	Duckweed (*L. minor*)	99.97	[158]
	0.2	7 d	Hydroponic	Duckweed (*L. minor*)	85	[159]
	0.655	7 d	Field	Duckweed (*L. minor*)	84	[146]
	7.5 µg/L	3 d	Field	Duckweed (*L. minor*)	1259	[137]
	10-41	21d	Field/peat	Cannaceae (*Canna indica L.*)	81.16	[179]
	0.5 and 0.25	7 d	Hydroponic	Duckweed (*L. minor*)	0	[166]
	200 µM	3 d	Hydroponic	Duckweed (*L. minor*)	20.2	[168]
	23.37 ppb	25 d	Hydroponic	Duckweed (*L. minor*)	99.61	[139]
	0.09-0.86	15 d	Field	Water hyacinth (*Eichhornia crassipes*)	36.09-84.41	[173]
	ND-0.55	15 d	Field	Water lettuce (*Pistia stratiotes*)	43.02-76.66	[173]
Zn	5- 40	12 d	Hydroponic	Water hyacinth (*Eichhornia crassipes*)	50-90	[142]
	1	15 d	Field	Duckweed (*L. minor*)	95.20	[153]
	< 0 µg/L	Inconsistent	Field	Poaceae (*Phragmites communis Trin*)	45.6-80	[141]
	< 0 µg/L	Inconsistent	Field	spiny water nymph, spiny naiad and holly-leaved naiad (*Najas marina*)	45.6-80	[141]
	< 0– 63.5	Inconsistent	Field	Poaceae (*Phragmites australis Cav.*)	50–80	[155]
		Inconsistent	Field	Sea clubrush, cosmopolitan bulrush, alkali bulrush, saltmarsh bulrush, and bayonet grass (*Bolboschoenus maritimus* L.)	50–80	[155]

Table 7. (Continute)

Metal	Concentration	Exposure duration	Experimental framework	Plant specie	Removal rate (%)	References
	0.04-98	60 d	Field	Duckweed (*L. minor*)	25-77.42	[156]
	0.003-10^{-7} M	7 d	Hydroponic	Duckweed (*L. minor*)	63.5	[143]
	0.2-30	7 d	Hydroponic	Duckweed (*L. minor*)	75	[180]
	0.816	7 d	Field	Duckweed (*L. minor*)	62	[146]
	1-5	4 w	Field	Duckweed (*L. minor*)	90	[167]
	730 µg/L	3 d	Field	Duckweed (*L. minor*)	628	[137]
	0.5 and 0.25	7 d	Hydroponic	Duckweed (*L. minor*)	0	[166]
	200 µM	3 d	Hydroponic	Duckweed (*L. minor*)	20.2	[168]
			Field	*Cyperus alternifolius*		[181] [182]
	0-12.39	28 d	Field	Duckweed (*L. minor*)	72-91	[148]
	0-12.39	28 d	Field	Water fern (*Azolla filiculoides*)		[148]
			Hydroponic	Alpine penny-cress (*Noccaea caerulescens*)		[183]
	49.59 ppb	25 d	Hydroponic	Duckweed (*L. minor*)	98.00	[139]
	0.91-1.67	15 d	Field	Water hyacinth (*Eichhornia crassipes*)	21.55-90.18	[173]
	0.26-1.31	15 d	Field	Water lettuce (*Pistia stratiotes*)	26.99-79.57	[173]

[a] used Cr^{6+}, [b] used Cr^{3+}; Concentrations are in (mg/L) unless otherwise noted; d-days, h-hour(s), w-week(s); field: water samples treated or plant used was collected from aquatic environment, outdoor experiment or involves a constructed wetland, Hydroponics: growing plants in water cultures, or nutrient solution, without soil as a rooting medium; Pilot with continuous flow: wastewater in a continuous flow pond system used to simulate a wastewater treatment pond and a natural wetland as habitat for the plants

hyacinth in clean wastewater at Sukinda chromite mines (SCM) area of Orissa (India) containing high levels of toxic hexavalent chromium (CrVI). Results showed that the plant could remove 99.5% Cr (VI) of the processed water of SCM in 15 days. Using hydroponics, they [48] tested different levels of Cd (5 to 20 mg L^{-1}) rate by three hydrophytes: *Gladiolous*, *Isoetes taiwaneneses* Dwvol and *Echinodorus amazonicus* and observed highest accumulation in *Gladiolous* than the other two plants. Also, high removal rates following phytofiltration were reported for *Elsholtzia argyi* (50-90 %) and *Elsholtzi splendens* (45-80 %) for Cu [164]. Boonyapookana et al [140] observed high phytoaccumulation rates (reaching 90 %) for Cd and Cr by *W. globosa*, which correlates positively with exposure time and metal concentration were increased. Small water fern (*Azolla caroliniana* Willd.), was investigated for water purification potential by [152]. The experiment was conducted

in 12 days using hydroponic solution polluted by Hg and Cr. Initial concentrations were 0.1, 0.5 and 1.0 mg/L for both metals and day 12, metal contents the solution decreased to 0–0.25 mg L^{-1}, corresponding between 74 – 100 % removal rates. Baldantoni et al [141] studied the leaves and roots *Phragmites communis* Trin. (an emergent plant), and *Najas marina* L. (submerged plant), taken from Lake Averno (Naples, Italy) for levels Cd, Cr, Cu, Fe, Ni, Pb, Zn and found higher accumulation in root than leaves. However, between the two plants, *Phragmites communis* showied high capability to accumulate trace metals in the roots better than *Najas marina* [141]. By constructing a wetland in the Venice lagoon watershed, they [155] investigated the removal efficiency of *Phragmites australis* and *Bolboschoenus maritimus* in removing Cr, Ni, Cu and Zn from water. Investigations were conducted over a vegetative season with various distances to the inlet point to assess effects on

vegetation. Results showed that overall heavy metal concentrations removed ranged from 50-80 % and *P. australis* was a better phytoaccumulator to in *B. maritimus* (accumulating more in roots). Using outdoor experiments, capacity examination of *Salvinia herzogii* (Salviniaceae) and *Pistia stratiotes* (water lettuce) to remove Cr (III) from water was conducted by [151]. Results from their study showed that both plants efficiently removed Cr (up 83 % for Salviniaceae and up 80 % for water lettuce, Table 7) from water. Furthermore, water lettuce was also found by [173] to be very effective with maximum removal rate over 15 days for Zn (80–90%), Pb (76–84%), Cu (72-87%) and Ni (68-81%) respectively from landfill leachates. The author reported that the plant exhibited low (< 1) bioconcentration factor (BCF) and translocation factor (TF), indicating low transport of heavy metals from roots to the upper parts of the plant. Another excellent Cr removal from polluted water was found in *Callitriche cophocarpa* (water-starwort) by [157]. The authors used a hydroponic culture for up to 3 weeks and reported removal rate up 80 % (Table 7). Nevena et. al., [179] tested an ornamental plant *C. indica* for phytoremediation of Pb in wastewater. Removal rates of 81.16 % was obtained and therefore concluded that *C. indica* can be used in rhizofiltration systems or floating islands for treatment of water polluted with lead [179]. Most recent studies have used duckweed more when compared to other plants. Axtell et al [176] examined the ability of *Lemna minor* using a batch process to remove Pb and Ni under different laboratory conditions. Initial concentrations were 0.0, 5.0, and 10.0 mg/l for Pb, and 0.0, 2.5, and 5.0 mg/l for Ni. Overall, *L. minor* removed 76% of Pb and 82% of Ni. They further observed that there was no synergistic/antagonistic effect for the multiple metal experiments, in terms of metal removal [176]. In a continuous flow pond system, Uysal [134] examined the ability of *Lemna minor* to remove Cr (VI) ions from wastewater. The authors used the system to simulate a wastewater treatment pond and a natural wetland as habitat for the plants and reported removal rates between 20

– 76.4 % suggesting the potentiality of the plants for Cr removal in wastewater. More recently, [150] studied the uptake of Cd, Cr, Pb, and Zn by four aquatic plants including umbrella palm (*Cyperus alternifolius*), duckweed (*Lemna minor*), water hyacinth (*Eichhornia crassipes*), and canna (*Canna × generalis*) in different environments i.e., Gohar Rood river, Zarjoob river, Eynak lagoon, Anzali lagoon, and control solution. Results showed that the highest uptake rates were observed for duckweed fronds (> 70 %) while highest removal throughout the study for specific plants was water hyacinth 68 %, umbrella 66 % and canna 31 % respectively. Based on the results of their study, duckweed was suitable for the uptake of most heavy metals [150].

4.3. Phytoremediation of organic pollutant in water

Few aquatic plants have been generally been tested recently for removal of aquatic organic pollutant. It has been less studied compared to heavy metals mainly due to the complex properties (physical and chemical) of organic pollutants. Aquatic organic pollutants to have been remediated from aqueous solution by aquatic plants using either field and/ or hydroponic experiment include the following: chemical and biological oxygen demand (COD and BOD), nitrate, phosphate, sulphate; from agricultural chemicals including atrazine, dimethomorph, pyrimethanil, Isoproturon, glyphosate, metazachlor, chloroacetamide, flazasulfuron, terbuthylazine, 4-chloro-2-fluorophenol (4-Cl-2-FP), lactofen, cyanophos, herbicide norflurazon; from pharmaceuticals and personal care products (PPCPs) including sucralose, fluoxetine, tyramine, putrescine, cadaverine, spermidine, spermine, cefadroxil, metronidazole, trimethoprim, sulfamethoxazole, triclosan, diclofenac, naproxen, caffeine, ibuprofen, clofibric acid, sulfachlorpyridazine, oxitetracycline, chlorpyrifos, venlafaxine, 3-fluorophenol, 3-trifluoromethylphenol, phenol, ibuprofen, fluoxetine, cisplatin, linear alkylbenzene sulfonate; from dyes and toxin including textile dyes (AB113, RB198, BR46), blue dye, triacontanol, cyanotoxin

microcystin-LR., perchlorate, toluidine Blue; and from petroleum hydrocarbons including 1H-benzotriazole, 4-methyl-1Hbenzotriazole, 5-methyl-1Hbenzotriazole, xylytriazole, 5-chlorobenzotriazole, 3-trifluoromethylphenol, phenantherene.

Few aquatic plants to have generally been tested recently for phytoremediation of aquatic organic pollutant include M. *spicatum* [103, 148, 187]; *Azolla filiculoides* [148], *Canna generalis* [188], *Pistia stratiotes* L [131, 173, 189]; *Eichornia sp.* [131, 173, 190, 191]; *Lemna sp.* [51, 131, 192]; *Salvinia sp.* [131], *Chara vulgaris* L. [82], *H. dubia* (Bl.) Backer [84], *Potamogeton perfoliatus*

L. [85], *Hydrilla verticillata* (L.f.) Royle [193], *Vallisneria natans* (Lour.) Hara [193], giant reed (*Arundo donax*) [194], Poaceae (*Phragmites australis*) [194], broadleaf plantain (*Plantago major L.*) [222] and *Ipomoea aquatica* [195] while *Myriophyllum aquaticum* (watermilfoil) [196] and bulrush (*Scirpus lacustris*) [197] have also been used earlier. For remediation of municipal effluents, some of these plants in some cases have been reported to better treat wastewater than normal wastewater treatment plant [198] and combination of two or more plant increased the effectiveness of removal [199-201]. Domestic as well as industrial
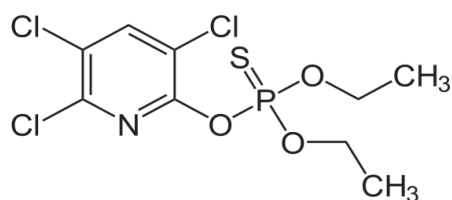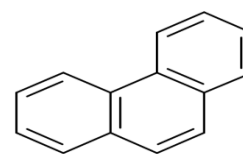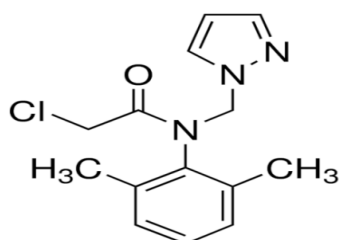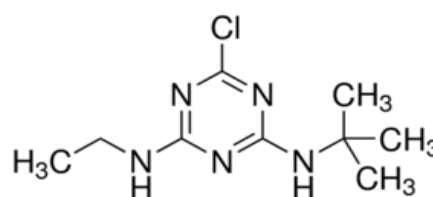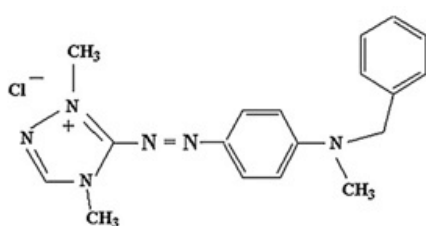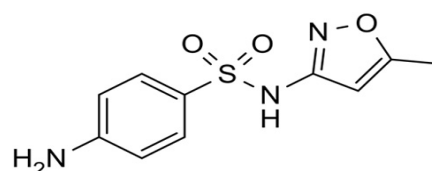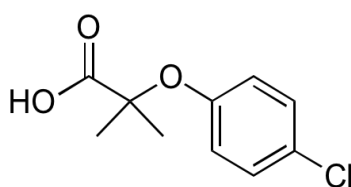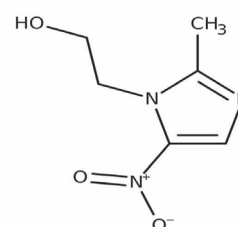
Fig. 5. Structures of some priority and emerging pollutants to have been treated from aqueous solution with aquatic plants. Emerging pollutants are mainly from pharmaceutical and personal care products (PPCPs). PPCPs maintain chemical properties that can vary widely, usually containing a non-polar core with a polar functional moiety [184-186].

activities introduced over 70 % organic pollutants into the aquatic environment. Bhaskara and coworkers [131] evaluated the phytoremediation potential of free floating macrophytes (*Eichornia*, *Pistia*, *Salvinia* and *Lemna*) in removing perchlorate from water. Among the plants tested, Pistia showed 63.8±4% (w/v) removal of 5 mg L^{-1} level perchlorate in 7 days, while other plants showed low removal (< 1 %). The mechanism involved in removal identified was phytoaccumulation (18.2 %) and rhizodegradation (45.68 %). Phenol from wastewater removal by water hyacinth was demonstrated [190]. *Myriophyllum spicatum* L., a submerged aquatic plant was tested for the accumulation of exogenous organic pollutant linear alkylbenzene sulfonate (LAS) [103]. Results showed that plant can accumulate LAS concentration of 50-100 mg/L without showing physiological changes. Previous studies conducted by [82], [84] and [85] respectively on the uptake LAS by *Chara vulgaris* L., *Lemna minor* L., *H. dubia* (Bl.) Backer and *Potamogeton perfoliatus* L. showed the potentiality of these plant in removing LAS (anionic surfactant) at moderate concentrations from water. Idris et. al., [194] evaluated and compared the removal ability of two emergent macrophytes, giant reed (*Arundo donax*) and Poaceae (*Phragmites australis*), in experimental subsurface flow, gravel-based constructed wetlands (CWs). Results showed that the BOD, total suspended solids (TSS), total phosphorus (TP), total nitrogen (TN), total ammoniacal nitrogen (TAN) and nitrate nitrogen (NO_3) removal in the *A. donax* and *P. australis* beds was 94%, 67%, 96%, 97%, 99.6%, and effectively 100% and 95%, 87%, 95%, 98%, 99.7%, and effectively 100%, respectively, with no significant difference in performance between the two aquatic plants. Tran et. al., [188] using *Canna generalis* (a common reed and easy to grow plant both in water and wet land conditions) to remove organic pollutants such as BOD_5, TSS, NH_4-N and PO_4-P from wastewater in two kinds of hybrid constructed wetlands viz Facultative pond combined with free watersub-surface constructed wetlands system and horizontal subsurface flow combined with Aerobic

pond system. Results showed that the ponds played an important role in the hybrid system performance and enhanced the performance of constructed wetlands. The pollutant removal efficiencies of the hybrid systems were all higher than the single constructed wetlands. The BOD_5, TSS, NH_4-N and PO_4-P removal efficiencies averaged 81%, 85%, 93% and 77%, respectively for the hybrid horizontal subsurface flow constructed wetlands system operated at a hydraulic loading rate of 0.075 m/day, while they were 89%, 97%, 97%, and 68%, respectively for the hybrid free water sub-surface constructed wetlands system operated at a hydraulic loading rate of 0.1 m/day. Yilmaz and Akbulut [199] reported a removal rate of 79 to 83% of BOD in effluent by *Lemna gibba*. Also, a removal rate of 94, 72, 63, 82, 82 and 82 % respectively for biochemical oxygen demand, ammonia, total suspended solids, total nitrogen, ammonium nitrate, and phosphate by duckweed in effluent was reported [57]. Blue dye and textile dyes were removed at a rate of 59.6 % and 10-96 % respectively by *L. minor,* indicating the plant can be very useful in textile industries to remediate effluents [203, 204], supported in further study by Neag *et al*. [205] using Toluidine Blue dye. The usefulness of duckweed for phytoremediation of wide range of organic pollutants has been extensively reviewed recently (see ref [57]). The review covers the state of duckweed application for the remediation of diverse aquatic pollutants including organic pollutants. The removal of diverse organic pollutants from aqueous solutions has been well demonstrated in many studies reviewed. Unfortunately, to the best of our knowledge, studies concerning the removal of POPs such as PCB and OCPs from aqueous solution are lacking.

5. Chemometrics for aquatic phytoremediation

The science of relating chemical data from chemical processes to state of system by applying mathematical or statistical methods/models is considered chemometrics [6]. It captures relationships between system variables and widely

used in environmental analytical research [6, 207]. Information from models is viewed as simplified concepts of environmental issues. Thereby making for easy understanding by policy makers, this way decisions on environmental issues are quickly arrived at [19, 21, 207-209]. Overall, in phytoremediation studies, chemometric models are used to assess plant performance after the experimental period. Commonly used models includes; Growth rate (GR), Growth rate inhibition (% Inhibition), Metal uptake (MU), translocation/transfer factor (TF), bioconcentration factor (BCF), Percent metal uptake (% MU), Removal capacity (RC) and Toxicity index (TI). These models are repeatedly used in aquatic phytoremediation studies of metals in aqueous medium [44, 48, 137, 139, 141, 146, 155-158, 165-168, 171-173, 175-177, 210-211] and can also be used in organic pollutant remediation studies. Growth rate (GR) value is an important index for predicting growth trends of plants used for remediation. GR is also referred to as relative growth rate (RGR). It was proposed by Fisher [212] and calculated using either equation (1) or (2), where DB_{AH} (g) and DB_{BP} (g) are the dry biomass after and before harvest, respectively, while TAH (days) and TBP (days) are the planting periods after and before harvest, measured over the study period. RGR stands for the relative growth rate (mg/g/d); $\ln(m_1)$: logarithm of the final dry mass (g); $\ln(m_0)$: logarithm of the initial dry mass (g); t_0: initial time (d); t_1: final time (d).

$$GR = \frac{DB_{AH} - DB_{BP}}{T_{AH} - T_{BP}} \quad (1)$$

$$RGR = \left(\frac{\ln(m_1) - \ln(m_0)}{t_1 - t_0}\right) * 1000 \quad (2)$$

The tolerance index (TI) was proposed by Wilkins [213]. It provides information regarding the tolerance of the plant to metal contamination in the solution; calculated using equation (3) as the ratio of growth rate of the plant in the solution contaminated to growth rate of the plant in the uncontaminated control solution. In the equation, RGR is the growth rate of the plant in the solution contaminated while RGR_c is the growth rate of the plant in the control solution, without contamination.

$$TI = \left(\frac{RGR}{RGR_c}\right) * 100 \quad (3)$$

Metal uptake (MU) shows the metal content in whole plant tissue or in a selected plant part; moreover, MU can be calculated by using equation (4): where C_{metal} (mg /kg or mg/L or any acceptable units) is the metal concentration in the plant tissue, and DB (g) is the dry biomass of the plant.

$$MU(g/plant) = C_{metal} * DB \quad (4)$$

The TF shows the efficiency of the plant to transport an element from the root to the shoot; and the BCF allows for evaluating the efficiency of the plant in accumulating the chemical element, taking into account its concentration in the medium or simply the ratio of concentrations of each metal in the roots to those in the water. Both the TF and BCF can be estimated according to equations (5) and (6) respectively [44, 211].

$$TF = \frac{C_{metal} \ in \ roots}{C_{metal} \ in \ shoots} \quad (5)$$

$$BCF = \frac{C_{metal} \ in \ plants}{C_{metal} \ in \ solution \ or \ medium} \quad (6)$$

The potential for metal uptake in plant tissue is shown by percent metal uptake (% MU); the uptake also corresponds with reduced metal concentration in solution. In addition, it can be calculated using Equation 7, where C_i and C_f are the initial and final metal concentrations in solution respectively.

$$\% \ MU = \left[\frac{(C_i - C_f)}{C_i}\right] * 100 \quad (7)$$

Removal capacity (RC) indicates the potential of plants for removing metal from solution over an entire study period and can be calculated using Equation 8; where RC is the removal capacity (mg/d/g), C_i and C_f remains as in Equation 6, V is the liquid volume (L), D (days) is the days, and B (g) is the mean dry biomass [49].

$$RC = (C_i - C_f) - VDB \quad (8)$$

Growth rate inhibition (% Inhibition) shows the extent of inhibition to growth of plant caused by the contaminant. % Inhibition can be calculated according equation (9), where variables remain the same as in equation (3).

$$\% \text{ Inhibition} = 1 - \left(RGR / RGR_c \right) \tag{9}$$

Rhizofiltration potential (RP) is based on adsorbed heavy metals by the aqueous system and inform on the performance of the plant to accumulate or remediate contaminants using roots. RP is calculated as equation (10), where, C is concentration of heavy metal; C_{leaves} is concentration of heavy metal in leaves; C_{roots} is concentration of heavy metal in roots; M is dry biomass yield, M_{total} is leaves and root biomass yield (g DW/m²/yr), M_{plant} is the mean of plant yield (g DW/m²/yr), M_{root} is the mean of root biomass yield (g DW/m²/yr), M_{leaves} is the mean of leaves biomass yield (g DW/m²/yr) (Rezania et al., 2016).

$$RP \, (mg/m^2 / year) = \left| \left(C_{leaves} * M_{leaves} \right) + \left(C_{root} * M_{root} \right) / M_{total} \right| * M_{plant} \tag{10}$$

However, in a batch or continuous flow system, the accumulation or absorption may be studied by using different sorption kinetics and isotherms models such as pseudo-first-order (PFO), pseudo-second-order (PSO), Freundlich, Langmuir and Temkin. Some of the models have significant limitations e.g PFO and PSO models, which only considers adsorption step on the active sites and predicts the internal diffusion while ignoring the external diffusion. In the use of Freundlich and Langmuir isotherms models, assumption is made that there is a local equilibrium between the contaminated aqueous medium and contaminant, an assumption that may be misleading [221]. However, they have been widely used in absorption studies [215-217] and recently used in phytoremediation studies [188, 205, 218-219]. The pseudo-first order kinetic equation and pseudo second order kinetic equation simply indicates if the reaction is more inclined towards physisorption or chemisorptions

depending on the closeness of regression coefficient value (r²) to unity (1). Furthermore, they represent the degradation rate of pollutants in the biological treatment system [188]. The kinetic equation for the pseudo-first order and pseudo second order can be calculated respectively following Equations 11 and 12: where Ce is the outflow concentration of metal at t day (d); C_i is the initial concentration of metal: and k is the first-order removal rate constant.

$$C_e = C_i * e^{-k.d} \tag{11}$$

$$d / C_e = 1 / k * C_e^2 + 1 / C_e * d \tag{12}$$

Langmuir adsorption equation is the very ubiqutes linear model for monolayer adsorption, and it is used to assess the adsorption process. Langmuir model can be calculated using Equation 13: where qL is the quantity of metal adsorbed per unit weight of sorbent (in this case, plant) and C_e is unadsorbed or outflow metal concentration remaining in water. Q corresponds to the maximum quantity of metal adsorbed per unit dry weight of the plant to form a complete monolayer on the surface and k is a constant associated with affinity of the binding site.

$$qL = \frac{Q * k * C_e}{1 + k * C_e} \tag{13}$$

Freundlich model explained adsorption onto a heterogeneous surface [219] as in Equation 14: where, C_e refers to solution equilibrium concentration (mg L⁻¹), q is the adsorption capacity (concentration of metal on adsorbing substrate, mg/kg), and k and (1/n) are constants connected to adsorption capacity.

$$q = k * C_e^{(1/n)} \tag{14}$$

Temkin isotherm model corresponds to a factor which is associated with explicitly taking into the account of sorbent-adsorbate interactions. Temkin model is given in Equation 15: where, q is the metal concentrations in the plant biomass (mg/kg), Ce corresponds to metal concentration (mg/L) remaining in outflow, B and kt are the constant

related to adsorption process [219].

$$q = Bln(kt) + Bln(C_e) \qquad (15)$$

The removal efficiency (RE %) of dye from aqueous solution in a batch study can be studied by equation (16) while the amount of dye in the plant phase can be calculated using equation (17); where q_e is the amount of dye adsorbed per gram of adsorbent at equilibrium (mg/g), C_0 and C_e are the initial and equilibrium concentrations of the dye in solution (mg/L); V is the volume of solution (mL); m is the weight of the adsorbent (plant) (g) [205].

6. Conclusion, Knowledge gap, and Future Areas of Research

Water resources management and protection from toxic chemicals pollution due to anthropogenic activities is of critical concern to scientist, governmental and non-governmental organizations and the general public. Phytoremediation is largely accepted and desirable to several conventional methods for the treatments of water pollution. Many aquatic plants (emerging, submerged or free flowing) have been applied extensively recently and mostly conducted using hydroponics or field experiment by constructed wetlands. Results from literature reviewed have generally established the effectiveness in remediating organic pollutants and heavy metals by aquatic plants, although heavy metals have been extensively studied than organic pollutants. Most commonly used plant include; duckweed (*L. minor*), water hyacinth (*Eichhornia crassipes*) and water lettuce (*P. stratiotes*), due to their ubiquitous nature, invasive mechanism, sporadic reproductive capacity, bioaccumulation potentials and resilience in polluted environment [57]. Heavy metals consider as water pulltant and must be removal from waters and reviers [223-226]. However, the removal rates are varied and mainly controlled by the physicochemical properties of the water, contaminants, plant and the experimental framework. Using modeling and interpretation of adsorption isotherms for performance assessment is particularly good and increases level of accuracy obtained from adsorption processes of

contaminant on plant. Despite the promising efforts so far, there are still limitations in certain areas to demonstrate the effectiveness of the aquatic plant in phytoremediation of chemical pollutants.

7. Knowledge gap and Future Areas of Research

(1) A need is there for studying the plant in the face of emerging chemicals (e.g polychlorinated dibenzo-*p*-dioxins and polychlorinated dibenzo-furans (PCDD/Fs) etc) which defy conventional remediation approaches for establishing acceptable remediation strategies and ecological benchmark for improvement of constructed wetlands for wastewater effluents treatment [57]. Some other priority organic pollutants such as 1,2,3-trichloro-benzene, pyrene, 1,3-Dinitrobenzene, lindane, and 2,4-Dinitrotoluene have been removed in terrestrial environment by terrestrial plant [220] while studies are lacking for their removal in aquatic environment. Therefore, there is need for an extensive study of aquatic plant for removal of these types of organic pollutants. (3) More studies are required to understand better the precise transfer pathways of pollutants and their temporal pattern, in order to pinpoint toxicity more precisely in aquatic plants. Such studies will generate an improved understanding which will help in controlling cumulative toxic effects of pollutants on plants and enhancing the role of aquatic plants as a vital ecological based bioremediation agent for water pollution.

8. Conflicts of interest

The researchers declares no conflicts of interest regarding the publication of this manuscript

9. References

[1] United States Geological Survey (USGS), Ground Water and Surface Water: A Single Resource, Circular, (1998) 1139.

[2] T. Zhang, Q. Lu, C. Su C., Y. Yang, D. Hu, Q. Xu, Mercury induced oxidative stress, DNA damage, and activation of antioxidative system and Hsp70 induction in duckweed (*Lemna minor*), Ecotox. Environ. Safe., 143 (2017) 46-56.

[3] C. Jiang, H. Chen, Y. Zhang, H. Feng, M.A. Shehzad, Y. Wang, T. Xu, Complexation electrodialysis as a general method to simultaneously treat wastewaters with metal and organic matter, Chem. Eng. J., 348 (2018) 952–959.

[4] M.N.V Prasad, Aquatic Plants for Phytotechnology, (2006) 259-274.

[5] C.F. Carolin, P.S. Kumar, A. Saravanan, G.J. Joshiba, Mu Naushad, Efficient techniques for the removal of toxic heavy metals from aquatic environment: a review, J. Environ. Chem. Eng., 5 (2017) 2782–2799.

[6] C.E. Enyoh, A.W. Verla, N.J. Egejuru, pH variations and chemometric assessment of borehole water in Orji, Owerri Imo State, Nigeria, J. Environ. Anal. Chem., 5 (2018) 1-9.

[7] CDC, Global WASH Fast Facts. Global Water, Sanitation, & Hygiene (WASH), (2016). https://www.cdc.gov/healthywater/global/wash_statistics.html Accessed 30/7/2019.

[8] World Health Organization and UNICEF, Meeting the MDG Drinking Water and Sanitation Target: The urban and rural challenge of the decade, 2006, 1-47. https://www.who.int/water_sanitation_health/monitoring/jmpfinal.pdf

[9] Z. J. Xu, Y. Cao, Y. Zhang, Z. Yuan, Z. Lou, X. Xu, X. Wang, A review of functionalized carbon nanotubes and graphene for heavy metal adsorption from water: preparation, application, and mechanism, Chemosphere, 195 (2018) 351–364.

[10] L. K. Charity, V. A. Wirnkor, A.C. Emeka, A.A. Isioma, C.E. Ebere, Health risks of consuming untreated borehole water from uzoubi umuna orlu, Imo State Nigeria, J. Environ. Anal. Chem., 5 (2018) 250-264.

[11] A. Bhatnagar, M. Sillanpaa, Utilization of agro-industrial and municipal waste materials as potential adsorbents for water treatment, Chem. Eng. J., 157 (2010) 277–296.

[12] E. Padilla-Ortega E., R. Leyva-Ramos, J.V. Flores-Cano, Binary adsorption of heavy metals from aqueous solution onto natural clays, Chem. Eng. J., 225 (2013) 535–546.

[13] A.W. Verla, E. N. Verla, C.E. Amaobi, C.E. Enyoh, Water pollution scenario at river uramurukwa flowing through owerri metropolis, Imo State, Nigeria, Inter. J. Appl. Sci. Res., 3 (2018) 40-46.

[14] K. H. Vardhan, S. K. Ponnusamy, C.P. Rames, A review on heavy metal pollution, toxicity and remedial measures: Current trends and future perspectives, J. Mole. Liq., 290 (2019) 111-197.

[15] L. West, World Water Day: A Billion people worldwide lack safe drinking water, 2018. http://environment.about.com/od/environmentalevents/a/waterdayqa.htm

[16] D.H. Pink, Investing in Tomorrow's Liquid Gold., 2019. https://web.archive.org/web/20060423172532/https://finance.yahoo.com/columnist/article/trenddesk/3748

[17] K. Kelland, Study links pollution to millions of deaths worldwide, 2017. https://www.reuters.com/article/us-health-pollution/study-links-pollution-to-millions-of-deaths-worldwide-idUSKBN1CO39B .

[18] L. Järup, Hazards of heavy metal contamination. Br. Med. Bull. 68 (2003) 167–182.

[19] E.N. Verla, A.W. Verla, C.E. Enyoh, Pollution assessment models of soils in portharcourt city, rivers state, Nigeria. World News Nat. Sci., 12 (2017) 1-23.

[20] A. W. Verla, C. E. Enyoh, E. N. Verla, Microplastics, an emerging concern: a review of analytical techniques for detecting and quantifying microplatics, Anal. Method. Environ. Chem. J., 2 (2019) 15-32. https://doi.org/10.24200/amecj

[21] A.W. Verla, E.N. Verla, C.E. Enyoh, K. Leizou, N.O. Peter, Using physicochemical properties in assessment of river water for consumption and irrigation in Nigeria, Eurasian J. Anal. Chem., 5(2019) 14-23.

[22] R. S. Boyd, Heavy metal pollutants and chemical ecology: exploring new frontiers, J. Chem. Ecol., 36 (2010) 46-58.

[23] LH. Gade, Highly polar metal-metal bonds in "early-late" heterodimetallic complexes. Angew. Chem. Int. Ed., 39 (2000) 2658–2678.

[24] K.V. Ragnarsdottir, D. Hawkins, Trace metals in soils and their relationship with scrapie occurrence, Geochim. Cosmochim. Acta, 69 (2005) 196–196.

[25] M.I. Lone, Z. He, P.J. Stoffella, X. Yang, Phytoremediation of heavy metal polluted soils and water: Progresses and perspectives, J. Zhej. Uni. Sci. B, 9 (2008) 210-220.

[26] J. Yabe, I. Mayuni, U. Takashi, Current levels of heavy metal pollution in Africa. J. Vet. Med. Sci., 72 (2010) 1257–1263.

[27] J.D. Appleton, M.R. Cave, B. Palumbo-Roe, J. Wragg, Lead bioaccessibility in top soils from lead mineralization and urban domains, UK. Environ.

Pollut., 178 (2013) 278-287.

[28] J.B. Diatta, W. Grzebisz, Simulative evaluation of Pb, Cd, Cu, and Zn transfer to humans: The case of recreational parks in Poznan, Poland. Pol. J. Environ. Stud., 20 (2011) 1433-1440.

[29] C. E. Enyoh, A.W. Verla, E.N. Verla, Uptake of microplastics by plant: a reason to worry or to be happy, World Sci. News, 131 (2019) 256-267.

[30] EEA report, Heavy metal emissions, Eur. Environ. Agency, (2019).

[31] M. van het Bolcher, H. Denier van der Gon, B.J. Groenenberg, I. Ilyin, G.J. Reinds, J. Slootweg, O. Travnikov, A. Visschedijk, W. de Vries, Heavy metal emissions, depositions, critical loads and exceedances in Europe-J.P. Hettelingh - J. Sliggers. VROM-DGM, Directie Klimaatverandering en Industrie, IPC 650, (2006) P.O. Box 20951, 2500 EZ Den Haag, Netherlands.

[32] Wang F., Kuehr R., Ahlquist D., Li J. E-waste in China: A country report; United Nations University, (2019). https://collections.unu.edu/ eserv/UNU:1624/ewaste-in-china.pdf.

[33] W. Barabasz, D. Albinska, M. Jaskowska, J. Lipiec, Ecotoxicology of aluminium. Pol. J. Environ. Stud., 11 (2002) 199–203.

[34] R. Grazuleviciene, R. Nadisauskiene, J. Buinauskiene, T. Grazulevicius, Effects of elevated levels of manganese and iron in drinking water on birth outcomes, Pol. J. Environ. Stud., 18 (2009) 819–825.

[35] M. Jaishankar, T. Tseten, N. Anbalagan, B.B. Mathew, K.N. Beeregowda Toxicity, mechanism and health effects of some heavy metals. Interdiscip. Toxicol., 7 (2014) 60–72.

[36] S. Martin, W. Griswold, Human health effects of heavy metals, Environ. Sci. Tech. Briefs Citizens 15 (2009) 1–6.

[37] C. B. de Souza, G.R. Silva, Phytoremediation of effluents contaminated with heavy metals by floating aquatic macrophytes species. Intertech Open book, (2019). http://dx.doi.org/10.5772/ intechopen.83645

[38] N. Sooksawat, M. Meetam, M. Kruatrachue, P. Pokethitiyook, K. Nathalang, Phytoremediation potential of charophytes: bioaccumulation and toxicity studies of cadmium, lead and zinc, J. Environ. Sci., 25(3) (2013) 596–604

[39] F.E.C. Sneller, L.M. van Heerwaarden, H. Schat, Toxicity, metal uptake, and accumulation of phytochelatins in silene vulgaris exposed to mixtures of cadmium and arsenate, Environ.

Toxicol. Chem., 19 (2000) 2982-2986.

[40] G. Brunetto, Heavy metals in vineyards and orchard soils. Revista Brasileira de Fruticultura, Jaboticabal. 39 (2017) e-263.

[41] F.V. de Campos, J. A. de Oliveira, A.A. da Silva, C. Ribeiro, F. F. dos Santos, Phytoremediation of arsenite-contaminated environments: is *Pistia stratiotes* L. a useful tool, Ecological Indicators 104 (2019) 794–801

[42] S. Jasrotia, K. Arun, M. Aradhana, Performance of aquatic plant species for phytoremediation of arsenic-contaminated water, Appl. Water Sci. 7 (2017) 889–896.

[43] S.H. Hasan, M. Talat, S. Rai, Sorption of cadmium and zinc from aqueous solutions by water hyacinth (Eichchornia crassipes), Bioresour. Technol. 98 (2007) 918–928

[44] L.Q. Ma, K.M. Komar, C. Tu, W. Zhang, Y. Cai, E.D. Kennely, A fern that hyperaccumulates arsenic, Nature, 409 (2001) 579.

[45] W. Samuel, B. Richard, E. Helen, L. Darkwah, Assessment of typha capensis for the remediation of soil contaminated with As, Hg, Cd and Pb, Environ. Monit. Assess., 191 (2019) 346. https:// doi.org/10.1007/s10661-019-7484-2

[46] S. Radic, M. Babic, D. Sˇkobic, V. Roje, B. Pevalek-Kozlina, Ecotoxicological effects of aluminium and zinc on growth and antioxidants in *Lemna minor* L, Ecotoxicol. Environ. Safe. 73 (2010) 336-342.

[47] J. Razinger, M. Dermastia, J.D. Koce, A. Zrimec, Oxidative stress in duckweed (Lemna minor L.) caused by short-term cadmium exposure, Environ. Pollut. ,153 (2008) 687-694.

[48] H. Li, F. Cheng, A. Wang, T. Wu, Cadmium removal from water by hydrophytes and its toxic effects, Proceeding of the international symposium of phytoremediation and ecosystem health, Hangzhou, China, (2005).

[49] T. Sricoth, W. Meeinkuirt, P. Saengwilai, J. Pichtel, P. Taeprayoon, Aquatic plants for phytostabilization of cadmium and zinc in hydroponic experiments, Environ. Sci. Pollut. Res. 25 (2018) 14964-14976. https://doi.org/10.1007/s11356-018-1714-y

[50] C. Jung-Chun, W. Kai-Sung, H. Chen, C. Lu, L. Huang, H. Li, T. Peng, S. Chang, Phytoremediation of Cr(III) by *Ipomonea aquatica* (water spinach) from water in the presence of EDTA and chloride: Effects of Cr speciation, Bioresour. Technol., 101 (2010) 3033–3039.

[51] M. Marcia, A. Christiane, R. Chafim, S. Jonatas,

Technical challenges and social, economic and regulatory barriers to phytoremediation of contaminated soils, Rev. Bras. Ciênc. Solo., 35 (2011) 1-11.

[52] G.A Leao, J.A. de Oliveira, R.T.A. Felipe, F.S. Farnese, G.S. Gusman, Anthocyanins, thiols, and antioxidant scavenging enzymes are involved in Lemna gibba tolerance to arsenic, J. Plant Interact., 9 (2014) 143-151.

[53] K. Jayakumar, M. Rajesh, L. Baskaran, P. Vijayarengan, Changes in nutritional metabolism of tomato (Lycopersicon esculantum Mill.) plants exposed to increasing concentration of cobalt chloride, Int. J. Food Nut. Safe., 4 (2013) 62–69.

[54] K. Jayakumar, C. A. Jaleel, M. M. Azooz, Phytochemical changes in green gram (Vigna radiata) under cobalt stress, Global J. Mol. Sci., 3 (2008) 46–49.

[55] K. Jayakuma, C. A. Jaleel, and P. Vijayarengan, Changes in growth, biochemical constituents, and antioxidant potentials in radish (Raphanus sativus L.) under cobalt stress, Turkish J. Biol., 31, 3 (2007) 127–136.

[56] W. Drost, M. Matzke, T. Backhaus, Heavy metal toxicity to Lemna minor: studies on the time dependence of growth inhibition and the recovery after exposure, Chemosphere, 67 (2007) 36-43.

[57] O. E. Abraham, F.D. Sikoki, E. O. Nwachukwu, Application of common duckweed (Lemna minor) in phytoremediation of chemicals in the environment: state and future perspective, Chemosphere 223 (2019) 285-309.

[58] A.W. Verla, E.N. Verla, C.E. Enyoh, Petroleum hydrocarbons and heavy metals risk of consuming fish species from oguta lake, Imo State, Nigeria, 6th International Science Congress, ISCA-ISC-8EVS-08-Poster, Pune, Maharastra, India, (2016).

[59] L. E. Okoumassoun, C. Brochu, C. Deblois, S. Akponan, M. Marion, D. Averill-Bates, F. Denizeau, Vitellogenin in tilapia male fishes exposed to organochlorine pesticides in Ouémé river in republic of Benin, Sci. Total Environ., 299 (2002) 163–172.

[60] H.B. Moon, H.S. Kim, M. Choi, H.G. Choi, Intake and potential health risk of polycyclic aromatic hydrocarbons associated with seafood consumption in Korea from 2005 to 2007. Arch. Environ. Contam. Toxicol., 58(1) (2010) 214–221.

[61] I. Tolosa, S.J. de Mora, S.W. Fowler, J.P. Villeneuve, J. Bartocci, C. Cattini, Aliphatic and aromatic hydrocarbons in marine biota and coastal sediments

from the Gulf and the Gulf of Oman , Mar. Pollut. Bull.,50 (2005) 1619-1633.

[62] M.A. Al-kahtani, Accumulation of Heavy metals in Tilapia fish (Oreochromisniloticus) from Al-khadoud spring, Al-Hassa, Saudi Arabia, Am. J. Appl. Sci., 6 (2009) 2024- 2029.

[63] P. A. Sreedevi, B. Suresh, B. Siraramkrishna, B. Prebhavarhi, K. Radhakrishriaiah, Bioaccumulation of Nickel in organs of the fresh water fish, Cyprinocarpio and the fresh water mussel Lamethdeimarginalis under lethal and sublethal nickel stress, Chemosphere, 24 (1992) 29-36.

[64] S.P. Kumar, J.K.P. Edward, Assessment of metal concentration in the sediment cores of Manakudy estuary, south west coastal of India, Indian J. Mar. Sci., 38 (2009) 235-248.

[65] C.E. Enyoh, E.A. Ihionu, A. W. Verla, N.P. Ebosie, Physicochemical Properties of Palm Oil and Soil from Ihube Community, Okigwe, Imo State, Nigeria, Int. Letter. Nat. Sci., 62 (2017) 35-49.

[66] A.W. Verla, E. N. Verla, C.M. Ajero, K.C. Lele, N.O. Stellamarris, C.E. Enyoh, Biomonitoring of heavy metals in blood and urine of African children from Owerri Metropolis, Eastern Nigeria, J. Chem. Health Risks, 9 (2019) 11-26.

[67] ATSDR, Toxicological Profile for Cadmium. CAS#: 7440-43-9. (2012) https://www.atsdr.cdc.gov/toxprofiles/tp.asp?id=48&tid=15

[68] ATSDR, Toxicological Profile for Chromium. CAS#: 7440-47-3 (2012). https://www.atsdr.cdc.gov/toxprofiles/tp.asp?id=62&tid=17

[69] ATSDR, Toxicological Profile for Cobalt. CAS#: 7440-48-4 (2004). https://www.atsdr.cdc.gov/toxprofiles/tp.asp?id=373&tid=64

[70] ATSDR, Toxicological Profile for Copper. CAS#: 7440-50-8 (2004). https://www.atsdr.cdc.gov/toxprofiles/tp.asp?id=206&tid=37

[71] ATSDR, Toxicological Profile for Nickel. CAS# 7440-67-2. (2005). https://www.atsdr.cdc.gov/toxprofiles/tp.asp?id=245&tid=44

[72] ATSDR, Toxicological Profile for Lead. CAS# 7439-92-1. (2019). https://www.atsdr.cdc.gov/ToxProfiles/tp.asp?id=96&tid=22

[73] ATSDR, Toxicological Profile for Zinc. CAS#: 7440-66-6 (2005). https://www.atsdr.cdc.gov/toxprofiles/tp.asp?id=302&tid=54

[74] N.D. Bedding, A.E. McIntyre, R. Perry, J.N. Lester, Organic contaminants in the aquatic environment I, Sources and occurrence, Sci. Total Environ., 25

(1982) 143–167.

[75] A.G. Burton, R. Pitt, Stormwater Effects Handbook: A Toolbox for Watershed Managers, Scientists, and Engineers, New York: CRC/Lewis Publishers, Chapter 2, (2001).

[76] Anonymous, Text of the stockholm convention, Amended in 2009, 2011, 2013 and 2015, (2008). http://chm.pops.int/TheConvention/Overview/TextoftheConvention/tabid/2232/Default.aspx

[77] A. David, M. Christiana, D. Godfred, J.W. Johan, S. Bjame, C.A. Robert, Uptake of antibiotics from irrigation water by plants, Chemosphere, 157 (2016) 107–114.

[78] E.M. Dettenmaier, W.J. Doucette, B. Bugbee. Chemical hydrophobicity and uptake by plant roots, Environ. Sci. Technol., 43 (2009) 324–329.

[79] M. Trapp, C. McFarlane, Plant contamination, Lewis Publisher, Boca Raton (1995).

[80] M.N.V. Prasad, A State-of-the-Art report on bioremediation, its applications to contaminated sites in India, ministry of environment & forests, government of India, Indian national science academy (2011). http://soilhealth.ucdavis.edu/application/files/2015/4207/9078/BioremediationBook.pdf

[81] Z. Cheng, F. Yao, L. Yuan-wang, C. Hui-qing, L. Zhao-jun, X. Jian-ming, Uptake and translocation of organic pollutants in plants: A review, J. Integr. Agric., 16 (2017) 1659–1668.

[82] N. Liu, Z. Wu, Toxic effects of linear alkylbenzene sulfonate on *Chara vulgaris* L, Environ. Sci. Pollut. Res., 25 (2018) 4934-4941.

[83] Z. Wang, J. Zhang, L. Song, E. Li, X. Wang, B. Xiao, Effects of linear alkylbenzene sulfonate on the growth and toxin production of *Microcystis aeruginosa* isolated from Lake Dianchi, Environ. Sci. Pollut. Res., 22 (2015) 5491-5499.

[84] Z. Wu, D. Yu, J. Li, G. Wu, X Niu, Growth and antioxidant response in *Hydrocharis dubis* (Bl.) Backer exposed to linear alkylbenzene sulfonate, Ecotoxic.,19: (2010) 761-769.

[85] J. Zhou, Z. Wu, D. Yu, Y. Pang, H. Cai, Y. Liu, Toxicity of linear alkylbenzene sulfonate to aquatic plant *Potamogeton perfoliatus* L, Environ. Sci. Pollut. Res., 25 (2018) 32303-32311.

[86] W. Wang, R. Li, Q. Zhu, X. Tang, Q. Zhao, Transcriptomic and physiological analysis of common duckweed *Lemna minor* responses to NH^{4+} toxicity, BMC Plant Biol., 16:92 (2016)1-13.

[87] S. Bayen, G.O. Thomas, H.K. Lee, E.L.Yong, J.P. Obbard, Occurrence of PCBs and PBDEs in green mussels (Perna viridis) sampled from Singapore's coastal waters, Environ. Toxicol. Chem., 22 (2003) 2432–2437.

[88] S. Bayen, Y.H. Gong, H.S. Chin, H. K. Lee, E.L. Yong, E. L., J.P. Obbard, Determination of polybrominated diphenyl ethers (PBDEs) in marine biological tissues using microwave assisted extraction (MAE), J. Chromatogr. A, 1035 (2004) 291–294.

[89] . Bayen, Y.H. Gong, H.S. Chin, H. K. Lee, E.L. Yong, E. L., J.P. Obbard, Organochlorine pesticides and heavy metals in green mussel, Perna viridis, in Singapore, Water Air Soil Pollut., 155 (2004) 103–116.

[90] Bayen, Y.H. Gong, H.S. Chin, H. K. Lee, E.L. Yong, E. L., J.P. Obbard,. Androgenic and estrogenic response of green mussel extracts from Singapore's coastal environment using a human cellbased bioassay, Environ. Health Perspect., 112 (2004) 1467–1471.

[91] S. Karups, S. Annamalai, J.P. Obbard, Barnacle, attached to the bottle-nose dolphin, Xenobalanus globicipitis (Cirripedia, Coronulidae), Tursiops truncatus (Mammalia, Cetacea) on the southeastern coast of India, J. Crustaceana, 77 (2004) 879–882.

[92] S. Karups, S. Annamalai, J.P. Obbard, Organochlorine residues in marine mammals from the southeast coast of India, Chemosphere, 60 (2004) 891–897.

[93] D. Yahia, E.E. Elsharkawy, Multi pesticide and PCB residues in Nile tilapia and catfish in Assiut city, Egypt, Sci. Total Environ., 466- 467 (2014) 306–314.

[94] Q. Q. Li , A. Loganath, Y.S. Chong, J. Tan, J.P. Obbard, Persistent Organic Pollutants and Adverse Health Effects in Humans, J. Toxicol. Environ. Health Part A, 69 (2006) 1987-2005

[95] S. Safe, Toxicology, structure-function relationship, and human and environmental health impacts of polychlorinated biphenyls: progress and problems, Environ. Health Perspect., 100 (1993) 259-268.

[96] K. Frische, J. Schwarzbauer, M. Ricking, Structural diversity of organochlorine compounds in groundwater affected by an industrial point source, Chemosphere., 81 (2010) 500-8.

[97] W. Brack, H.J. Klamer, M. López de Alda, D. Barceló, Effect-directed analysis of key toxicants in European river basins a review, Environ Sci. Pollut. Res. Int., 14 (2007) 30-38.

[98] E. T. Pawłowicz, Organic pollution of water and human health, Health Problems Civilization, 1 (2017) 32–39.

[99] D. Skutlarek, M. Exner, H. Färber, Perfluorinated surfactants in surface and drinking waters, Environ. Sci. Pollut. Res. Int., 13 (2006) 299-307.

[100] G.C. Windham, D. Lee, P. Mitchell, M. Anderson, M. Petreas, B. Lasley, Exposure to organochlorine compounds and effects on ovarian function. Epidemiol., 16 (2005) 182–190.

[101] R. W. Bretveld, M. Hooiveld, G.A. Zielhuis, A. Pellegrino, I.A. van Rooij, N. Roeleveld, Reproductive disorders among male and female greenhouse workers. Reprod. Toxicol., 25 (2008) 107–114.

[102] J. P. Arrebola, H. Belhassen, F. Artacho-Cordón, R. Ghali, H. Ghorbel, H. Boussen, F. Perez-Carrascosa, J. Expósito, A. Hedhili, N. Olea, Risk of female breast cancer and serum concentrations of organochlorine pesticides and polychlorinated biphenyls: a case-control study in Tunisia, Sci. Total Environ., 520 (2015) 106–113.

[103] Y. Liua, N. Liua, Y. Zhoub, F. Wangb, Y. Zhangb, Z. Wua, Growth and Physiological Responses in Myriophyllum spicatum L. Exposed to Linear Alkylbenzene Sulfonate, (2019). Doi:10.1002/etc.4475

[104] UNEP (Undated), Phytoremediation: An environmentally sound technology for pollution prevention, control and redmediation, an introductory guide to decision-makers, newsletter and technical publications freshwater management series No. 2, United Nations environment programme division of technology, industry, and economics, (2019). http://www.unep.or.jp/Ietc/Publications/Freshwater/FMS2/1.asp , Assessed 18/8/2019

[105] R.R. Brooks, M.F. Chambers, L.J. Nicks, B.H. Robinson, Phytomining, Trends Plant Sci., 3 (1998) 359–362.

[106] Ernst, W.H.O., Bioavailability of heavy metals and decontamination of soil of soil plants, App. Geochem., 11 (1996) 163–167.

[107] A.W. Erakhrumen, Phytoremediation: an environmentally soundtechnology for pollution prevention, control andremediation in developing countries, Edu. Res. Review, 2 (2007) 151-156.

[108] M. Ghosh, S.P. Singh, A review on phytoremediation of heavy metals and utilization of its byproducts, Appl. Ecol. Environ. Res., 3 (2005) 1-18.

[109] USEPA, Treatment technologies for site cleanup: annual status report (12th Edition), Tech. Rep. EPA-542-R-07-012, Solid Waste and Emergency Response (5203P), Washington, DC, USA, (2007).

[110] M. Kuperberg, G. Banuelos, R.L. Chaney, M. Coia, S. Dushenkov, G. Hulet, R. Kristich, M. Kucharski, M. Lasat, S. Lee, Y.M. Li, K. Rose, N. Terry, Removal from soil report, Proceedings from the workshop on phytoremediation of inorganic contaminants, Argonne Natl. Lab, Chicago, IL., (1999).

[111] M.M. Lasat, Phytoextraction of toxic metals: a review of biological mechanisms, J. Environ. Quality, 31 (2002) 109–120.

[112] J. Vymazal, The use of hybrid constructed wetlands for wastewater treatment with special attention to nitrogen removal: A review of recent development, Water Res., 47 (2013) 4795–4811.

[113] Y.K. Kumar, N. Gupta, A. Kumar, L.M. Reece, N. Singh, S. Rezania, S. A. Khan, Mechanistic understanding and holistic approach of phytoremediation: A review on application and future prospects, Ecol. Eng., 120 (2018) 274–298.

[114] P.J.C. Favas, J. Pratas, N. Rodrigues, R. D'Souza, M. Varun, M.S. Paul, Metal (loid) accumulation in aquatic plants of a mining area: potential for water quality biomonitoring and biogeochemical prospecting, Chemosphere, 194 (2018) 158–170.

[115] USDA, The PLANTS Database, National Plant Data Team, NRCS, United States Department of Agriculture, Greensboro, NC 27401-4901 USA, (2018). http://plants.usda.gov

[116] E. Aksorn, P. Visoottiviseth, Selection of Suitable Emergent Plants for Removal of Arsenic from Arsenic Contaminated Water, Sci. Asia, 30 (2004) 105-113.

[117] M.N.V. Prasad, M. Greger, P. Aravind, Biogeochemical cycling of trace elements by aquatic and wetland plants: relevance to phytoremediation. In: Prasad MNV, Sajwan KS, Naidu R (eds), Trace elements in the environment: Biogeochemistry, Biotechnology and Bioremediation. CRC Press, Florida, USA, Taylor and Francis, Chap 24, 443-474 (2005).

[118] M.N.V. Prasad, M. Greger, B.N. Smith, Aquatic macrophytes, in metals in the environment: Analysis by biodiversity, Prasad MNV (ed) Marcel Dekker Inc., New York, 259 (2001).

[119] T.G. Sors, D.R. Ellis, D.E. Salt, Selenium uptake, translocation, assimilation and metabolic fate in plants, Photosynth. Res., 86 (2005) 373–389.

[120] X.Yu, J. Gu, Phyto-transport and assimilation of selenium, plant-based remediation processes, Springer, 159-175 (2013). https://doi.org/10.1007/978-3-642-35564-6_9

[121] J. Kania, M. Hannigan, T.E. Kujundzic, Phytoremediation, *Halifax*, *Canada*, 1-7 (2002). http://www.colorado.edu/MCEN/EnvTox/Phytoremedy.pdf

[122] HCSM, Constructed Stormwater Wetlands, Pervious Pavement. Horry County Stormwater Management,(2016). http://stormwater.horrycounty.org/Home/LowImpactDevelopment/ConstructedStormwaterWetlands.aspx . Accessed 6/9/2019.

[123] D.C. Adriano, W.W. Wenzel, J. Vangronsveld, N.S. Bolan, Role of assisted natural remediation in environmental cleanup, Geoderma, 122 (2004) 121-142.

[124] M.N.V. Prasad, Heavy metal stress in plants: from biomolecules to ecosystems, Narosa Publishing House, New Delhi, 2nd Ed., 462, 2004.

[125] P. K. Rai, Heavy metal pollution in aquatic ecosystems and its phytoremediation using wetland plants: An ecosustainable approach, I. J. Phytoremed., 10 (2008) 133-160.

[126] I.T. Cousins, D. Mackay, Strategies for including vegetation compartments in multimedia models, Chemosphere, 44 (2001) 643-654.

[127] J. Fismes, G.C. Perrin, B.P. Empereur, J.L. Morel, Soil-to-root transfer and translocation of polycyclic aromatic hydrocarbons by vegetables grown on industrial contaminated soils, J. Environ. Quality, 31 (2002) 1649–1656.

[128] C. Moeckel, G. Thomas, J.L. Barber, K.C. Jones, Uptake and storage of PCBs by plant cuticles. Environ. Sci. Technol., 42 (2008)100-105.

[129] J. Y. Liu, L.S. Jerald, Uptake and translocation of lesser-chlorinated polychlorinated biphenyls (PCBs) in whole hybrid poplar plants after hydroponic exposure, Chemosphere, 73 (2008)1608–1616.

[130] X. Hua, M. Li, Y. Su, D. Dong, Z. Guo, D. Liang, The degradation of linear alkylbenzene sulfonate (LAS) in the presence of light and natural biofilms: The important role of photosynthesis, J. Hazard. Mater., 229 (2012) 450-454.

[131] K. Bhaskaran, V. Nadaraja, S. Tumbath, B. Shah, G. P. Veetil, Phytoremediation of perchlorate by free floating macrophytes, J. Hazard. Mater., 260 (2013) 901–906.

[132] Öztürk M, Ashraf M, Aksoy A, Ahmad M S A, Hakeem K R, eds., Plants, pollutants and remediation, Springer Netherlands, USA, 241-305, 2015.

[133] Y. Uysal, F. Taner, Effect of pH, temperature, and lead concentration on the bioremoval of lead from water usingLemna minor, Int. J. Phytoremed., 11 (2009) 591–608.

[134] Y. Uysal, Removal of chromium ions from wastewater by duckweed, Lemna minor L. by using a pilot system with continuous flow, J. Hazard. Mater., 263 (2013) 486–492.

[135] V.A. Nzengung, C.H. Wang, G. Harvey, Plant-mediated transformation of 329 perchlorate into chloride, Environ. Sci. Technol,. 33 (1999) 1470–1478.

[136] S. Alvarado, M. Guédez, M.P. Lué-Merú, G. Nelson, A. Alvaro, A.C. Jesús, Z. Gyula, Arsenic removal from waters by bioremediation with the aquatic plants Water Hyacinth (*Eichhornia crassipes*) and Lesser Duckweed (*Lemna minor*), Bioresour. Technol., 99 (2008) 8436-8440.

[137] M. Sasmaz, E. Obek, A. Sasmaz, Bioaccumulation of uranium and thorium by *Lemna minor* and *Lemna gibba* in Pb-Zn-Ag tailing water, Bull. Environ. Contam. Toxicol., 97 (2016) 832-837.

[138] A. Sandhi, T. Landberg, M. Greger, Phytofiltration of arsenic by aquatic moss (Warnstorfia fluitans), Environ. Pollut., 237 (2017) 1098-1105.

[139] F. Tufaner, Post-treatment of effluents from UASB reactor treating industrial wastewater sediment by constructed wetland, Environ. Technol., (2018) accepted manuscript.

[140] B. Boonyapookana, E. S. Upatham, M. Kruatrachue, P. Pokethitiyook, S. Singhakaew, *Phytoaccumulation and Phytotoxicity of Cadmium and Chromium in Duckweed Wolffia globose,* Int. J. Phytoremed., 4 (2002) 87–100.

[141] D. Baldantoni, A. Alfani, P. Di Tommasi, G. Bartoli, A. V. De Santo, Assessment of macro and microelement accumulation capability of two aquatic plants, Environ. Pollut.,130 (2004) 149–156.

[142] X. Lu, M. Kruatrachue, P. Pokethitiyook, K. Homyok, Removal of cadmium and zinc by water hyacinth, Sci. Asia, 30 (2004) 93–103.

[143] A. Basile, S. Sorbo, B. Conte, R.C. Cobianchi, F. Trinchella, C. Capasso, V. Carginale, Toxicity, Accumulation, and removal of heavy metals by three aquatic macrophytes, Int. J. Phytorem., 14

(2012) 374-387.

[144] D. Chaudhuri, A. Majumder, A.K. Misra, K. Bandyopadhyay, Cadmium removal by Lemna minor and Spirodela polyrhiza, Int. J. Phytorem., 16 (2013) 1119-1132.

[145] F. Hadi, A. Ahmad, N. Ali, Cadmium (Cd) removal from saline water by Veronica anagallis and Epilobium laxum in hydroponic system, Sci. Res., 14 (2014) 935–944.

[146] H. Vaseem, T.K. Banerjee, Efficacy of phytoremediation technology in decontaminating the toxic effluent released during recovery of metals from polymetallic sea nodules, Int. Aquat. Res., 7 (2015) 17-26.

[147] E.Ü. Tunca, K. Terzioğlu, H. Türe, The effects of alginate microspheres on phytoremediation and growth of Lemna minor in the presence of Cd, Chem. Ecol., 33 (2017) 1-17.

[148] E. Amare, F. Kebede, W. Mulat, Wastewater treatment by *Lemna minor* and *Azolla filiculoides* in tropical semiarid regions of Ethiopia, Ecolog. Eng., 120, (2018) 464-473.

[149] Q. Lu, T. Zhang, W. Zhang, C. Su, Y. Yang, D. Hu, Q. X u, Alleviation of cadmium toxicity in Lemna minor by exogenous salicylic acid, Ecotoxicol. Environ. Saf., 147, (2018) 500-508.

[150] A. Shirinpur-Valadi, A. Hatamzadeh, S. Sedaghathoor, Study of the accumulation of contaminants by Cyperus alternifolius, Lemna minor, Eichhornia crassipes, and Canna × generalis in some contaminated aquatic environments, Environ. Sci. Pollut. Res., 26 (2019) 21340–21350.

[151] M.A. Maine, N.L. Sune, S.C. Lagger, Chromium bioaccumulation: comparison of the capacity of two floating aquatic macrophytes, Water Res., 38 (2004) 1494–1501.

[152] R. Bennicelli, Z. Stępniewska, A. Banach, K. Szajnocha, J. Ostrowski, The ability of Azolla caroliniana to remove heavy metals (Hg(II), Cr(III), Cr(VI)) from municipal waste water, Chemosphere J., 55 (2004) 141–146.

[153] P. Miretzky, A. Saralegui, C.A. Fernandez, Aquatic macrophytes potential for the simultaneous removal of heavy metals (Buenos Aires, Argentina), Chemosphere J., 57 (2004) 997-1005.

[154] T. P. Choo, C. K. Lee, K. S. Low, O. Hishamuddin, Accumulation of chromium (VI) from aqueous solutions using water lilies (Nymphaea spontanea), Chemosphere J., 62 (2006) 961–967.

[155] C. Bragato, H. Brix, M. Malagoli, Accumulation of

nutrients and heavy metals in Phragmites australis Steudel and Bolboschoenus maritimus (L.) Palla in a constructed wetland of the Venice lagoon watershed, Environ. Pollut., 144 (2006) 967-975.

[156] P.K. Rai, Phytoremediation of heavy metals in a tropical impoundment of industrial region, Environ. Monit. Assess., 165 (2010) 529-537.

[157] J. Augustynowicza, M. Grosickia, E. Hanus-Fajersk, M. Lekka, A. Waloszek, H. Kołoczek, Chromium(VI) bioremediation by aquatic macrophyte *Callitriche cophocarpa* Sendtn. Chemosphere, 79 (2010) 1077-1083.

[158] E. Üçüncü, E, Tunca, S. Fikirdeşici, A.D. Özkan, A. Altındağ, Phytoremediation of Cu, Cr and Pb mixtures by Lemna minor, Bull. Environ. Contam. Toxicol., 91 (2013) 600-604.

[159] E. Üçüncü, E, Tunca, S. Fikirdeşici, A. Altındağ, Decrease and increase profile of Cu, Cr and Pb during stable phase of removal by duckweed (*Lemna minor* L.), Int. J. Phytorem., 15 (2013) 376-384.

[160] C. Tang, J. Song, X. Hu, X. Hu, Y. Zhao, B. Li, D. Ou, L. Peng, Exogenous spermidine enhanced Pb tolerance in Salix matsudana by promoting Pb accumulation in roots and spermidine, nitric oxide, andantioxidant system levels in leaves, Ecol. Eng., 107 (2017) 41-48.

[161] J. Vymazal, Concentration is not enough to evaluate accumulation of heavy metals and nutrients in plants, Sci. Total Environ., 544 (2016) 495–498.

[162] P. Saha, O. Shinde, S. Sarkar, Phytoremediation of industrial mines wastewater using water hyacinth, Int. J. Phytoremed. 19 (2017) 87–96.

[163] Y. Kara, Bioaccumulation of copper from contaminated wastewater by using *Lemna minor*, Bull. Environ. Contam. Toxicol., 72 (2004) 467-471.

[164] L. Zhang, S. Tian, Z. Ye, H. Peng, The efficiency of heavy metal removal from contaminated water by *elsholtzia argi* and *elsholtzia splendens*; Proc. of the international symposium of phytoremediation and ecosystem health, Health J., 10 (2005) 17-28.

[165] S. Mishra, M. Mohanty, C. Pradhan, H.K. Patra, R. Das, S. Sahoo, Physico-chemical assessment of paper mill effluent and its heavy metal remediation using aquatic macrophytes-a case study at JK paper mill, Rayagada, India, Environ. Monit. Assess., 185 (2012) 4347-4359.

[166] J.A. Romero-Hernández A., Amaya-Chávez P. Balderas-Hernández G. Roa-Morales N. González-

Rivas, M.A. Balderas-Plata, Tolerance and hyperaccumulation of a mixture heavy metals (Cu, Pb, Hg and Zn) by four aquatic macrophytes, Int J Phytorem, 19 (2016) 239-245.

[167] R. Othman, R. Ramya, Z.M. Baharuddin, K.S.H. Hashim, M. Yaman, Response of *Lemna minor* and *Salninia natans* as phytoremediation agents towards Fe, Cu and Zn toxicities via in vivo model system, J. Teknologi. Sci. Eng., 77 (2015) 101-109.

[168] R. Sallah-Ud-Din, M. Farid, R. Saeed, S. Ali, M. Rizwan, H.M. Tauqeer, S.A.H. Bukhari, Citric acid enhanced the antioxidant defense system and chromium uptake by *Lemna minor* L. grown in hydroponics under Cr stress, Environ. Sci. Pollut. Res., 24 (2017) 17669-17678,

[169] T.M. Galal, E.M. Eid, M.A. Dakhil, L.M. Hassan,. Bioaccumulation and rhizofilteration potential of Pistia stratiotes L. for mitigating water pollution in the Egyptian wetlands, Int. J. Phytoremediation., 5 (2017) 10-19.

[170] T.M. Galal, F.A. Gharib, S.M. Ghazi, K.H. Mansour, Phytostabilization of heavy metals by the emergent macrophyte Vossia cuspidata (Roxb.) Griff.: a phytoremediation approach, Int. J. Phytoremediation, 19 (2017) 992–999.

[171] I. Panfili, M.L. Bartucca, E. Ballerini, D.D. Buono, Combination of aquatic species and safeners improves the remediation of copper polluted water, Sci. Total. Environ., 601 (2017) 1263-1270.

[172] C. Hu, L. Liu, X. Li, Y. Xu, Z. Ge, Y. Zhao, Effect of graphene oxide on copper stress in *Lemna minor* L.: evaluating growth, biochemical responses, and nutrient uptake, J. Hazard. Mater., 17 (2017) 30570-30578.

[173] Z. Abbas, F. Arooj, S. Ali, I. E. Zaheer, M. Rizwan, M. A. Riaz, Phytoremediation of landfill leachate waste contaminants through floating bed technique using water hyacinth and water lettuce, Int. J. Phytoremed., 7 (2019) 1–12.

[174] J. Marrugo-Negrete,, , G. Enamorado-Montes, J. Durango-Hernández, J. Pinedo-Hernández, S. Díez, Removal of mercury from gold mine effluents using Limnocharis flava in constructed wetlands, Chemosphere, 167 (2017) 188–192.

[175] R. Zurayk, B. Sukkariyah, R. Baalbaki, D. A. Ghanem, Ni Phytoaccumulation in *Mentha Aquatica* L. and mentha sylvestris L. Water, Air, and Soil Pollut., 139 (2002) 355–364.

[176] N.R. Axtell, S.P.K. Sternberg, K. Claussen, Lead and nickel removal using microspora and lemna minor, Bioresour. Technol., 89 (2003) 41–48.

[177] S. T. Hussain, T. Mahmood, S. A. Malik, Phytoremediation technologies for Ni by water hyacinth, African J. Biotech., 9 (2010) 8-23.

[178] S. Pal, H.B. Singh, A. Rakshit, Potential of different crop species for nickel and cadmium phytoremediation in peri-urban areas of Varanasi district (India) with more than twenty years of wastewater irrigation history, Italian J. Agron., 8 (2013) e8.

[179] C. Nevena, D. Vilotic, M. Nesic, M. Veselinovic, D. Drazic, S. Mitrovic, Phytoremediation potential of *canna indica* L in water contaminated with lead Fresenius, Environ. Bull., 259 (2016) 3728-3733.

[180] E. Lahive, J. O'Halloran, M.A.K. Jansen, A marriage of convenience; a simple food chain comprised of *Lemna minor* (L.) and *Gammarus pulex* (L.) to study the dietary transfer of zinc, Plant Biology, 17 (2013) 75-81.

[181] J. Yang, J. Yang, J. Huang, Role of co-planting and chitosan in Phytoextraction of As and heavy metals by Pteris vittata and castor bean – a field case, Ecol. Eng., 109 (2017) 35–40.

[182] J. Yang, G. Zheng, J. Yang, X. Wan, B. Song, W. Cai, J. Guo, Phytoaccumulation of heavy metals (Pb, Zn, and Cd) by 10 wetland plant species under different hydrological regimes. Ecol. Eng., 107 (2017) 56–64.

[183] N. Dinh, A.V.D. Ent, D.R. Mulligan, A.V. Nguyen, Zinc and lead accumulation characteristics and in vivo distribution of Zn in the hyperaccumulator Noccaea caerulescens elucidated with fluorescent probes and laser confocal microscopy, Environ. Exp. Bot., 147 (2018) 1–12.

[184] B.O. Clarke, S.R. Smith, Review of 'emerging' organic contaminants in biosolids and assessment of international research priorities for the agricultural use of biosolids, Environ. Int., 37 (2011) 226–247.

[185] N.S. Thomaidis, A.G. Asimakopoulos, A.A. Bletsou, Emerging contaminants: a tutorial mini-review, global NEST J., 14 (2012) 72-79.

[186] M.O.C. Ogwuegbu, C. K. Enenebeaku, C.S.Obi, N. P. Ebosie, C.E. Enyoh, Stoichiometric Determination of Fe (II), Ni (II) and Cu (II) Complexes of Metronidazole, Int. J. Chem. Sci., 3 (2019) 25-29.

[187] M. Qu, N. Li, H. Li, T. Yang, W. Liu, Y. Yan, X. Feng, D. Zhu, Phytoextraction and biodegradation of atrazine by *Myriophyllum spicatum* and evaluation of bacterial communities involved in atrazine degradation in lake sediment, Chemosphere, 209 (2018) 439-448.

[188] D.H. Tran, T.M.H. Vi, T.T.H. Dang, R. Narbaitz, Pollutant removal by Canna Generalis in tropical constructed wetlands for domestic wastewater treatment, Global J. Environ. Sci. Manage., 5 (2019) 331-344.

[189] P. Prasertsup, N. Ariyakanon, Removal of Chlorpyrifos by Water Lettuce (*Pistia stratiotes* L.) and Duckweed (*Lemna minor* L.), Int J, Phytoremed., 13 (2011) 383-395.

[190] M. Uddin, M. Islam, M. Abedin, Adsorption of phenol from aqueous solution by water hyacinth, ARPN J., Engin. Appl. Sci., 2 (2007) 11-16.

[191] A. L. Seyfferth, M. K. Henderson, D. R. Parker, Effects of common soil anions and pH on the uptake and accumulation of perchlorate in lettuce, Plant Soil, 302 (2008) 139-148.

[192] J. Wang, X. Liu, X. Zhang, X. Liang, W. Zhang, Growth response and phytoremediation ability of Reed for diesel contaminant, Procedia Environ. Sci., 8 (2011) 68-74.

[193] Zhong G, Wu Z, Yin J, Chai L, 2018. Responses of Hydrilla verticillata (L.f.) Royle and Vallisneria natans (Lour.) Hara to glyphosate exposure, Chemosphere, 193 (2018) 385-393.

[194] S. M. Idris, P. L. Jones, S. A. Salzman, G. Croatto, G. Allinson, Evaluation of the giant reed (Arundo donax) in horizontal subsurface flow wetlands for the treatment of recirculating aquaculture system effluent, Environ.Sci. Pollut. Res., 19 (2011) 1159–1170.

[195] Ha W., D. L. Suarez, S. M. Lesch, Perchlorate uptake in Spinach as related to perchlorate, nitrate, and chloride concentrations in irrigation water, Environ. Sci. Technol., 45 (2011) 9363–9371.

[196] S. Susarla, S.T. Bacchus, N.L. Wolfe, S.C. Mccutcheon, Phytotransformation of perchlorate and identification of metabolic products in Myriophyllum aquaticum, Int. J. Phytoremed., 1 (1999) 97–107.

[197] T. Machate, H. Noll, H. Behrens, A. Kettrup, Degradation of phenanthrene and hydraulic characteristics in a constructed wetland, Water Res., 31 (1997) 554-560.

[198] A. Priya, K. Avishek, G. Pathak, Assessing the potentials of Lemna minor in the treatment of domestic wastewater at pilot scale, Environ. Monit. Assess., 184 (2012) 4301-4307.

[199] D.D. Yilmaz, H. Akbulut, Effect of circulation on wastewater treatment by Lemna gibba *and Lemna minor* (floating aquatic macrophytes), Int. J.

Phytorem., 13 (2011) 970-984.

[200] X. Zhao, G.K. Moates, N. Wellner, S.R.A. Collins, M.J. Coleman, K.W. Waldron, Chemical characterisation and analysis of the cell wall polysaccharides of duckweed (Lemna minor), Carbohydr. Polym., 14 (2014) 436-446.

[201] W. Van Echelpoel, P. Boets, P.L.M. Goethals, Functional response (FR) and relative growth rate (RGR) Do not show the known invasiveness of Lemna minuta (Kunth), PLoS, 11 (2016) e0166132.

[202] K.K. Yadav, N. Gupta, V. Kumar, J.K. Singh, Bioremediation of heavy metals from contaminated sites using potential species: a review, Indian J. Environ. Prot., 37 (2017) 65-84.

[203] N.K. Kilic, E. Duygu, G. Dönmez, Triacontanol hormone stimulates population, growth and Brilliant Blue R dye removal by common duckweed from culture media, J. Hazard. Mater., 182 (2010) 525-530.

[204] D.A. Yaseen, M. Scholz, Comparison of experimental ponds for the treatment of dye wastewater under controlled and semi-natural conditions, Environ. Sci. Pollut. Res. Int., 24 (2017) 16031-16040.

[205] E. Neag, D. Malschi,, A. Măicăneanu, Isotherm and kinetic modelling of toluidine blue (TB) removal from aqueous solution using Lemna minor, Int. J. Phytorem., 20 (2018) 1049-1054.

[206] Souza, T. D. de, Borges, A. C., Matos, A. T. de, Veloso, R. W., & Braga, A. F. (2018). Kinetics of arsenic absorption by the species Eichhornia crassipes and Lemna valdiviana under optimized conditions, Chemosphere, 209 (2018) 866–874.

[207] A.W. Verla, E. N. Verla, C. E. Enyoh, Chemometrics in environmental analytical chemistry: A review of mathematical models and their applications. Proceedings of 3rd world environment day conference, Imo State University, Nigeria, 16, 2019.

[208] A.W. Verla, E.N. Verla, C.M. Ajero, K.C. Lele, N.O. Stellamarris, C.E. Enyoh, Biomonitoring of heavy metals in blood and urine of African children from Owerri Metropolis, Eastern Nigeria, J. Chem. Health Risk., 9 (2019) 11-26.

[209] A.W. Verla, C.E. Enyoh, V.E. Ngozi, P.N. Okeke, S.S. Pingale, Chemometric assessment of orashi river after confluence with oguta lake, Indonesian J. Fundamental Appl. Chem., (2019). Accepted manuscript.

[210] M.S. Islam, T. Saito, M. Kurasaki, Phytofiltration

of arsenic and cadmium by using an aquatic plant, micranthemum umbrosum: phytotoxicity, uptake kinetics, and mechanism, Ecotoxicol. Environ. Safe., 112 (2015) 193-200.

[211] M. Srivastava, L.Q. Ma, N. Singh, S. Singh, Antioxidant responses of hyperaccumulator and sensitive fern species to arsenic, J. Exp. Bot., 56 (2005) 1335-1342.

[212] R.A. Fisher, Some remarks on the methods formulated in a recent article on 'The quantitative analysis of plant growth, Ann. Appl. Biol., 7 (1921) 367-372.

[213] D.A. Wilkins, The measurement of tolerance to edaphic factors by means of root growth, New Phytol., 80 (1978) 623-633.

[214] J.A. Romero-Hernández, A. Amaya-Chávez, P. Balderas-Hernández, G. Roa-Morales, N. González-Rivas, M.A. Balderas-Plata, Tolerance and hyperaccumulation of a mixture heavy metals (Cu, Pb, Hg and Zn) by four aquatic macrophytes, Int. J. Phytorem., 19 (2016) 239-245.

[215] V. Vadivelan, K.V. Kumar, Equilibrium, kinetics, mechanism, and process design for the sorption of methylene blue onto rice husk, J. Colloid Interface Sci., 286 (2005) 90-100.

[216] A.W. Verla, M. Horsfall (Jnr), E.N Verla, A.I. Spiff, Some aspect of surface chemistry of activated carbon prepared from fluted pumpkin (*Telfairia occidentalis Hook. F.*) by physical activation, Int. J. Chem. Sci. Technol., 2 (2012) 224-230**.**

[217] B. O. Isiuku, C. N. Nwosu, Fixed-bed adsorption of metanil yellow from aqueous solution on HNO_3-treated-H_3PO_4-activated carbon frm gmelina bark, Asian J. Chem., 29 (2017) 475-479.

[218] F. Zurita, J. De Anda, M.A. Belmont, Treatment of domestic wastewater and production of commercial flowers in vertical and horizontal subsurface-flow constructed wetlands, Ecol. Eng., 35 (2009) 861–869.

[219] O. C. Türker, A. Yakar, N. Gür. Bioaccumulation and toxicity assessment of irrigation water contaminated with boron (B) using duckweed (Lemna gibba L.) in a batch reactor system, J.Hazard. Mater., 324 (2017) 151–159.

[220] Y.H. Su, Y.G. Zhu, Transport mechanisms for the uptake of organic compounds by rice (Oryza sativa) roots, Environ. Pollut., 148 (2007) 94–100.

[221] V.A. Wirnkor, E.C. Ebere, V.E. Ngozi, N.K. Oharley, Microplastic-toxic chemical interaction: A review study on quantified levels, mechanism and implication, SN Appl. Sci., (2019). https://10.1007/s42452-019-1352-0

[222] A. A. Romeh, Phytoremediation of cyanophos insecticide by *Plantago major* L. in water, J. Environ. Health Sci. Eng., 12 (2014) 38.

[223] M. Michel, B. Buszewski, HPLC determination of pesticide residue isolated from food matrices, J. Liq. Chromatogr. Related Technol., 25 (2002) 2293-2306.

[224] C. Ferrer, M.J. Gomez, J.F. Garcıa-Reyes, I. Ferrer, Determination of pesticide residues in olives and olive oil by matrix solid-phase dispersion followed by gas chromatography/mass spectrometry and liquid chromatography/tandem mass spectrometry, J. Chromatogr. A, 1069 (2005) 183−194.

[225] C. Tsoutsi, C. I. Konstantinou, D. Hela, T. Albanis, Screening method for organophosphorus insecticides and their metabolites in olive oil samples based on headspace solid-phase microextraction coupled with gas chromatography, Anal. Chim. Acta, 573 (2006) 216− 222.

[226] N. Chamkasem, L.W. Ollis, T. Harmon, S. Lee, G. Mercer, Analysis of 136 Pesticides in Avocado Using a Modified QuEChERS Method with LC-MS/MS and GC-MS/MS, J. Agric. Food Chem., 61 (2013) 315−2329.

Separation and determination of lead in human urine and water samples based on thiol functionalized mesoporous silica nanoparticles packed on cartridges by micro column fast micro solid-phase extraction

Maling Gou[a,b] and Baharak Bahrami Yarahmadi[c,*]

[a] *State Key Laboratory of Biotherapy and Cancer Center, West China Hospital, Sichuan University and Collaborative Innovation Center for Biotherapy, Chengdu 610041, China*

[b] *Department of Thoracic Oncology, Cancer Center, West China Hospital, Medical School, Sichuan University, Chengdu 610041, China*

[c,*] *Occupational Health Engineering Department, School of Public Health, Kerman University of Medical Sciences, Kerman, Iran*

A B S T R A C T

An efficient method based on thiol functionalized mesoporous silica nanoparticles (HS-MSNPs) was used for extraction of lead ions (PbII) from urine and water samples by packed column micro solid phase extraction (PC-MSPE). By procedure, 15 mg of HS-MSNPs packed in syringe cartridges (SC, 5mL) with cellulose membrane and pH adjusting at 5.5-6.5. Then, the lead of urine and water sample was efficiently extracted on HS-MSNPs after pushing the plunger of a syringe. Finally, the Pb (II) was back-extracted with inorganic acid solution and the remained solution determined by electrothermal atomic absorption spectrometry (ET-AAS). By optimization conditions, the enrichment factor, LOD, linear range and RSD% was obtained 24.8, 0.04 μg L^{-1}, 0.12-5.5 μg L^{-1} and less than 5%, respectively for 5 mL of urine samples. The validation was confirmed by spiking of real samples and using certified reference material (CRM, NIST) in water and urine sample.

1. Introduction

Heavy metals such as; arsenic (As), lead (Pb), Cobalt (Co), chromium (Cr) and mercury (Hg) and nickel (Ni) with densities about 5 gram per cubic centimeter are called heavy metals. Natural and human sources of heavy metals are mineral resources development, metal processing and smelting, petrochemical company, factory emissions, and sewage irrigation [1]. Exposure to heavy metals especially mercury caused to different disease in humans. For example, disorders of the

cardiovascular, CNS, Liver, renal, and others, may be lead to dangers acute and chronic disease such as, cancer and multiple sclerosis [2-5]. So heavy metals enter to human body and cause many problem with adverse health effects [6]. Heavy metals have a normal range in environment (air, soil, water), but industrial activity increase their concentrations in the environment matrix and humans [7]. The Pb(II) was widely used in industrial processes and has highly toxic effect in humans as a major environmental pollutant [8]. In battery factory, the lead exposure is still the main subject in the human workplace and occupational health but some

protective instruments used to reduce the emission of lead [9-11]. Lead is used for pipe, instruments and medical device as a resistant to corrosion and X-ray. The lead with melting point of 327 °C and evaporation pressure out 1.77 mmHg was used in industrial process with different application such as, battery, ceramic, balls, rubber, crystals, and pesticide [12]. The international agency for research on cancer (IARC) reported, the inorganic and organic lead caused to carcinogenic effect in humans [7, 12, 13]. Also, the half-life of Pb in blood, soft tissue and bone was obtained about 35 days, 50 days and 20 years, respectively [6, 14, 15]. The previously papers showed that, the lead poisoning has adverse health effects in human systems and acute and chronic exposure caused to disorder in cardiovascular, digestive, and nervous systems [12]. Car exhausts, contaminated food, industrial emission, and air and soil pollution could be a good example of lead exposure by skin, inhalation or ingestion. Symptoms of lead toxicity included, abdominal pain, anorexia, tremor, CNS problem, MS, constipation, myalgia, irritability, and anemia. Lead poisoning can be caused an acute abdominal pain [16, 17]. The toxicity of lead evaluates in the blood, hair, urine, and stool samples by ET-AAS or ICP instruments. Lead can be excreted in urine by the renal, so, nephrotoxicity was occurred in both acute and chronic exposure of lead in adults and children's. The nephrotoxic effects of lead has been observing at high blood concentrations 1.93 -2.42 μmol L^{-1} (40-50 μg dL^{-1}) [15, 18]. The various methods was used for determination lead in different matrix samples [13, 19]. The most well-known methods are; flame atomic absorption spectrometry (FAAS) [20], graphite furnace atomic absorption spectrometry (GFAAS) [21], inductively coupled plasma-optical emission spectrometry (ICP-OES) [13], and inductively coupled plasma-mass spectrometry (ICP-MS) [22]. Due to the low concentration of lead in biological matrix, interferences ions and difficulty analysis of lead, a sample preparation step before the determination process is necessary [23, 24]. Liquid-liquid extraction/micro extraction(LLE/LLME) [25], co-

precipitation [26], cloud point extraction(CPE) [27], and solid-phase extraction/micro solid-phase extraction (SPE&MSPE) [28] are the most effective pre-concentration procedures. Also, different sorbets were evaluated for SPE methods. Recently, nanosorbents as favorite sorbent was considered for extraction heavy metals in water and human samples [29]. As reliable analytical performance for metal adsorption /determination, a variety of nanomaterials include; modified macromolecules [28], carbon nanotubes [30], magnetic materials [31], mesoporous materials [32], and ion-imprinted polymers [33], ferric oxide [34], titanium oxide [35], manganese oxide [36], and aluminum oxide [37] have been used in SPE. Nanomaterials with high surface area, high adsorption, usability, good recovery, low time extraction are candidate for SPE analytical approach[13]. Some advantages such as high sensitivity, low sample requirement, low solvent consumption, simplicity, and easy automation, Solid-phase micro extraction (SPME) as successful technique has been used for extraction metals from liquid phase [38]. Other nanomaterials include; polymer nanoparticles, nanocarbon, nanozeolites, functionalized nanomaterials and mesoporous silica nanoparticles was used as efficient sorbent for extraction heavy metals by SPE or MSPE [39]. Due to excellent dispensability and high adsorption capacity with large specific surface area, mesoporous silica based on monolithic column have attracted by SPE/SPME procedure [40]. For analyzing heavy metals based on SPE method, various functionalized mesoporous silica with thiol, amine, phosphonate, etc. have been used. Recently, the syringe-based SPE device containing thiol and amine functionalized mesoporous silica was used for the simultaneous uptake of As(III) and As(V) in liquid samples [38, 40]. In this work, lead in urine and waters were extracted based on HS-MSNPs by PC-MSPE technique before determined by ET-AAS. By proposed method, HS-MSNPs as an adsorbent were validated by CRM. The thiol functionalized MSNPs was used as complexing agent for extraction of lead from samples. The chemical bonding of HS-MSNPs was occurred

based on the thiol-lead bonding by sorbent in liquid phase.

2. Material and method

2.1. Apparatus and Reagents

The ultra-pure reagents such as, sodium hydroxide (NaOH), hydrogen peroxide (H_2O_2), inorganic and organic acids(H_2SO_4, HNO_3, HCl, CH_3COOH), T-ethoxysilane (TEOS, CAS N: 800-6580025), Triethanolamine hydrochloride (TEAH$_3$, HOCH2CH2)3N , HCl, CAS N: 102-71-6), hexadecyltrimethylammonium bromide as ammonium surfactant; (CTAB, $C_{19}H_{42}BrN$, N: 57-09-0), sodium hydroxide, lead nitrate salt (CAS number: 10099-74-8) and - 3-Triethoxysilyl-1-propanethiol ($C_9H_{22}SO_3Si$, CAS N: 14814-09-6) was purchased from Sigma Aldrich (Darmstadt,Germany). Sodium silicate solution ($Na_2O(SiO_2)_x \cdot xH_2O$, N: 338443, Sigma Germany), pure ethanol solution and acetone were prepared from Merck(Germany). The standard solution of Pb(II) was prepared from the lead chloride [liquid of $Pb Cl_2$] as 1 g L^{-1} solution in HCl 1%. The micro gram concentrations of Pb Cl2 were prepared daily by dilution HCl. For evaluation of the purity of HS_ MSNPs toxic metals such mercury; lead determined by ET-AAS. The pH of samples was adjusted by buffer solutions. The $CH_3COONa/$ CH_3COOH and ammonium buffer solutions were selected for pH of 3-7and 7.5-10. The results were obtained by electrothermal atomic absorption spectrometer (GBC, ET-AAS, Australia). A deuterium background correction lamp (UV) and hollow cathode lamp with 5 mA and a wavelength of 283.3 nm was adjusted. The pH of samples was determined by pH meter of Metrohm, Germany.

2.2. Synthesis of thiol functionalized MSNPs

In a typical synthesis, tri-ethoxysilane was added to predetermine amounts of Triethanolamine hydrochloride. The solution was heated up to 140 °C under vigorous stirring. After cooling down to 90 °C, CTAB was added to this solution. The final molar compositions of the reactants were 1.0 TEOS: 3.5 TEAH$_3$: 0.25 CTAB: 90 H_2O [41-43]. For thiol functionalization of calcined MSNPs, 1.4 g of 3-mercaptopropyltriethoxysilane ($C_9H_{22}SO_3Si$) and 1.5 g of calcined MSNPs in presence of toluene, were refluxed for 24 h and then washed with DW. The obtained thiol functionalized MSNPs (HS MSNPs was dried at 75ºC.

2.3. Characterization

The scanning electron microscopy (SEM) and transmission electron microscopy (TEM) was used for morphology and size morphology of the HS-MSNPs by Philips Co., Netherland (model PW3710 & model CM30) (Fig. 1a and b). The elemental analyzer was used for determination of elemental composition ratio H/C, N/C, S/C or C/N (GBC, AUS). X-ray diffraction (XRD) peak of HS-MSNPs and MSNPs were obtained with by wavelength 0.15 nm (Fig. 2) (Seifert TT 3000, Germany). Functional groups of SH on MSNPs
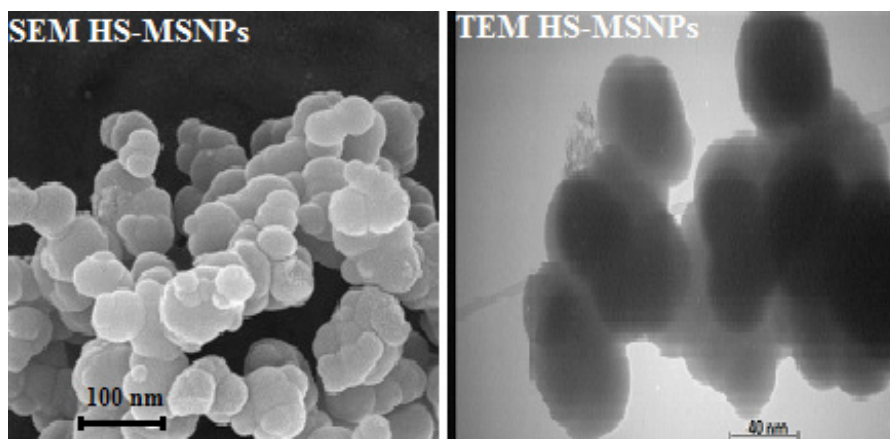
Fig. 1. (a)SEM of HS-MSNPs and (b) TEM of HS-MSNPs
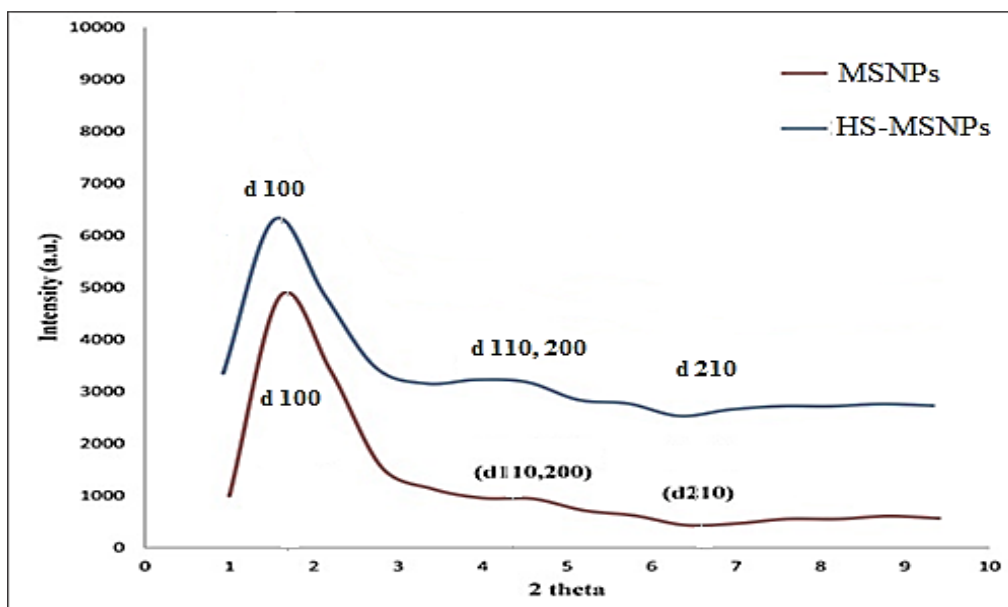
Fig. 2. The XRD of HS-MSNPs

as HS-MSNPs material were analyzed by FTIR in Waveland between 300 cm^{-1} to 4000 cm^{-1} (Fig. 3). The HS band was showed in Waveland of 2500 cm^{-1} (Germany).

2.4. General procedure

The packed column micro solid phase extraction (PC-MSPE) was used for separation and preconcentration of Pb(II) ions in human urine, standard solution and water samples. First, 5 mL

of the lead standard solution containing 0.1 -5.5 µg L^{-1} as a LLOQ and ULOQ was used and pH adjusted up to 6 by buffer solution. After optimized pH, the standard and urine samples directly transferred to in 5 mL of syringe cartridges with cellulose membrane which was already packed with 15 mg of HS-MSNPs and MSNPs as a sandwich form between membranes manually. The syringe cartridges (SC) included packed sorbent in cellulose membrane (PSCM) was used as solid
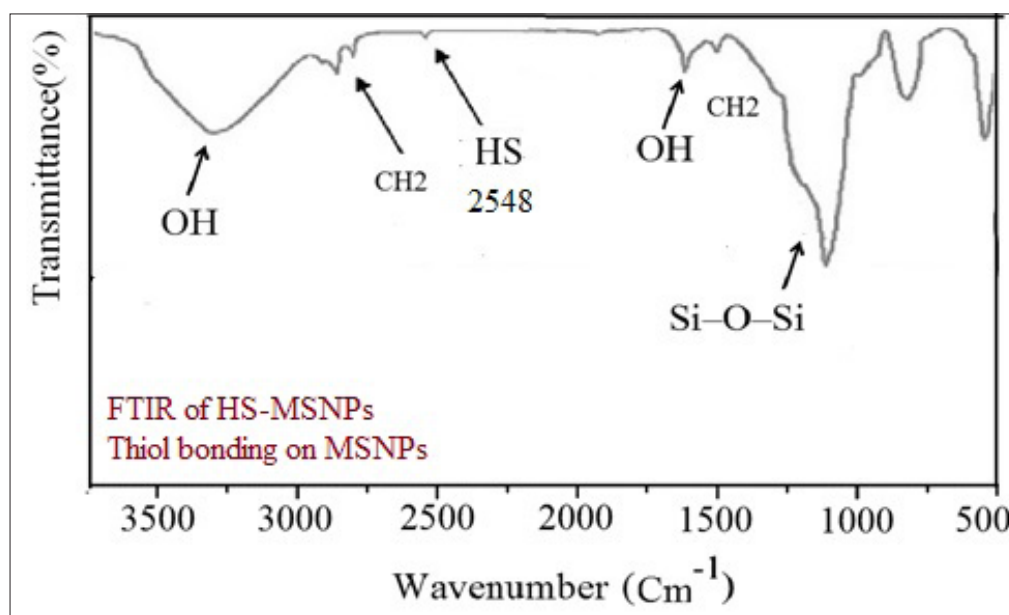
Fig. 3. FT-IR spectra patterns HS-MSNPs in 2500 cm^{-1}
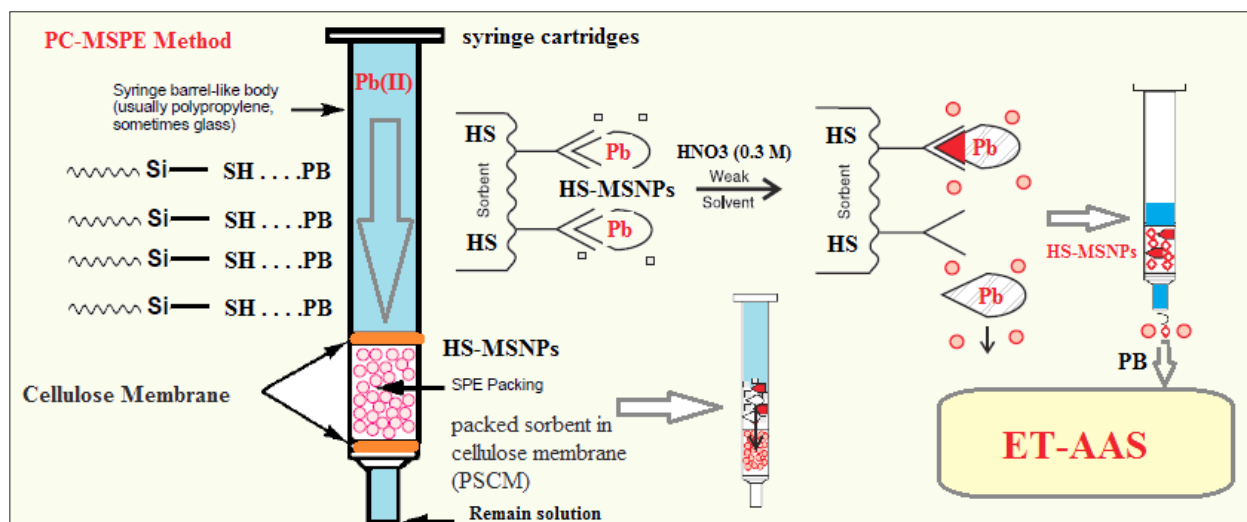
Fig. 4. The general procedure for lead extraction by PC-MSPE

phased for extraction Pb (II) from liquid phase by PC-MSPE. Then the urine and standard samples were fast extracted through PSCM of HS-MSNPs with pushing the plunger and the solid/liquid phases were separated.   The Pb(II) ions chemically and physically absorbed on HS-MSNPs in PSCM. Finally, Pb(II) ions retained on the HS-MSNPs were eluted by passing 0.2 mL of nitric acid (0.3 mol L^{-1}) through the SC and the concentration of lead ions in the eluent was determined by ET- AAS (Fig. 4).The project approved by the ethical committee of K.U.M.S. (Ethical Code:IR.KMU.REC. 1398. 453)

3. Results and Discussion

3.1. The pH optimization

The pH is one of the most important parameters which were affected on lead extraction by PC-MSPE procedure. The effect of urine and standard pH on the extraction of Pb (II) by HS-MSNPs and MSNPs has investigated from pH of 1-12 containing 0.1-5.5 µg L^{-1} of lead ions by PC-MSPE method. Also, the extraction Pb ions in human urine sample were investigated in human pH. The results showed us, the extraction efficiencies of Pb (II) in urine samples were increased in pH from 5.5 to 6.5. The maximum recoveries were achieved in optimized pH (more than 97%) and decreased in 5.5 > pH > 6.5. So, the pH of 6.0 was selected as optimized pH for Pb extraction in urine and water samples. Furthermore, the Pb(II) and other metals was more extracted by extra mass (50 mg) of HS-

MSNPs as physically adsorption simultaneity. In optimized conditions, the mean extraction of Pb was obtained less than 98.7% and 34.6% by 15 mg of HS-MSNPs and MSNPs, respectively at pH=6. The extraction mechanism of Pb ions on the HS-MSNPs is mainly based on the electrostatic attractions of deprotonated sulfur of thiol groups with the positively charged Pb ions.

3.2. The mass optimization

For optimization of proposed method, the amounts (mg) of HS-MSNPs and MSNPs in the range of 1 to 30 mg were studied for extraction of 0.1-5.5 µg L^{-1} of Pb(II) in human urine and water samples. The results showed us, more than 12.5 mg of HS-MSNPs had good extraction recovery for Pb(II) in standard samples. So, 15 mg of HS-MSNPs was used as optimized amount of HS-MSNPs by PC-MSPE method (Fig. 6). More than 15 mg of HS-MSNPs got no significant extraction on the recovery of lead urine and water samples. For 15 mg of MSNPs, the extraction recovery was obtained less than 35% at pH=6 and was increased up to 44.4 % at pH=3.

3. 3. The sample volume optimization

The sample volume effected on the recovery of Pb(II) ions based on PC-MSPE in standard and human urine samples. So, the sample volume was evaluated from 1-20 mL in optimized conditions.
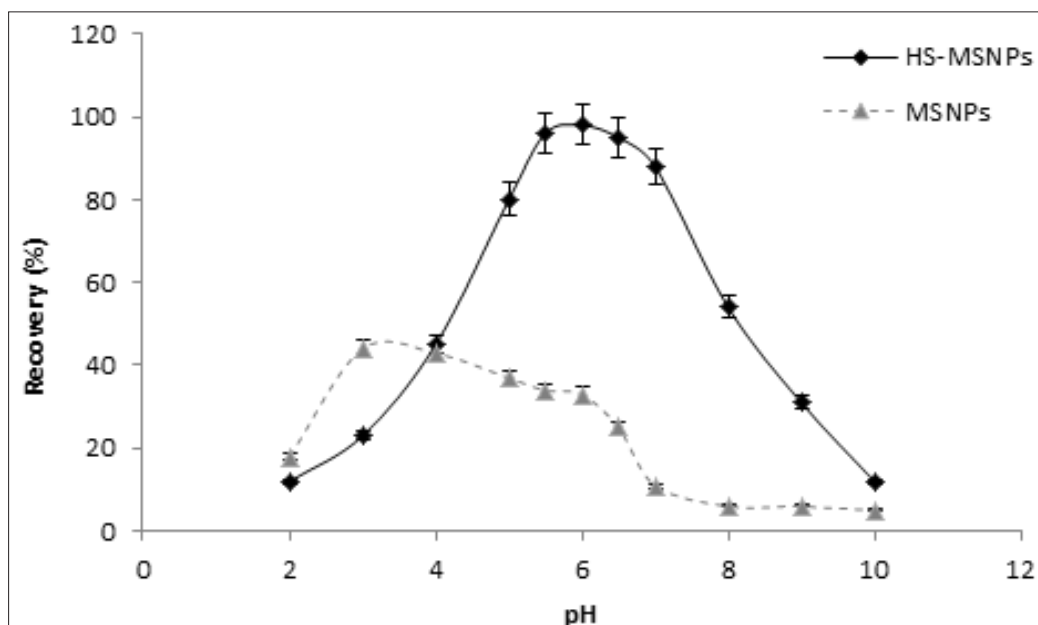
Fig. 5. The effect of pH on lead extraction by HS-MSNPs and MSNPs

The results showed us, the quantitative extraction was achieved less than 5 mL sample by $0.1 - 2.5$ µg L^{-1} of Pb as LLOQ and ULOQ range (≈97%). The extraction recovery was reduced more than 8 m and 10 mL of sample volume for urine and standard/water samples, respectively. As normal range of Pb in urine and waters (TLVs) a syringe cartridges (SC) of 5 mL were used for urine and water samples (Fig. 7).

3. 4. Adsorption capacity and separation time

In the batch system, the adsorption capacity (AC) of HS-MSNPs and MSNPs for lead extraction was calculated by ET-AAS. The adsorption capacity of Pb (II) was investigated for 5 mL of human urine sample and standard solution at pH=6 (15 mg HS-MSNPs and MSNPs). The pH was adjusted by using buffer solution and after shaking of SC, lead ions chemically and physically absorbed on sorbents. The residual solutions were determined
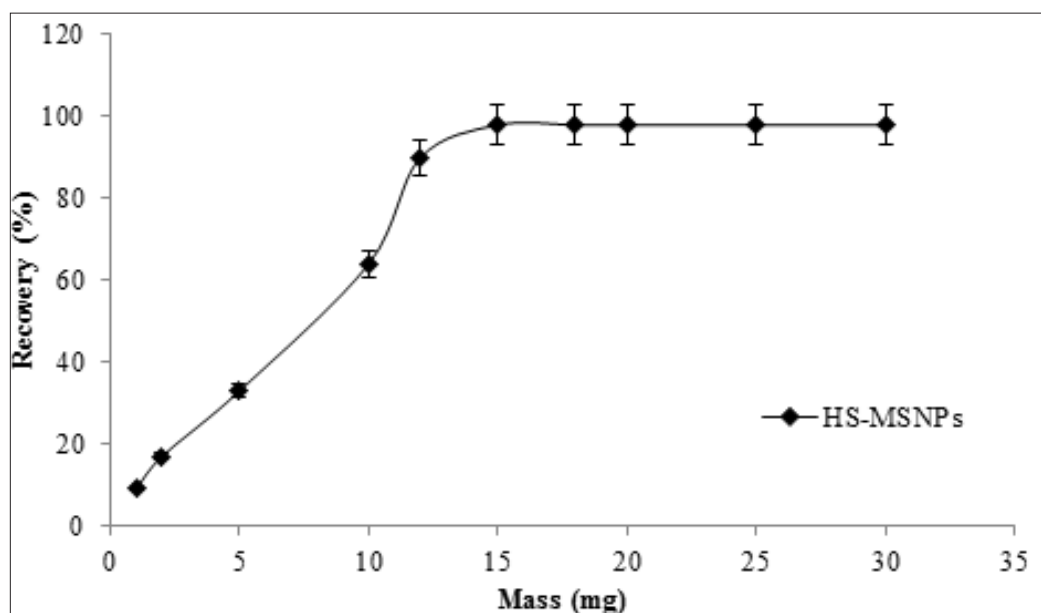
Fig. 6. The effect of mass of HS-MSNP on lead extraction by PC-MSPE method
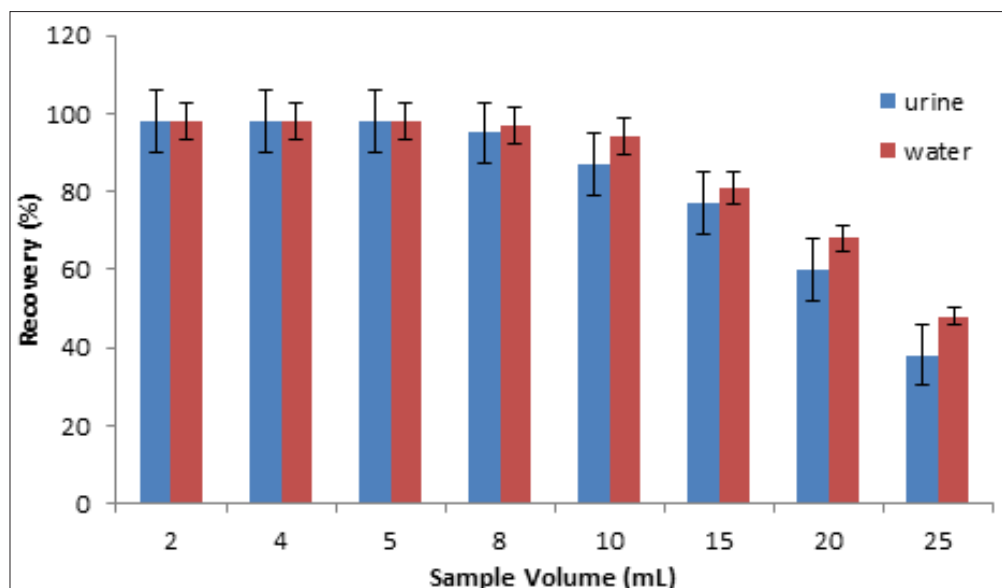
Fig. 7. The effect sample volume on lead extraction in water and urine samples

by ET-AAS. The adsorption capacity of HS-MSNPs and MSNPs for Pb ions was 186.3 mg g^{-1} and 64.8 mg g^{-1}, respectively. The results showed, the recovery of HS-MSNPs was higher than MSNPs as characterization and chemical bonding. So, the HS-MSNPs were used as excellent sorbent for extraction of Pb (II) in this study. Also separation time for extraction of lead ions was investigated between 2 min to 10 min. The result showed that, 4.5 min was an optimum time for excellent recovery. This time was controlled by pushing the plunger.

3. 5. Back extraction process
The maximum recovery for lead extraction was carried out in optimum conditions. The lead was back extracted from HS-MSNPs by different concentration of inorganic and organic acids such as HNO_3, HCl, CH_3COOH and H_2SO_4. The chemical adsorption between HS-MSNPs and Pb ions was dissociated at acidic pH. For optimizing, 0.1-0.5 mL of acids with different concentration from 0.1- 0.5 mol L^{-1} was studied. Based on results, 0.2 mL of HNO_3 (0.3 mol L^{-1}) had good recovery (Fig. 8).

3. 6. Interference study
By PC-MSPE method, the interference of coexisting

ions (cations and anions)such as; SO_4^{2-}, Cl$^-$, Br$^-$, NO_3^-, CO_3^{2-}, Cd^{2+}, AS^{3+}, Hg^{2+}, Ag^+, Co^{2+}, CU $^{2+}$, Zn^{2+}, Mn^{2+}, V^{3+}, Al^{3+} and Ni^{2+} in water and urine samples was studied. So, different concentration of coexisting ions (1—5 mg L^{-1}) was added to 5 mL of standard sample solution with lead concentration of 5.5 μg L^{-1}. Based on results, the most concomitant ions cannot effect on extraction of Pb in samples. The mean of concentration ratio of above coexisting ions per lead was less than 500. Therefore, the Pb ions in urine samples were efficiently extracted with HS-MSNPs in present of coexisting ions (less than 5%).

3.7. Discussion
Mortada et al investigated the pre-concentration of Pb^{2+} from blood and urine samples with mesoporous strontium titanate nanoparticles and determined the samples by FAAS. The characterization was obtained by FT-IR, XRD, SEM-EDX, and TEM. In optimized conditions, the pH, shaking time, mass sorbent and adsorption capacity was achieved at 6, 20 min, 50 mg and 155.6 mg g^{-1} which was lower than PC-MSPE procedure in this study. The limit of detection and relative standard deviation was 1.75 μg L^{-1} and 2.5%, respectively which was higher than our proposed method by HS-MSNPs (LOD=0.04 μg L^{-1}, 2.2 %)[44]. In another research,
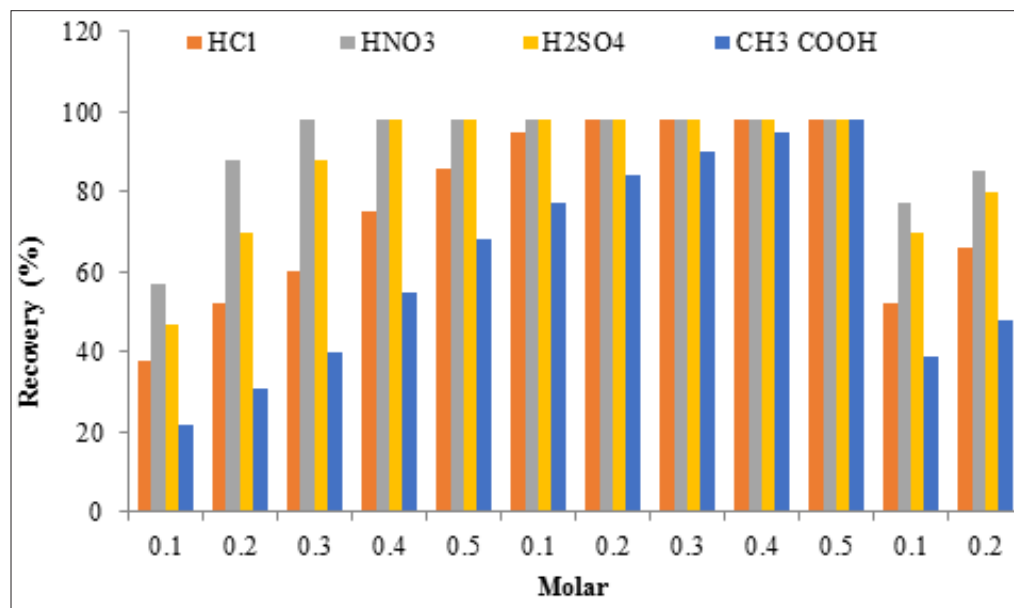
Fig. 8. The effect acids on lead extraction with HS-MSNPs

Behbahani et al used the method of solvent-assisted dispersive solid-phase extraction (SA-DSPE) to determine lead in fruit and water samples. After lead extraction the samples was determined by flame atomic absorption spectrophotometer (F-AAS). Based on results, LOD =1.2 µg L^{-1} was obtained as compared to lower LOD (0.04 µg L^{-1}) by PC-MSPE method [45]. Kakavandi et al, reported ultrasonic assisted-dispersive solid-phase extraction based on ion-imprinted polymer (UA-DSPE-IIP) nanoparticles as a selective extraction for lead ions. Box-Behnken design (BBD) was used for the optimization of sorption and desorption steps in UA-DSPE-IIP. Under the optimized conditions, the limit of detection and relative standard deviation for the detection of lead ions by UA-DSPE-IIP was found to be 0.7 µg L^{-1} and <4%, respectively which was higher than proposed method based on HS-MSNPs by PC-MSPE method [46]. Also, a magnetic sorbent (MoS2-Fe3O4) based on dispersive solid-phase microextraction (DSPME) was used for separation Pb(II) and copper(II) ions from water samples by Soylak. LODs and RSD of 3.3 µg·L^{-1}, 4.9 for Pb(II) and of 1.8 µg·L^{-1}, 1.5% for Cu(II), was achieved by F-AAS. So, PC-MSPE method had better results as compared to MoS2-Fe3O4 sorbent [47]. Jiamei at al showed mesoporous silica-grafted graphene oxide (GO-SBA-15) as sorbent and packed it in an SPE microcolumn with solution-cathode glow discharge-atomic emission spectrometry (SCGD-AES) method. The detection limit (DL) of Pb(II) was calculated to be 0.91 µg L− 1 which was higher than PC-MSPE procedure [48]. Shahad et al used mesoporous silica with nanospheres as a substrate and the organic ligand of 2,5-di mercapto-1,3,4-thiadiazole, for lead removal from wastewater with LOD of 0.48 µg L^{-1} and adsorption capacity of 67.20 mg g^{-1}[49]. sobhi et al suggested ultrasonic-assisted dispersive micro-solid phase extraction (d-µSPE) method with GF-AAS for measuring of lead in water and urine samples by silica-based amino-tagged nano sorbent (MCM-41@NH2. The result showed that linear range, RSD and recovery was obtained 0.1–1.0 µg L^{-1}, 4.8–9.2% and 92–110%, respectively. The wide linear range and lower RSD was achieved for PC-MSPE as compared to d-µSPE method [50]. Amiri et al synthesized magnetic natural clinoptilolite (CP for simultaneous determination of lead (II) and cadmium (II) ions by FAAS. The limit of detection (LOD) using this method were found to be 0.93[51]. Raoof et al use the graphene oxide-soluble eggshell membrane protein (GO-SEP)

by inductively coupled plasma-optical emission spectrometry (ICP-OES). The GO-SEP-ICP-OES with LOD of 0.1 µg.L^{-1} was equal to PC-MSPE method [52]. Baile et al used magnetic dispersive solid-phase microextraction (MDSPME) method, based on ZSM-5 zeolite decorated with iron oxide magnetic nanoparticles (*i.e.*, ZSM-5/Fe2O3) for the simultaneous separation and preconcentration of cadmium (Cd), mercury (Hg) and lead (Pb) from urine [53].

3.8. Validation of procedure

A novel method based on HS-MSNPs was applied for lead extraction for 5 mL of urine and water samples by PC-MSPE. For validation, real samples (water and urine) were spiked by standard lead samples in different concentration from LLOQ to ULOQ. The method was approved with good precision and accuracy results with low RSD% (Table 1). Also, the proposed method was validated by power instrumental analysis (ICP-MS) as compared to PC-MSPE procedure (Table 2). The certified reference material (CRM, NIST) in water and wastewater samples were used for validating of results by PC-MSPE method. Experimental results of the CRM sample were satisfactorily confirmed the certified values of lead (Table 3). The recoveries of spiked water and urine samples

Table 1. Validation of PC-MSPE method based on spike of lead standard concentration

Sample	Added (µg L^{-1})	*Found(µg L^{-1})	Recovery%
Urine A	------	2.34 ± 0.09	------
	2.0	4.28 ± 0.17	97
Urine B	------	1.02± 0.04	------
	1.0	1.97± 0.11	95
Well Water	------	0.46 ± 0.02	------
	0.5	0.97± 0.05	102
[a] Wastewater	------	2.16 ± 0.12	------
	2.0	4.14± 0.18	99

* Mean of three determinations ± confidence interval (P = 0.95, n =10).
[a] Wastewater samples was diluted with DW (1:20)

Table 2. Comparing of PC-MSPE method with ICPMS for lead determination

Sample	Added	ICP-MS	PC-MSPE	ICP-MS Recovery%	PC-MSPE Recovery%
Urine	------	1.82 ± 0.04	1.78 ± 0.09	------	------
	2.0	3.79 ± 0.05	3.69 ± 0.21	98.5	95.5
Water	------	0.73 ± 0.02	0..68 ± 0.03	------	------
	0.5	1.21± 0.03	1.19 ± 0.05	96.0	102.0

* Mean of three determinations ± confidence interval (P = 0.95, n =10).

Table 3. Validation methodology by Sigma CRM and ICP-MS for PC-MSPE method

CRM sample	ICP-MS	CRM (µg/L)	*Found(µg L^{-1})	Recovery%
*ERMCA713	4.92 ± 0.12	4.97 ± 0.17	4.88 ± 2.4	98.2
1640a	1.19 ± 0.02	1.21 ± 0.02	1.23± 0.06	101.6
Urine	2.07 ± 0.09	------	1.98 ± 0.09	95.6
Drinking water	0.51± 0.01	------	0.49± 0.03	96.2

*Mean of three determinations ± confidence interval (P = 0.95, n =10)
[a] Sigma Aldrich, Cat. No. ERMCA713, lead in wastewater diluted up to 10.
[b] NIST SRM 1640a, lead in water, diluted up to 10.

for Pb(II) were ranged from 95% to 102%, which demonstrated that the PC-MSPE method was satisfactory extracted and determined Pb ions in human urine samples (n=10).

4. Conclusions

The simple, applied and reliable SPE technique for determination of trace levels of Pb (II) ions in real water and urine samples was developed based on HS-MSNPs by ET-AAS. The PC-MSPE method provided good recoveries (>95%) in optimized conditions. By procedure, reproducibility and reliability data with low RSD (under 5%) in 10 experiments were obtained. The batch adsorption capacities of lead on MSNPs and HS-MSNPs were found to be 64.8 and 186.3 mg g^{-1}, respectively. The PC-MSPE procedure has some advantages such as, excellent separation, high surface area, low consumption of only 15 mg of HS-MSNPs, good enrichment factor for 5 mL of sample, only 0.2 mL of eluent per extraction, high absorption capacities, low LOD, and favorite reusability (more than 20). It is expected that the PC-MSPE procedure based on nanotechnology could successfully be extracted lead ions from urine and water samples.

5. References

[1] X. Zhang, T. Zhong, L. Liu, X. Ouyang, Impact of soil heavy metal pollution on food safety in China, PLOS ONE., 10 (2015) 135-182.

[2] L. Han, X. Wang, R. Han, M. Xu, Y. Zhao, Q. Gao, H. Shen, H. Zhang, Association between blood lead level and blood pressure: An occupational population-based study in Jiangsu province, China. PlOS. ONE., 13 (2018) 200-289.

[3] H Shirkhanloo, M Ghazaghi, HZ Mousavi, Chromium speciation in human blood samples based on acetyl cysteine by dispersive liquid–liquid biomicroextraction and in-vitro evaluation of acetyl cysteine/cysteine for decreasing of hexavalent chromium concentration, J. pharm. Biomed. Anal.,118 (2016) 1-8.

[4] X. Wang, P. Jin, Q. Zhou, S. Liu, F. Wang, S. Xi, Metal biomonitoring and comparative assessment in urine of workers in lead-zinc and steel-iron mining and smelting, Bio. tra. elem. res, 189 (2019) 1-9.

[5] Q. Yang, Z. Li, X. Lu, Q. Duan, L. Huang, J. Bi, A review of soil heavy metal pollution from industrial

and agricultural regions in China: pollution and risk assessment, Sci. Total. Environ, 642 (2018) 690-700.

[6] T. Vlasak, G. Jordakieva, T. Gnambs, C. Augner, R. Crevenna, R. Winker, A. Barth, Blood lead levels and cognitive functioning: A meta-analysis, Sci. Total. Environ, 668 (2019) 678-684.

[7] M. Andjelkovic, A. Buha Djordjevic, E. Antonijevic, B. Antonijevic, M. Stanic, J. Kotur-Stevuljevic, V. Spasojevic-Kalimanovska, M. Jovanovic, N. Boricic, D. Wallace, Toxic effect of acute cadmium and lead exposure in rat blood, liver, and kidney, Inter. J. Environ. Res. Pub. health, 16 (2019) 274.

[8] Z. Shraideh, D. Badran, A. Hunaiti, A. Battah, Association between occupational lead exposure and plasma levels of selected oxidative stress related parameters in Jordanian automobile workers, Inter. j. Occup. Med. Environ. Health, 31 (2018) 517-525.

[9] I.E. Castro, D.A. Larsen, B. Hruska, P.J. Parsons, C.D. Palmer, B.B. Gump, Variability in the spatial density of vacant properties contributes to background lead (Pb) exposure in children, Environ. Res., 170 (2019) 463-471.

[10] A.S. Dickerson, J. Hansen, A.J. Specht, O. Gredal, M.G. Weisskopf, Population-based study of amyotrophic lateral sclerosis and occupational lead exposure in Denmark, Occup. Environ. Med., 76 (2019) 208-214.

[11] J. Xie, G. Du, Y. Zhang, F. Zhou, J. Wu, H. Jiao, Y. Li, Y. Chen, L. Ouyang, D. Bo, ECG conduction disturbances and ryanodine receptor expression levels in occupational lead exposure workers, Occup. Environ. Med., 76 (2019) 151-156.

[12] M. Mohammadyan, M. Moosazadeh, A. Borji, N. Khanjani, S.R. Moghadam, Investigation of occupational exposure to lead and its relation with blood lead levels in electrical solderers, Environ. Mon. Ass., 191 (2019) 126.

[13] W.I. Mortada, A.M. Abdelghany, Preconcentration of Lead in Blood and Urine Samples Among Bladder Cancer Patients Using Mesoporous Strontium Titanate Nanoparticles, Bio. Tra. Elem. Res., (2019) 1-11.

[14] Y. Chen, X. Xu, Z. Zeng, X. Lin, Q. Qin, X. Huo, Blood lead and cadmium levels associated with hematological and hepatic functions in patients from an e-waste-polluted area, Chemosphere, 220 (2019) 531-538.

[15] G.M. Daley, C.J. Pretorius, J.P. Ungerer, Lead Toxicity: an Australian Perspective, Clin. Bioch. Rev., 39 (2018) 61.

[16] M.J. Ahmed, M.T. Islam, S. Aziz, A Highly Selective and Sensitive Spectrophotometric Method for the

Determination of Lead at Ultra-trace Levels in Some Real, Environmental, Biological, Food and Soil Samples Using 5, 7-Dibromo-8-Hydroxyquinoline, Chem. Sci. Inter. J., (2019) 1-19.

[17] K. Soltaninejad, S. Shadnia, Lead poisoning in opium abuser in Iran: A systematic review, Inter. J. Pre. Med., 9 (2018).

[18] J.E. Forsyth, K.L. Weaver, K. Maher, M.S. Islam, R. Raqib, M. Rahman, S. Fendorf, S.P. Luby, Sources of Blood Lead Exposure in Rural Bangladesh, Environ. Sci. Tech., (2019).

[19] A. Ogunfowokan, A. Adekunle, B. Oyebode, J. Oyekunle, A. Komolafe, G. Omoniyi-Esan, Determination of Heavy Metals in Urine of Patients and Tissue of Corpses by Atomic Absorption Spectroscopy, Chem. Afr., (2019) 1-14.

[20] P.A. da Silva, G.C. de Souza, D.M.d.S. Leotério, M.F. Belian, W.E. Silva, A.P. Paim, A.F. Lavorante, Synthesis and characterization of functionalized silica with 3, 6-ditia-1, 8-octanediol for the preconcentration and determination of lead in milk employing multicommuted flow system coupled to FAAS, J. Food. Com. Anal., 40 (2015) 177-184.

[21] J. Chen, S. Xiao, X. Wu, K. Fang, W. Liu, Determination of lead in water samples by graphite furnace atomic absorption spectrometry after cloud point extraction, Talanta, 67 (2005) 992-996.

[22] Y. Cao, B. Deng, L. Yan, H. Huang, An environmentally-friendly, highly efficient, gas pressure-assisted sample introduction system for ICP-MS and its application to detection of cadmium and lead in human plasma, Talanta, 167 (2017) 520-525.

[23] J. Caroline, S. Choiriyah, G. Cristata, An Analysis of Lead (Pb) Levels in the Urine of Gas Station Operators Based on Individual Characteristics (A Case Study at Kali Rungkut and Panjang Jiwo Gas Station Surabaya), IOP. Con. Ser. Mater. Sci. Eng, IOP Publishing, 2019, pp. 012042.

[24] A.K. Maria das Graças, J.B. de Andrade, D.S. de Jesus, V.A. Lemos, M.L. Bandeira, W.N. dos Santos, M.A. Bezerra, F.A. Amorim, A.S. Souza, S.L. Ferreira, Separation and preconcentration procedures for the determination of lead using spectrometric techniques: A review, Talanta, 69 (2006) 16-24.

[25] A.E. Visser, R.P. Swatloski, S.T. Griffin, D.H. Hartman, R.D. Rogers, Liquid/liquid extraction of metal ions in room temperature ionic liquids, Sep. Sci. Tech., 36 (2001) 785-804.

[26] A.A. Gouda, A new coprecipitation method without carrier element for separation and preconcentration of some metal ions at trace levels in water and food

samples, Talanta, 146 (2016) 435-441.

[27] W. Mortada, I. Kenawy, M. Abdel-Rhman, G. El-Gamal, S. Moalla, A new thiourea derivative [2-(3-ethylthioureido) benzoic acid] for cloud point extraction of some trace metals in water, biological and food samples, J. Tra. Elem. Med. Bio., 44 (2017) 266-273.

[28] W. Mortada, I. Kenawy, Y.A. El-Reash, A. Mousa, Microwave assisted modification of cellulose by gallic acid and its application for removal of aluminium from real samples, Inter. J. Bio. Macro., 101 (2017) 490-501.

[29] B. Hu, M. He, B. Chen, Nanometer-sized materials for solid-phase extraction of trace elements, Anal. bio. chem., 407 (2015) 2685-2710.

[30] B. Feist, Selective dispersive micro solid-phase extraction using oxidized multiwalled carbon nanotubes modified with 1, 10-phenanthroline for preconcentration of lead ions, Food Chem., 209 (2016) 37-42.

[31] H.-m. Jiang, T. Yang, Y.-h. Wang, H.-z. Lian, X. Hu, Magnetic solid-phase extraction combined with graphite furnace atomic absorption spectrometry for speciation of Cr (III) and Cr (VI) in environmental waters, Talanta, 116 (2013) 361-367.

[32] H. Shirkhanloo, A. Khaligh, H.Z. Mousavi, A. Rashidi, Ultrasound assisted-dispersive-micro-solid phase extraction based on bulky amino bimodal mesoporous silica nanoparticles for speciation of trace manganese (II)/(VII) ions in water samples, Microchem. J., 124 (2016) 637-645.

[33] T. Bicim, M. Yaman, Sensitive determination of uranium in natural waters using UV-Vis spectrometry after preconcentration by ion-imprinted polymer-ternary complexes, J. AOAC. Inter., 99 (2016) 1043-1048.

[34] N. Limchoowong, P. Sricharoen, Y. Areerob, P. Nuengmatcha, T. Sripakdee, S. Techawongstien, S. Chanthai, Preconcentration and trace determination of copper (II) in Thai food recipes using Fe3O4@ Chi–GQDs nanocomposites as a new magnetic adsorbent, Food Chem., 230 (2017) 388-397.

[35] W. Mortada, A. Moustafa, A. Ismail, M. Hassanien, A. Aboud, Microwave assisted decoration of titanium oxide nanotubes with CuFe 2 O 4 quantum dots for solid phase extraction of uranium, RSC. Adv., 5 (2015) 62414-62423.

[36] E. Yavuz, Ş. Tokalıoğlu, H. Şahan, Ş. Patat, Nano sponge Mn2O3 as a new adsorbent for the preconcentration of Pd (II) and Rh (III) ions in sea water, wastewater, rock, street sediment and catalytic converter samples prior to FAAS determinations,

Talanta, 128 (2014) 31-37.

[37] M. Ghaedi, K. Niknam, A. Shokrollahi, E. Niknam, H.R. Rajabi, M. Soylak, Flame atomic absorption spectrometric determination of trace amounts of heavy metal ions after solid phase extraction using modified sodium dodecyl sulfate coated on alumina, J. Haz. Mater., 155 (2008) 121-127.

[38] L.-y. Zhao, Q.-y. Zhu, X.-q. Zhang, Y.-j. Chen, L. Mao, H.-z. Lian, X. Hu, Preparation and analytical application of novel thiol-functionalized solid extraction matrices: From mesoporous silica to hybrid monolithic capillary column, Talanta, 189 (2018) 517-526.

[39] P. Li, X.-q. Zhang, Y.-j. Chen, T.-y. Bai, H.-z. Lian, X. Hu, One-pot synthesis of thiol-and amine-bifunctionalized mesoporous silica and applications in uptake and speciation of arsenic, RSC. Adv., 4 (2014) 49421-49428.

[40] H. Shirkhanloo, M. Ghazaghi, A. Rashidi, A. Vahid, Arsenic speciation based on amine-functionalized bimodal mesoporous silica nanoparticles by ultrasound assisted-dispersive solid-liquid multiple phase microextraction, Microchem. J., 130 (2017) 137-146.

[41] H. Shirkhanloo, A. Khaligh F. Golbabaei, Z. Sadeghi, A. Vahid, Rashidi A. On-line micro column preconcentration system based on amino bimodal mesoporous silica nanoparticles as a novel adsorbent for removal and speciation of chromium (III, VI) in environmental samples. J. Environ. Health Sci. Eng., 3 (2015) 47.

[42] H. Shirkhanloo, A. Khaligh, HZ Mousavi, A. Rashidi. Ultrasound assisted-dispersive-ionic liquid-micro-solid phase extraction based on carboxyl-functionalized nanoporous graphene for speciation and determination of trace inorganic and organic mercury species in water and caprine blood samples. Microchem. J., 130 (2017) 245-54.

[43] H. Shirkhanloo, A. Khaligh, HZ. Mousavi, A. Rashidi. Ultrasound assisted-dispersive-micro-solid phase extraction based on bulky amino bimodal mesoporous silica nanoparticles for speciation of trace manganese (II)/(VII) ions in water samples. Microchem. J., 124 (2016) 637-45.

[44] W.I. Mortada, A.M. Abdelghany, Preconcentration of lead in blood and urine samples among bladder cancer patients using mesoporous strontium titanate nanoparticles, Biol. Trace Elem. Res., 2019 10 (2019)1-10.

[45] M. Behbahani, P.G. Hassanlou, M.M. Amini, F. Omidi, A. Esrafili, M. Farzadkia, A. Bagheri, Application of solvent-assisted dispersive solid phase extraction as a new, fast, simple and reliable preconcentration and trace detection of lead and cadmium ions in fruit and water samples, Food chem., 187 (2015) 82-88.

[46] M.G. Kakavandi, M. Behbahani, F. Omidi, G. Hesam, Application of ultrasonic assisted-dispersive solid phase extraction based on ion-imprinted polymer nanoparticles for preconcentration and trace determination of lead ions in food and water samples, Food Anal. Method., 10 (2017) 2454-2466.

[47] N. Baghban, E. Yilmaz, M.A. Soylak, magnetic MoS 2-Fe 3 O 4 nanocomposite as an effective adsorbent for dispersive solid-phase microextraction of lead (II) and copper (II) prior to their determination by FAAS, Microchim. Acta, 184(2017) 3969-3976.

[48] J. Mo, L. Zhou, X. Li, Q. Li, L. Wang, Z. Wang, On-line separation and pre-concentration on a mesoporous silica-grafted graphene oxide adsorbent coupled with solution cathode glow discharge-atomic emission spectrometry for the determination of lead. Microchem. J., 130 (2017) 353-3 59.

[49] A. Shahat, H.M. Hassan, H.M. Azzazy, E.A. El-Sharkawy, H.M. Abdou, M.R. Awual, Novel hierarchical composite adsorbent for selective lead (II) ions capturing from wastewater samples, Chem. Eng. J., 332 (2018) 377-386.

[50] H.R. Sobhi, A. Mohammadzadeh, M. Behbahani, A. Esrafili, Implementation of an ultrasonic assisted dispersive μ-solid phase extraction method for trace analysis of lead in aqueous and urine samples, Microchem, J., 146 (2019) 782-788.

[51] T. Amiri-Yazani, R. Zare-Dorabei, M. Rabbani, A. Mollahosseini, Highly efficient ultrasonic-assisted pre-concentration and simultaneous determination of trace amounts of Pb (II) and Cd (II) ions using modified magnetic natural clinoptilolite zeolite: response surface methodology, Microchem. J., 146 (2019) 498-508.

[52] A.R. Mahmood, I.Q. Abdallah, M.A. Alheety, H. Akbaş, A.N. Karadağ, O-rich graphene oxide based eggshell membrane polymer: Preparation, characterization and its utility as nano sorbent for solid phase extraction of Pb (II) in various water samples. AIP conference proceeding, AIP Publishing, 2144(2019) 020003.

[53] P. Baile, L. Vidal, M.A. guirre, A. Canals, A modified ZSM-5 zeolite/Fe 2 O 3 composite as a sorbent for magnetic dispersive solid-phase microextraction of cadmium, mercury and lead from urine samples prior to inductively coupled plasma optical emission spectrometry, J. Anal. Atom. Spec., 33 (2018) 856-66.

Modification of graphene for speciation of chromium in wastewater samples by suspension solid phase microextraction procedure

Ahmad Ghozatloo[a,*]

[a,*] *Research Institute of Petroleum Industry (RIPI), West Blvd. Azadi Sport Complex, P.O. Box: 14665-137, Tehran, Iran*

A B S T R A C T

In this study, the surface modification of graphene (SMG) was developed for efficient speciation and determination of chromium in water and wastewater samples. First surface of the graphene was modified with acid mixtures, potassium persulfate (KPS) in an alkaline media, tetra hydro furan (THF), Octadecyl amine and sodium dodecyl benzene sulfonate (SDBS) as synthesis. By procedure, the chromium ions was extracted from water/wastewater sample based on sulfonated and amine graphene (S-NG, N-NG) by suspension solid phase microextraction procedure (SMSPE). Hydrophobic ionic liquid ([HMIM] [PF6]) was used for separation graphene from 10 mL of waters. After shaking and centrifuging, the phase of Cr→ S-NG, Cr→N-NG was back extracted by 0.2 mL of HNO_3 (0.4 mol L^{-1}) and finally chromium concentration determined with electrothermal atomic absorption spectrometry (ET-AAS). The results showed, the sulfonated and amine graphene can successfully extracted Cr(III) and Cr(VI) from water and wastewater samples at pH=3.5-5.5 and pH<3, respectively. Also, the most Cr(VI) extracted by N-graphene at pH=2($NH_3^+ → Cr_2O_7^-$). Under the optimal conditions, the linear range, limit of detection and preconcentration factor were obtained 0.02–2.4 μg L^{-1}, 5.0 ng L^{-1} and 20.2 for 10 mL of water samples, respectively for Cr(III,VI) (%RSD<5%, pH=4). The validation of methodology for speciation of chromium was confirmed by spiking real samples.

1. Introduction

Different synthesis of graphene was used for extraction metals from waters [1]. Novel materials, such as graphene with various structures, have numerous advantages that make them favorable for many analytical chemistry applications [2]. Because of inherent low coefficient thermal expansion of graphene and its lightweight, high thermal and mechanical properties and ease for nanocomposites, it has been widely used in aqua phase materials such as water and wastewater samples [3]. Then

grapheme sheets have been used for extraction metals and VOCs. As solid phase extraction (SPE) with graphene, it is big to be dispersed in solution and cannot too long dispersion in polar solvents. Also, graphene nano sheets was hold together in bundles by van der Waals interactions [4, 5]. The grapheme nano sheets are hydrophobic and thus have a non-homogeneous form in water, so, simply used for heavy metal extraction as physical adsorption. But chemical methods involve surface modification of graphene for chemical bonding between graphene and function group. Surface control of nano particles to receive semi or full hydrophilic or hydrophobic properties has attracted

extensive research interests over the few years due to its importance in chemistry research and potential applications such as extraction ions from different matrixes. All the existing modification methods of graphene for chemical applications are wet-chemical method [6-7]. As synthesis of graphene modification, carboxylic acid, hydroxyl, nitrogen and sulfur group are the most common functional groups for absorption analysis [8]. Although this approach can increase the dispersion property but it can also have a detrimental effect on the conductivity of the composites and nano fluids [9]. Surfactants have also been used to disperse nanostructures, since this prevents them from becoming aggregated over time [10].

The wide application exists for modification of graphene specially sulfonated and amidation graphene (S…NG, N…NG). Recently, metal extraction occurred with graphene and modification graphene in water, human matrix and foods. Some toxic metal such as mercury, chromium and lead in drinking water and human blood or serum cause physiological or neuro-logical damage in human body. Chromium, specially Cr(VI) is a toxic pollutant in the environment, industries and factories. Cr determination in human body and waters is important because of health problem such as chromosome aberration, mutations, and carcinogenicity in cells. So, ultra-trace determination of Cr is very important in water samples. Many methods developed for Cr extraction in water samples by graphene sorbents. Cr enter the human body through food or drinking water, and its level in the air, water and biological samples is very low. Cr concentration in drinking water is generally less than 2g L^{-1}. The World Health Organization (WHO) states that the guideline values of 50 g L^{-1} for   Cr (VI) is considered as high concentration value in human [11-14]. In this paper, the extraction recovery and absorption capacity of different functionalized graphene for chromium was calculated by SMSPE procedure after synthesis. Also, the behavior of different functionalized graphene for extraction of chromium was investigated and compared together.

The sulfonated (:S^--NG) and amine graphene (:N^+-NG) was used for extraction cations of Cr(III)$^+$ and anions of Cr(VI)$^-$ from water and wastewater samples at pH=4 and pH=2, respectively. Other compounds have low extraction efficiency as compared to (:S-NG) and (:N-NG).

2. Experimental
2.1. Chemical materials
In the present work, acetone, toluene, Thionyl Chloride (SOCl2) >98%, potassium persulphate (KPS) >99.9% and Sodium hydride (NaH)>90% obtained from Sigma-Aldrich. Also Methyl ethanesulfonate (C3H8O3S) >97%, Ethylmethylamine (C3H9N)>98% and Sodium 2-dodecylbenzenesulfonate (SDBS) obtained from ChemSpider. The reagents such as; HNO$_3$, H$_2$SO$_4$, HCl, NaOH, KOH, as analytical grade were purchased from Internal Companies, Iran. Deionized water was purchased from Bahre-e Zolal-e Tehran Company.

2.2. Synthesized and Characterization of Graphene
Graphene was synthesized by chemical vapor deposition (CVD) with methane as a carbon feed under hydrogen atmosphere at 1100°C [15]. Provided graphene is pure with nano sheet structure. The CVD graphene was characterized with X-ray diffraction (XRD) and TEM imaging. X-ray diffraction measurements were carried out using a X-pert Philips diffractometer equipped with a CuKα source (wavelength λ = 0.154 nm). The XRD pattern of CVD graphene was shown in Figure 1. As shown in Figure 1, one high-intensity broad peak was appear about 2θ=26.5 corresponding to (002) diffraction line (d-space 3.4A) plane of graphite. It was proved the pure and crystalline of CVD graphene structure [16]. By using Scherrer equation, the crystalline size of graphene is calculated as 1.8 nm and when it is divided by the distance of graphene layers (3.4 Å), the number of graphene sheets is calculated as 5.3 layers. In order to evaluate the morphology and diameter distribution of the graphene, TEM image was taken for the pristine graphene of CVD. Transmission
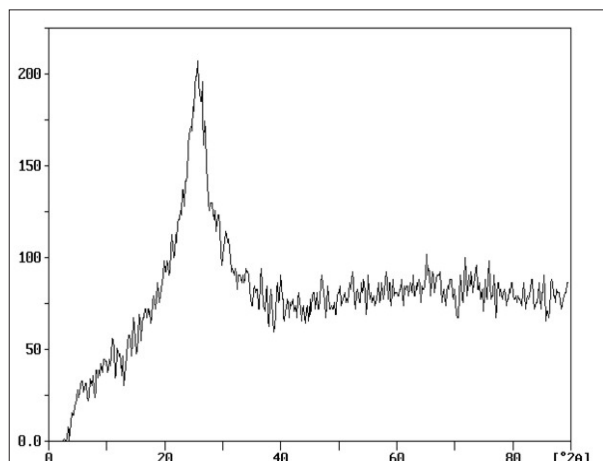
Fig. 1. XRD patterns of CVD Graphene

Fig. 2. TEM image of CVD Graphene

Electron Microscopy (TEM) was carried out using a ZEISS EM900 KNL groups at 100kV. The TEM image of CVD graphene was shown in Figure 2. It exhibits a high magnification TEM image of CVD graphene, showing a completely sheet structure and ordered with few layers [17].

2.3. Surface modification methods for graphene

The main motive of this paper is to provide a framework for using an appropriate functional group from the upcoming options when using graphene nanofluids. Surfactant treatment was used as surface modification methods. Surfactant has been used to disperse graphene, since this prevents them from becoming aggregated over time [18]. These treatments improve the dispersion of graphene in aqueous media. To improve graphene dispersion in water the sheets were dispersed with the aid of SDBS surfactant as follows [19]. The samples formed from graphene treated with SDBS were designated as SDBS-GNSs. The reaction scheme for the treatment of graphene using SDBS shows in Figure 3 (a). Also, basic treatment was used as another way for surface modification methods. For basic treatment, the surface modification of graphene was performed with KPS at 100°C refluxed for 8 hr. as follows [20]. The samples formed from graphene treated with basic method were designated as K-GNSs. The reaction scheme for the treatment of graphene using KPS shows

in Figure 3(b). In addition, surface modification methods flowed by K-GNSs which were treated with SDBS for 24 h at room temperature to obtain surfactant treated K-GNSs [21]. The samples formed from K-GNSs treated with SDBS were designated as SDBS-KGNS. Figure 3(c) gives a schematic diagram of the process of the SDBS-KGNSs. In order to achieve the highest stability, the amount of consumed SDBS was considered twice as much as graphene amount in the fluid. Acid treatment and surfactant based acid treatment were used for functionalized graphene. For acid treatment, the surface modification of graphene was performed with 1:3 mixtures of concentrated HNO_3 and H_2SO_4 at 60 °C for 3 hr. as follows [22]. The samples formed from graphene treated with acid mixture were designated as A-GNSs. The reaction scheme for the treatment of graphene using Acid treatment shows in 3(d). For surfactant – acid treatment, the A-GNSs were treated with SDBS for 24 h at room temperature to obtain surfactant treated A-GNSs as follows [21]. The samples formed from A-GNSs treated with SDBS were designated as SDBS-AGNSs. 3(e) gives a schematic diagram of the process of the SDBS-AGNS. Finally, amidation and sulfate treatment was prepared for this research. For amidation treatment, acyl-chlorinated graphene was added to an amine compound (octa decyl amine). This mixture was sonicated using an ultrasound bath at 70°C for 2
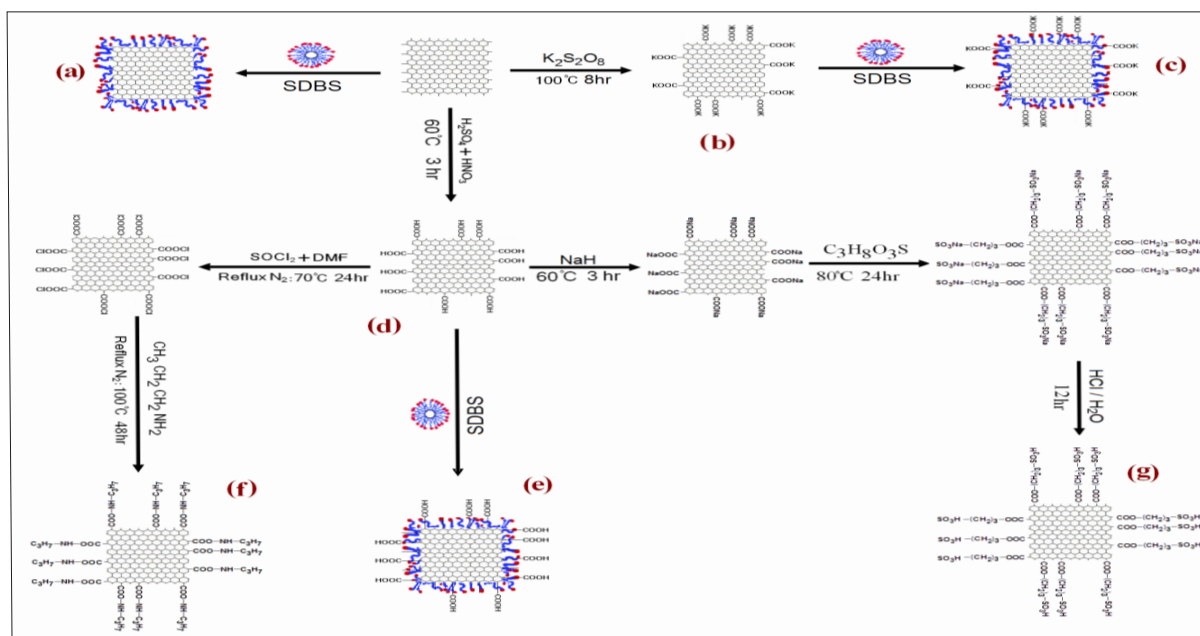
Fig. 3. Schematic representations of surface modification of graphene by (a) Surfactant   (b) alkaline method   (c) Surfactant & alkaline   (d) acid media   (e) Surfactant & acid   (f) Amidation N-NG   (g) Sulfate treatment, S-NG

hr, and then refluxed for 2 days. After cooling to room temperature the product were washed with ethanol to remove excess amine. Finally the black solid was dried at 70°C overnight. The samples formed from graphene treated with amidation were designated as :N-NG. Corresponding chemical reactions are illustrated in 3(f) [22]. For sulfate treatment, graphene was added to anhydrous THF under vigorous mechanical stirring. To replace the terminated Na with H in graphene, sodium hydride (NaH) was added slowly to the graphene/THF mixture at 60°C for 6 hr. Propane sultone was then added drop wise to the mixture, and this mixture was reacted at 80°C for 24 hr. with constant stirring. After the reaction, filtered reactant was immersed into an HCl/water solution for 12 h and then washed with ethanol several times to remove the residuals. The product was dried in vacuum at 70°C for 6 hr. [23]. The samples formed from graphene treated with Sulfate treatment were designated as :S-NG. 3(g) gives a schematic diagram of the sulfonation process of the sulfonated graphene.

2.4. General Procedure
Chromium was separated and determined based on functionalized graphene (S-NG, N-NG) from

water sample with SMSPE coupled by ETAAS. For speciation of chromium, 20 mg of N-NG/S-NG dispersed in 10 mL of standard and water sample at pH=4 and pH=2 for complexation with sulfur and amide group for extraction cations of Cr(III)$^+$ and anions of Cr(VI)$^-$ from water and wastewater samples. After shaking and centrifuging processes, the Cr(III) and Cr (VI) complexation was achieved [Cr$_{III}$→:S-NG, Cr$_{VI}$→:N-NG] and trapped with [HMIM] [PF6] in conical tube. Then, the chromium in remained IL/sorbent back extracted by 0.2 mL of HNO$_3$ (0.4 mol L^{-1})/ NaOH(0.2 M) and finally Cr(III) and Cr (VI) concentration determined with ET-AAS after dilution with DW up to 1 mL. The results showed us, the Cr(III) and Cr(VI) can be extracted by S-NG at and N-NG at pH=4 and pH=2, then back extracted by HNO$_3$ and NaOH. The validation of methodology was confirmed by spiking chromium standard solution and certified reference materials in water (SRM). The optimized conditions were shown in Table 1.

3. Results and Discussion
All parameters for chromium extraction was studied and optimized by graphene sorbents by ET-AAS. The results showed that. The sulfur and amide group

Table 1. The conditions for chromium extraction based on S-NG /IL and N-NG/IL by SMSPE procedure (μg L⁻¹)

Factor	Water	Standard
PF[a]	20.2	20.4
LOD[b]	0.005	0.0045
%RSD[c]	3.9	3.2
Linear range	0.02 – 2.2	0.02 – 2.1
Correlation coefficient	0.9992	0.9996

[a] Preconcentration factor

[b] Limit of detection

[c] Relative standard deviation(V=10 mL, n=10).

of graphene was more extraction of chromium from waters as compared to other function group graphene in this study. The matrix effects in water samples were calculated as extracted chromium from a wastewater matrix to extract chromium from Standard solution by SMSPE-ETAAS procedure (Q1). The recovery efficiency (RE) was obtained by equation Q2.

% ME= (Peak area of the Hg extraction in human matrix)/(Peak area of the Hg extraction in matrix free solution)×100   (Q1)

$$\text{Re cov ery}\% = \frac{(C_i - C_f)}{C_i} \times 100 \qquad (Q2)$$

3.1. FTIR analysis

The presence of variety functional groups were confirmed by FTIR spectra. Therefore in this paper in order to study the structural changes in the graphene after surface modification, FTIR analysis was performed. FTIR spectrometer (Thermo Scientific, Nicolet 6700) was recorded typically 100 scans over the range 450-4000cm⁻¹ were taken from each sample with a resolution of 2 cm⁻¹ and summed to provide the spectra. Figure 4 shows FTIR spectra for prepared of the functionalized graphene. The peak at 1574 cm⁻¹ corresponds to the FTIR-active phonon mode of the graphene. This spectrum peak is assigned to the (C=C) stretching mode associated with graphene edge defects [24]. Peak of 1574 cm⁻¹ can be attributed aromatic structures [25]. The FTIR spectra of the SDBS treated graphene (SDBS-GNSs, SDBS-AGNSs and SDBS-KGNSs) showed peaks at 2924 cm⁻¹, which apparently correspond to the symmetrical stretching of (CH₂), at 1378 cm⁻¹ due to the asymmetrical
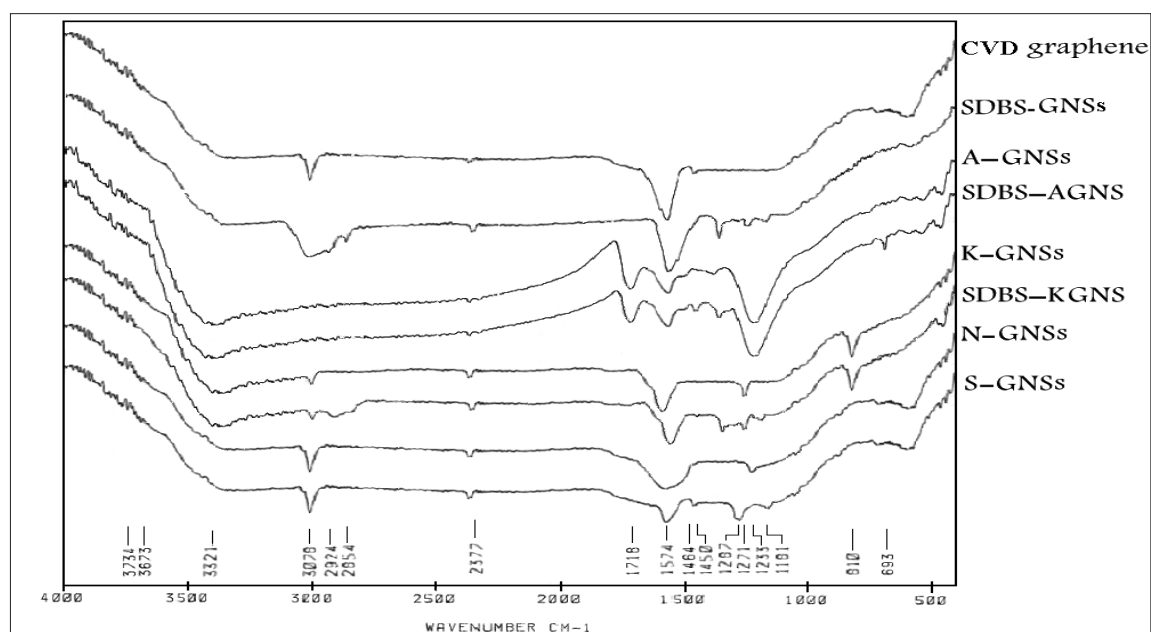
Fig. 4. FTIR spectra for the functional graphene for N-NG (N-GNSs) and S-NG(S-GNSs)

vibration of (CH$_3$) two peaks at 1181 cm^{-1} and 1236 cm^{-1} due to the asymmetrical vibration of (S–O) and (S=O) respectively [26]. These peaks indicate successful adhesive of SDBS on graphene. The broad band of FTIR spectra 3400 cm^{-1} corresponds to the presence of the oxygenated groups [27]. In addition, the spectra of the A-GNSs showed peak at around 1718 (C=O) cm^{-1}, asymmetric and 1079 (C-O) cm^{-1}, apparently corresponding to the stretching mode of the carboxylic acid group (COOH) [24]. These peaks indicate successful generation of (COOH) groups on graphene. In the case of the oxidized graphene by basic treatment with KPS, the two main peaks observed. A peak in the 810 cm-1 due to the symmetrical stretching of the (C–S) [20], and Peaks of 1233 cm^{-1} , 1572 cm^{-1} 1585 cm^{-1} are associated with resonance of the (C-O), stretching of the (C-O), and stretching of the (C=O) respectively related to (-COOK) groups [18]. Therefore, hydroxyls, carboxylate groups in K-GNSs were formation the graphene have been successfully to K-GNSs. The peak observed at 1618 cm^{-1} is associated with the (C=O) bond shifted to 1636 cm^{-1} (amido-functionalized of graphene) [26]. The existence of vibration modes corresponding to (C–N) at 1287 cm^{-1}, (N–H) at 1507 and 3421 cm^{-1} indicate the formation of the amine bond [28].

In the spectrum of S-AGNSs the two main peaks observed, a peak in 1271 cm^{-1} and a peak in 1181 cm^{-1} due to the symmetrical stretching of the (S=O) and (S–O) respectively which have shown typical absorbance for the sulfonic acid groups (SO$_3$H) [17].

3.2. Raman spectroscopy

Raman spectroscopy is a very valuable tool for the characterization of carbon-based nanostructures and confirmed that the structure how mach ruptured after treatment. Raman spectroscopy (Renishaw RM1000 -Invia) was used to investigate graphene structural changes during the surface modification treatments. The ratio between D and G band is a good indicator of the quality on bulk samples and is very important factor in the way that allows distinguishing between the functional graphene samples after treatment with different agents. The degree of functionalization can be estimated by the intensity of the D and G band [19]. Figure 5 shows the Raman spectrum of the samples reported in Table 1.

These typical peaks, which still present after surface treatments were prove the structure of graphene didn't damage during that varies treatments. Generally the ratio of I$_D$/I$_G$ is increased
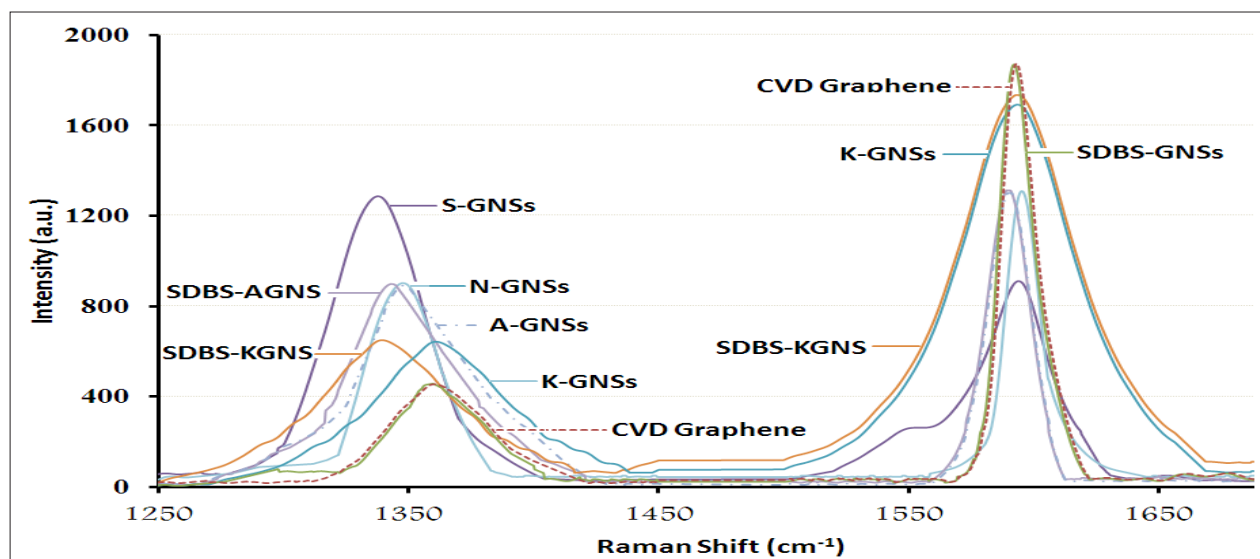

Fig. 5. *Raman spectra of CVD and Functionalized graphene after treatment with different agents* The D band of Raman spectra of CVD graphene is 1361 cm^{-1} and its intensity (I$_D$) is 455 and the G band is 1592 cm^{-1} and its intensity (I$_G$) is 1853 so its I$_D$/I$_G$= 0.246.

Table 2. I_D/I_G ratio of the functionalized graphene

Intensity	I_D	I_G	I_D/I_G
CVD graphene	455	1853	0.246
SDBS-GNSs	458	1871	0.245
K-GNSs	641	1691	0.379
SDBS-KGNS	648	1732	0.374
A-GNSs	893	1302	0.686
SDBS-AGNS	898	1312	0.684
N-GNSs	901	1308	0.689
S-GNSs	1288	911	1.414

for functionalized graphene as compared to CVD graphene in all treatment methods. It means that chemical treatments of graphene breaks some bonds and insert functional groups that can be considered as defects on the structure. The I_D/I_G ratio of functional graphene was summarized in Table 2. Sulfate treatment gave larger I_D/I_G (1.414) than amidation (0.689) and other method treatment of graphene. The measured intensity I_D/I_G ratio of the functionalized graphene were in the order of S-GNSs > N-GNSs> A-GNSs > SDBS-AGNS > K-GNSs >K-GNSs > SDBS-GNSs.

3.3 Preparing and Stability of graphene nanofluids
The dispersion stability of nano structures is an important factor in fabricating uniformly dispersed NFs. The thermal properties of the resulting NFs will also be strongly influenced by the dispersion stability of graphene. In order to prepare the samples (graphene NFs), two-step process was used. Functionalized graphene with the 0.075wt% mix up with deionized water (DI) and place in the ultrasonic bath (frequency range 20 kHz and power of 80 watts) for 60 min. The specifications of the samples were tabulated on Table 3.

Figure 6 shows the pictures of the functionalized graphene which dispersed in water. Sample (1), includes CVD graphene without any treatment, instability of graphene was observed. Therefore CVD graphene without any treatment has poor dispersion stability in water [29].   Sample (2), includes graphene with SDBS, few aggregations was observed. However, in samples 3~8 good dispersion were observed which functionalized
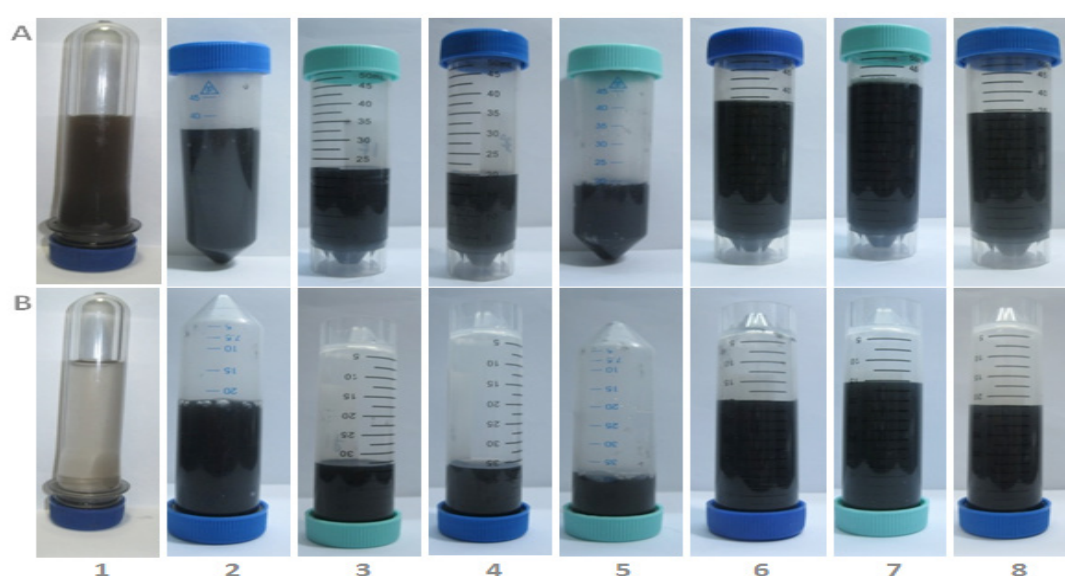
Fig. 6. The images of the dispersed graphene in water (a) immediately after sonication, (b) after 7 days (1)CVD graphene, (2)SDBS-GNS, (3)K-GNSs, (4)SDBS-KGNS, (5)A-GNSs, (6)SDBS-AGNS, (7)N-GNSs & (8)S-GNSs

**Table 3.** Specification of 0.075wt% functionalized graphene nanofluids

Sample	Nano Structure	Type of Treatment	Type of Agent
1	CVD graphene	----------	---------
2	SDBS-GNSs	Surfactant	SDBS
3	K-GNSs	Alkaline	$K_2S_2O_8$-KOH
4	SDBS-KGNS	Surfactant - Basic	SDBS-$K_2S_2O_8$
5	A-GNSs	Acid	H_2SO_4-HNO_3
6	SDBS-AGNS	Surfactant - Acid	SDBS-H_2SO_4
7	N-GNSs	Amine	Octa Decyl Amine
8	S-GNSs	Sulfate	THF-NaH

graphene was used with different treatments.

The results of stability were semi quantified by measuring the absorbance of visible light [30]. The dispersion stability of the surface-modified graphene in water was measured by UV–visible spectroscopy (UVS-2100 SCINCO spectrophotometer between 200 and 1100nm) at ambient temperature. If the nanomaterials dispersed in fluids have characteristic absorption bands in the wavelength 200–1100 nm, it is an easy and reliable method to evaluate the stability of nanofluids using UV-vis spectral analysis. The Samples were diluted up to the extents that were suitable for UV–VIS measurements. Figure 7 shows the peak absorbance of the samples around the range of 220-290 nm. As shown in Figure 7, the high peak of the SDBS-AGNS, A-GNSs show a well dispersion in water. Significant increase in their absorbance

is good agreement (Fig. 7). According to Figure 7, N-CNTs and S-CNTs also show fine dispersion in water. After 7 days, the suspensions were still homogeneous but for the SDBS-GNSs scarcely any sedimentation was observed. This is due to the fact that the defect of the graphene carries more dissociated (-COO) groups, which can stabilize the nano sheets via an electrostatic stabilization mechanism [31].

Furthermore, the SDBS present will act as a self-assembly template. Consequently, functionalized treatments have a different stability and dispersion for graphene in water. The measured dispersion stabilities are in the order of SDBS-AGNS > A-GNSs > SDBS-KGNS > K-GNSs > S-GNSs > SDBS-GNS > N-GNSs. The results showed us, maximum Cr (III) extracted by S-GNSs and extraction efficiency in the order of S-GNSs >
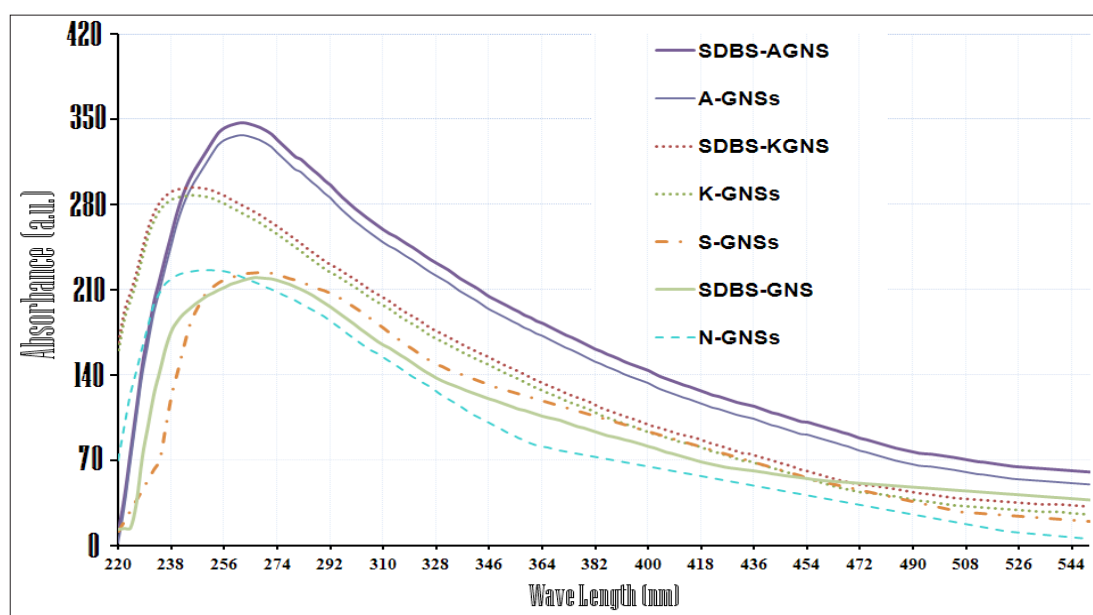
Fig. 7. UV–visible spectra of surface-modified graphene nanofluids

SDBS-GNS > SDBS-KGNS> SDBS-AGNS> N-GNSs> K-GNSs, respectively. Also, Cr (VI) extracted by N-GNSs and extraction efficiency in the order N-GNSs> K-GNSs> SDBS-AGNS, respectively.

3.4. Thermal conductivity variations vs. temperature

Thermal conductivities of the graphene /water NFs were measured by KD2 Pro thermal properties analyzer (Decagon devices, Inc., USA). The instrument had a specified accuracy of 0.1% and meets the standard of IEEE 442-1981. The instrument had a probe of 60 mm length and 1.3mm diameter, a thermo resistor and a microprocessor to control and measure the conduction in the probe. The instrument had a specified accuracy of 5%. In order to obtain precise results, the sample and the probe were maintained at constant temperature for about 15 min. In order to study the effect of temperature, a thermostat bath was used, which meets the standards of ASTM D5334 at temperature range of 10 to 60. Each data presented is the average value of the measurements from five tested the samples. In general, compare to base fluid, thermal conductivity of NFs is more sensitive due to temperature and increases with increasing of temperature. In order to study the temperature effect on thermal conductivity of the samples a thermostat bath was used. Experimental data were indicate

thermal conductivity of the samples involving functionalized graphene/water NFs increases with temperature and the results were shown in Figure 8. The thermal conductivity of all samples was dramatically increased by the introduction of the graphene. Among the samples, the highest thermal conductivity value (0.728w/mK) was observed for SDBS-KGNS and then (0.704w/mK) K-GNSs.

This may be due to the fact that after their oxidation by the base treatment, the surfaces of graphene contain more function groups. According to Boehm titration, results were observed functional group in alkaline method is about 3%, while the acid treatment is top 5%. Alkaline method usually provides less functional group than acid treatment but provides more stability. It must be noted that alkaline treatment was done in a mild condition, thus the structure of graphene at acid treatment would be more damage than alkaline treatment. Based on Brownian motion of fluids, the functionalized graphene move fast in the water, so that energy transport inside the liquid becomes strong and thermal conductivity increases [33]. Therefore, thermal conductivity gradually ascends in the functionalized graphene /water nano fluids by increasing of temperature. According to Figure 8, by increasing temperature, there are semi linear increases for thermal conductivity of all the samples. For example, thermal conductivity of the
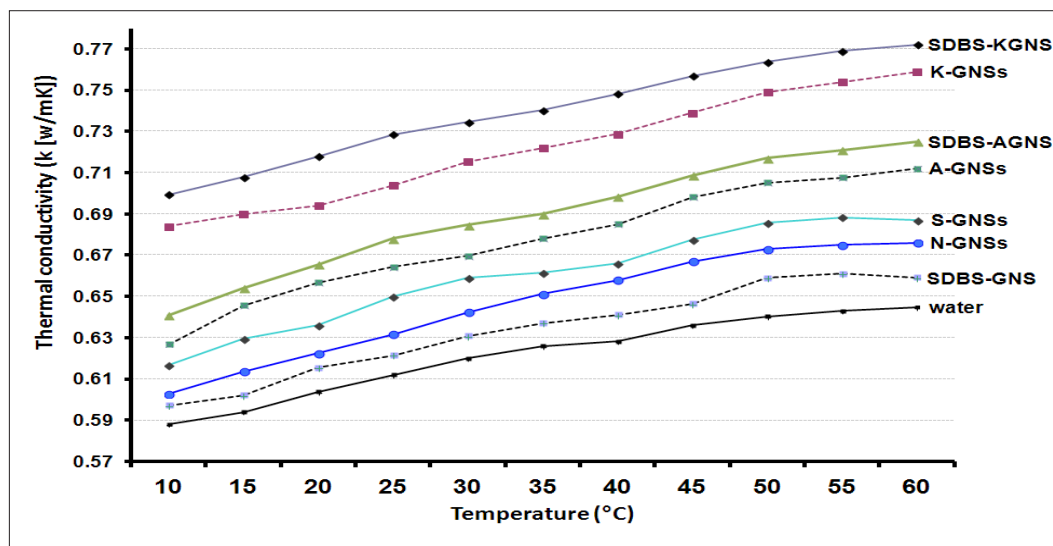

Fig. 8. Thermal Conductivity of the samples vs. Temperature

Table 4. Thermal conductivity of 0.1wt% functionalized graphene nanofluids

Samples	nano structure	k @ 25°C	k @ 60°C	Improvement (%)
		(w/m.K)		
1	water	0.612	0.645	5.39
2	SDBS-GNSs	0.621	0.659	6.12
3	K-GNSs	0.704	0.759	7.81
4	SDBS-KGNS	0.728	0.772	6.04
5	A-GNSs	0.664	0.712	7.23
6	SDBS-AGNS	0.678	0.725	6.93
7	N-GNSs	0.632	0.676	6.96
8	S-GNSs	0.650	0.687	5.69

SDBS-KGNS increases about 10.5% at 10 to 60°C and 18.9% enchantment for SDBS-KGNS compare to water at 25°C. Table 4 represents the measured thermal conductivity of 0.1wt% functionalized graphene NFs. For Cr(III) and Cr (VI) analysis with electrochemistry , thermal conductivity is main factor for cyclic voltammetry analysis(CVA) at upper 60°C.

3.5 Optimizing of Parameters

The pH of the sample solution is an important factor for quantitative extraction of chromium in waters [34-37]. The pH was affected on surface charge of the graphene or function group of graphene (FNG) for separation of chromium from liquid phase by SMSPE procedure. So, the effect of sample pH on the chromium recovery by NG and FNG was examined in pH ranges from 1 to 12 by using buffered sample solutions containing 0.2-2 μg L^{-1} of chromium. The recovery of Cr (III) and Cr(VI) extraction for sulfonated (S-NG) and amidation graphene (N-NG) was obtained at pH=4 and pH=2, respectively (more than 96%, Fig. 9). Also, Cr(VI) can be extracted by S-NG at pH=1-3.

Also, the effect of amount of sulfonated and amine graphene (S-NG, N-NG) by ionic liquid [HMIM][PF$_6$] for chromium extraction in waters was investigated. The various amounts of S-NG,
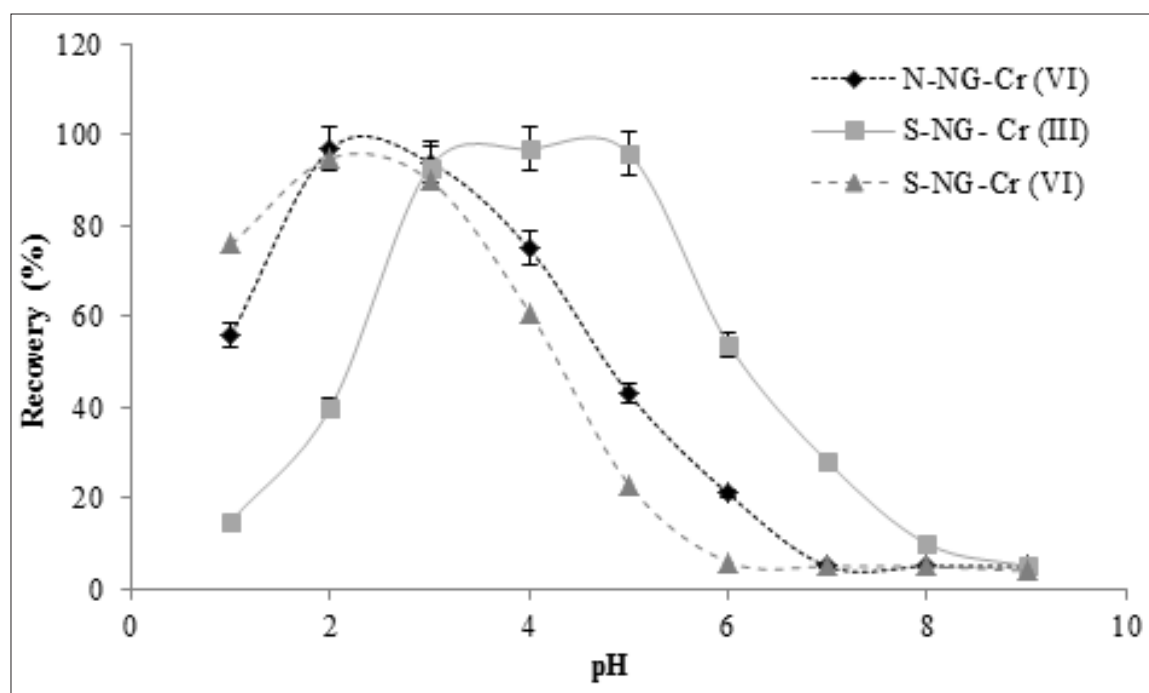
Fig. 9. The effect of pH on chromium extraction by FNG

N-NG in the ranges of 2 to 30 mg were studied, respectively. Other modified graphene set aside from study because of low efficient recovery as compared to S-NG and N-NG sorbents. The results showed, the amount of 12 mg of both graphene was efficient extracted in present of [HMIM][PF$_6$] in waters. So, 15 mg of sorbents were considered as the optimum mass (Fig. 10).

The volume of samples for extraction of chromium was tested by proposed method and 10 mL of sample volume selected for further study (Fig. 11).

Also, some inorganic acid prepared for back extraction of chromium (III) from S-NG was examined and finally, 0.2 mL of HNO$_3$, 0.4 mol L^{-1} (0.4 M) was obtained by optimizing (Fig. 12). The 0.2 mL 0f NaoH (0.2 M) used for back extraction of Cr (VI) as optimized reagent for N-NG at pH=2.

The different mass of vary ILs was used for extraction chromium by S-NG, N-NG. I n
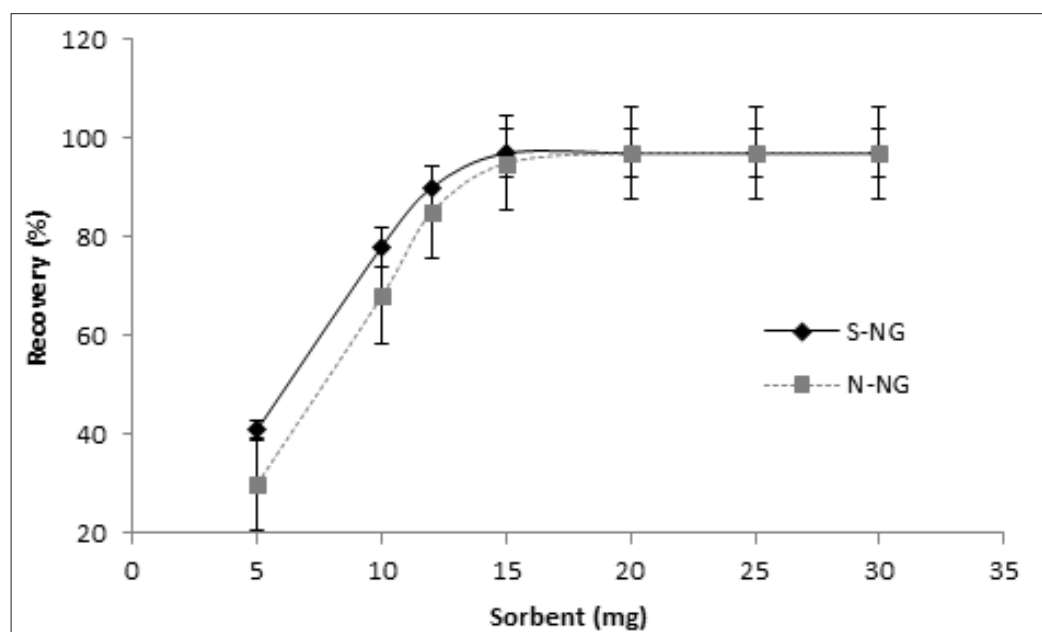
Fig. 10. The effect of amount of FNG on chromium extraction
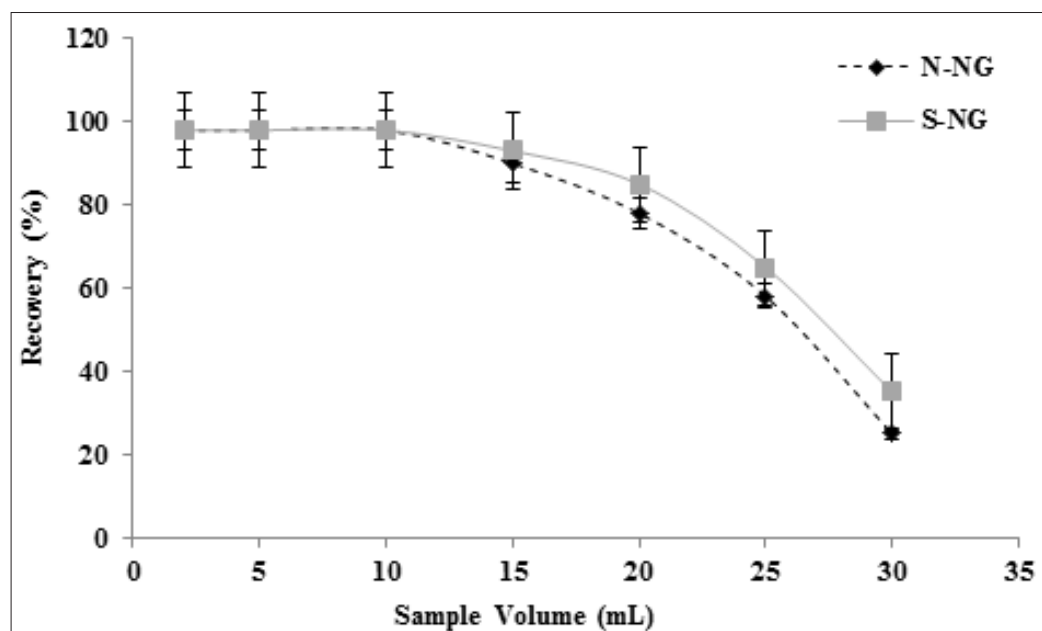
Fig. 11. The effect of sample volume on chromium extraction by FNG
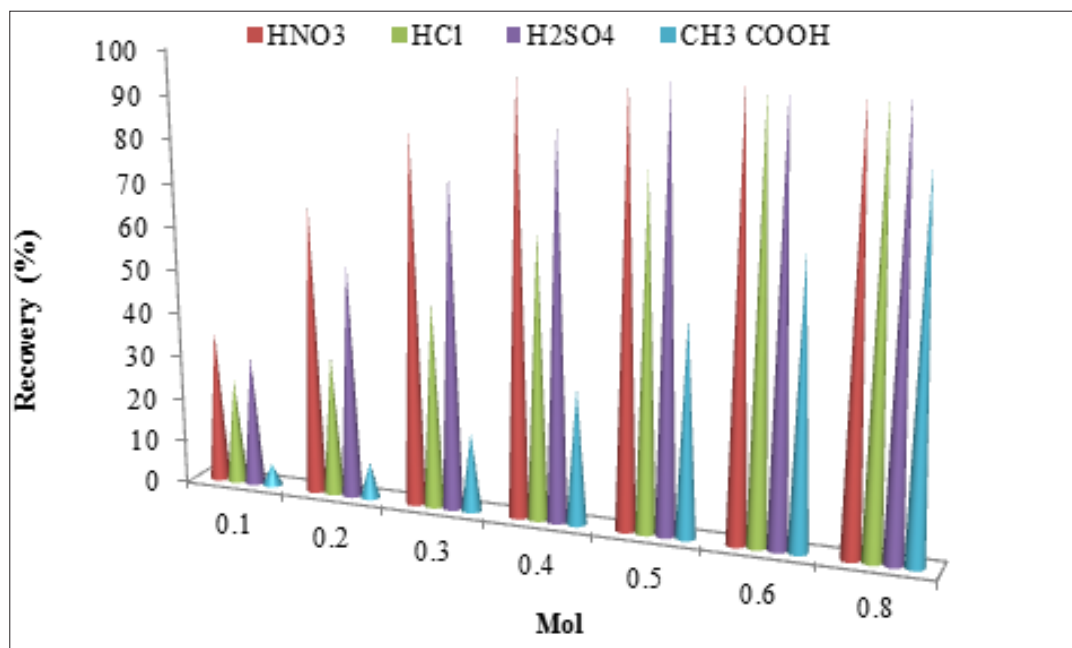
Fig. 12. The effect of inorganic and organic acids on Cr(III) back extraction by S-NG

optimized conditions, 80 mg of $[HMIM][PF_6]$ had more efficiency for chromium extraction by procedure (Fig. 13).

 The SMSPE method based on S-NG, N-NG was used for real samples, the interference of some coexisting ions encountered in water samples on the recovery of Cr (III) ions was investigated in optimized condition. This procedure was performed by adding various amounts of the interfering ions to

10 mL of standard sample solution containing 2.5 $\mu g\ L^{-1}$ of Cr (III) and Cr(VI). The results showed, the most of the concomitant had no considerable effect on chromium extraction (less than 5%).

3.6. Validation of speciation chromium by FNG
The chromium complexation was evaluated with different modified graphene as novel Nano-materials by SMSPE method. The analysis of
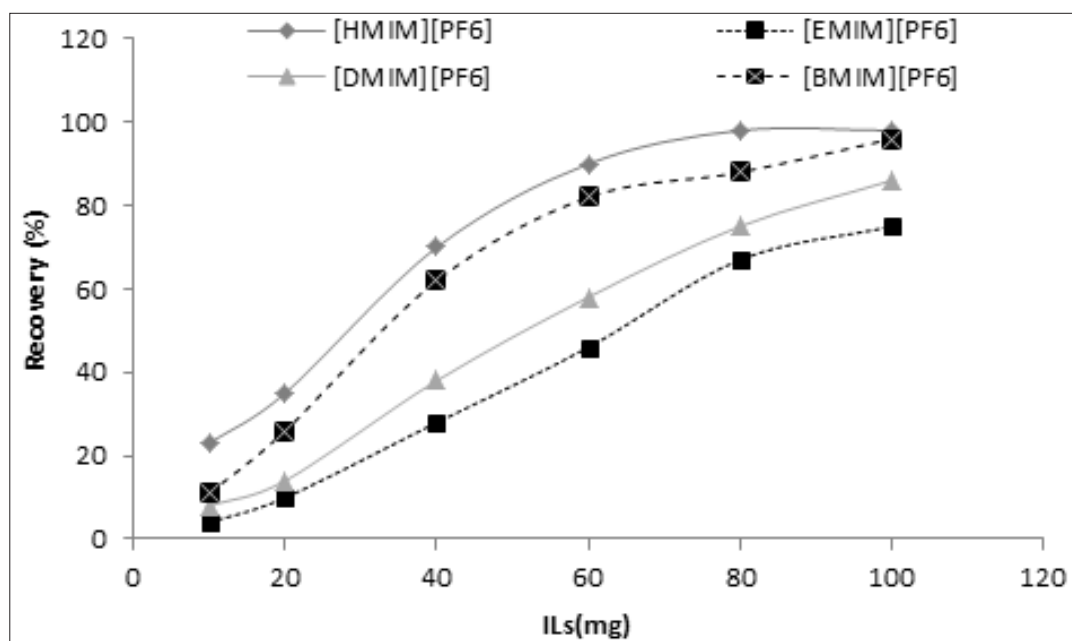
Fig. 13. The effect of different ILs on chromium extraction by FNG

chromium was validated by spiking chromium standard solution to real water samples. Based on result; S-NG is good adsorbent for chromium extraction by SPE. The SMSPE procedure was used for trace chromium analysis in water and wastewater samples. The experimental results based on average of three determinations, for Cr (III) were achieved in real water samples. For evaluation, real samples in standard and water samples was validated by chromium spiking to real samples (Table 5). The good recovery and accuracy with S-NG was achieved by proposed method in water and wastewater samples. The mean recoveries of spiked samples were satisfactory obtained at 98.6%. Also, The high recovery with N-NG was achieved for Cr (VI) by proposed method in water and wastewater samples. The recoveries of spiked samples were satisfactory obtained more tha 95% (Table 6).

4. Conclusions

NG and FNG was synthesis and used for chromium

Table 5. Validation of SMSPE method based on S-NG /IL by spiking of mercury standard concentration in water samples ($\mu g\ L^{-1}$)

Sample	Added	Found [a]	Recovery (%)
	Cr (III)	Cr (III)	Cr (III)
Drinking Water	-----	0.17 ± 0.01	-----
	0.2	0.38 ± 0.02	105
	0.4	0.56 ± 0.04	97.5
River Water	-----	1.04 ± 0.05	-----
	1.0	1.99 ± 0.09	95
	1.5	2.47 ± 0.12	96.3
Wastewater	-----	0.88± ٠,04	-----
	1.0	1.89 ± 0.10	101
	1.5	2.36 ± 0.12	98.6
Wastewater*	-----	1.22 ± 0.05	-----
	1.0	2.19 ± 0.11	97
	2.0	3.15 ± 0.14	96.5

[a] Mean of three determinations ± confidence interval (P= 0.95, n=10)

* Wastewater diluted with DW 1:10

Table 6. Validation of SMSPE method based on N-NG /IL by spiking of mercury standard concentration in water samples ($\mu g\ L^{-1}$)

Sample	Added	Found [a]	Recovery (%)
	Cr (VI)	Cr (VI)	Cr (VI)
Tab Water	-----	0.113 ± 0.014	-----
	0.1	0.209 ± 0.017	96.0
	0.2	0.315 ± 0.026	101.1
Well Water	-----	0.503 ± 0.025	-----
	0.5	0.997 ± 0.048	98.8
	1.0	1.498 ± 0.073	99.5
Wastewater of petrochemical factory	-----	1.011 ± ٠,٠57	-----
	0.5	1.495 ± 0.074	96.8
	1.0	2.033 ± 0.096	102.2
Wastewater of color factory	-----	0.954 ± 0.044	-----
	0.5	1.443 ± 0.063	97.8
	1.0	1.938 ± 0.121	98.4

[a] Mean of three determinations ± confidence interval (P= 0.95, n=10)

extraction (CrIII ,Cr VI) in water samples by SMSPE procedure. An effective function treatment was reported for graphene by using KPS as oxidant in alkaline media to prepare graphene stable solution. The atomic structure in the functional groups, as well as their method and mechanism of their stabilization on graphene, are two essential factors that can determine the phenomenon in graphene nanofluids. Surface and amine modification of graphene based on SMSPE was used for separation/ preconcentration of Cr(III) and Cr(VI) in waters, repetively. The results showed us, the surface modification of graphene has a strong influence on the dispersion stability, thermal conductivity of NG and help to chemically adsorption of chromium speciation. The FNG (S-NG and N-NG) can be extracted chromium in different pH by physical and chemical adsorption. All of FNG such as SDBS-GNSs, K-GNSs, SDBS-KGNS, A-GNSs, SDBS-AGNS, N-GNSs and S-GNSs can be extracted chromium with different recovery by proposed method. The results showed, N-GNSs (Cr_{VI}) and S-GNSs (Cr_{III}) had more efficient recovery for chromium extraction from waters by chemical adsorption. The developed method based on N-GNSs and S-GNSs was low interference, simple and easy preparation, low RSD% and high precision /recoveries for chromium speciation/ extraction n water and wastewater samples (more than 96%).

5. References

[1] C. He, Z. Yang, J. Ding, Y. Chen, X. Tong, Y. Li , Effective removal of Cr(VI) from aqueous solution by 3-aminopropyltriethoxysilane-functionalized graphene oxide. Colloid Surf. Physicochem. Eng. Asp., 520 (2017) 448–458.

[2] L. Wang., D. Han., J. Luo, Li T., Z. Lin., Y. Yao, Highly efficient growth of boron nitride nanotubes and the thermal conductivity of their polymer composites, phys. Chem. C, 122 (2018) 1867-1873.

[3] C.T. Hsieh, Y.F. Chen, C.E. Lee, Y.M. Chiang, H. Teng, Thermal transport in stereo carbon framework using graphite nanospheres and graphene nanosheets, Carbon, 106 (2016) 132-141.

[4] A.B. Showkat, A. Tariq, A. Moheman, Z. Ngaini, Functionalized graphene nanocomposites for water treatment, functionalized graphene nanocomposites and their derivatives synthesis, processing and applications micro and nano technologies, Chapter 5 (2019) 98-107

[5] H.J. Salavagione, M.A. Gomez, G. Martinez, Polymeric modification of graphene through esterification of graphite oxide and poly(vinyl alcohol), Macromol., 42 (2009) 6331-6334.

[6] L. Sun , T. Wang , M. Wu , Z. Wang , Y. Yang , G. Pan , Inhibiting the corrosion-promotion activity of graphene, Chem. Mater., 27 (2015) 2367-2373.

[7] B. Ramezanzadeh, S. Niroumandrad, A. Ahmadi, M. Mahdavian, M.H. Mohamadzadeh, Enhancement of barrier and corrosion protection performance of an epoxy coating through wet transfer of amino functionalized graphene oxide, Corros. Sci., 103 (2016) 283-304.

[8] Y.C. Seong, K. Minsu, K. Min, L. Min, K. Bum Kim, Effect of Cu surface treatment in graphene growth by chemical vapor deposition, Mater. Lett., 236 (2019) 403-407

[9] S. Li, K. Tu, C. Lin, C.W. Chen, Chhowalla M., Solution-processable graphene oxide as an efficient hole transport layer in polymer solar cells, ACS Nano, 4 (2010) 3169-3174.

[10] M. Lotya, Y. Hernandez, P.J. King, R.J. Smith, Nicolosi V., Karlsson L.S., Liquid phase production of graphene by exfoliation of graphite in surfactant/ water solutions, Am. Chem. Soc., 131 (2009) 3611-3620.

[11] P. Liang, H. Sang, Speciation of chromium in water samples with cloud point extraction separation and preconcentration and determination by graphite furnace atomic absorption spectrometry, J. Hazard. Mater., 154 (2008) 1115–1119.

[12] H Shirkhanloo, M Ghazaghi, HZ Mousavi, Chromium speciation in human blood samples based on acetyl cysteine by dispersive liquid– liquid biomicroextraction and in-vitro evaluation of acetyl cysteine/cysteine for decreasing of hexavalent chromium concentration, J. pharm. Biomed. Anal.,118 (2016) 1-8.

[13] A. Zhitkovich, Importance of chromium-DNA adducts in mutagenicity and toxicity of chromium

(VI), Chem. Res. Toxicol., 18 (2005) 3–11.

[14] M.S. Hosseini, F. Belador, Cr(III)/Cr(VI) speciation determination of chromium in water samples by luminescence quenching of quercetin, J. Hazard. Mater., 165 (2009) 1062–1067

[15] A. Ghozatloo, M. Shariaty-Niasar, A.M. Rashidi, Preparation of nanofluids from functionalized Graphene by new alkaline method and study on the thermal conductivity and stability, Int. Commun. Heat Mass, 42 (2013) 89–94.

[16] W. Guoxiu, Y. Juan, J. Park, G. Xinglong, B. Wang, H. Liu, J. Yao, Facile synthesis and characterization of graphenee nano sheets, Phys. Chem. C, 112 (2008) 192–195.

[17] L. Luqi, Z. Shuang, H. Tengiao, G. Zhi-Xin, Solubilized multi walled carbon nanotubes with broadband optical limiting effect, Chem. Phys. Lett., 359 (2009) 191-195.

[18] T.M. McCoy, G. Turpin, M. Teo, R.F. Tabora, Graphene oxide: surfactant or particle, curr. Opin. in colloid interface Sci., 39 (2019) 98-109.

[19] L. Jiang, L. Gao, J. Sun, Production of aqueous colloidal dispersions of carbon nanotubes, Colloid Interface Sci., 260 (2003) 89-94.

[20] O. Park, T. Jeevananda, N.H. Kim, S. Kim, L.J. Hee, Effects of surface modification on the dispersion and electrical conductivity of carbon nanotube/polyaniline composites, Scripta Mater., 60 (2009) 551–554.

[21] J.Y. Hye, H.K. Kyoung, K.Y. Santosh, W.C. Jae, Effects of carbon nanotube functionalization and annealing on crystallization and mechanical properties of melt-spun carbon nanotubes/poly(ethylene terephthalate) fibers, Composites Sci. Technol., 72, (2012) 1834–1840

[22] S. Safari Kish, A.M. Rashidi, H.R. Aghabozorg, L. Moradi, Increasing the octane number of gasoline using functionalized carbon nanotubes, Appl. Surf. Sci., 256 (2010) 3472–3477.

[23] H. Yuseon, I.M. Hyungu, K. Jooheon, The effect of sulfonated graphene oxide on sulfonated poly membrane for direct methanol fuel cells, Membrane Sci., 425 (2012) 11-22.

[24] C.A. Dyke, J.M. Tour, Covalent functionalization of single-walled carbon nanotubes for materials appli-cations, Phys. Chem., 108 (2004) 151-159.

[25] Y.Rike, O. Holia, S. Sudirman, S. Yukie, I. Tadahisa, I. Jun, Analysis of functional group sited on multi-wall carbon Nanotube surface, The Open Mater. Sci., 5 (2011) 242-247.

[26] H. Arıa, Z. Büyükmumcub, T. Özpozanb, Vibrational spectroscopic study of isotopic effect on TcX^{3+} and TcX_3OH (X: O, S and Se) by DFT, Mol. Structure, 1165 (2018) 259-266.

[27] C. Li, J. Lin, S. Huang, J. Lee, C. Chen, A new and acid exclusive method for dispersing carbon multi walled nanotubes in aqueous suspensions, Colloids Surf. A: Physicochem. Eng. Aspects, 297 (2007) 275-281.

[28] R. Wang, H. Fan, W. Jiang, G. Ni, Amino-functionalized graphene quantum dots prepared using high-softening point asphalt and their application in Fe^{3+} detection, App. Surf. Sci., 467 (2019) 446-455.

[29] J. Paredes, S. Villar-Rodil, A. Martinez-Alonso, J.M.D. Tascon, Graphene oxide dispersions in organic solvents, Langmuir, 24 (2008) 560-566.

[30] V. G. Kravets, A.N. Grigorenko, R.R. Nair, P. Blake, S. Anissimova, K.S. Novoselov, Spectroscopic ellipsometry of graphene and an exciton-shifted van Hove peak in absorption, Phys. Rev. B, 81 (2010) 413-422.

[31] S. Vadukumpully, J. Paul, N. Mahanta, S. Valiyaveettil, Flexible conductive graphene/poly(vinyl chloride) composite thin films with high mechanical strength and thermal stability, Carbon, 49 (2011) 198-211.

[32] S. Ganguli, A.K. Roy, D.P. Anderson, Improved thermal conductivity for chemically functionalized exfoliated graphite/epoxy composites, Carbon, 46 (2008) 806-812.

[33] X.B. Sun, P. Ramesh, M.E. Itkis, E. Bekyarova, R.C. Haddon, Dependence of the thermal conductivity of two-dimensional graphite nanoplatelet-based composites on the nanoparticle size distribution, Phys, Condens Mat., 22 (2010) 4216-4223.

[34] T.S. Munonde, N.W. Maxakato, P.N. Nomngongo, Preconcentration and speciation of chromium species using ICP-OES after ultrasound-assisted magnetic solid phase extraction with an amino-modified magnetic nanocomposite prepared from Fe_3O_4, MnO_2 and Al_2O_3, Microchim. Acta, 184

(2017)1223–1232.

[35] H. Peng, N. Zhang, M. He, B. Chen, B. Hu, Simultaneous speciation analysis of inorganic arsenic, chromium and selenium in environmental waters by 3-(2-aminoethylamino) propyl trimethoxysilane modified multi-wall carbon nanotubes packed microcolumn solid phase extraction and ICP-MS, Talanta, 131 (2015) 266–272

[36] A. Sheikhmohammadi, S.M. Mohseni, R. Khodadadi, M. Sardar, M. Abtahi, S. Mahdavi, H. Keramati, Z. Dahaghin, S. Rezaei, M. Almasian, M. Sarkhosh, M. Faraji, S. Nazari (2017) Application of graphene oxide modified with 8-hydroxyquinoline for the adsorption of Cr (VI) from wastewater: Optimization, kinetic, thermodynamic and equilibrium studies, J. Mol. Liq., 233 (2017) 75–88.

[37] X. Qia, S. Gao, G. Ding, A.N. Tang, Synthesis of surface Cr (VI)-imprinted magnetic nanoparticles for selective dispersive solid-phase extraction and determination of Cr (VI) in water samples, Talanta, 162 (2017) 345–353.

A novel sorbent based on metal–organic framework for mercury separation from human serum samples by ultrasound assisted- ionic liquid-solid phase microextraction

Negar Motakef-Kazemi[a,*]

[a,*] *Department of Medical Nanotechnology, Faculty of Advanced Sciences and Technology, Tehran Medical Sciences, Islamic Azad University, Tehran, Iran.*

A B S T R A C T

In this research, the metal–organic framework (MOF) as a solid phase was used for separation mercury [Hg (II)] inhuman serum sample by ultrasound assisted- Ionic Liquid-solid phase microextraction procedure (USA- IL-μ-SPE). Mercury extracted from serum sample by $[Zn_2(BDC)_2(DABCO)]_n$ as MOF at pH=8. Hydrophobic ionic liquid ([BMIM] [PF6]) was used as solvent trap for Hg-MOF-NC from the sample solution. The phase of Hg-MOF-NC was back extracted by 0.5 mL of HNO_3 (0.2 mol L-1) and finally mercury concentration determined with cold vapor-atomic absorption spectrometry (CV-AAS) after dilution with 0.5 mL of DW. Under the optimal conditions, the linear range, limit of detection and preconcentration factor were obtained 0.02– 5.5 μg L^{-1}, 6.5 ng L^{-1} and 9.8 for serum samples, respectively (%RSD<5%). The validation of methodology was confirmed by standard reference materials (SRM).

1. Introduction

Today, metal-organic frameworks have received considerable attention as porous coordination polymers (PCPs) and porous hybrid organic–inorganic materials because of their unique properties [1-2]. MOFs can be synthesized via self-assembly of metal ions (or metal clusters) as metal centers, and bridging ligands as linkers [3-4]. In recent years, MOFs wildly have been studied for their potential applications in many areas such as gas storage [5], separation [6], catalysis [7], optics

[8], photonic [9], ion exchange [10], molecular array [11], biomedicine [12], sensing [13], drug delivery [14], luminescent [13, 15], magnetic [16], and semiconductors [17]. Several methods have been proposed to remove hazardous materials from water such as electrochemical [18], chemical coagulation [19], reverse osmosis membrane [20], and adsorbent [21-23]. The absorbent materials have been studied for different species such as nitrobenzene [24-26], phenol [27], p-xylene hydrocarbon [28], dye [29-32], heavy metal [33-34], humic acid [35], and nitrate [36-37] from the waste water. Mercury is a chemical element and heavy metal with very toxic effect. This non-essential metal can be distributed

in the environment, natural products, and human body [38-39]. The exposure to high mercury can be resulted to the changes in the central nervous system, irritability, fatigue, behavioral changes, tremors, headaches, hearing and cognitive loss, dysarthria, incoordination, and hallucinations [40]. Mercury compounds can be harmed the liver and kidneys, resulting some disorder in enzyme activity, illness, and death [41-42]. Recently, the applications of mercury adsorbents are expanded due to increased level and toxic effect [43-44]. In present study, $Zn_2(BDC)_2(DABCO)$ MOF was synthesized by solvothermal method for mercury absorption from serum and standard solution with CV-AAS by USA- IL-μ-SPE procedure. The 1-octyl-3-methylimidazolium hexafluorophosphate ($[OMIM][PF_6]$) as a hydrophobic ionic liquid was used for separating of Hg-MOF from liquid phase. The proposed method was validated by spike of real samples and CRM (NIST).

2. Experimental
2.1. Reagents and Materials
All reagents with high purity and analytical grade were purchased from Merck (Darmstadt, Germany), unless otherwise stated. Materials including zinc acetate ehydrate ($Zn(Oac)_2.2H_2O$), 1,4 benzenedicarboxylic acid (BDC), 1,4-diazabicyclo [2.2.2] octane (DABCO), dimethylformamide (DMF) were used for synthesis of $Zn_2(BDC)_2(DABCO)$ MOF. All aqueous solutions were prepared in ultra-pure deionized water (R≥18 MΩ cm^{-1}) from Milli-Q plus water purification system (Millipore, Bedford, MA, USA). An Hg (II) standard stock solution (1000 mg L^{-1} in 1% nitric acid, 250 mL) was purchased from Fluka, Buchs, Switzerland. The experimental and working standard solutions were prepared daily by diluting the stock solutions with deionized water. The solutions were freshly prepared and stored just in a fridge (4 °C) to prevent decomposition. A 0.6% (w/v) sodium borohydride reagent solution was prepared daily by dissolving an appropriate amount of $NaBH_4$ in 0.5% (w/v) sodium hydroxide and used as a reducing agent. 1-butyl-3-methylimidazolium hexafluorophosphate

[HMIM][PF6] was obtained from Sigma–Aldrich (M) Sdn. Bhd., Malaysia. The pH adjustments of samples were made using nitric acid (0.1 mol L^{-1}) for pH 1-2, and appropriate buffer solutions including sodium acetate (CH_3COONa/CH_3COOH, 1-2 mol L^{-1}) for pH 3.75-5.75, sodium phosphate (Na_2HPO_4/NaH_2PO_4, 0.2 mol L^{-1}) for pH of 5.8-8.0, and ammonium chloride (NH_3/NH_4Cl, 0.2 mol L^{-1}) for pH 8-10. All the laboratory glassware and plastics were cleaned by soaking in nitric acid (10%, v/v) for at least 24 h and then rinsed with deionized water before use. Due to hazardous effects of Hg solutions, gloves, safety mask, and laboratory hood should be used when mercury standard solutions are prepared.

2.2. Characterization
The MOF was characterized by Fourier transform infrared spectroscopy (FTIR), powder X-ray diffraction (XRD), and scanning electron microscope (SEM). FTIR spectra were recorded on a Shimadzuir 460 spectrometer in a KBr matrix in the range of 400–4000 cm^{-1}. Powder X-ray diffraction pattern was performed for evaluation of crystalline structure of bismuth oxide NP using a Philips Company X'pert diffractometer utilizing Cu-Ka radiation (ASENWARE, AW-XBN300, China). Scanning electron microscope was investigated the morphology and MOF (KYKY, EM3200, China). Determination of mercury was performed with an atomic absorption spectrometer (GBC 932– HG3000-AUS, Australia) equipped with a flow injection cold vapor module (FI-CV-AAS), deuterium-lamp background corrector, Hg hollow-cathode lamp, and a circulating reaction loop. The working conditions of FI-CV-AAS were given in Table 1. The pH values of the solutions were measured by a digital pH meter (Metrohm, model 744, Herisau, Switzerland). A Hettich centrifuge (model EBA 20, Germany) and an ultrasonic bath with heating system (Tecno-GAZ SPA, Italy) were used throughout this study.

2.3. Synthesis of MOF
The $Zn_2(BDC)_2(DABCO)$ MOF was prepared via

Table 1. The FI-CV-AAS conditions for determination of mercury in standard samples.

Features	Value
Linear range, $\mu g\ L^{-1}$	0.2-55
Wavelength, nm	253.7
Lamp current, mA	3.0
Slit, nm	0.5
Mode	Peak area
HCl carrier solution 37%, mol L^{-1}	3.0
$NaBH_4$ reducing agent, % (m/v)	0.6 (in 0.5% w/v NaOH)
Argon flow rate, mL min^{-1}	10.0
Sample flow rate, mL min^{-1}	3.0
Reagent flow rate, mL min^{-1}	5.0

the self-assembly of primary building blocks. In a typical reaction, Zn $(OAc)_2.2H_2O$ (0.132 g, 2 mmol), BDC (0.1 g, 2 mmol), and DABCO (0.035 g, 1 mmol) were added to 25 ml DMF [3]. The reactants were sealed under reflux and stirred at 90 °C for 3 h. Then, the reaction mixture was cooled to room temperature, and filtered. The white crystals were washed with DMF to remove any metal and ligand remained, and dried in a vacuum. DMF was removed from white crystals with a vacuum furnace at 150 °C for 5 h.

2.4. General procedure of mercury adsorption

By USA-IL-μ-SPE procedure, 10 mL polytetrafluoroethylene (PTFE) centrifuge tube was used for this study. First, 10 mL of serum sample or standard aqueous solution containing Hg (II) with concentration in the range of 0.1-5.5 $\mu g\ L^{-1}$ was adjusted to optimum pH of 8 with sodium phosphate buffer solution (Na_2HPO_4/ NaH_2PO_4, 0.2 mol L^{-1}) and transferred into the 10 mL PTFE centrifuge tube. Then 50 mg of [OMIM][PF6] dispersed in 100 μL acetone was mixed with 20 mg $Zn_2(BDC)_2(DABCO)$ as MOF sorbent and rapidly injected by a syringe into the serum/ standard solution. The resulting mixture was shaken in ultrasonic bath for 5 min at 25 ºC. Hg (II) was extracted and separation by MOF. The $[Zn_2(BDC)_2(DABCO)]_n$-Hg was trapped with IL and centrifuged at 4000×g for 3 min. The Hg-MOF /IL was settled down in bottom of the conical centrifuge tube and the aqueous phase was removed

with a transfer pipette. Finally, mercury species retained on the sorbent were eluted by adding 0.5 mL of 0.3 molar HNO_3 and vigorously shaking the tube for 1 min. The eluent phase was separated by centrifuging of the remaining mixture and Hg (II) ions were analyzed by CV-AAS after dilution with deionized water up to 1 ml. Figure 1 was shown general procedure of mercury adsorption.

3. Results and Discussion

3.1. Fourier transforms infrared spectroscopy for MOF

The FTIR spectra of MOF were recorded in the range of 400–4000 cm^{-1} with KBr pellets by fourier transforms infrared spectroscopy (Fig. 2). The C–H aromatic band is shown at 3424 cm^{-1}. The aliphatic C–H asymmetric stretching is assigned at 2960 cm^{-1}. The peak at 2357 cm^{-1} is related to CO_2 which exist in environment. The C=O stretching and carboxylic group are assigned at 1587 cm^{-1} and 1387 cm^{-1} respectively. FTIR spectra corresponded to the reported results [1].

3.2. X-ray diffraction of MOF

The XRD measurement was used to determine the crystalline structure of MOF in 2θ range ۵° to ۳۰° (Fig. 3). The position and diffraction properties of the peaks are similar to the pattern of previously reported result [1].

3.3. Scanning electron microscopy for MOF
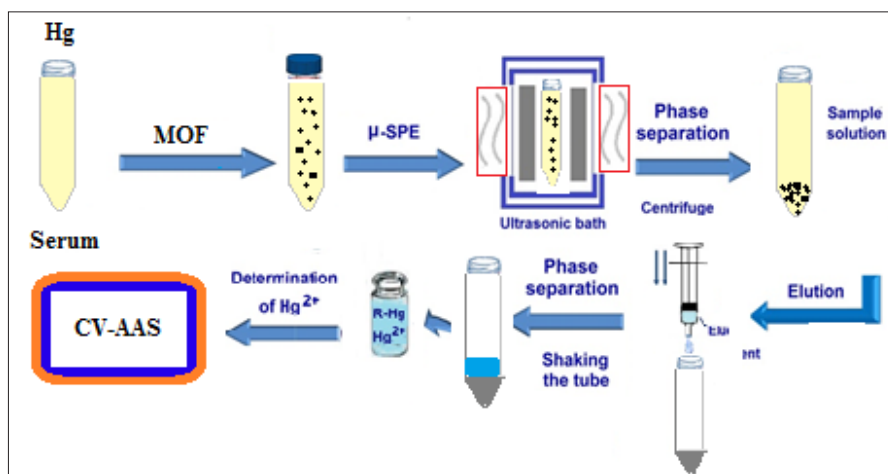
The size and morphology structures of samples

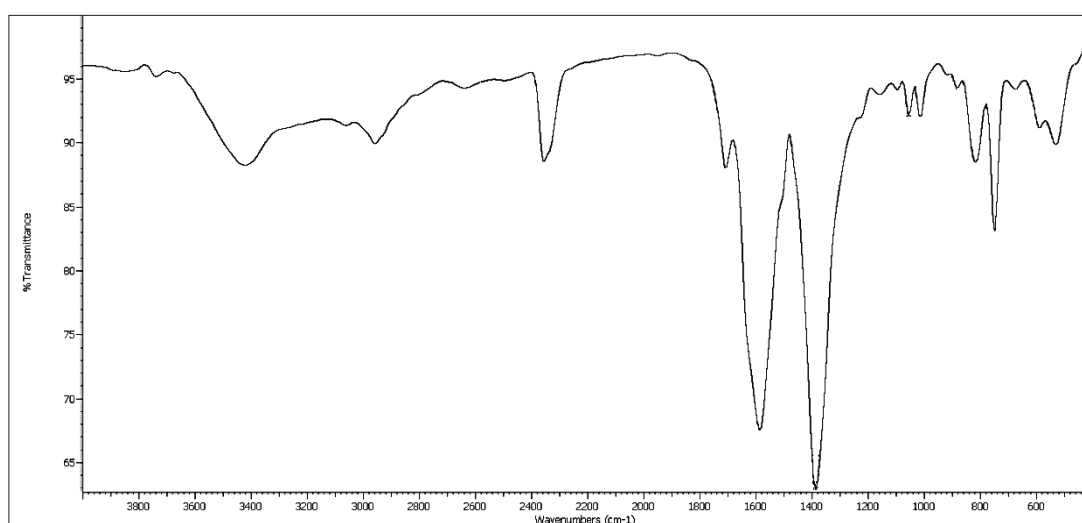**Fig. 1.** General procedure of mercury adsorption based on MOF by USA-IL-µ-SPE

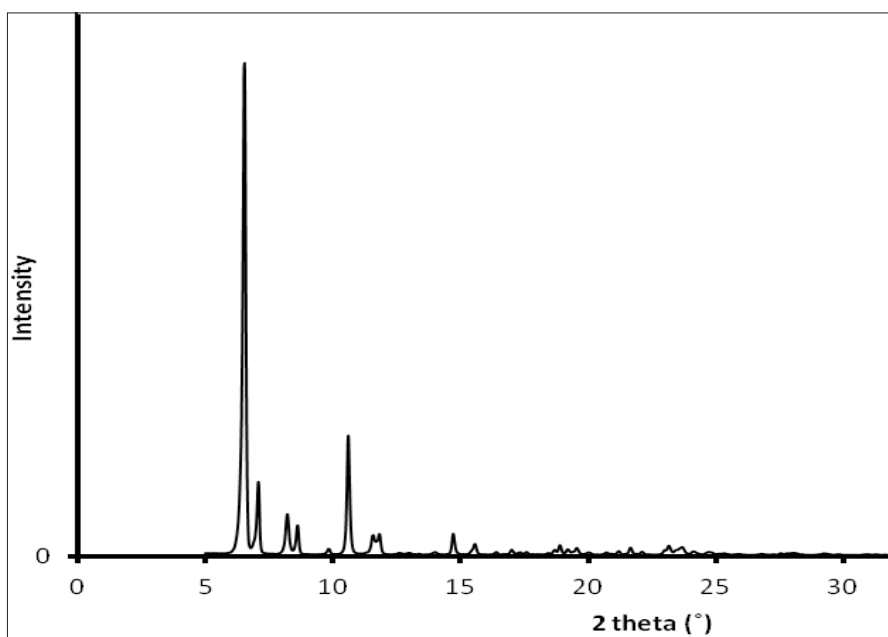**Fig. 2.** FTIR spectra of $Zn_2(bdc)_2(dabco)$ MOF

Fig. 3. XRD pattern of $Zn_2(bdc)_2(dabco)$ MOF

were studied using SEM that shown rod-shaped with an average diameter of 70 nm, and the length of 350 nm (Fig. 4).

3.4. Adsorption mechanism

The compounds of MOF $[Zn_2(bdc)_2(dabco)]_n$ such as, bdc (COO-) and dabco(N:) was used for chemical extraction of mercury from serum and standard solution samples at optimized pH. These ligands as a suitable material can be extracted the mercury ions in human biological sample at pH=8. The MOF are coordinating with the cations of Hg via nitrogen and carbocyclic bond which was deprotonated at basic pH. The mechanism of chemical and physical adsorption carried out by MOF at pH 7.5-8.5 for mercury in serum samples. The results showed us the recovery of physical adsorption in low pH without nitrogen covalence bonding (pH=3─6) was achieved 43.8 % and

increased more than 95% by chemical bonding of MOF with Hg(MOF─N:→Hg) at pH=7.5─8.5 (Fig. 5)

3.5. The optimization

The optimization was investigated for the ultrasound-assisted ionic liquid-micro solid phase extraction conditions. The USA-IL-µSPE procedure provides novel and interesting approach using the MOF sorbent for extraction of mercury from water and serum samples. In order to obtain optimum speciation conditions and quantitative recoveries of inorganic and organic mercury species with good sensitivity and precision, the presented USA- IL-µSPE method was optimized for various analytical parameters. Moreover, in order to optimization of effecting parameters, standard solutions containing different concentrations of Hg (II) in the range of 0.1–5.5 µg L^{-1} were examined.
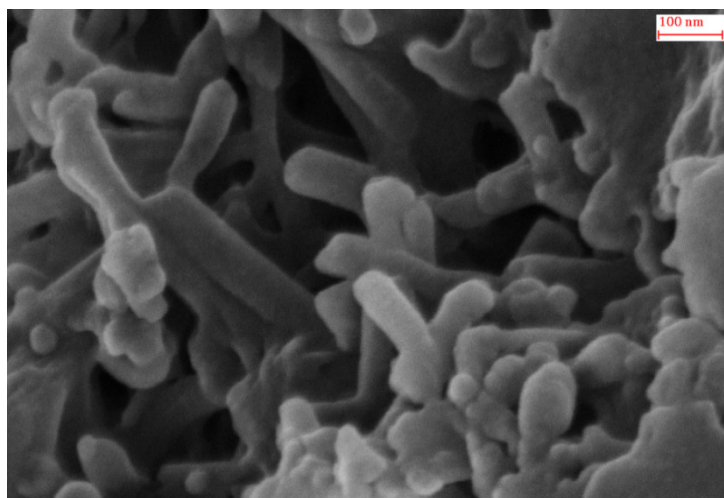
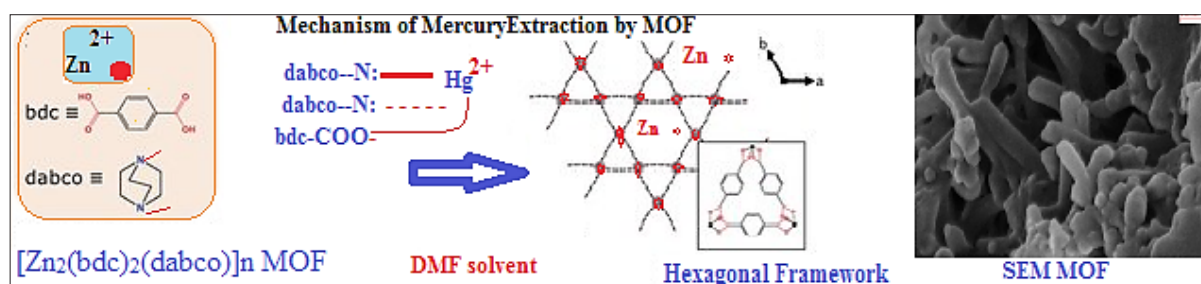

Fig. 4. SEM of $Zn_2(bdc)_2(dabco)$ MOF

Fig. 5. The mechanism of mercury absorption by MOF

3.5.1. Back extraction of mercury from MOF

The recovery percentage was investigated for mercury absorption by MOF in presence of different acids such as HNO_3, HCl, H_2SO_4, and CH_3COOH (Fig. 6), and selected 0.3 molar HNO_3 as optimum.

3.5.2. The pH effect of MOF

The pH of the sample is an important role to high recovery and extraction of Hg in human serum matrixes. The effect of serum pH on the extraction of Hg(II) based on MOF has studied from pH of 2 to 11, containing 0.1-5.5 µg L^{-1} of standard Hg(II) by USA- IL-µ-SPE method. Based on Figure 7, the extraction of Hg ions in serum and standard solution samples were increased between pH from 7.5 to 8.5. The recovery of mercury extraction were achieved more than 95% in pH=8 and decreased at pH more than 8.5 and less than 7.5. Consequently, the pH of 8 was used in further study for Hg extraction from serum and standard solution samples. In addition, the extra extraction of mercury was achieved by increasing MOF mass but, some of essential metals (Cu, Zn, Ca, Mn, Mg,) may be removed from
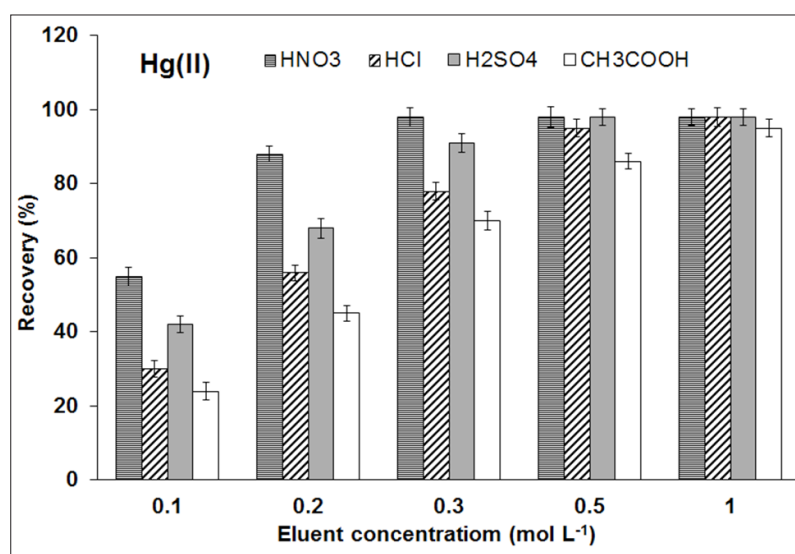
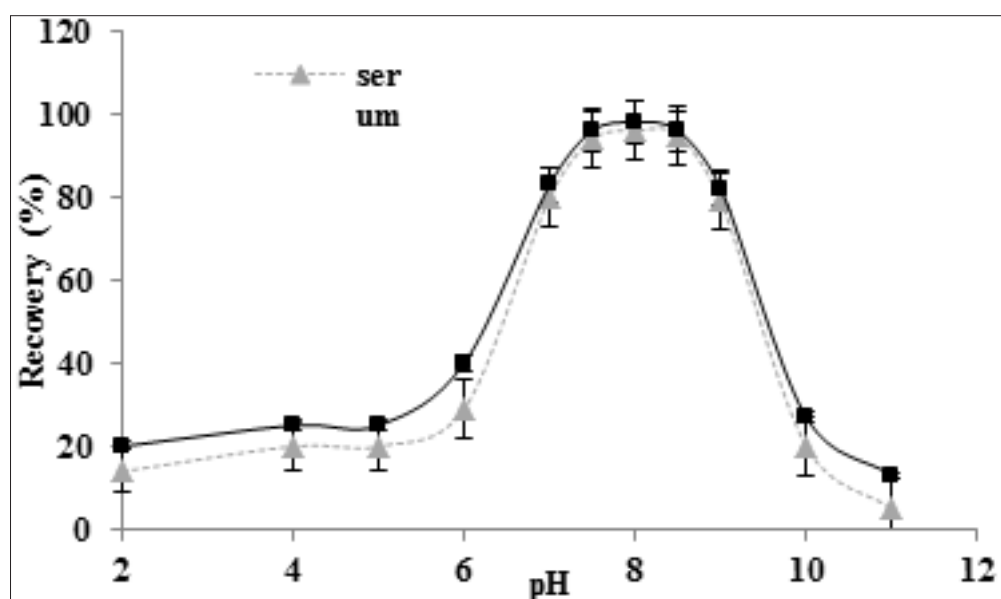**Fig. 6.** Recovery percentage in presence of different acids

Fig.7. The effect of pH on mercury extraction by MOF

human body and caused different acute disease. In proposed conditions, the recovery of Hg extraction was obtained 25% and 97.6% by IL and MOF/IL, respectively at pH=8. The mechanism of mercury extraction of MOF/IL was mainly obtained by the electrostatic attractions of deprotonated nitrogen and carbocyclic groups (N, COO) with the positively charged mercury ions at pH=8. At acidic pH, the surface of MOF, especially charge of groups have positive (+) and similar to Hg^{2+}, so, the recovery of extraction mercury was decreased. However, in optimized pH, the MOF sorbent had negative charge and electrostatic attraction caused to extract mercury. At high pH more than 8.5, the recovery efficiencies were decreased due to the formation of hydroxyl complexes of mercury [Hg(OH)2]. Therefore, Ph=8 selected as optimized pH by USA- IL-µ-SPE procedure.

3.5.3. Effect of MOF Mass
The mass of MOF was evaluated as effective parameter for mercury absorption among 1-40 mg. Based on mass results, the optimal value was mass 20 mg for mercury absorption by the MOF. For optimization of proposed method, the amounts of $[Zn_2(bdc)_2(dabco)]_n$ in the range of 1 to 40 mg were studied for mercury extraction in serum and standard samples. The results showed us, less than 18 mg of MOF caused to decrease the extraction efficiency of mercury. So, 20 mg of $[Zn_2(bdc)_2(dabco)]_n$ was used by USA- IL-µ-SPE procedure (Fig. 8).

3.5.4. Effect of volume of serum
The optimized sample volume on the recovery of Hg(II) ions based on USA- IL-µ-SPE procedure were examined from 1 mL to 25 mL of standard and serum samples. The volume of serum was investigated as effective parameter for mercury absorption. Based on the results, the optimal value was obtained less than 18 ml for water sample by the MOF. By results, the quantitative recovery was achieved (< 95%) for 15 mL and 12 mL of standard solution and serum, respectively with concentration of $0.1 - 5.5$ µg L^{-1} of mercury (CV-AAS). The recovery was decreased more than 12 mL and 15 mL for volume of serum and standard samples by proposed method. So, 10 mL of volume sample was used by USA- IL-µ-SPE method at pH=8 (Fig. 9).
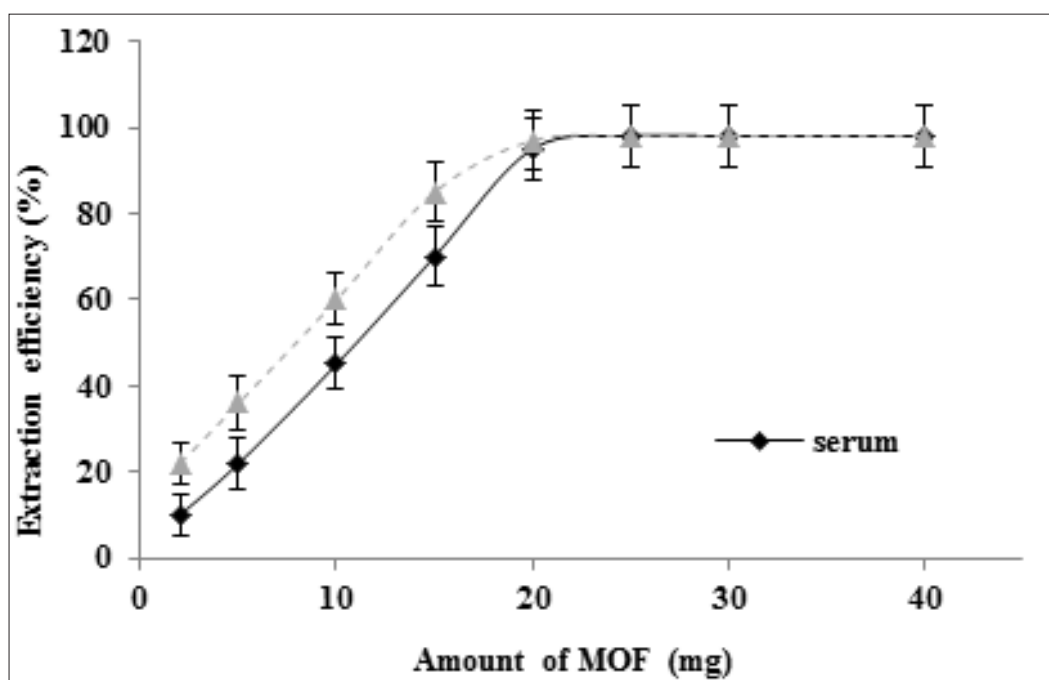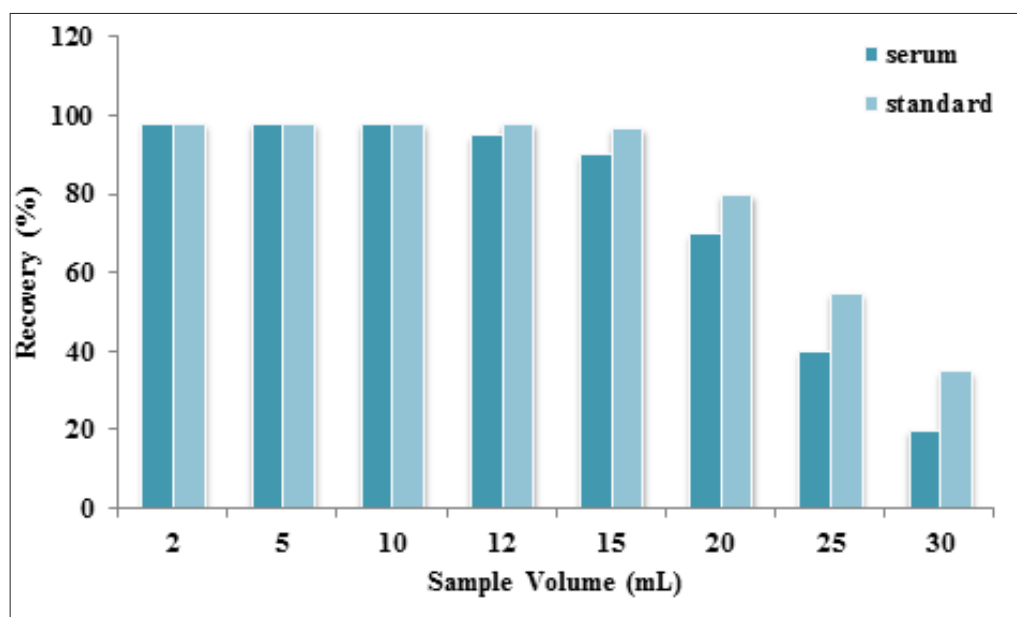

Fig. 8. The effect of MOF mass on mercury extraction

Fig. 9. The effect of sample volume on mercury extraction

3.5.5. Effect of ILs for mercury extraction

The IL was investigated as effective parameter for mercury absorption between 5-100 mg, and the optimized result was selected 50 mg. A hydrophobic ionic liquids such as; [MMIM] [PF$_6$], [HMIM] [PF$_6$] and [OMIM][PF$_6$] as a green solvent was used to separate MOF from the serum and standard solution (Fig. 10). The different amount of IL (5-100 mg) for separation of [Zn$_2$(bdc)$_2$(dabco)]$_n$ from serum phase were used and examined. The results

showed us, the good recovery was achieved with 65 mg of [HMIM][PF$_6$] and 45 mg of [OMIM][PF$_6$]. Therefore, 50 mg of [OMIM][PF$_6$] was selected by proposed method. In addition, the effect of [OMIM][PF6] for extraction of mercury in serum matrix was investigated without [Zn$_2$(bdc)$_2$(dabco)]$_n$ sorbents. The results showed us, the extraction recoveries of Hg were obtained about 12 % by [Zn$_2$(bdc)$_2$(dabco)]$_n$ which was depended to amino acid complexation in serum.
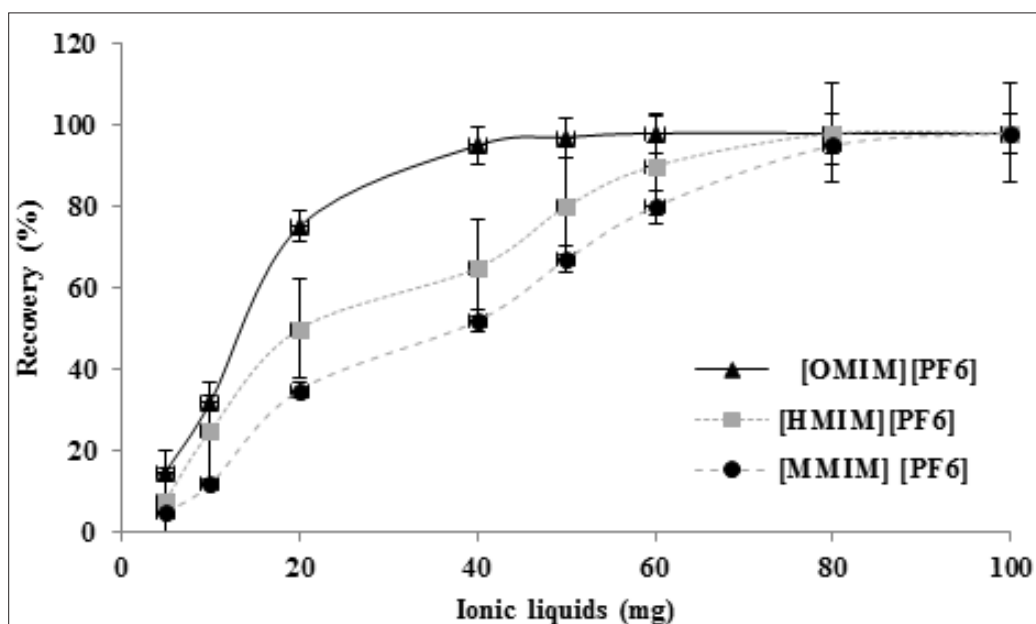

Fig. 10. The effect of different ionic liquids on mercury extraction

Table 2. The interference of some coexisting ions in serum samples on the recovery of mercury ions under the optimal condition.

Ions	Concentration ratio ($C_{interferent\ ion}/C_{Hg}^{2+}$)		Mean of Recovery (%)	
	Standard	Serum	Standard	Serum
Cr^{3+}, Co^{2+}, Pb^{2+}, V^{3+}, Mn^{2+}	500	400	96.4	95.9
I^-, Br^-, F^-, NO_3^-,	750	620	98.6	96.2
Na^+, K^+, Cl^-, Ca^{2+}, Mg^{2+}	1400	1100	97.7	95.1
Ni^{2+}, Ag^+, Cd^{2+}	35	20	99.3	97.5
Zn^{2+}, Cu^{2+}	120	100	97.0	96.8

3.5.6. Adsorption capacity

The important factor for analyzing of mercury with $[Zn_2(bdc)_2(dabco)]_n$ as MOF sorbent was adsorption capacity factor (ACF). In batch system, the ACF of Hg (II) was studied for 10 mL of human serum and standard solution at pH=8. The ACF of MOF for mercury vapor in GC closed glass was 149.56 mg g^{-1}. Based on characteristics of $[Zn_2(bdc)_2(dabco)]_n$ the most ACF related to chemical bounding of MOF as compared to physical adsorption by MOF. So, $[Zn_2(bdc)_2(dabco)]_n$ with high ACF was considered as excellent MOF sorbent for extraction of Hg (II) from serum and standard solution samples.

3.6. Interference Study

By USA-IL-µ-SPE procedure based on MOF for real samples, the interference of some coexisting ions encountered in serum samples on the recovery of Hg (II) ions was investigated under the optimal condition. This procedure was performed by adding various amounts of the interfering ions to 10 mL of standard sample solution containing 5.5 µg L^{-1} of Hg (II). Taking as criterion for interference the deviation of the recovery more than ±5%, the obtained results (Table 2) showed that most of the probable concomitant cations and anions had no considerable effect on the recovery efficiencies of

Hg (II) ions under the selected conditions.

3.7. Validation of results

The mercury absorption capacity was examined among different applications of MOF as hybrid inorganic-organic nanoporous materials by USA-IL-µ-SPE method. The intra-day analysis of mercury was shown in Table 3 and based on this result; MOF is good candidate for mercury adsorption.

The USA-IL-µ-SPE method was used for ultra-trace mercury determination in standard solution and serum samples. The results based on average of three determinations, for Hg (II) were achieved in serum samples. For validation of results, real samples in serum and standard solution was verified by spiking of mercury standard concentration (Tables 4). The favorate recovery showed that the proposed method had good accuracy in serum matrix. The recoveries of spiked samples for serum and standard solution were obtained more than 95%. The developed method based on MOF /IL was satisfactory demonstrated for mercury analysis in serum. The concentration of Hg in petroleum (subject) and office worker (control) were studied by USA-IL-µ-SPE procedure (N=-50). There were no significant differences between

Table 3. The intra-day analysis of mercury with MOF by USA-IL-µ-SPE method

Parameter (Intra-day)	Serum sample	Standard sample
PF[a]	9.8	10.2
LOD[b] (n=10, ng L^{-1})	6.5	6.8
RSD[c] (n=6, %)	4.2	3.3
Linear range (μg L^{-1})	0.02 – 5.5	0.02 – 6.0
Correlation coefficient	0.9988	0.9992

[a] Preconcentration factor, [b] Limit of detection, [c] Relative standard deviation.

Table 4. Validation of USA-IL-μ-SPE method based on MOF/IL by spiking of mercury standard concentration in real samples (μg L^{-1})

Sample	Added	Found[a]	Recovery (%)
	Hg (II)	Hg(II)	Hg(II)
Serum	-----	0.48 ± 0.02	-----
	0.5	0.97 ± 0.05	98
	1.0	1.51 ± 0.07	103
Serum	-----	2.55 ± 0.13	-----
	1.0	3.52 ± 0.12	97
	2.0	4.48 ± 0.23	96.5
Water	-----	3.11 ± 0.14	-----
	1.0	4.07 ± 0.21	96
	2.0	5.14 ± 0.27	102
Water	-----	0.26 ± 0.01	-----
	0.2	0.47 ± 0.02	105
	0.4	0.65 ± 0.02	97.5

[a] Mean of three determinations±confidence interval (P= 0.95, n=5)

exposed subjects and unexposed controls in terms of age and sex. The mean concentration of mercury in control groups was obtained under 1.0 μg L^{-1}. In addition, for validation of methodology, standard reference material (SRM 1641e) for inorganic mercury was analyzed by MOF/IL. Table 5 was approved the validation of developed USA- IL-μ-SPE method. The Ethical Committee of Tehran Medical Sciences, Islamic Azad University, approved the blood sampling guidance in the human body based on the Helsinki rules (E.C.: IR.IAU.PS.REC.1398.272).

using DMF solvent. Based on the results, the MOF was propped as a good candidate for mercury absorption. The highest mercury absorption was observed in pH=8, mass of MOF 20 mg, volume of serum 10 ml, volume of water 15 ml, and IL optimized 50 mg in presence of HNO$_3$ as optimized acid. Also, the interference of concomitant cations and anions had no considerable effect on the recovery efficiencies of Hg (II) ions under the selected conditions. Therefore, these properties can be resulted to many advantages in the future to absorb of hazardous materials.

4. Conclusions

In this study, Zn$_2$(BDC)$_2$(DABCO) MOF was synthesized by solvothermal method at 90 °C for 3 h via the self-assembly metal centers and linkers

5. References

[1] N. Motakef-Kazemi, S.A. Shojaosadati, A. Morsali, Evaluation of the effect of nanoporous nanorods

Table 5. Validation of developed USA- IL-μ-SPE method based on MOF with standard reference material (SRM)

Sample	Certified (μg L^{-1})	Added (μg L^{-1})	Found[a] (μg L^{-1}) Hg (II)	Recovery (%)
SRM 1641e [b]	1.016 ± 0.017	---	0.952 ± 0.048	----
		0.5	1.446 ± 0.087	98.8
		1.0	1.921 ± 0.126	96.9
SRM 3668[c]	0.910 ± 0.055	---	0.897 ± 0.052	----
		0.5	1.380 ± 0.092	96.6
		1.0	1.875 ± 0.103	97.8

[a] Mean of three determinations ± confidence interval (P = 0.95, n =5).
[b] NIST, SRM 1641e, total mercury in water (p=0.95).
c Mercury in Frozen Human Urine

Zn$_2$(bdc)$_2$(dabco) dimension on ibuprofen loading and release, J. Iran. Chem. Soc. 13 (2016) 1205–1212.

[2] S. Hajiashrafi, N. Motakef Kazemi, Preparation and evaluation of ZnO nanoparticles by thermal decomposition of MOF-5, Heliyon 5 (2019) e02152.

[3] N. Motakef-Kazemi, S.A. Shojaosadati, A. Morsali, In situ synthesis of a drug-loaded MOF at room temperature, Micropor. Mesopor. Mat. 186 (2014) 73–79.

[4] B. Miri, N. Motakef-Kazemi, S.A. Shojaosadati, A. Morsali, Application of a nanoporous metal organic framework based on iron carboxylate as drug delivery system, Iran. J. Pharm. Res. 17(4) (2018) 1164-1171.

[5] S.I. Noro, S. Kitagawa, M. Kondo, K. Seki, A new methane adsorbent, porous coordination polymer, Angew Chem. Int. Ed. 39 (2000) 2082–2084.

[6] K.S. Min, Self-assembly and selective guest binding of three-dimensional open-frame work solids from a macrocyclic complex as a trifunctional metal building block, Chem. Eur. J. 7 (2001) 303–313.

[7] M. Fujita, Y.J. Kwon, S. Washizu, K. Ogura, Preparation, clathration ability, and catalysis of a two-dimensional square network material composed of cadmium(II) and 4,4'-bipyridine, J. Am. Chem. Soc. 116 (1994) 1151–1152.

[8] O.R. Evans, W. Lin, Crystal engineering of NLO materials based on metal−organic coordination networks, Acc. Chem. Res. 35 (2002) 511–522.

[9] O.R. Evans, W. Lin, Crystal engineering of nonlinear optical materials based on interpenetrated diamondoid coordination networks, Chem. Mater. 13 (2001) 2705–2712.

[10] M. Oh, C.A. Mirkin, Ion exchange as a way of controlling the chemical compositions of nano- and microparticles made from infinite coordination polymers, Angew Chem. Int. Ed. 45 (2006) 5492–5494.

[11] R. Kitaura, S. Kitagawa, Y. Kubota, T.C. Kobayashi, K. Kindo, Y. Mita, A. Matsuo, M. Kobayashi, H. Chang, T.C. Ozawa, M. Suzuki, M. Sakata, M. Takata, Formation of a one-dimensional array of oxygen in a microporous metal-organic solid, Sci. 298 (2002) 2358–2361.

[12] P. Horcajada, T. Chalati, C. Serre, B. Gillet, C. Sebrie, T. Baati, J.F. Eubank, D. Heurtaux, P. Clayette, C.

Kreuz, J.S. Chang, Y.K. Hwang, V. Marsaud, P.N. Bories, L. Cynober, S. Gil, G. Ferey, P. Couvreur, R. Gref, Porous metal-organic-framework nanoscale carriers as a potential platform for drug delivery and imaging, Nat. Mater. 9 (2010) 172–178.

[13] B. Chen, L. Wang, F. Zapata, G. Qian, A luminescent microporous metal−organic framework for the recognition and sensing of anions, J. Am. Chem. Soc. 130 (2008) 6718–6719.

[14] A.J. Fletcher, K.M. Thomas, M.J. Rosseinsky, Flexibility in metal-organic framework materials: impact on sorption properties, J. Solid State Chem. 178 (2005) 2491–2510.

[15] M.D. Allendorf, C.A. Bauer, R.K. Bhakta, R.J.T. Houk, Luminescent metal–organic frameworks, Chem. Soc. Rev. 38 (2009) 1330-1352.

[16] S.M. Humphrey, T.J. Angliss, M. Aransay, D. Cave, L.A. Gerrard, G.F. Weldon, P.T. Wood, Bimetallic metal-organic frameworks containing the [M2,x-pdc)$_2^{-2}$](M = Cu, Pd, Pt; x = 4, 5) building block–synthesis, structure, and magnetic properties, Z. Anorg. Allg. Chem. 633 (2007) 2342-2353.

[17] C.G. Silva, A. Corma, H. García, Metal–organic frameworks as semiconductors. J. Mater. Chem. 20 (2010) 3141-3156.

[18] M. Hunsom, K. Pruksathorn, S. Damronglerd, H. Vergnes, P. Duverneuil, Electrochemical treatment of heavy metals (Cu^{2+}, Cr^{6+}, Ni^{2+}) from industrial effluent and modeling of copper reduction, Water Res. 39 (2005) 610-616.

[19] A. El-Samrani, B. Lartiges, F. Villiéras, Chemical coagulation of combined sewer overflow: heavy metal removal and treatment optimization. Water Res. 42 (2008) 951-960.

[20] H. Ozaki, K. Sharma, W. Saktaywin, Performance of an ultra-low-pressure reverse osmosis membrane (ULPROM) for separating heavy metal: effects of interference parameters, Desalination 144 (2002) 287-294.

[21] Z. Wang, J. Xu, Y. Hu, H. Zhao, H. Zhou, Y. Liu, Z. Lou, X. Xu, Functional nanomaterials: Study on aqueous Hg(II) adsorption by magnetic Fe$_3$O$_4$@SiO$_2$-SH nanoparticles, J. Taiwan Inst. Chem. Eng. 60 (2016) 394-402.

[22] L. Rahmanzadeh, M. Ghorbani, M. Jahanshahi, Effective removal of hexavalent mercury from aqueous solution by modified polymeric nanoadsorbent, J. Water Environ. Nanotechnol. 1

(2016) 1-8.

[23] K. Yaghmaeian, R. Khosravi Mashizi, S. Nasseri, A.H. Mahvi, M. Alimohammadi, S. Nazmara, Removal of inorganic mercury from aquatic environments by multi walled carbon nanotubes, J. Environ. Health Sci. Eng. 13 (2015) 55.

[24] Q.D. Qin, J. Ma, K. Liu, Adsorption of nitrobenzene from aqueous solution by MCM-41, J. Colloid Interface Sci. 315 (2007) 80–86.

[25] L. Xie, D. Liu, H. Huang, Q. Yang, C. Zhong, Efficient capture of nitrobenzene from waste water using metal–organic frameworks, Chem. Eng. J. 246 (2014) 142–149.

[26] D.V. Patil, P.B. Somayajulu Rallapalli, G.P. Dangi, R.J. R.S. Tayade, Somani, H.C. Bajaj, MIL-53(Al): An efficient adsorbent for the removal of nitrobenzene from aqueous solutions, Ind. Eng. Chem. Res. 50 (2011) 10516–10524.

[27] N. T. Abdel-Ghani, G. A. El-Chaghaby, F. S. Helal, Individual and competitive adsorption of phenol and nickel onto multiwalled carbon nanotubes, J. Adv. Res. 6 (2015) 405-415.

[28] Z. Zhaoa, X. Li, Z. Li, Adsorption equilibrium and kinetics of p-xylene on chromium-based metal organic framework MIL-101, Chem. Eng. J. 173 (2011) 150–157.

[29] A.A. Adeyemo, I.O. Adeoye, O.S. Bello, Metal organic frameworks as adsorbents for dye adsorption: overview, prospects and future challenges, Toxicol. Environ. Chem. 94(10) (2012) 1846–1863.

[30] M.M. Tong, D.H. Liu, Q.Y. Yang, S. Devautour-Vinot, G. Maurin, C.L. Zhong, Influence of framework metal ions on the dye capture behavior of MIL-100 (Fe, Cr) MOF type solids, J. Mater. Chem. A 1 (2013) 8534–8537.

[31] M.A. Al-Ghouti, M.A.M. Khraisheh, S.J. Allen, M.N. Ahmad, The removal of dyes from textile wastewater: a study of the physical characteristics and adsorption mechanisms of diatomaceous earth, J. Environ. Manage. 69 (2003) 229–238.

[32] J. Galán, A. Rodríguez, J.M. Gómez, S.J. Allen, G.M. Walker, Reactive dye adsorption onto a novel mesoporous carbon, Chem. Eng. J. 219 (2013) 62–68.

[33] A. Sayari, S. Hamoudi, Y. Yang, Applications of pore-expanded mesoporous silica: removal of heavy metal cations and organic pollutants from

wastewater, Chem. Mater. 17 (2005) 212-216.

[34] S. Babel, T.A. Kurniawan, Low-cost adsorbents for heavy metals uptake from contaminated water: a review, J. Hazard. Mater. B97 (2003) 219–243.

[45] L. Rasuli, A.H. Mahvi, Removal of humic acid from aqueous solution using MgO nanoparticles, J. Water Chem. Tech. 38(1) (2016) 21–27.

[36] M.R. Mehmandoust, N. Motakef-Kazemi, F. Ashouri, Nitrate adsorption from aqueous solution by metal–organic framework MOF-5, Iran. J. Sci. Technol. Trans. A-Science. 43(2) (2019) 443–449.

[37] A. Bhatnagara, E. Kumarb, M. Sillanpää, Nitrate removal from water by nano-alumina: Characterization and sorption studies, Chem. Eng. J. 163 (2010) 317–323.

[38] J.D. Park, W. Zheng, Human exposure and health effects of inorganic and elemental mercury, J. Prev. Med. Public Health 45 (2012) 344–352.

[39] M.A. Bradley, B.D. Barst, N. Basu, A review of mercury bioavailability in humans and fish, Int. J. Environ. Res. Public Health 14 (2017) 169.

[40] B.F. Azevedo, L.B. Furieri, F.M. Pecanha, G.A. Wiggers, P.F. Vassallo, M.R. Simoes, J. Fiorim, P.R. Batista, M. Fioresi, L. Rossoni, I. Stefanon, M.J. Alonso, M. Salaices, D.V. Vassallo, Toxic effects of mercury on the cardiovascular and central nervous systems, J. Biomed. Biotechnol. 2012 (2012) 1-11.

[41] K.M. Rice, E.M. Walker Jr, M. Wu, C. Gillette, E.R. Blough, Environmental mercury and its toxic effects, J. Prev. Med. Public Health 47 (2014) 74–83.

[42] S.E. Orr, C.C. Bridges, Chronic kidney disease and exposure to nephrotoxic metals, Int. J. Mol. Sci. 18 (2017) 1039.

[43] E. Afshar, H. Mohammadi-Manesh, H. Dashti Khavidaki, Removal of Hg (I) and Hg (II) ions from aqueous solutions, using TiO_2 nanoparticles, Pollution. 3 (2017) 505-516.

[44] K. Suresh Kumar Reddy, B. Rubahamya, A. Al Shoaibi, C. Srinivasakannan, Solid support ionic liquid (SSIL) adsorbents for mercury removal from natural gas, Int. J. Environ. Sci. Technol. 16 (2019) 1103–1110.

Air pollution Analysis: Nickel paste on Multi-walled carbon nanotubes as novel adsorbent for the mercury removal from air

Ali Ebrahimi[a,*] and Ahmad Salarifar[b]

[a,*] *Occupational Health Engineering Department, School of Public Health, Qom University of Medical Sciences, Qom, Iran.*
[b] *Environmental Engineering, Faculty of Natural Resources, Islamic Azad University, Bandar Abbas Branch, Bandar Abbas, Iran*

ABSTRACT

Mercury as a hazardous material can be released in air and caused renal failure and CNS problem in humans. In this study, mercury vapor removed from air based on nickel-coated on multi-walled carbon nanotubes (Ni-MWCNTs) as a novel sorbent at room temperature. By procedure, amalgamation of mercury with Ni-MWCNTs was achieved by solid-gas phase removal method (SGPR). In bench scale set up, the mercury vapor generated and mixed with purified air with electro air cleaner and moved to sorbent at optimized flow rate. After thermal desorption of Ni-MWCNTs at 200 °C, the mercury vapor flowed to quartz glass cell with argon gas and determined by cold vapor atomic absorption spectrometer technique (CV-AAS). In optimized conditions, 25 mg of Ni-MWCNTs and MWCNTs with different size from 30-100 nm was used and the adsorption capacity of sorbents was obtained 194 mg g^{-1} and 64 mg g^{-1}, respectively. The efficient recovery was obtained at optimized conditions such as, temperature of 25-40 and flow rate of 200 mL min^{-1}. Due to results, the surface of Ni-MWCNTs had good potential for removal of mercury vapor from the air and can be used as a low cost and efficient sorbent in industrial workplace.

1. Introduction

Mercury was ranked as a hazardous material for human health and animals such black fish and extra concentration cause dangers disease in human body [1,2]. Mercury is a toxic element and has no essential biological function in human body and normal range was reported less than 20 µg L^{-1} and 2 µg L^{-1} in urine and blood serum, respectively by ACGIH. Organic and inorganic mercury occurs in fishes, foods, vegetables, waters and air [3].

It is emitted to the atmosphere from chlor-alkali factory, sea, chemical process, coal, oil combustion for energy generation, and metal mining, The contribution of industrial sources for mercury and other heavy metals emissions to the atmosphere, rivers and fish and humans [4]. Human exposure to mercury evaluated and studied in occupational and environmental health [5]. Mercury generated from chemicals, petrochemical and electrical industries [6]. The mercury exposure caused many health problems in human body such as, central nervous system defects, erythrism, arrhythmias, cardiomyopathies, and kidney damage. Necrotizing

bronchitis and pneumonitis arising from inhalation of mercury vapor can result in respiratory failure [5, 6]. Mercury is listed and suggested as one of the hazardous air pollutants in the 1990 and recently many methods was used for mercury removal from air [7]. The air sampling and analysis methods was used for mercury determination by the national institute for occupational safety and health (NIOSH) and the occupational safety and health administration (OSHA), respectively(NIOSH 6009). The main disadvantages of these methods related to interference by other metal compounds and organic mercury in air. the sample tube be The fragile of sample tube, low adsorption capacity, impurities and contamination of reagents used for sample preparation, the use of nitric acid and hydrochloric acid, as well as being time consuming, the mercury loss during sample preparation, operator skills and the costs of solid sorbent tubes caused to consider as a weak procedure [8, 9]. Many Nano carbon compound such as carbon nanotubes (MWCNTs, SWCNTs), graphene and mesoporous silica nanoparticles (MSN) was syntheses and used as a sorbent for removal of mercury from air. Carbon nanotubes are unique wall porous structures with nanometer diameter and can be simply removed mercury from air with two type's single walled carbon nanotubes (SWNTs) and multiple walled carbon nanotubes (MWNTs) [16]. MWCNT and SWCNT were used in many published papers for mercury removal from air/gas. Adsorption of mercury was achieved by montmorillonite powder modified with Copper Compounds or amorphous of MoS_3 pasted on TiO_2 was used for removal metals from gas/air . Also, the bimetallic sorbents such as Pd–Fe and catalytic compounds such as Ce–Mn/TiO_2 applied for Hg^0 removal in air [10-15]. In fact, CNTs with chemical and physical properties have good potentially in many applications such as, nanotechnology, electronics, optics, water, chemistry, environment and other fields of materials science [16-20]. Low diameter (nm), low weight, thermal conductivity and high surface area, thermal resistance, high tensile strength and a very high Young modulus

caused to introduce as novel adsorbent in many science [21-22]. Also, these compounds also have been used for absorb the gases and metal cations and volatile organic compounds [23-27]. The carbon nanotubes have a good repeatability in high temperature, So, CNTs introduce a favorite sorbent for mercury removal from air by thermal desorption method [28, 29], Also, the health effect of exposure to solvents, acids and other chemical methods were reduced by proposed method. Recently, different instruments coupled with techniques was reported for mercury analysis by researchers, activated carbon from mixed recyclable waste modified by phosphonium-based ionic liquid (IL-ACMRW) based on Inductively Coupled Plasma- mass spectroscopy (ICP-Ms) was used for mercury removal from wastewater. Inductively coupled plasma atomic emission spectroscopy *(ICP* OES), high-performance liquid chromatography coupled hydride generation atomic absorption spectrometry (HPLC-*HG*-AAS), hydride generation atomic absorption spectrometry (*HG*-AAS), hydride generation atomic absorption spectrometry coupled mercury concentration (HG-AAS-MC3000). In this work, Ni-MWCNTs and MWCNTs was removed the mercury vapor from air due to their unique physicochemical properties. Strong chemical interactions between Ni and Hg^o (Hg→Ni-MWCNTs) caused to increase removal efficiency of sorbent by SGPR. The reusable of Ni-MWCNTs can be considered as a cost effective sorbent.

2. Experimental
2.1. Material and Methods
All reagents such as, Sodium borohydride, nitric acid, sodium hydroxide and hydrochloric acid were prepared from Sigma Aldrich. Mercury standard solutions were prepared from a stock solution of 1000 mg L^{-1} in 1% ultra-pure nitric acid. Working standard solutions were freshly prepared by dilution of stock and intermediate standards. Sodium borohydride ($NaBH_4$) prepared fresh daily. 3.0 g of NaBH4 and 3.0 g of sodium hydroxide (NaOH) were mixed and diluted by deionized water (DW) up to 500mL. Deionized water obtained from a

water purification system (Millipore, Bedford, MA, USA) was used for preparing all solutions. All containers (quartz crucibles, plastic tubes) were cleaned with detergent and treated successively by the hydrochloric acid and rinsed with deionized water. Argon was used as the pure gas (99.99%). The present research is an experimental study and it includes stages such as preparation of the various concentrations of mercury vapor, adsorption of mercury vapor in various concentration, time, temperature optimized as well as retention time of adsorbed mercury by multi-walled carbon nanotubes. The atomic absorption spectrometer (GBC) Model (AAS–932 Puls) with cold vapor technique (CV-AAS/HG3000) has been used for the analysis of samples. Instrumental parameters for cold vapor atomic absorption spectrometry are shown in Table 1. The mercury concentrations were prepared from 1 μgL^{-1} to 50 μgL^{-1}. The Ni-MWCNTs (25 mg) as solid phase was used and placed in a glass tube with length of 5 cm and the internal and external diameters of 5 and 8 mm respectively. Then, end-capping with some silica /cotton was performed to prevention of humidity. MWCNTs were provided by Nano department of RIPI, Tehran. Also, all solutions and materials were purchased from Merck, Germany.

2.2. Synthesis of nickel coated on MWCNTs

The Ni-MWCNTs has prepared as follows, 2.0 g of the pure MWCNTs was added to 50 mL of DW with 0.25 g of Sodium sulfosuccinate esters ($NaO_3SCH(CO_2R')CH_2CO_2R$)as a surfactant by low heating at 300 rpm stirring speed. The nickel nitrate (0.5 g) was added to the Final solution without heat in 200 rpm stirring speed. Then, ammonia solution (2 mL) was added to solution and diluted with DW up to 200 mL with stirring in 20 min at 300 rpm speed. Then finally, 10 mL of formalin slowly was added for five minutes as a reducing agent. The synthesis of Ni-MWCNTs nanoparticles was obtained by increasing the speed of Stirring after addition formalin for 10 min (800 rpm). The extra formalin and ammonia on Ni-MWCNTs cleaned by DW washing after filtration

Table 1. Conditions of cold vapor atomic absorption spectrometry (CV-AAS) for mercury

Parameters	Value
5 mA	Lamp Current
253.7 nm	Wavelength
0.5 nm	Band pass
Cold vapor	Flame Conditions
HCL	Lamp
400 k Pa	Argon gas pressure
100 mL/min	Gas flow to the mixer block
35 mL/min	Gas flow to the separator

by Whatman filter. In addition, oxidation of the Ni-MWCNTs nanoparticles was prevented by washing with Ethanol.

2.3. Experimental Procedure

In bench scale set up, the air was purified with electro air cleaner (EAC, Canada, model EAHEPA600M-3) by HEPA. The HEPA act for efficient removing particles under 300 nm (99.97%) from air. Then, the pure air of EAC passed through polyethylene tubes and entered to polyethylene bag (1 Li) by a SKC pump. All of the gas lines were PE tubes and those that enter to PE bag were covered with heating jackets capable of controlling the temperature at 50 °C to prevent water vapor and mercury vapor from condensing. In SGPR, trace of elemental mercury vapor in air was prepared by aqueous standard solution of mercury (1-50 μgL^{-1}). The aqueous standard solutions entered to hydride generator system and mercury vapor generated in a continuous flow rate. The system was designed by a peristaltic pump that can be pumped standard solutions of mercury, tin chloride as reducing agent and ionized water into a mixer continuously. Peristaltic pump rotation rate was 1.5 rounds per second or 90 rpm. The solution mixed thoroughly in reaction tube and then pushed into a liquid–gas separator where the mercury vapor is separated from the liquid using an inert carrier gas. The mercury vapor mixed with pure air and flowed to Ni-MWCNT by flow rate 100-300 ml min^{-1}. After adsorption mercury by Ni-MWCNTs, the remained air stored in polyethylene bag 1(1 L). The air into air bag was determined by CV-AAS and MC3000
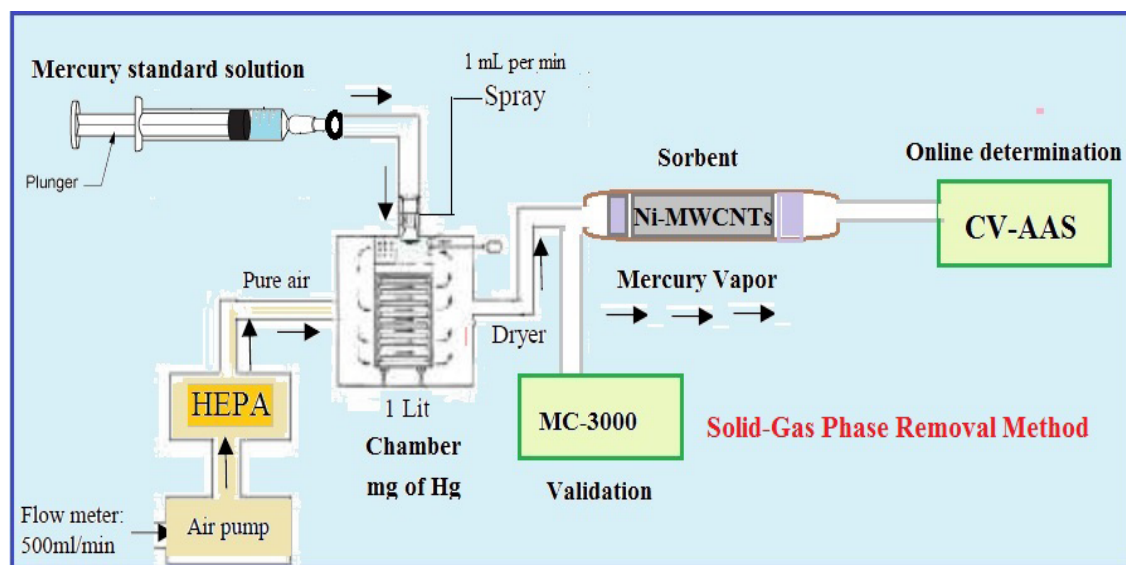
Fig. 1. Scheme of pilot plan for mercury removal from air

(gold trap). After thermal desorption of MWCNT, the mercury vapor flowed with Ar gas and stored in another bag (bag 2, 1L) and mercury determined by CV-AAS and MC 3000. The pilot plan for mercury removal from air was shown in Figure 1.

3. Results and Discussion

3.1. Scanning electron microscopy images from carbon nanotubes

The scanning electron microscopy (SEM) and Transmission electron microscopy (TEM) images of MWCNT and Ni-MWCNTs was shown in Figures 2 and 3, respectively. Elemental analysis conditions showed that Ni-MWCNTs included 8% nickel and 90% carbon. Mercury was removed by sorbent 0.55% by Ni-MWCNTs (Table 2).

3.2. Adsorption efficiency for different amounts of MWCNTs

The adsorption efficiency with 25 mg of Ni-MWCNTs and MWCNTs was examined for 0.01-0.1 µg of mercury concentration by SGPR. According to the results, the adsorption efficiency for Ni-MWCNTs was more than 95% as compared
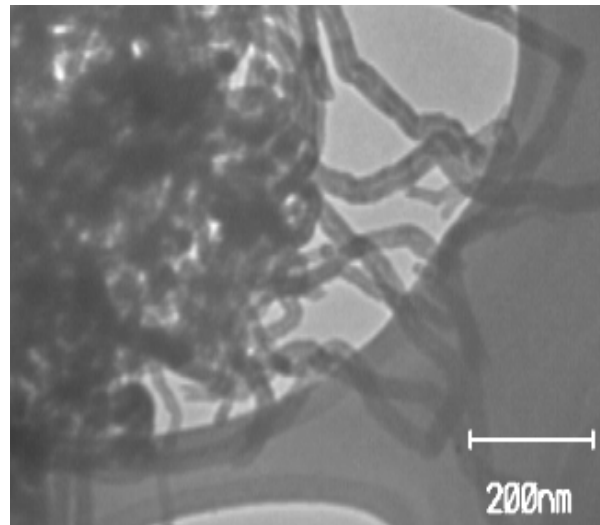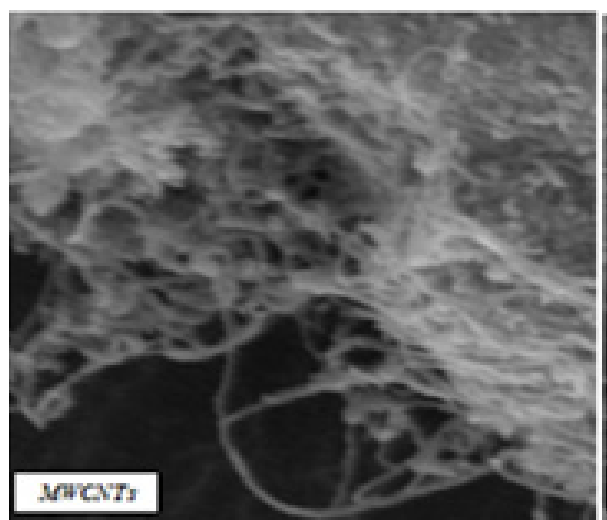

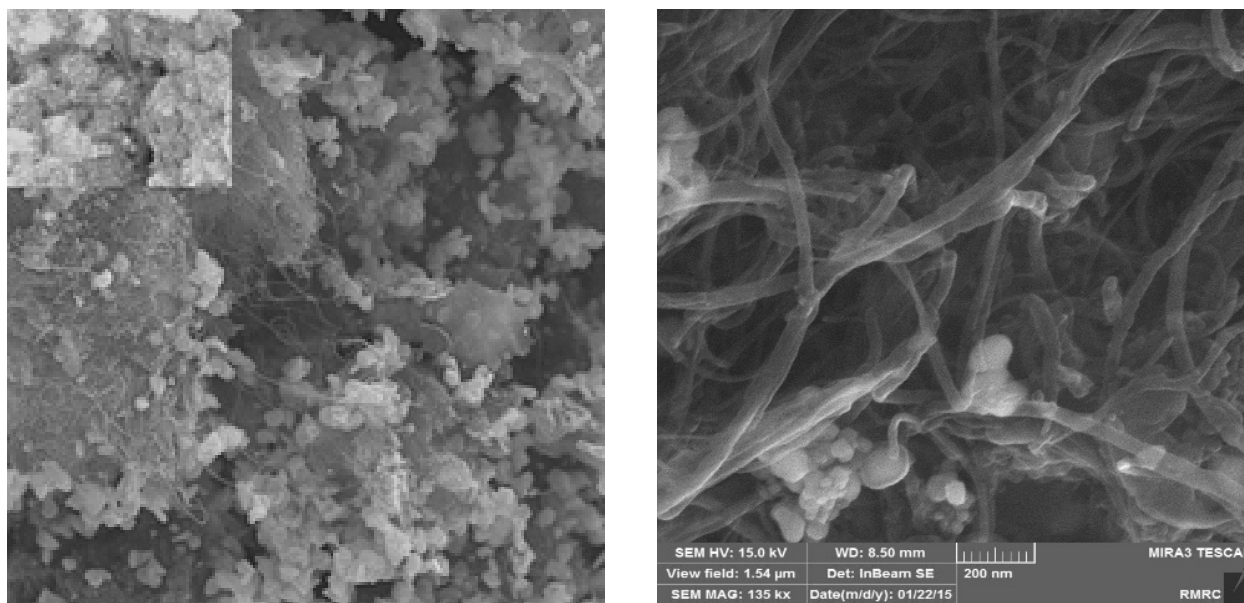**Fig. 2.** SEM (L) and TEM (R) images of multi-walled carbon nanotubes

Fig. 3. SEM (L) and TEM (R) images of Nickel coated on multi-walled carbon nanotubes

Table 2. Energy Dispersive X-Ray Analysis of Ni-MWCNTs (EDX) for mercury removal

Elt	Line	Int	Error	K	Kr	W%	A%	ZAF	Ox%	Pk/Bg	Class	LConf	HConf	Cat#
C	Ka	676.1	80.3865	0.4213	0.2945	48.21	90.22	0.6107	0.00	37.86	A	47.66	48.76	0.00
Ni	La	1269.7	6.5990	0.4792	0.3350	41.14	8.57	0.8142	0.00	26.05	A	40.79	41.48	0.00
Au	La	7.0	0.5642	0.0839	0.0586	9.29	1.06	0.6307	0.00	2.41	B	8.25	10.34	0.00
Hg	Ma	47.1	6.5990	0.0157	0.0110	1.36	0.55	0.8077	0.00	3.20	B	1.30	1.42	0.00

to MWCNTs (less than 70%). Also the RSD had different value from 5 to 8%. The results showed that the good recoveries for mercury removal by two sorbents were achieved in low and high mercury concentration (Table 3).

3.3. Adsorption capacity of Ni- MWCNTs and MWCNTs

In batch system, 10 mg L^{-1} of mercury standard solution (Merck) selected and injected in closed special glass (CSG) after put into Ni- MWCNTs

Table 3. Recovery of adsorption for different concentration of mercury from low to high range (n=10; Mean SD of results ± 0.0032)

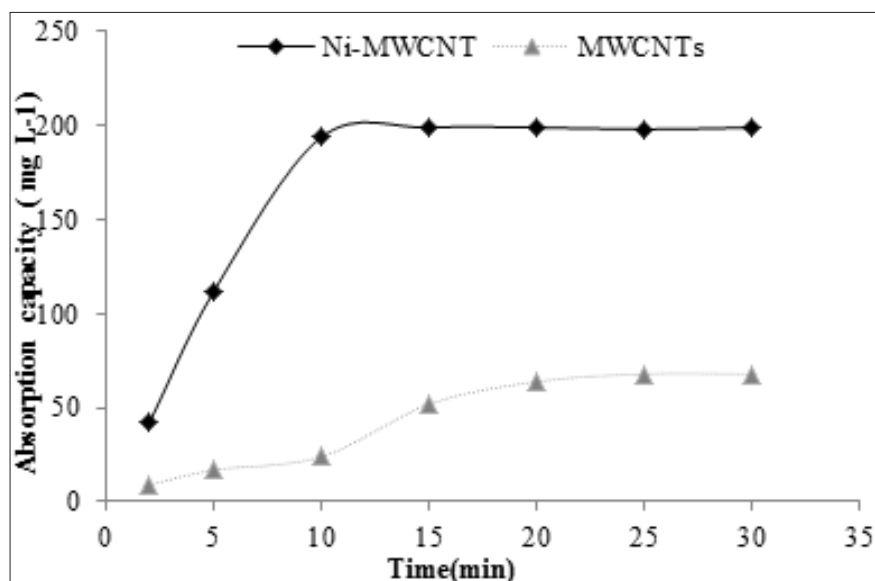| 25 mg of NI-MWCNTs			
Pilot concentrations (µg)	Found desorption	RSD%	Recovery (%)
0.01	0.00944	0.67	94.4
0.02	0.0195	0.52	97.5
0.03	0.0286	0.73	95.3
0.05	0.0487	0.81	97.4
0.1	0.0976	0.76	97.6
25 mg of MWCNTs			
0.01	0.00654	0.74	65.4
0.02	0.0148	0.63	74.0
0.03	0.0206	0.73	68.6
0.05	0.0388	0.54	77.6
0.1	0.0683	0.59	68.3

Fig. 4. The absorption capacity (AC) of mercury vapor in Ni- MWCNTs and MWCNTs (n=10).

and MWCNTs as sorbents in CSG. After heating, the temperature increased up to 80 °C for 10 min. The mercury was vapored and absorbed on sorbents. The results showed us, the absorption capacity (AC) of Ni- MWCNTs and MWCNTs for mercury removal was obtained 194.7 mg g^{-1} and 64.4 mg g^{-1}, respectively (Fig. 4). In temperature of 50°C for 10 min, AC was decreased about 8% but after 20 min AC was similar to proposed procedure.

3. 4: Determine the optimum time and temperature for desorption

For optimization of temperature, the rate of desorption at different temperatures was studied by SGPR. The maximum of desorption rates on the Ni-MWCNTs was achieved in 160-250°C. So, 200°C was selected as an optimum temperature for desorption point by Ni-MWCNT. Based on the optimum temperature and after several experiments, the results showed that the best time
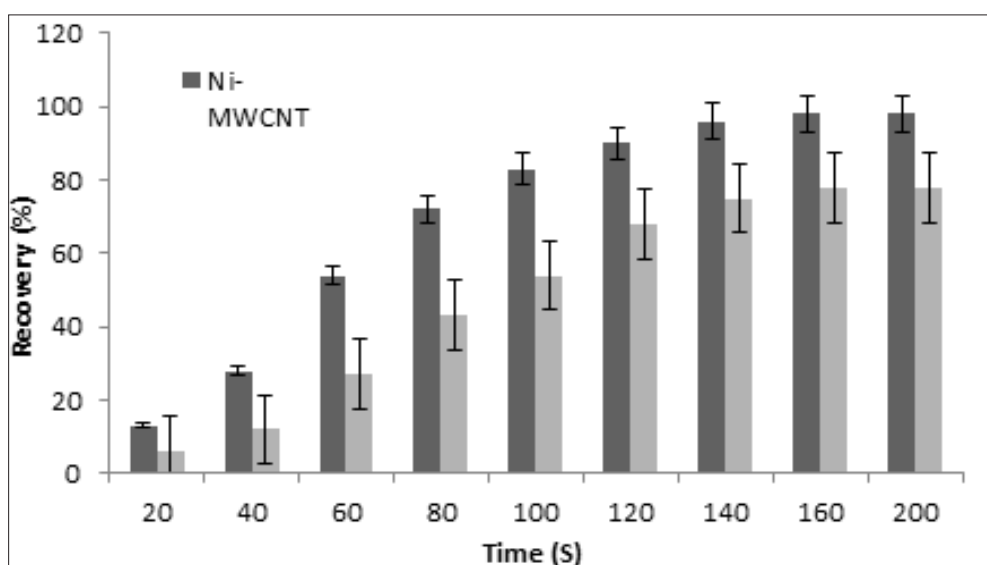

Fig. 5. The effect of time desorption of Ni-MWCNTs and MWCNTs by SGPR (n=10).
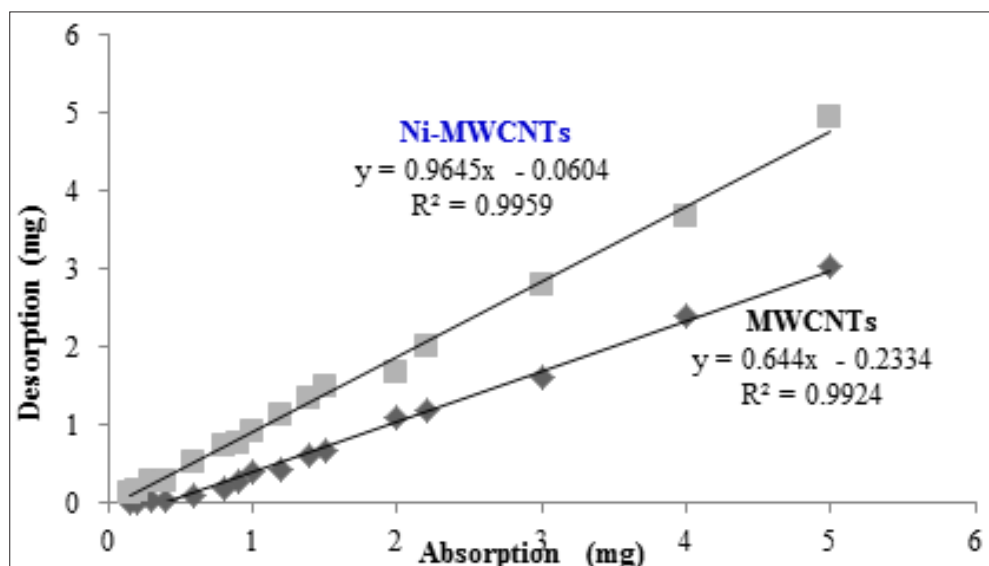
Fig. 6. The linear regression of adsorption / desorption for Ni-MWCNTs and MWCNTs

for desorption high efficiency was about 2.33 min with average desorption efficiency equals to 94.5 - 98.2% by peak area mode (Fig. 5).

3.5. Adsorption/desorption efficiency

Removal efficiency and linear regression between the mean values of the mass adsorption and desorption by Ni-MWCNTs and MWCNTs have been shown in Figure 6. The mercury concentration (0.02-0.1 mg L^{-1}) was used for calculating of removal efficiency by proposed procedure. Based on Figure 6 the removal efficiency of Ni-MWCNTs (25 mg) was more than MWCNTs (25 mg) as compared to adsorption/desorption procedure for mercury removal from air by 200 ml min^{-1}.

3.6. Repeatability and retention time

The retention time evaluated for 0.02-0.1 mg of mercury concentration for Ni-MWCNTs and MWCNTs in different temperature. For calculation of retention time, the two ends of sorbents tube with Ni-MWCNTs and MWCNTs were kept at zero 0°C and 25°C. After various times, carbon nanotubes were desorbed in optimum conditions (200°C and 10 min) and then, this procedure followed in different times (1-5 weeks). The results showed us, the main mass of mercury in sorbent tubes was similar to primary mercury concentration after

3 weeks by desorption procedures (0°C). But, in room temperature, only Ni-MWCNTs were stable mass after 1 week. So, Ni-MWCNTs is suitable sorbent for mercury removal from air and saving in room temperature. The adsorption / desorption procedure for Ni-MWCNTs and MWCNTs was repeated based on proposed method and after flashing point , 25 and 27 usage times was achieved as an optimum point for Ni-MWCNTs and MWCNTs, respectively.

3.7. Discussions

According to the results, Ni-MWCNTs were able to absorb mercury from air by SGPR. The atomic absorption spectrometer (GBC) Model (AAS–932 Puls) with cold vapor technique (HG3000) was used for determination of mercury in air, liquid and gas. Previous studies have been researched to attract mercury vapor in gas/air [23-27]. In this study, the Ni-MWCNTs with average diameter of (less than 100 nm) were used to form a stationary phase (sorbent) of glass tubes containing a length of 10 cm, internal diameter of 4cm and external diameter of 6 cm [8, 9]. Shirkhanloo et al. used silver nanoparticles in glassy balls. They showed that silver nanoparticles (AgNPs) had good removal efficiency for mercury from air but it was more expensive as compared to our study.

Also silver nanoparticles can be oxidizing by air, so storage is very hard in room temperature as compared to Ni-MWCNTs [7]. The average absorption rate and absorption capacity (AC) of mercury mass in different concentrations was increased by increasing the mass of nanotubes. In this study, the adsorption capacity of mercury for the Ni-MWCNTs (Ni→Hg) was obtained 194 mg g^{-1} which was higher than other published methods (less than 170 mg g^{-1}) and MWCNTs (64 mg g^{-1}). This amount is more than the adsorption capacity of adsorptions such as activated carbon. [30]. According to results in optimized conditions, it seems that the factors such as, concentration of mercury in air, the mass of sorbents, air flow rate, surface area, temperature, and type of the adsorbent effected on the adsorption efficiency of mercury from air up to 80%. Also, the other parameters such as layout of the sorbent tube, length, diameter, O$_2$ and H$_2$O in air, had low affected less than 20%. The optimum point for concentration and temperature desorption was obtained 1-50 µgL^{-1} and 200 **°C**, respectively. In other studies that designed on the activated carbon, graphene and carbon nanotubes, similar to proposed method [31, 32]. After one month, the retention time of mercury on Ni-MWCNTs, at temperature of 0**°C** was obtained 98.8% ± 1.05 was near to initial concentration amount. Many papers were used CNTs sorbents for removal mercury from air. The adsorption capacity of Ni-MWCNTs was higher than other sorbents such as MWCNTs, activated carbon and graphene which was previously reported.

4. Conclusions

In present work, a novel sorbent based on Ni-MWCNTs was used for mercury removal from air by SGPR. By proposed procedure, the Ni-MWCNTs were synthesized and put on quartz glass cell. By laboratory bench scale set up, mercury generated in chamber and flowed to sorbent and by amalgamation procedure mercury removed from artificial pure air. After optimizing conditions, the adsorption and desorption point for Ni-MWCNTs was obtained 20-45°C and 200°C, respectively.

The results showed us, the efficiency of mercury removal from air was more than 95% and less than 65% for Ni-MWCNTs and MWCNTs, respectively. The removal recovery was decreased less than 5 % in present of O$_2$ and H$_2$O by SGPR method. So, the Ni-MWCNTs introduced as novel sorbent with high efficiency for mercury removal from air in flow rate of 200 mL min-1 which was acted by physical and chemical adsorption mechanism.

5. Acknowledgements

6. References

[1] A. Wilk, E. Kalisińska, D. I. Kosik-Bogacka, Cadmium, lead and mercury concentrations in pathologically altered human kidneys, Environ. Geochem. Health, 39 (2017) 889–899.

[2] B. Mansouri, R. Baramaki, M. Ebrahimpour, Acute toxicity bioassay of mercury and silver on Capoeta fusca (black fish), Toxicol. Indus. Health, 28 (2012) 393-398.

[3] M. Gochfeld, Cases of mercury exposure, bioavailability, and absorption, Ecotoxicol. Environ. Saf. J., 56 (2003) 174-179.

[4] R. Afrin, M. Y. Mia, M. A. Ahsan, A. Akbor, Concentration of heavy metals in available fish species in the Turag river, Bangladesh, Pakistan, J. Sci. Ind. Res., Series B: Biol. Sci., 58 (2015)104–110.

[5] S. Cwan, Occupational toxicology, CRC Press. (2003) 317-319.

[6] PB. Tchounwou, WK. Ayensu, N. Ninashvili, D. Sutton, Environmental exposure to mercury and its toxicopathologic implications for public health, Environ. Toxicol. J., 18 (2003) 149-175.

[7] H. Shirkhanloo, M. Osanloo, M. Ghazaghi, H. Hassani, Validation of a new and cost-effective method for mercury vapor removal based on silver nanoparticles coating on micro glassy balls, Atmos. Pollut. Res., 8 (2017) 359-365

[8] NIOSH Manual of analytical methods (NMAM, 5 Edition), U.S. department of health and human services, 2017.

[9] Occupational Safety and Health Administration (OSHA), Air contaminants, 29 CFR

1910.1000,2017. http://www.osha.gov/laws- regs/ regulations/standardnumber/1910/1910.1000.

[10] M. Marczak, S. Budzyń, J. Szczurowski, K. Kogut, P. Burmistrz, Active methods of mercury removal from flue gases, Environ. Sci. Pollut. Res. Int., 26 (2019) 8383-8392.

[11] JG. Evan, WP. Henry, AH. Richard, Novel sorbents for mercury removal from flue gas, Ind. Eng. Chem. Res., 39 (2000) 1020-1029.

[12] Wu. Xiang, D. Yufeng, Li. Na, Hu. Peng, Y.Ting, M. Jialin, R. Shaojun, W. Hongqi, Regenerable Ce–Mn/TiO$_2$ catalytic sorbent for mercury removal with high resistance to SO$_2$. Energ. Fuel., 33(2019) 8835-8842.

[13] M. Lingjun, Y. Caixia, Y. Liang, H. Qihuang, H. Lina, C Liping, B Weiren, W Jiancheng, Effects of supports on Pd–Fe bimetallic sorbents for Hg^0 removal activity and regeneration performance from coal-derived fuel gas, Energ. Fuel., 33 (2019) 8976-8984.

[14] Z. Xiaoyang, C. Lin, L. Yuzhong, Z. Yongchun, D Yong, C Shensong, Adsorption and oxidation of mercury by montmorillonite powder modified with different copper compounds, Energ. Fuel., 33 (2019) 7852-7860.

[15] M. Jian, W. Chang, K. Lingnan, L. Xiaoli, H, Qixing, Z Hui, Y. Shijian, Outstanding performance of recyclable amorphous MoS$_3$ supported on TiO$_2$ for capturing high concentrations of gaseous elemental mercury: mechanism, kinetics, and application., Environ. Sci. Technol., 53 (2019) 4480-4489.

[16] F. Seef Saadi, KA. Mohamed, J. Wan Zurina Binti, A. Mohammed Abdulhakim A, F. Sabah Saadi, K. Suhana Binti, L. Sai Hin, C. Ming Fai, A. Ali Najah, ES. Ahmed, Artificial neural network approach for modelling of mercury ions removal from water using functionalized CNTs with deep eutectic solvent, Int. J. Mol. Sci., 17(2019) 4206-4212.

[17] S.S. Fiyadh, M.A. AlSaadi, .M.K AlOmar, S.S. Fayaed, A.R. Hama, S. Bee, A. El-Shafie, The modelling of lead removal from water by deep eutectic solvents functionalized CNTs: Artificial neural network (ANN) approach, Water Sci. Technol., 76(2017) 2413–2426.

[18] S.S. Fiyadh, M.A. AlSaadi, .M.K AlOmar, S.S. Fayaed, A. El-Shafie, Lead removal from water using DES functionalized CNTs: ANN modeling approach. Desalin. Water Treat., 150(2019) 105-113.

[19] M.A. AlSaadi, A. Al Mamun A., Alam M.Z., Amosa M.K., Atieh M.A. Removal of cadmium from water by CNT–PAC composite: Effect of functionalization, Nano., 11(2016) 1650011.

[20] M. Lu M, T, Ohba, K. Kaneko, K. Hata, M. Yumura, S. Iijima, H. Komatsu, A. Sakuma, H. Kanoh, Electron density modification of single wall carbon nanotubes (SWCNT) by liquid-phase molecular adsorption of hexaiodobenzene., Materials., 6(2013) 535–543.

[21] R. Yan, D.T. Liang, J.H. Tay, Control of mercury vapor emissions from combustion flue gas. Environ. Sci. Pollut. Res., J., 10 (2003) 399-407.

[22] PM. Ajayan, O.Z. Zhou, Applications of carbon nanotubes, Carbon Nanotubes J., 80 (2001) 391-425.

[23] P.E. Díaz-Flores, J.A. Arcibar-Orozco, N.V. Perez-Aguilar, J.R. Rangel-Mendez, V.M. Ovando Medina, J.A. Alcalá-Jáuegui, Adsorption of organic compounds onto multiwall and nitrogen-doped carbon nanotubes: Insights into the adsorption mechanisms, Water, Air Soil Pollut. J., 228 (2017) 133- 147.

[24] J. Xu, Z. Cao, Y. Zhang, Z. Yuan, Z. Lou, X. Xu, X. Wang, A review of functionalized carbon nanotubes and graphene for heavy metal adsorption from water: Preparation, application, and mechanism, Chemosphere. J., 195 (2018) 351- 364.

[25] W.N. Nyairo, Y. Ramazan Eker, C. Kowenje, I. Akin, H. Bingol, A. Tor, D.M. Ongeri. Efficient adsorption of lead (II) and copper (II) from aqueous phase using oxidized multiwalled carbon nanotubes/polypyrrole composite, Sep. Scie. Technol. J., 52(2018) 1498-1510.

[26] O. Moradi, K. Zare, M. Yari, Interaction of some heavy metal ions with single walled carbon nanotube, Int. J. Nano Dimens., 1 (2011) 203-20.

[27] F. Su, C. Lu, S. Hu, Adsorption of benzene, toluene, ethylbenzene and p-xylene by NaOCl-oxidized carbon nanotubes, Colloids Surf., A Physicochem. Eng. Asp., 353 (2010) 83-91.

[28] A. Safavi, N. Maleki, M.M. Doroodmand, Fabrication of a selective mercury sensor based on the adsorption of cold vapor of mercury on carbon nanotubes: Determination of mercury in industrial wastewater, J. Hazard. Mater., 173 (2010) 622-9.

[29] C.K Kuo, Desorption and re-adsorption of carbon nanotubes: Comparissons of sodium hydroxiid and microwave irradiation processes, J. Hazard. Mater., 152 (2008) 949-54.

[30] E. Granite, H. Pennline, R. Hargis, Novel sorbents for mercury removal from flue gas, Ind. Eng. Chem. Res., J., 39 (2000) 1020-1029.

[31] S.E. Lindberg, W.J, Stratton, Atmospheric mercury speciation, concentrations and behavior of reactive gaseous mercury in ambient air, Environ. Sci. Technol., 32 (1998) 49-57.

[32] T.G. Lee, Comprison of Hg captuer efficiencies of three in situ generated sorbent, Environ. Energy Eng., AIChE J., 47 (2001) 954-961.

The importance of microplastics pollution studies in water and soil of Nigeria ecosystems

Verla Andrew Wirnkor[a], Enyoh Christian Ebere[a,*], Verla Evelyn Ngozi[b]

[a,*] Group Research in Analytical Chemistry, Environment and Climate change (GRACE&CC), Department of Chemistry, Faculty of Science, Imo State University, Owerri, Imo State Nigeria

[b] Department of Environmental Technology, Federal University of Technology, Owerri, Imo State Nigeria

ABSTRACT

The ubiquity of microplastics in the environment is a novel problem to scientist, public media, governmental and non-governmental organization. The major problem is from the difficultness in removing them from the ecosystem. Elsewhere studies are being conducted while in Nigeria studies are relatively lacking. Production (10.3 %) and consumption (6.5 %) of plastics is on the increase annually, thereby, causing an increase in the amount of plastic waste generated annually. This is turn may potentially causing high microplastics pollution in Nigeria. Many reports have shown that microplastics could cause harm to man, animals and plants and exposure (or ingestion) could come from air, water and soil. Few studies have been conducted in Nigeria and reports have suggested high abundance of microplastics in Nigeria freshwater system. Following these observations, there is a clear need for more detailed studies focusing on the quantitative and qualitative determination of occurrence of microplastics in Nigeria ecosystem. Finally, from such studies, data generated will provide insight and understanding into the extent of microplastic pollution in Nigeria. Furthermore, the data will be important not only for both remediation and minimization of effects, but could be employed in averting occurrence through policies such as ban on some types of plastic uses in Nigeria. In this study, four manually generally microplastic types (PVC, acrylics, polyesters, silicones) were evaluated for heavy metals (Pb, Cd, Hg, and As) adsorption at optimized pH by ETAAS.

1. Introduction

According to Plastic Europe [1], producing and using plastics are vital in creating a more sustainable future because of specific properties including their light-weight, versatility and durability. However, the proposed sustainable future is not sustainable since plastic (including macro, meso and microplastics) pollution is now potentially deleterious and harmful to global ecosystem. As an increasing global issue, microplastic (from the degradation of macroplastic) contamination in marine, terrestrial and atmospheric environments is attracting significant attention from scientists, policy makers, and the public [2-7]. Microplastics are now naturally ubiquitous and have been detected in pelagic and neritic regions, deepest part of the ocean and highest (Tibetan Plateau) plateau of the world in significant quantities [6, 8-10]. In an effort to combat microplastic pollution, many governments in different continents worldwide have banned plastic use (especially single-use) and are encouraging recycling of plastics. Notable continents include Europe (England, Italy, Wales, Scotland, Germany), Asia (India, China, Bangladesh, Cambodia, Hong Kong, Indonesia, Malaysia, and

Taiwan), Australia, America (California, certain areas in Argentina, Brazil, Chile, and Colombia) while some African countries (Kenya, Mali, Cameroon, Tanzania, Uganda, Ethiopia, Malawi, Morocco, South Africa, Rwanda, and Botswana) have also banned plastic bags [11], though in principle but not in practice. In Nigeria, the problem of plastic pollution still persist and potentially on the increase, even though there are existing laws that may tackle these problems [12], but are not implemented or are poorly enforced [13]. Plastic industry in Nigeria is receiving massive investment and thus experiencing significant growth. In Sub-

Sahara Africa, excluding South Africa, Nigeria is the largest importer of plastics technology. The plastic types produced and imported in Nigeria are thermoplastics comprised mainly of polypropylene (PP), polyamide (PA; PA6 + PA66), polyethylene terephthalate resin (PET), polyethylene (PE; high density-PE, low density-PE, Linear low-density-PE), poly vinyl chloride (PVC), polystyrene (PS), acrylonitrile butadiene styrene (ABS), styrene-acrylonitrile resin (SAN) and polycarbonate (PC) [14]. There is a strong steady increase in plastic production (Figure 1) and consumption (Figure 2) in Nigeria (with negligible recycling). In the last
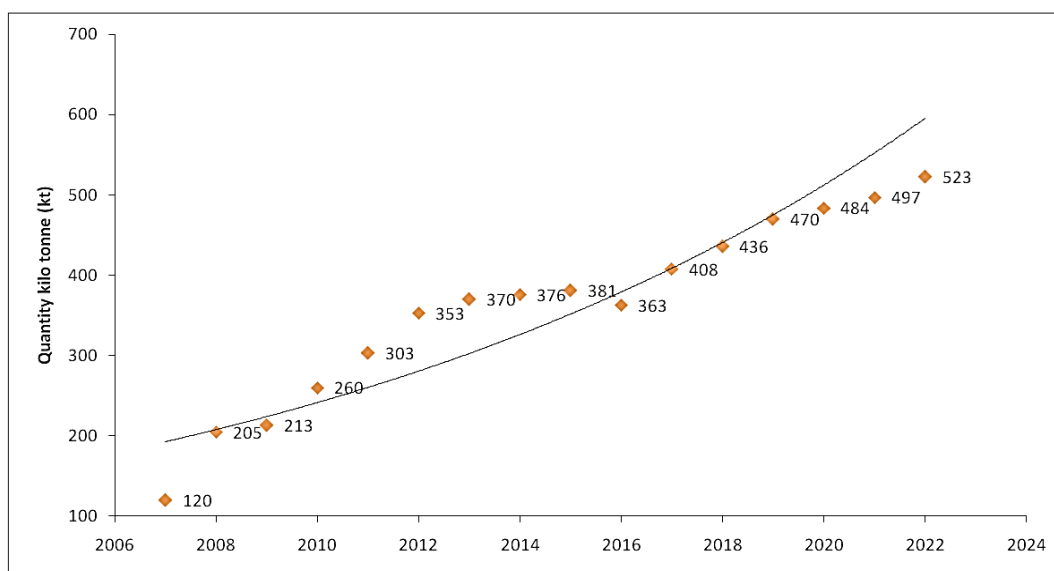

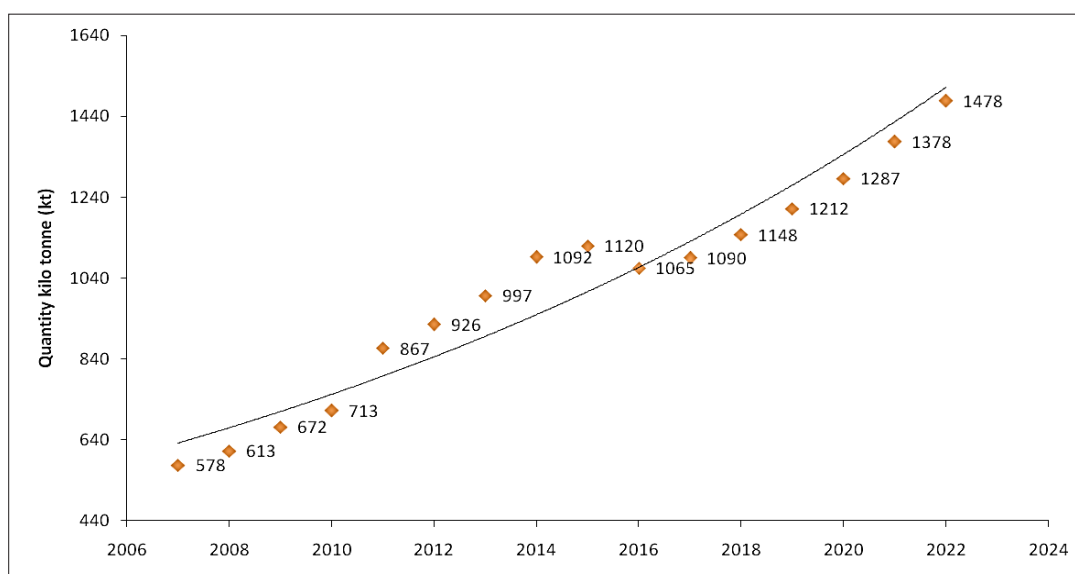**Fig. 1.** Plastic production in Nigeria (Data source: [14]).

Fig. 2. Plastic consumption in Nigeria (Data source: [14]).

decade, Nigeria's plastics production has grown by 10.3% annually, from 120 kt in 2007 to 436 kt in 2018 and is estimated to be 523 kt in 2022 while consumption (by application) has grown by 6.5% annually, from 578 kt in 2007 to 1.148 kt in 2017 and is estimated to be 1.478 kt in 2022 (Figure 2). Majority of plastic consumed (by application) is by packaging (55 %), 16 % by construction, 6 % for automotive and the remainder by various industries. So it is expected that the problem of microplastic pollution will increase as well (Figure 3), since there are currently no measure for curbing plastic waste in Nigeria. It is estimated that 10 % of plastic consumed annually in Nigeria end up as wastes in the environment and may continue to rise with increasing population. According to the estimates of United nations environment program [15], 6.4 million tons of plastic litter enters the world oceans each year, of which Nigeria is a major contributor (9th largest emitters), largely through the river Niger [16]. The river receives its wastes mainly from inland waterbodies in the country. Furthermore, 90 % of all the plastic that reaches the world's oceans are from ten countries, with Nigeria as one of them [17-18].

Plastics persist in the environment and can "outlive" humans by several hundred years (e.g PET degradation time ranged from 450-1000 years while average lifespan of human is < 100 years). So the first produced plastics in 1907 called "Bakelite" may still be in the environment till now (if not recycled). Sadly, plastic production in Nigeria is on the increase annually. The steady and huge increase in production and consumption is responsible for high plastic waste generation in Nigeria (Figure 3). Recent studies have shown that plastic is abundance in inland freshwater systems in Nigeria, often received from cities via surface run off [13]. Enyoh et. al., in 2019 [13] reported that plastic contributed 59 % of the 3487 macrodebris items/m^2 counted from shore of Rivers in Nwangele Local Government Area of Imo state. Similarly, a study of Cross River, Qua Iboe River and Jaja Creek in Akwa Ibom, Nigeria for suspended marine litter also reported high quantity of plastic (> 5000 kg/m^2) compared to other waste (can, foil etc < 1000 kg/m^2) [19]. Reports have shown that Macroplastics correlated strongly with microplastics indicating that wherever there is high abundance of macroplastics, there will be a corresponding high abundance of microplastics in that area [13,20]. Therefore, quantifying the abundance of microplastics and identifying their major sources in Nigerian environments is important to understand the potentially adverse impacts of microplastics to ecological systems in the country.
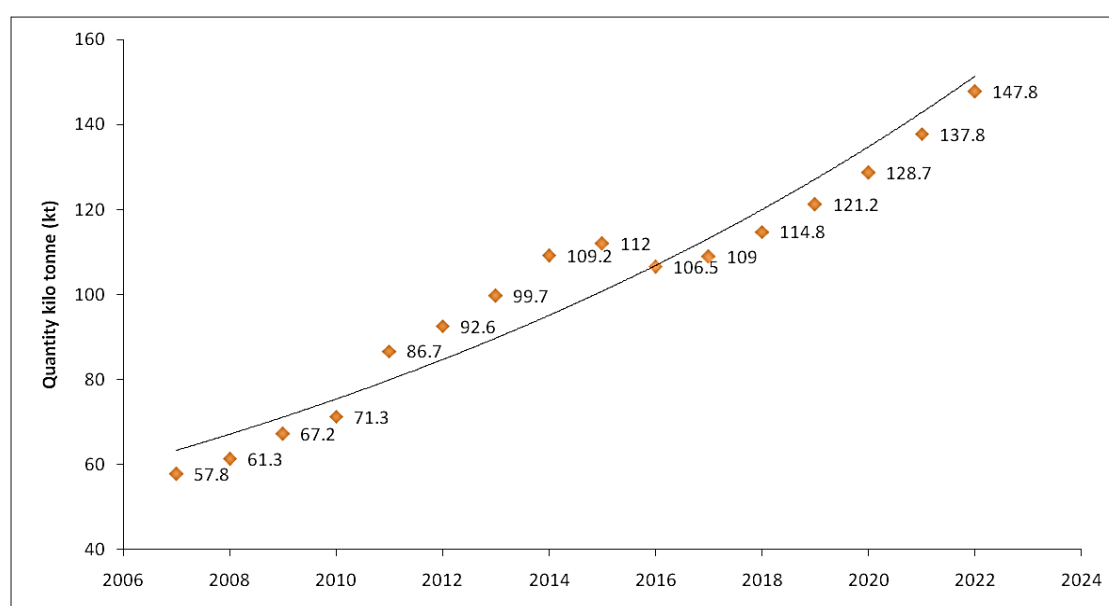

Fig. 3. Plastic waste (estimated) generated from plastic consumption in Nigeria

Extensive studies are being conducted in other countries regarding the occurrence, fate, and implication of microplastic in ecosystems [3-4, 6, 8, 21-23], while similar studies in Nigerian environment are very scarce [13]. This is probably due to lack of awareness and/or lack of standard methods for analysis [24]. Many people including government officials and health workers are not aware of the dangers associated with microplastic pollution because they have been taught that plastic is a safe material. Microplastics can serve as vectors to toxic chemicals in the environment and due to their small sizes; they can easily be ingested, where it may pose particle and chemical toxicity as well as microbial toxins through formed biofilm [6]. To the best of our knowledge, few studies (n = 3) covering 7 areas have been conducted in Nigeria till date (Table 1). Three invertebrates (L. varicus., M. tuberculata and T. fluviatilis) studied

from Osun river system as bioindicators for microplastics pollution in Nigeria revealed high quantity of fibre and three polymer types via PE, PP and nylon [25]. Briggs et al., focused on method development, however from re-interpretation of their results, one could say that there is high abundance of microplastics in surface water from Elechi creek (an area which experiences petroleum-industry related activities) [26]. Reconnaissance survey indicated that microplastics may be made up of PE, PS, PET and PA [26]. Enyoh et. al., in 2019 [13] reported small microplastics (11 µm) in surface water of Obiaraedu, Nwangele, Okumpi, Ogbajarajara and Onuezuze rivers which ranged from 440 to 1556 particles per liter. The shapes were generally fibre, film, fragment with PET, PE, PVC, PP as types of polymer. Overall studies have implicated significant microplastics pollution in Nigeria linked to anthropogenic activities.

Table 1. Available studies on microplastics in Nigeria ecosystem

Study area	Region	Media studied	Method used	MP load	Characteristics			Remark	References
					Size (µm)	Polymer type	Shape/ form		
Osun River (Osun state)	South Western, Nigeria	Invertebrates (*L. varicus.*, *M. tuberculata* and *T. fluviatilis;* as bioindicators)	Micro-FTIR	1.71 ± 0.46 to 6.1 ± 1.05 per g	0.2	PE, PP, nylon	Fibre, Film	Gives the first chemical identification of polymer types in freshwater invertebrates	[25]
Elechi creek (Rivers state)	South South, Nigeria	Freshwater	N/A	N/A	N/A	N/A	N/A	Work document for the first time, the sampling and sample extraction of microplastics in Nigeria.	[26]
Obiaraedu, Nwangele, Okumpi, Ogbajarajara and Onuezuze rivers (Imo state)	South Eastern, Nigeria	Freshwater	Microscopy	440 to 1556 particles/L	11	PET, PE, PVC, PP	Fibre, Film, Fragment	First report on MP quantification, distribution and composition of freshwater MP in Nigeria. Results from the study indicated high load of microplastics and provided baseline information for future assessments	[13]

N/A- not reported, FTIR-Fourier Transform Infrared Spectroscopy.

In Nigeria, knowledge about microplastic contamination of the ecosystem is still negligible, while such studies have been conducted elsewhere, especially in Europe, Asia and America. Preliminary studies show that in Nigeria there are microplastics in freshwater system and may be on the rise with increasing plastic production and consumption. There is a clear need for more detailed studies focusing on the quantitative and qualitative determination of occurrence in Nigeria ecosystem [air (indoor and outdoor), soil (including soil animals) and water (surface and groundwater)]. Such studies will provide insight and understanding into the extent of microplastic pollution in Nigeria. Importantly, increasing attention and studies on atmospheric microplastic pollution would be particularly beneficial to the protection of ecosystems in Nigeria, since the country is most polluted in Africa and fourth in the world regarding air pollution [27]. Furthermore, studies have shown that microlastics may be consumed from open meal in the house from indoor airborne microplastics during fall out and high during cooking periods [8, 23]. Finally, similar studies would be very important in Nigeria, where cooking is mostly done with stoves, charcoal, firewood etc. Furthermore, habits such as microwaving of food are rampant in Nigeria. This has been fingered as one possible way by which microplastics enter our food.

As stated earlier, heavy metals (with adverse effects associated with mutagenic, teratogenic and carcinogenic effects [28]) can be absorbed on microplastics and introduce as a major problem in environment [6]. Many methods used for determination heavy metals which were absorbed on microplastics from waters [29-32]. In an attempt to study this phenomenon, four manually generally microplastic types (PVC, acrylics, polyesters, silicones) were evaluated for heavy metal adsorption. Heavy metals such as Pb, Cd, Hg, and As was used with different concentration from 100-1000 μg L^{-1} in batch system with 20 mg of microplastics by vary times (min). Results showed in pH=3-6 high adsorption was achieved by surface of microplastics (PVC) at 60 min (pH=4-5). After, 60 min. the heavy metals desorption from PVC powder (1 g) with nitric acid 0.5 M(5 mL) and after dilution with 5 mL of DW, determined by atomic absorption spectrometry (AAS). The results showed, the adsorption capacity for PVC for Hg, Pb, Cd, and As was obtained 68.4 mg g^{-1}, 52.3 mg g^{-1}, 48.5 mg g^{-1} and 35.6 mg g^{-1}, respectively(Hg>Pb>Cd >As). So, microplastics (PVC powder) help in the removal heavy metals from waters and convert to new solid pollution in waters which must be removed (Fig. 4-6).
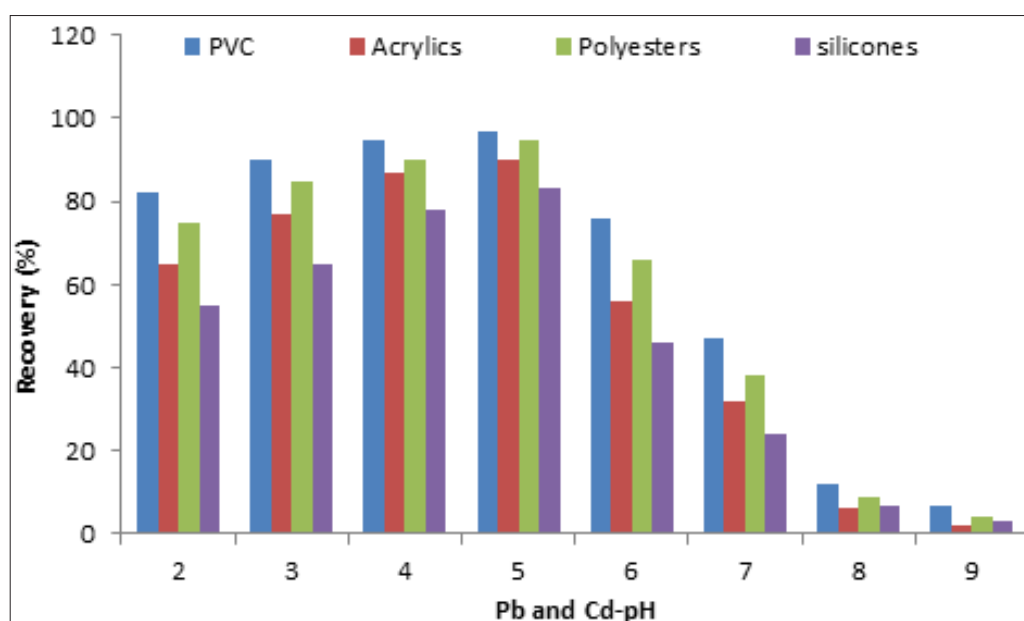

Fig. 4. The effect of pH on lead and cadmium extraction by microplastics
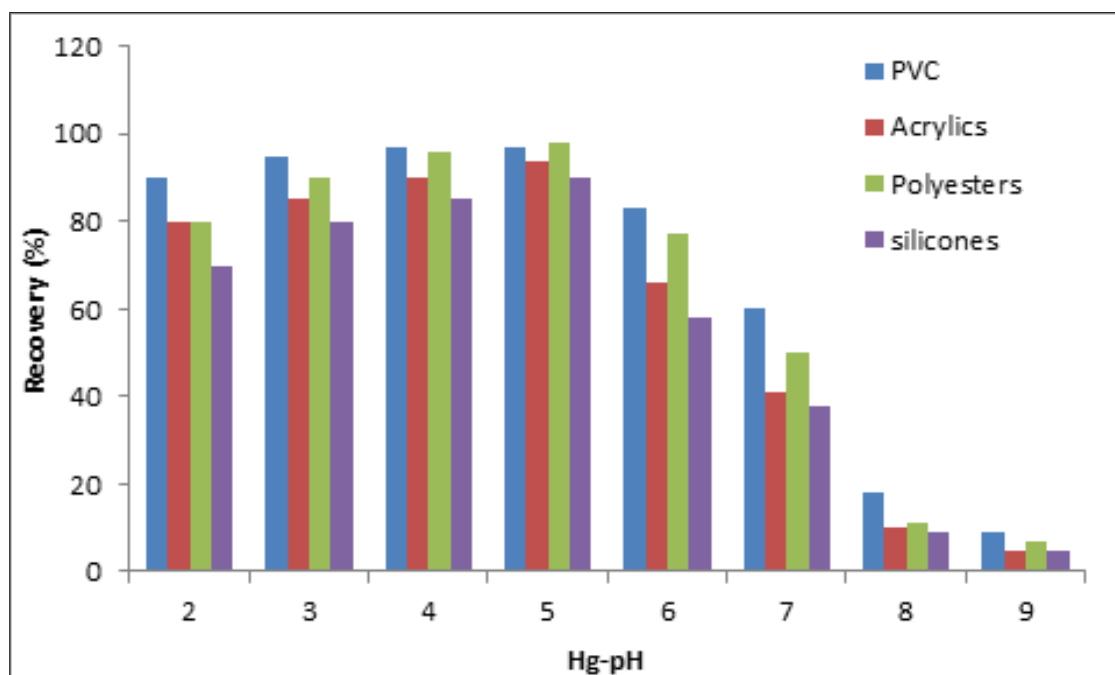
Fig. 5. The effect of pH on mercury extraction by microplastics

2. Conclusion

Microplastic studies are conspicuously absent from the huge volumes of journal papers from Nigerian authors. This unawareness is exacerbated by the general belief that plastics are non-toxic, biochemically inert and safe. Researchers elsewhere in the world are exploring the validity and veracity of this statement with many proposing that plastics degrade to microplastics and are responsible for the environment pollution called microplastics pollution. Occasionally microplastics absorbed toxic heavy metal from liquid matrix such as sea and rivers. In Nigeria, studies are not even a foot in understanding this pollution not to
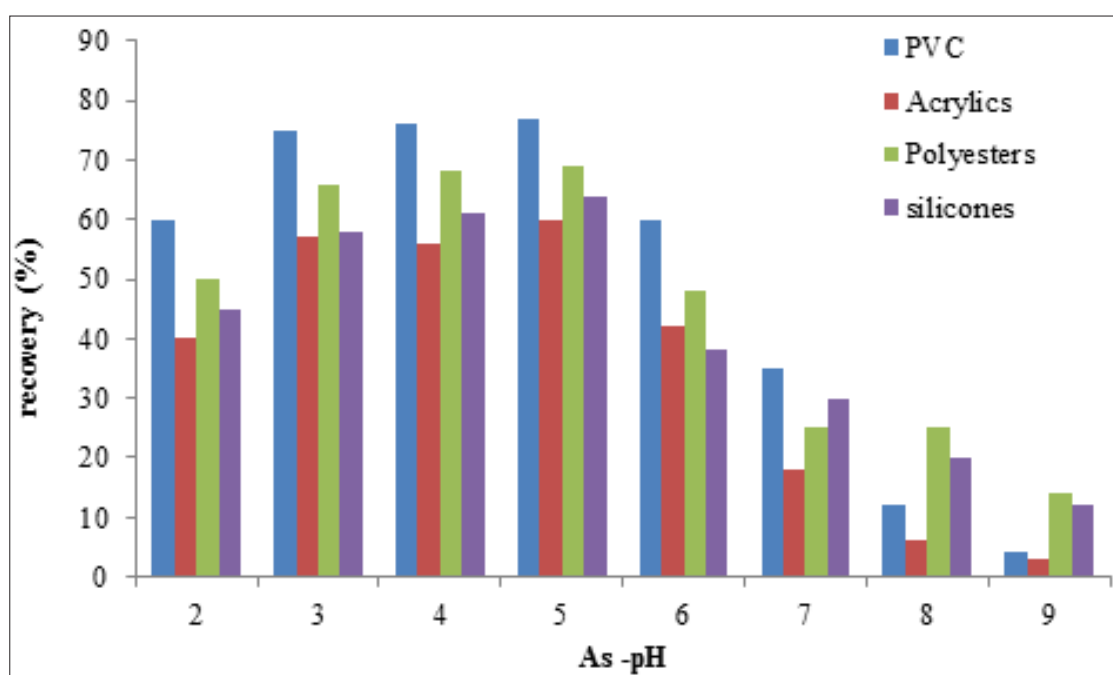

Fig. 6. The effect of pH on arsenic extraction by microplastics

talk of awareness. Despite the potential toxicity, there is research currently focusing on method of quantification and identification of microplastics in Nigeria as well as its removal in freshwater system. Also, determination heavy metals in water and microplastics are very important. As a matter of fact, when fully understood and the adverse effects of microplastics on man, his plants and animals are supported with data, the Nigerian government and policy makers with call for a ban of plastics as is currently done in developed countries. Therefore, a call is made here for more studies and awareness of this pollutant because a stich in time serves nine.

3. Conflict of interest
The authors declares no conflicts of interest

4. Acknowledgement

5. References
[1] Plastics europe, Plastics-the Facts: An analysis of European plastics production, demand and waste data, (2018). http://www.plasticseurope.org

[2] C. E. Enyoh, A. W. Verla, E. N. Verla, Uptake of microplastics by Plant: a Reason to Worry or to be Happy, World Sci. News, 131 (2019) 256-267.

[3] L. Van Cauwenberghe, A. Vanreusel, J. Mees, C.R. Janssen, Microplastic pollution in deep-sea sediments, Environ. Pollut., 182 (2013) 495–499.

[4] L. Van Cauwenberghe, L. Devriese, F. Galgani, J. Robbens, C. R. Janssen, Microplastics in sediments: A review of techniques, occurrence and effects, Marine Environ, Res,, 111 (2015) 5-17.

[5] A. W. Verla, C. E. Enyoh, E. N. Verla Microplastics, an emerging concern: A review of analytical techniques for detecting and quantifying microplatics, Anal. Method. Environ. Chem. J., 2 (2019) 15-32.

[6] A.W. Verla, C.E. Enyoh, E.N. Verla, K.O. Nwarnorh, Microplastic toxic chemical interaction: a review study on quantified levels, mechanism and implications. Appl. Sci. (2019). Accepted manuscript

[7] M.A. Browne, P. Crump, S.J. Niven, E. Teuten, A. Tonkin, T. Galloway, Accumulation of microplastic on shorelines worldwide: Sources and sinks, Environ. Sci. Technol, 45 (2011) 9175–9179.

[8] C.E. Enyoh, A.W. Verla, E.N. Verla, F.C. Ibe, C.E. Amaobi, Airborne microplastics: a review study on method for analysis, occurrence, movement and risks. Environ. Monit. Assess., (2019). Accepted manuscript

[9] M. Masó, J.M. Fortuño, S. de Juan, M. Demestre, Microfouling communities from pelagic and benthic marine matter to microplastic addition in Chinese loess soil, Chemosphere, 185 (2016) 907–917.

[10] Y. Zhang, T. Gao, S. Kang, M. Sillanpää, Importance of atmospheric transport for microplastics deposited in remote areas, Environ. Pollut., 254 (2019) PtA.

[11] E. Riskey, Which countries have banned plastic bags, Curr. Event., (2017) Accessed 27/09/2019. https://study.com/blog/which-countries-have-banned-plastic-bags.html

[12] NESREA, National Environmental Standards and Regulations Enforcement Agency; Laws and Regulations. (2009). https://www.nesrea.gov.ng/publications-downloads/laws-regulations/

[13] C.E. Enyoh, A.W. Verla, E.N. Verla, S.C. Ihenetu SC, Macrodebris and microplastics pollution in Nigeria: first report on abundance, distribution and composition, Inter. J. Environ. (*preprint* 2019). https://10.20944/preprints201908.0255.v1)

[14] J. Reisser, B. Slat, K. Noble, K. du Plessis, M. Epp, M. Proietti, J. de Sonneville, T. Becker, C. Pattiaratchi, The vertical distribution of buoyant plastics at sea: An observational study in the north Atlantic Gyre." *Biogeosci.,* ١٢ (٢٠١٥) ٥٦–١٢٤٩.

[15] UNEP, Marine Litter: A Global Challenge, Nairobi, (2009) 232.

[16] J.R. Jambeck, R. Geyer, C. Wilcox, T.R. Siegler, M. Perryman, A. Andrady, R. Narayan, K.L. Law, Plastic waste inputs from land into the ocean, Sci., 347 (2015) 768–771.

[17] C. Schmidt, K. Tobias, W. Stephan, Export of plastic debris by rivers into the sea, Environ. Sci. Technol., 51 (2017) 12246–12253.

[18] P. Jan, A. J. Löhr, F. G. A. J. Van Belleghem, A. M. J. Ragas, Wear and tear of tyres: A stealthy source of microplastics in the environment, *Int. J.*

Environ. Res. Pub. Health ١٤ (2017) 1265. https://doi.org/10.3390/ijerph14101265.

[19] B.B. Babatunde, O.U. Arinze, Suspended marine litter in Akwa Ibom state, Nigeria: A case study of cross river, QUA Iboe river and Jaja Creek, J. Geography Environ. Earth Sci. Inter., 18 (2018) 1-13.

[20] J. Lee, S. Hong, Y.K. Song, S.H. Hong, Y. C. Jang, Y.C., M. Jang, W.J. Shim, Relationships among the abundances of plastic debris in different size classes on beaches in South Korea. Marine Pollut. Bull., 77 (2013) 349–354.

[21] H. Liu, X. Yang, G. Liu, C. Liang, S. Xue, H. Chen, C.J. Ritsema, V. Geissen, Response of soil dissolved organic matter to microplastic addition in Chinese loess soil, Chemosphere, 185 (2017) 907-917.

[22] A. Lusher, P. Hollman, J. Mendoza-Hill, Microplastics in fisheries and aquaculture: status of knowledge on their occurrence and implications for aquatic organisms and food safety, FAO Fish. Aquacult. Tech. Paper, 615 (2017).

[23] A.I. Catarino, M. Valeria, G.S. William, C.T. Richard, B.H. Theodore, low levels of microplastics (MP) in wild mussels indicate that MP ingestion by humans is minimal compared to exposure via household fibres fallout during a meal, Environ. Pollut., 237 (2018) 675-684.

[24] C.E. Enyoh, Microplastic pollution in Nigeria: A call for concern. 26Th meeting of the Imo State chapter of the chemical society of Nigeria (CSN) held at Imo State University, Nigeria, (2019) 1-15.

[25] E.O. Akindele, M.E. Sonja, H.E.K Jochen, First empirical study of freshwater microplastics in West Africa using gastropods from Nigeria as bioindicators, Limnologica J., 78 (2019) 125708.

[26] E. Briggs, E.A.B. de Moura, H.A. Furusaw, M.E.B. Cotrim, E.E. Oguzie, A.B. Lugao, Microplastics: A Novel method for surface water sampling and sample extraction in elechi Creek, rivers state, Nigeria, characterization of minerals, metals and materials, the minerals, metals and materials society, (2019) 269-281.

[27] C.E. Enyoh, A.W. Verla, We are breathing Plastic; Don't Just Look down, Look up, Presented at the 3rd IMSU World Environment Day International Conference (2019).

[28] A.W. Verla, E.N. Verla, M.A. Chigbo, C.L. Kelechi, O.S. Ngozi, C.E. Enyoh, Biomonitoring of heavy metals in blood and urine of African children from Owerri Metropolis, Eastern Nigeria. J. Chem. Health Risks, 9 (2019) 11-26.

[29] D. Brennecke, B. Duarte, F. Paiva, I. Caçador, J. Clode, (2016) Microplastics as vector for heavy metal contamination from the marine environment, Estuar. Coast. Shelf Sci., 178 (2016)189-195.

[30] F. Fu, Q. Wang, (2011) Removal of heavy metal ions from wastewaters: A review, J. Environ. Manage., 92 (2011) 407-418.

[31] L. A. Holmes, A. Turner, R. C. Thompson, Adsorption of trace metals to plastic resin pellets in the marine environment, Environ. Pollut., 160 (2012) 42-48.

[32] J. Wang, J. Peng, Z. Tan, Y. Gao, Z. Zhan, Q. Chen, L. Cai, 2017): Microplastics in the surface sediments from the Beijiang River littoral zone: Composition, abundance, surface textures and interaction with heavy metals, Chemosphere 171(2017) 248-258

A Review: Analytical methods for heavy metals determination in environment and human samples

Mojtaba Arjomandi[a,b] and Hamid Shirkhanloo[c,*]

[a] *Department of Water Sciences and Engineering, Science and Research Branch, Islamic Azad University, Tehran, Iran / Research Institute of Petroleum Industry (RIPI), Tehran, Iran*
[b] *Department of Geophysics, Geological Survey and Mineral Explorations of Iran (GSI),Tehran, Iran*
[c,*] *Research Institute of Petroleum Industry, West Entrance Blvd., Olympic Village, P.O. Box: 14857-33111, Tehran, Iran.*

A B S T R A C T

Heavy metals are vital and necessary in our daily lives. Moreover, if the amounts of heavy metals are more than the acceptable amounts (mentioned by WHO) in soil, water, and air, indeed, they cause a lot of diseases in human bodies. Therefore, monitoring and measuring the amounts of heavy metals which are arduous and difficult are so important. In this review paper, a lot of studies which have been carried out on the determination and quantification of heavy metals in human bodies, soil, and water are considered. Moreover, the effect of toxicity of each heavy metal on human health is assessed. According to WHO, EPA, NIOSH, ACGIH, and clinical chemistry, determination of heavy metals such as Cd, Pb, Zn, Hg, Cu, Mn is very important in human body and Environmental matrixes. For example, the range concentration of heavy metals in human body such as, cadmium is about 0.3 to 0.98, and for cooper, it is about 0.01 – 1.107 ppm. In addition, most obtained results demonstrate that the lowest and highest range concentration of heavy metals in blood of human body has been equal to 0.56–8.78 ppm and 0.08 – 4.67 ppm respectively. Finally, in this review paper, the approaches of quantification of heavy metals using atomic absorption spectrometry, gas chromatography, inductively coupled plasma mass spectrometry etc. in human bodies, water, and soil are assessed.

1. Introduction

Many different techniques have been applied for determination of heavy metal in different samples. Atomic absorption spectrometry (AAS) is a quantitative method of metals analysis which was suitable for the determination of 70 elements by three option accessory (flame, furnace, Hydride generation). AAS measures the concentration of the metals by passing light (wave length emitted) by a radiation source of a particular element such as Hg, As, Pb and etc. Many metals determined by electrothermal atomic absorption spectrometry (ET-AAS) [1-9], flame atomic absorption spectrometry (F-AAS and FS-AAS) [10-18], atom trapping flame atomic absorption spectrometry (AT-FAAS), Hydride generation atomic absorption spectrometry, Cold vapor-atomic absorption spectrometry (HG-AAS, CV-AAS)[19, 20] and fluorescence spectrometry (XRF) [21-24]. Also, direct current polarography (DCP) [25, 26], differential pulse polarography (DPP), neutron activation analysis (NAA), inductively coupled plasma-optical emission spectrometry (ICP OES) [27, 28], inductively

coupled plasma- mass spectrometry (ICP-MS) [29, 30], UV-VIS [31], HPLC-inductively coupled plasma-mass spectrometry (HPLC - ICP - MS) [32], electrophoresis(EP) [33], Anodic striping voltammetry (AVS) and inductively coupled plasma-mass spectrometry (ICP-MS) was used for heavy metal determination in different matrix [34, 35]. Arida et al showed that the assessment of heavy and toxic metals in the blood and hair by modern analytical techniques in review paper. Heavy metals and toxic metal effect in blood and hair of some smokers was determined by modern analytical techniques. The levels of Hg, Pb, Cd, As, Se, Mn, Zn, Ni, and Cr were determined using inductively coupled plasma-atomic emission spectrometer (ICP-AES) [36]. A review procedure based on heavy metal analyzing in soil was developed with sequential extraction by Zimmerman et al in 2010. They showed that the quantification extraction and determination of heavy contamination in soil cannot give reliable results. They showed, the procedures of community bureau of reference (BCR) and geological society of Canada (GCS) procedures were examined to clarify benefits and limitations of each [37]. Also, determination of heavy metal in blood evaluated with AAS by Batool and Ahmad at 2018. The blood samples were divided into two parts .First for analysis of total blood and other for serum. By centrifuging the blood and serum sample separated. Serum after adding de ionized water analyzed by instrument after digestion. For whole blood samples wet digestion apply before analysis. Before analysis, blood samples were kept in freezer at 4 °C. In this study, wet digestion includes decomposition by acids carried out on hotplate and continued by AAS model Varian AA 240 [38]. Yuan Fu et al used Titanate/TiO$_2$ as adsorption sorbent for heavy metals determination and adsorption by nanotechnology. The titanate/TiO2 Nanomaterials were synthesized by Biomolecules (lignin). The titanate/TiO$_2$ characterized by XRD, FESEM, TEM, FTIR and BET, and their adsorption for heavy metals were studied. The found the maximum adsorption capacity of heavy metal ions (Pb^{2+}, Cu^{2+}, Cd^{2+}) based on procedure

[39]. Zhang et al showed, the nanomaterials can be treatment in water and wastewater samples. They introduce a novel nanotehecnology which was used by researcher included, the synthesis and physiochemical properties of nanomaterials, carbon based nanomaterial, metal and metal oxides nanoparticles were focused on removal of various heavy metals in water and wastewater [40]. Chromium speciation in natural water samples was developed by solid phase extraction procedure. Cr(VI) can be extracted with ammonium pyrrolidine dithiocarbamate (APDC) pasted on multi walled carbon nanotubes (MWNTs). The total chromium was determined by oxidation of Cr(III) to Cr(VI). The Cr(III) concentration is calculated by subtracting of total chromium and Cr(VI) [41]. Cr (VI) compounds, once inside the bloodstream, are actively transported into red blood cells (RBC) via nonspecific anionic channels and then rapidly reduced to Cr (III) which becomes bound to hemoglobin. As canceroginic effect of Cr (VI) determination of Cr (VI) very important. Also, in Figure 1, metabolism and formation of DNA damage by CrVI at pH 7.4 are shown.

Zendehdel et al studied on a HAp/NaP nanocomposite by adding a synthesized nano-hydroxyapatite to zeolite NaP gel. They used HAp/NaP for the removal of lead(II) and cadmium(II) ions from aqueous solution. This nanocomposite was characterized by FTIR, X-ray, SEM, energy-dispersive X-ray analysis and thermal analyses [42]. Microwave-assisted method was used for synthesizing of graphene nanosheet/δ-MnO$_2$ (GNS/MnO$_2$) composite. TheGNS/MnO$_2$ as sorbent was used for removal of NI(II) from waters. SEM, TEM and FTIR show that nanoscale δ-MnO$_2$ deposit well on GNS. The adsorption process was achieved in optimized pH [43]. Ojea-Jiménez et al showed that the removal of mercury from the Ebro River by Colloidal gold nanoparticles (Au NPs). Au NPs have been used for sequestration removal of Hg(II) from multicomponent waters. Under optimized conditions, sodium citrate was reduced Au NPs as the catalyst in the reduction of Hg(II), which is efficiently trapped in the presence of Cu(II) and
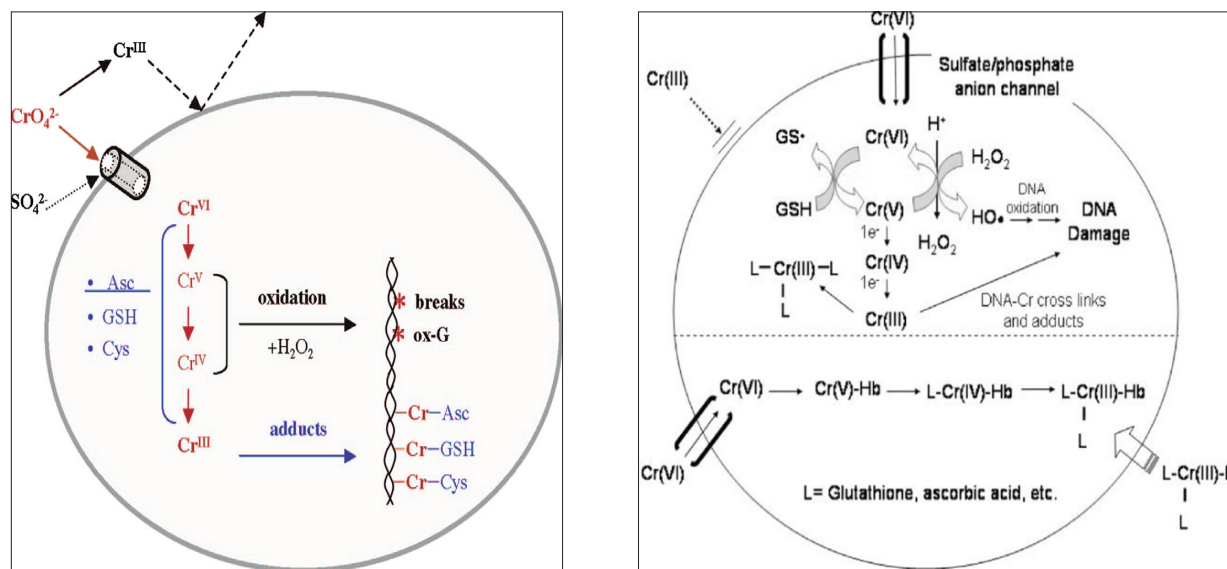
Fig. 1. Metabolism, and formation of DNA damage by Cr (VI) at pH 7.4.

Fe(III) [44]. Many references existed for separation and preconcentration and determination based on LLME, SPE, MSPE, IL/MSPE, USA-MSPE etc. in water, human biological and food samples by nanotechnology [45-56]. Also many developed methods was reported by researchers by green solvents such as ionic liquid for extraction of heavy metals in different matrixes [57-88]. In addition, an advanced approach for separating As(III) and As(V) ions in environmental matrixes was presented by Soylak et al in 2009 [89]. In their research, when dilute $KMnO_4$ was used to oxidize As(III), then the developed coprecipitation was used to determine total arsenic [89]. The difference between the total arsenic content and As(V) content was calculated as Arsenic(III) [89]. Moreover, in their study, hydride generation atomic absorption spectrometry (HG-AAS) was used to determine arsenic levels. Also, after calculating the factor of preconcentration, it was found out that the factor was equal to 25. In addition, the detection limits (LOD) for As(V) was 0.012 μg.L^{-1} [89]. A new approach for solid phase extraction (SPE) of gold(III) by using Dowex M 4195 chelating resin was developed by Soylak et al in 2007 [90]. The quantitative sorption of gold^{3+}, effect of flow rates, pH, sorption capacity, eluent types, and the effect of diverse ions on the sorption of Au^{3+} were investigated to find optimum experimental conditions [55]. In their work, for

more than 100 cycles of sorption–desorption, the chelating resin was reused without any considerable change in sorption of Au^{3+} [90]. In their work, the preconcentration factor was calculated to be 31. Detection limit (LOD) of Au was greater than 1.60 μg L^{-1} and the recovery values for Au^{3+} was greater than 96% [90]. The adsorption capacity of the resin was 8.1 mg.g^{-1}. Their proposed approach has been determining Au^{3+} in some real soil and water samples were used and showed the best results [90]. For characterizing As(III) biosorption from aqueous solution, green algae (*Ulothrix cylindricum*) biomass was used by Soylak et al in 2009 [91]. According to their studies, the biosorption capacity of *Ulothrix cylindricum* biomass was equal to 67.2 mg g^{-1} [91]. The outcomes of their work indicated that the processes of biosorption of As^{3+} followed well pseudo-second-order kinetics [91]. Separation of Cu^{2+} in environmental matrixes by using solid phase extraction on multi-walled CNT (carbon nanotubes) was studied by Soylak and Ercan in 2009 [92]. The optimum adsorption was obtained on MWNTs column in their study when pH was equal to 7.0. The preconcentration factor was equal to 60. Also, the detection limit for Cu^{2+} was equal to 1.46 μg L^{-1} [92]. For atomic absorption spectrometry, separation of trace heavy metals in sediment, urine, and dialysis concentrates by coprecipitation with samarium hydroxide was

carried out by Elci et al in 2003 [93]. In their study, the optimum pH for collecting trace heavy metals on samarium hydroxide was equal to 12.2. Also, coprecipitation occurs after 30 minutes, and when quantitative recovery is governed, and the precision is about 5% for the analytes [93]. Determining heavy Metals in plants, soil, and groundwater which followed high-rate sewage sludge was studied by Speir et al in 2003 [94].The pH of samples was less than 4. Also, during five years, the concentration of Zn in the soil reduced from 27 mg kg^{-1} to 0.04 mg kg^{-1}. Moreover, based on their study, there is a direct relation between the concentration of heavy metals in plants and the concentration of heavy metals in the soil [94]. An advanced biological treatment plant for removing heavy metals in groundwater was presented by Scheeren et al in 2007. Groundwater below the zinc production plant was contaminated with sulphate and heavy metals. To avoid contamination of nearby drinking-water aquifers in the future, a treatment plant for extracting contaminated ground water was established by them [95]. Effluent treatment based on activity of Sulphate Reducing Bacteria (SRB) for excess sulphide in solids for achieving the discharge criteria was designed by them. The reducing the sulphate to sulphide and thereby, precipitation of metal sulphides were obtained when anaerobic bacteria are there in the soil or the bacteria are injected [95].

Determination of trace heavy metals in harvested rainwater by ICP-MS was used by Malassa et al in 2018 [96]. Inductively coupled plasma mass spectrometry (ICP-MS) was used to quantify the content of each trace heavy metal (Cr, Co, Mn, Ni, Cu, Zn, Mo, Ag, Cd, Bi, and Pb) in a few rainwater samples. Their results indicated that that the concentrations of Cr, Mn, Ni, Ag, and Pb are more than the WHO limits in drinking water [96]. Contamination of heavy metals in sediments of the Karasu spring in Nigde, Turkey has been investigated by Yalcin and Narin in 2007 [97]. A few sediment matrixes were collected from contaminant sites along the spring. Moreover, concentrations of heavy metals have been

determined by X-ray Fluorescence Spectrometer [97]. The amount of Co, Cu, As, Sn, Ni, Zn, Ca, Pb, Al, Fe, Ti, Cr, and Mn contents of the Karasu creek sediments were equal to 18.30–69.00, 12.40–595.0 5.50–345.3, 5.80–15.1, 10.9–64.1, 28.90–103,300, 4.1–356.2, 7.70–37,840, 13,460–109,400, 11,740–62,900, 22.18–59.04, 41.70–369 and 12.09–3,480 mg/kg respectively. Moreover, according to their results, the presence of a contamination in the Karasu creek is obvious. In the case study, all the metal concentrations are more than acceptable limit values. In addition, in the Karasu creek and the Akkaya dam, eutrophication has been being developed. Also, it sounds that the accumulation of heavy metal in the creek is come from the discharge of mine quarries, domestic, and industrial wastes [97]. Separation of arsenic(III) and arsenic(V) by using *Streptococcus pyogenes* which has been immobilized on Sepabeads SP 70 resin has been considered by the approach of solid-phase extraction by Uluozlu et al in 2010 [98]. In sample solutions, hydride generation atomic absorption spectrometry (HGAAS) has been used to quantify the arsenic levels [98]. Their procedure has been governed when recovery of As^{3+} was more than 95%. Moreover, recovery of As^{5+} which was obtained was less than 5%. By using KI and ascorbic acid, As(V) has been reduced; in addition, after 1 hour later, for determining total arsenic, their system has been applied. As^{5+} has been calculated by subtracting the total As from As(III) content [98,99]. Some experimental parameters such as pH, amount of microorganism, sample volume have been assessed in their study. The capacity of biosorbent for As^{3+} has been equal to 7.3 mg g^{-1}. The preconcentration factor has been found to be equal to 36 [99]. The relative standard deviation has been obtained less than 8% [99]. Moreover, the contamination of trace heavy metal ions in drinking water samples has been investigated by Tuzen et al in 2005. According to their studies, if the amount of lead in drinking water samples is more than 10 microgram per liter, brain tissues and kidneys will be damaged [100]. Assessment of the amount of each metal in Drinking Waters from the

Tokat-Black Sea Region of Turkey was studied by Tuzen and Soylak in 2006. In their study, atomic absorption spectrometry was used to determine the amount of Cr, Ni, Cu, Mn, Zn, Fe, Co, and Al ions. According to their study, the amount of the heavy metals was lower than the maximum acceptable limits which were set by the World Health Organization [101-138]. In this review paper, the amounts of heavy metals and their toxicity in water, soil, air, and human bodies which have been studied and quantified by other researchers during the last decade are considered.

2. Experimental

Kaipei Qiu used ultrafine mesoporous magnetite nanoparticles (UFMNPs) for removal of heavy metals from waters (Scheme 1). Ultrafine magnetite NPs(UFMNPs, Fe_3O_4) were synthesized by co-precipitation method and successfully used as adsorbents for the removal of Pb^{2+}, Cd^{2+}, Cu^{2+}, and Ni^{2+} ions from contaminated river water. Also, the adsorption/desorption tests demonstrated that the ultrafine Fe_3O_4 NPs were reusable and can be used several times [139].

Gollavelli et al and Luo et al used Magnetic Graphene and magnetic chitosan/cellulose microspheres for removal of heavy metal from dinking waters, waters [140,141]. Mahmoudi ,Chen and Neyaz can be extracted heavy metals from different matrix by iron oxide nanoparticles (SPIONs), Fe_3O_4 @ SiO_2 and functionalized iron

oxide nanomaterials [142-144]. Tuzen et al showed a novel method based on switchable hydrophilicity microextraction syringe system (μS-SHS) by electrothermal atomic absorption spectroscopy (ETAAS). The proposed method was developed for separation and determination of vanadium in waters by complexing 2-(5-Bromo-2-pyridylazo)-5-diethylaminophenol (5- Br-PADAP). In this study, LOD, EF, and RSD were achieved 7.5 ng L^{-1}, 120 and 2.91 %, respectively. In addition, the μS-SHS is consisting of micropipette tip and syringe system was designed. First, the 10 mL of real sample was placed on beaker and then, 5- Br-PADAP solutions as ligand were used by sucking into syringe system. Finally, 0.1 mL of decanoic acid as a hydrophobic effect sucked into to solution which was followed by 500 μL of 1.0 mol L-1 Na_2CO_3 solution as a switchable hydrophobicity for the decanoic acid ($CH_3(CH_2)_8COOH$) in liquid phase. The surface response methodology was used to calculate response surface between [pH]/[V of SHS] and [pH]/[V of Na_2CO_3] of the vanadium. The results showed, high recovery based on 112 μL of SHS and 624 μL of Na_2CO_3 was obtained at pH=3.28. The design of experiments (DOE) was used for analyzing data and optimizing by surface response methodology [102]. Xiaogang Luo et al explained a novel sorbent for absorption heavy metals from waters. The carboxyl decorated magnetite (Fe_3O_4) nanoparticles (MN-CA) were obtained by modifying the magnetite surface with
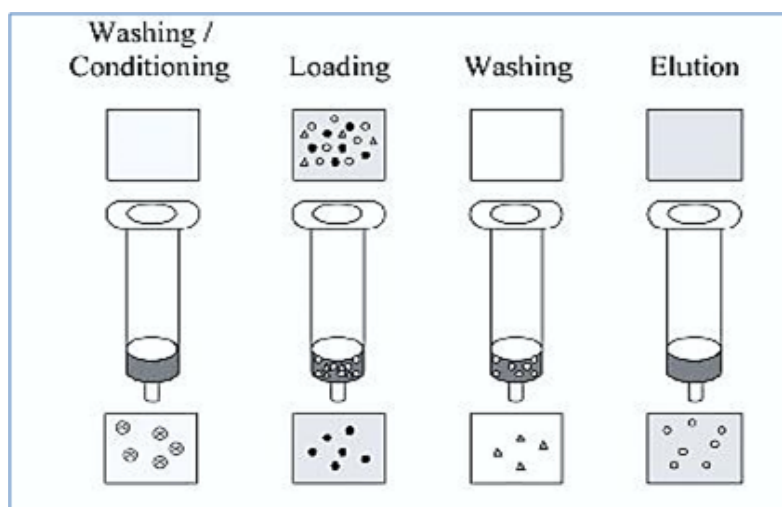
Scheme 1. SPE method for extraction heavy metals from liquids

citric acid. .In this research, the combination of specifically modified magnetic nanoparticles and activated carbon(AC) to cellulose may create new nanocomposite adsorbents, which possess high adsorption capacity for heavy metals removal and easy recovery by magnetic field. It could be deduced that electrostatic attraction between negatively charged magnetic cellulose-based beads (MCB) samples and positively charged Cu^{2+}, Pb^{2+}, and Zn^{2+} was the initial driving force of heavy metals binding to the adsorption site of the adsorbents [145]. Researcher such as Shannon, Luo, Gericke, Karami and Zhao et al worked for removal heavy metals from water, water Purification, wastewater treatment and methyl orange removal by novel technique with different sorbents such as; activated magnetic cellulose Microspheres, functional cellulose beads, magnetite nanoparticles,and hierarchical $MWCNTs/Fe^3O_4/PANI$ magnetic composite [146-150]. For determining the amount of metals in drinking water samples, the Perkin Elmer Analyst 700 atomic absorption spectrometer was used by Tuzen and Soylak in 2006 [101]. A 10 cm long slot-burner head, a lamp and an air-acetylene flame were applied. In solid phase extraction (SPE) studies, a glass column with 100 mm high and 10 mm in diameter was applied [101]. The solid phase materials such as Amberlite XAD-1180, Amberlite XAD-4 and Diaion HP-2MG was purchased, and they were prepared with the washing steps as reported previously in literature. They collected the drinking water samples in prewashed (with detergent, doubly de-ionized distilled water, diluted HNO_3 and doubly de-ionized distilled water, respectively) polyethylene bottles from eight stations in Tokat and villages around Tokat in July 2004. The samples were obtained from the water pump directly after the water had run for at least twenty minutes. They filtered the samples by using a Millipore cellulose membrane with a 0.45 µm pore diameters [101]. After the process of filtration, nitric acid was used to acidify the samples to 1%, and then the samples were stored in 1 L polyethylene bottles. The samples were thereby stored at 4 °C for a short time, afterwards they were analyzed until the

changes of the physicochemical form of the metals were minimized [101]. Electroplating industry, tanneries, electronics manufacturing industry, coal-fired power plants and mining operation are key sources of heavy metal pollution in water [151]. Lead (Pb) is discharged into water sources from various industries and is highly toxic to human beings even at trace concentrations. Maximum contaminant level of Pb(II) in drinking water is set at 15 µg L−1 by US Environmental Potential Agency (US EPA). Chromium(Cr), another toxic heavy metal pollutant, is mainly present in the effluents of leather tanning, electroplating and chromate preparations. Chromium is found in two oxidation states Cr(III,VI) and Cr (VI) is more toxic. World Health Organization (WHO) guideline for Cr(VI) in drinking water is 50 µg L⁻¹. So determination and separation this pollutant from waters with novel technique based on sorbent adsorption is very important [151]. Santhosh et al showed lead and Cr simply extracted from water solutions by PG-C and CNF-C [151]. By using thermal process, cobalt ferrites ($CoFe_2O_4$) paste on porous graphene (PG) and carbon nanofibers (CNF)), which was named PG-C and CNF-C nanocomposites as magnetic adsorbents [151]. In Figure 2, removal of heavy metals using nanographene is shown.

Sarika Singh et al used a functional oxide nanomaterials and nanocomposites for the removal of heavy metals and dyes in liquid phase. They showed that the oxide-based nanomaterials, such as Fe_3O_4, ZnO and TiO_2 for the removal of different toxic metals and organic dyes at optimized pH. Magnetic nanoparticles as excellent sorbent can be used as highly effective, efficient and economically-viable for removal toxic metals with advantages of easy separation under a magnetic field for reuse. Shen et al have observed that the adsorption efficiency of Ni^{2+}, Cu^{2+}, Cd^{2+} and Cr^{6+} ions by Fe_3O_4 nanoparticles is strongly dependent on pH, temperature, and the amount of the adsorbent. In optimized conditions, 3.5 mg mL⁻¹ dose of nano-adsorbent with an optimum pH=4 was used for removal heavy metals from contaminated water [152]. Phoebe Zito Ray et al studied on Inorganic
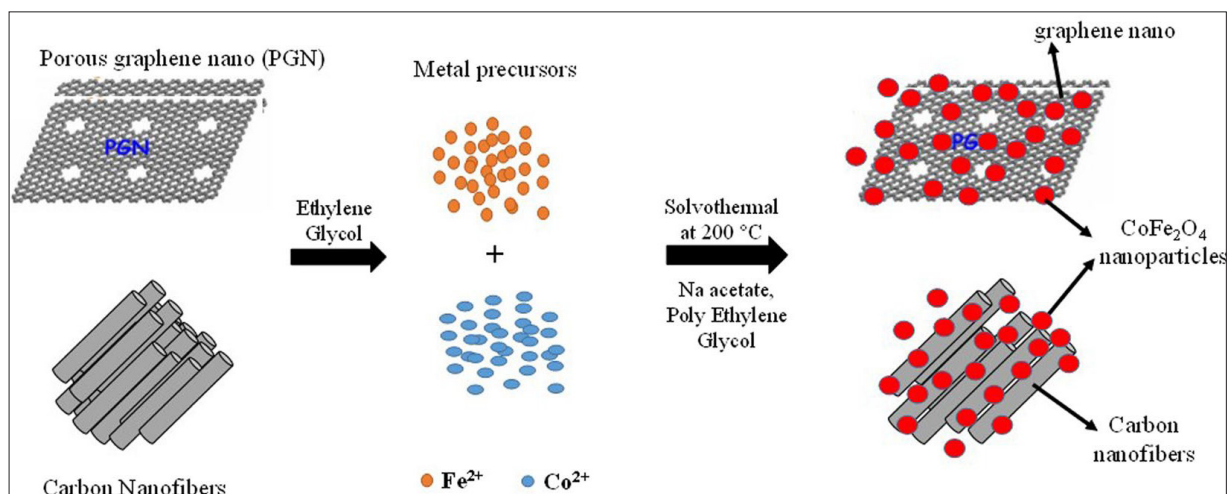
Fig. 2. Removal of heavy metals using nano-graphene [151].

nano-adsorbents for the removal of heavy metals and arsenic in aqueous solutions. They were explained that metal oxides and CNTs as nanoadsorbents were used for heavy metal removal in aqueous solutions. Phoebe Zito Ray et al used the iron oxide (hematite, magnetite and maghemite), carbon nanotubes (CNT), and metal oxide based (Ti, Zn) and polymeric nanoadsorbents for this study. Based on reults, metal oxides can have increased surface area and possess favorable sorption to heavy metals. ZnO nanoplates showed complete removal of Cu^{2+} in aqueous solutions [153]. Recently, CNTs and nZVI synthetized by coupling these nanomaterials and was efficient used for removal of Cr(VI), Se and Co from polluted water by Giorgio Vilardi et al. Regeneration studies were performed fixing CNTs-nZVI concentration and the initial metal concentration equal to $10 \, mg \, L^{-1}$, as already reported in a previous study [154]. Experimental results of adsorption batch tests showed that the removal efficiency of nanomaterials was in decreasing order: CNTnZVI>nZVI>CNTs>CNTs-nZVI, except for the Cr(VI) that nZVI was the most efficient material. Furthermore, the removal of Cr(VI) was found to not be affected by varying the pH in the case of using nZVI, but decreased with increasing pH when using the other three nanomaterials [154]. Also, Majed Alrobaian and Hassan Arida studied on Assessment of Heavy and Toxic Metals in the Blood and Hair of Saudi Arabia Smokers Using Modern Analytical Techniques. The levels of some selected heavy and toxic metals (e.g.; Hg, Pb, Cd, As, Se, Mn, Zn, Ni, and Cr) were determined using inductively coupled plasma-atomic emission spectrometer (ICP-AES). Prior to the analysis, the blood and hair samples of Saudi Arabia smokers were collected, treated, and digested by microwave digestion system. The validation measurement of ICP-AES was performed using working calibration solutions of the investigated toxic heavy metal ions (Hg, Pb, Cd, As, Se, Mn, Zn, Ni, and Cr) [155]. Kaiser, Zheng and Feng was introduced a novel two-dimensional polymers synthesis with nano size in water which was different application such as heavy metal removal. They reported the controlled synthesis of few-layer two-dimensional polyimide crystals on the surface of water through reaction between amine and anhydride monomers, assisted by surfactant monolayers [156]. Heavy metals such a lead or cadmium has devastating health effects on human body. So, removal of heavy metals from industrial wastewater and drinking water is very important. Rosillo-Lopez et al showed that carboxylated graphene nanoflakes (cx-GNF) and nano-graphene oxide (nGO) can be extracted Fe^{2+}, Cu^{2+}, Fe^{3+}, Cd^{2+} and Pb^{2+} ions from water sample. The sorption capacity for Pb^{2+}, , is more than six times greater for the cx-GNF compared to GO which is attributed to the efficient formation of lead carboxylates as well as strong cation–π interactions [157]. Zhao et al introduced a novel multi-throughput dynamic microwave-assisted leaching

(MDMAL) combined with ICP-AES was used for the simultaneous determination of Cu, Mn, Zn and Pb in soil. The MDMAL method was more rapid than the simple digestion method or microwave digestion process and could be an alternative approach for the analysis of heavy metals in solid samples [158]. Aaron et al reported an efficient chemical strategy for the crosslinking of polymer chains based on the N- and C- of proteins(CPC→N/C-P), producing hybrid hydrogels which was related to biomolecules. This compound is largely independent of the protein's sequence; it can in principle be used to incorporate of polypeptide into a polymer based on uniform linkages. They used cysteine for this strategy to convert metallothioneins into a recyclable polymer gel that can remove heavy metals from water samples [159]. Shirkhanloo et al reported a novel method based on amine-functionalized mesoporous silica UVM-7 as nanoadsorbent for manganese (II) and manganese (VII) extraction in waters by ultrasound assisted-dispersive-micro-solid phase extraction (US-D-μ-SPE) procedure. They were used NH2-UVM7 for speciation of Mn(II) and Mn(VII) ions at pH of 8 and 5, respectively which was determined by(AT-F AAS. The validation of the method was also performed by the standard reference material [160]. Also, Shirkhanloo et al introduced a carboxyl-functionalized nanoporous graphene (NG-COOH) as solid phase sorbent for speciation of trace Hg (II) and R-Hg (CH$_3$Hg$^+$ and C$_2$H$_5$Hg$^+$) in waters by US-D-IL- μ-SPE (pH=8). Ionic liquid was used for trapping of sorbent from water sample. After back extraction, Hg (II) concentration determined with flow injection-cold vapor-atomic absorption spectrometry (FI-CV-AAS) [161]. Also they were reported a new method based on ultrasound assisted-dispersive solid-liquid multiple phase microextraction (USA-DSLMPME) for speciation of trace amounts of inorganic arsenic (III and V) and total organic arsenic (TOA) in waters and human urine samples. By procedure NH2-UVM7 were immersed in ionic liquid (IL) as an extraction phase. Then, the mixture of NH2-UVM7 and IL/acetone [HMIM][PF6]/AC) was injected to sample at pH of 3.5.

After ultrasonic, As(V) anion extracted by binding to amine group. Total amount of inorganic arsenic (TIA) was determined after oxidization of As(III) to As(V) by ETAAS and As(III) was calculated by the subtracting TIA and As(V) content [162].

3. Results and Conclusions

Kaipei Qiu was introduced a novel adsorption process for heavy metals from waters. In the adsorption process, the desorption and repeatability are significant parameters for developing new adsorbents for practical applications. The heavy metals such as, Pb^{2+}, Cd^{2+}, Cu^{2+}, and Ni^{2+} were adsorbed by UFMNPs which was shown in Scheme 2. The adsorption kinetics is one of the important characteristics defining the effectiveness of an adsorbent, which describes the solute uptake rate by controlling the diffusion process and the residence time of an adsorbate uptake at the solid/solution interface. The results in this quaternary Pb–Cd–Cu–Ni system indicated that the rate constant of Pb^{2+} (0.045 g mg^{-1} min^{-1}) was higher than the rate constants of Cu^{2+} (0.008 g mg^{-1} min^{-1}), Cd^{2+} (0.005 g mg^{-1} min^{-1}), and Ni^{2+} (0.003 g mg^{-1} min^{-1}), further demonstrating the strong affinity of Fe$_3$O$_4$ NPs for Pb^{2+}[139].

Soylak and Tuzen studied on the amounts of Cr, Cu, Ni, Zn, Mn, Fe, Co, and Al in drinking water samples based on novel extraction technique using atomic absorption spectrometry in Turkey. According to their studies, the concentration of Cr in natural water was often very small. Based on results, the hexavalent form of chromium (Cr $_{VI}$) is ranged between 3.14 and 6.08 μgL^{-1}. The mean of Cr levels in the waters of the area of Turkey was equal to4.40 μgL^{-1}. Maximum tolerable limit of concentration of total chromium in drinking water was less than 50 μg L^{-1} (Tlv of chromium by WHO > 50 μg L^{-1}) [101]. The permissible value of Ni in drinking water was less than 20 μg L^{-1}. The mean level of Ni in the water samples, in the area of Tokat, Turkey was equal to 3.82 μg L^{-1} which was lower than standard references such as EPA, WHO. Also, according to their study, the drinking water sample from Turhal was the highest nickel value
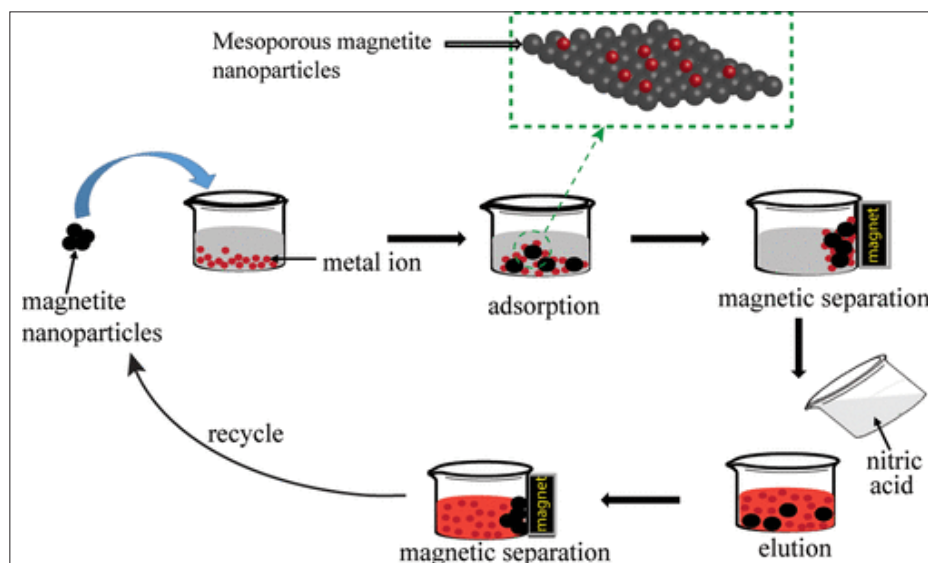
Scheme 2. Removal of heavy metal Ions by desorption process [139]

$(5.35\pm0.28 \mu g$ L^{-1}) and the city center of Tokat was the lowest $(2.16\pm0.19 \mu gL^{-1})$ [101]. They showed, the amount of Cu was in the range of 4.44-7.43 μgL^{-1}. In Erbaa, Turkey, Cu was substantially lower than the permissible limit defined by WHO (1.0 μgL^{-1}) in drinking waters [101]. In addition, mean level of concentration of Cu was equal to 6.01 μg L^{-1}. Therefore, no contamination of Cu was there in the drinking water samples. The guideline value for zinc in drinking-water is given as 5.0 mg/l by WHO. The concentration of Zinc ranged from 4.16 to 8.44 μg L^{-1} in the drinking water samples. The mean level of zinc was obtained 6.12 μg L^{-1}, which was more than the permissible limit value (5.0 mg/L^{-1}) [101]. Many published methods were reported for determination and sample preparation of heavy metals in water and biological samples [Table 1-3]. Chromium speciation based on acetylcysteine (NAC) by dispersive liquid–liquid bio-microextraction was achieved in human blood samples by shirkhanloo et al. By method, Ionic liquid (1-hexyl-3-methylimidazolium hexafluorophosphate) was rapidly injected into the blood samples containing Cr^{3+}, which have already complexed by NAC at pH from 5 to 8. By optimizing, the linear range, limit of detection and preconcentration factor were achieved 0.03–4.4 μg L^{-1}, 0.005 μg L^{-1}, and 10 respectively [163,164]. Also, chromium speciation was reported by other

researcher [165-172]. Xiaogang Luo et al explained a novel sorbent for absorption heavy metals from waters by syntesis of MCB. The carboxyl decorated magnetite (Fe_3O_4) nanoparticles (MN-CA) were obtained by postmodifying the magnetite surface with citric acid. The nanoparticles of Fe_3O_4 were added to 0.1 M citric acid under ultrasonic condition for 45 min, and the reaction was kept for 4 h at room temperature. A magnet was used to separate the MN-CA, and then the prepared MN-CA samples were rinsed thoroughly with acetone and double distilled water. The proposed method based on MN-CA followed by Scheme 3 for adsorption heavy metals from waters [145].

Naeemullaha et al showed, the effect of main parameters on extraction of vanadium in waters was evaluated by μS-SHS procedures [102]. For optimizing, Statistical assessment of μS-SHS method, Screening and optimization of experimental variables and selectivity of the μS-SHS method was studied and finally, the method was validated by CRM (SLRS-4 Riverine water samples). The optimization of experimental variables followed with screen out of the volume of SHS, pH, volume of Na_2CO_3 and volume of H_2SO_4 solution as a extraction efficiency with t-value (95 %) of 2.365. The simple, fast and switchable hydrophilicity microextraction (SHM) couple with ETAAS through micropipette tip
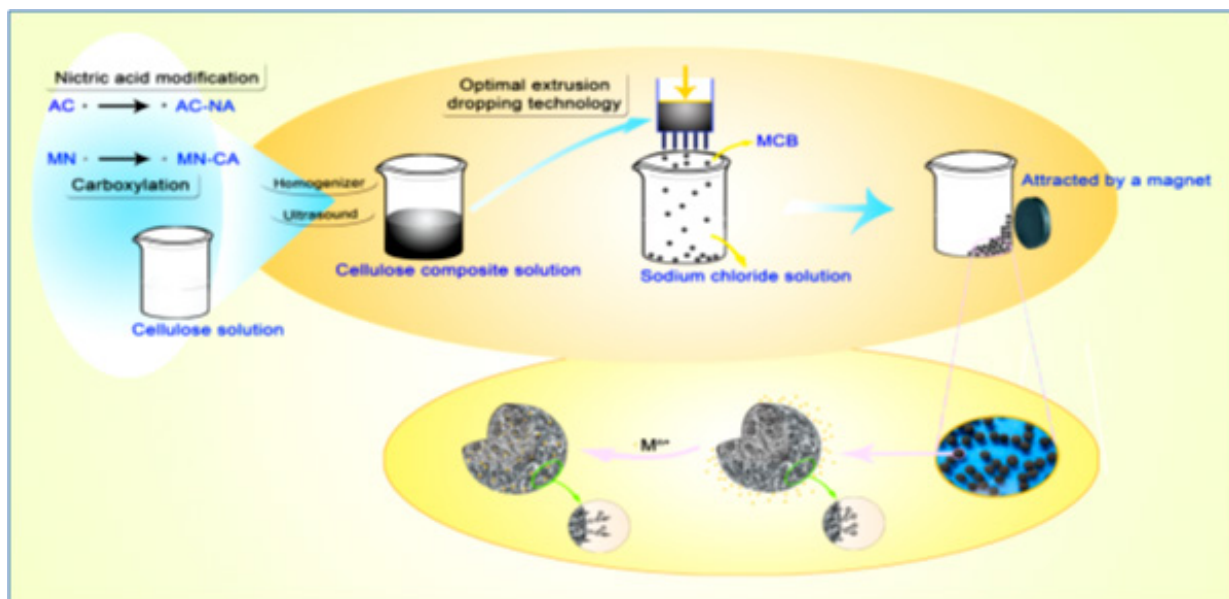
Scheme 3. depiction of preparation of MCB and the adsorption mechanism of heavy metal ions by MCB [145].

syringe system (µS-SHS) was used for separation and determination of vanadium in food and water samples. The µS-SHS method introduced an ideal sample preparation for vanadium extraction. The simple, fast and applied method based on SHM had good efficiency as compared with conventional methods for extraction of vanadium [102]. Also, the proposed method based on µS-SHS compared with published method and results showed high precision and accuracy results with low LOD and RSD (Table 1). Moreover, the graphical abstract of the µS-SHS was shown in Figure 3.

Many separation methods were used for determination of ultra-trace metals in different matrix, such as Liquid-liquid microextraction, dispersive liquid–liquid microextraction, solid-phase microextraction, selective dispersive micro solid-phase extraction, traditional organic solvents, and switchable solvent, ultrasound assisted-dispersive-ionic liquid-micro-solid phase extraction and ultrasound assisted-dispersive solid-liquid multiple phase microextrbased on

action [Table 1-3]. Kaiser, Zheng and Feng used a novel two-dimensional polymers crystals (TDPC) synthesis with nano size in waters through reaction between amine and anhydride monomers by surfactant monolayers. They showed high crystallinity polymers (CsP) with thickness (2 -3 nm) and an crystal size (3.5 µm²). The molecular structure of the materials, were characterized using X-ray scattering and TEM. The structure and TEM was shown in Figure 4. The formation of CsP is attributed to the pre-organization of monomers at interface phase (water- surfactant). Finally, micrometre-sized and few layer TDPC were grown. This material was used in different application such as removal heavy metals [156].

Rosillo-Lopez et al used carboxylated graphene nanoflakes (CX-GNF) and nanographene oxide (GO) for extracting of heavy metals such as, Fe^{2+}, Cu^{2+}, Fe^{3+}, Cd^{2+} and Pb^{2+} in waters. The carboxylic acid groups (cx-GNF) have strong binding with heavy metal cations. CX-GNF with additional chemical-functionalization procedures can easily compete

Table 1. The proposed method based on µS-SHS compared with published method [102]

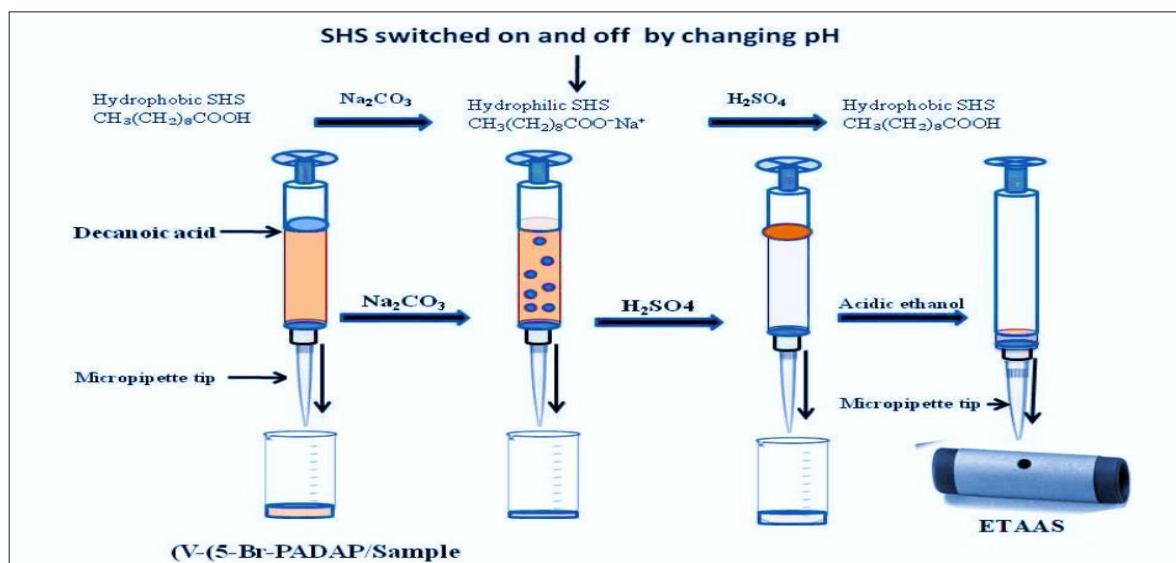| Sample preparation	Technique	SV	RSD%	LOD (µg.L⁻¹)	EF/PF	References
SPE	ICP-OES	10	3.4	0.06	45	68
CPE approach	Spectrometric	….	….	1.4	….	70
CPE	ETAAS	50	….	0.042	125	71
µS-SHS	ETASS	10	2.2	0.0075	120	76

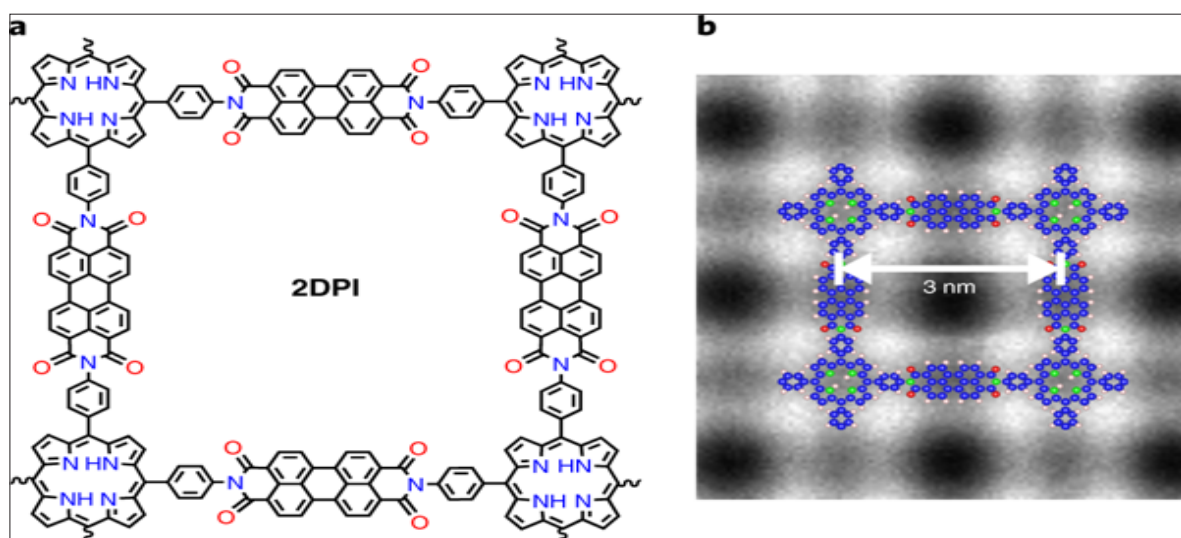**Fig. 3.** The graphical abstract of the µS-SHS [102].

Fig. 4. The structurea and b) TEM of two-dimensional polymers crystals (TDPC)[156]

with other carbon materials such as G and GO for heavy-metal extraction (Fig. 5). Furthermore, the cx-GNF material extracted Pb^{2+} ions in the presence of excess Ca^{2+} or Mg^{2+} cations which were already existed in environmental matrix. So, the CX-GNF material showed the highest potential for extraction of heavy-metal from water as compared to other graphene materials [157]. Zhao et al used multi-throughput dynamic microwave-assisted leaching (MDMAL) for determination of Cu, Mn, Zn and Pb in soil . This method combines the microwave and dynamic leaching technique for five samples within 15 min (Fig. 6). HNO_3 aqueous solution was
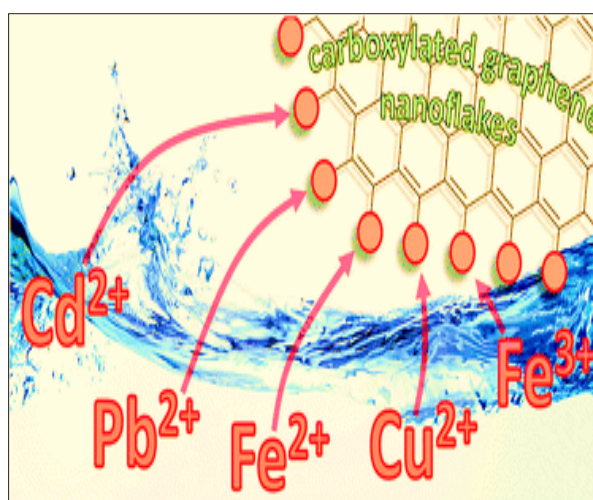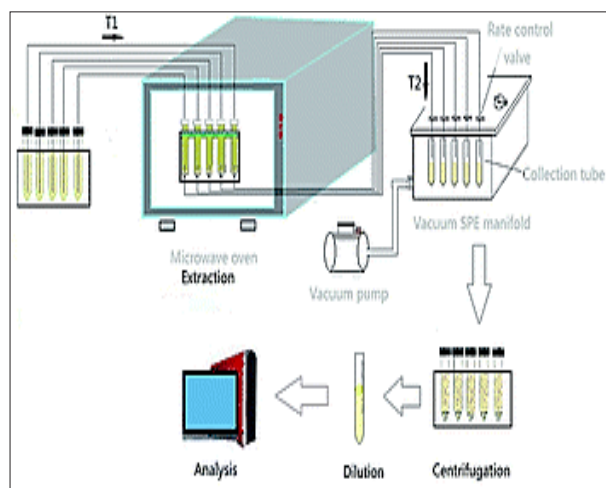

Fig. 5. Heavy metal extraction by cx-GNF.

Fig. 6. Heavy metal extraction by MDMAL

employed as leachant at a flow rate of 1.5 mL min⁻¹. The leaching condition were above 95% for Cu, Mn, Zn, Pb and lower for Cr, Cd, Ni and Co, compared to the conventional method. The mean of RSD of intra- and inter-day of Cu, Mn, Zn, and Pb were 4% and 6%, respectively. The proposed method was more rapid than the conventional digestion method and could be an alternative approach for the analysis of heavy metals in complex solid samples [158].

Aaron et al, showed that, the crosslinking of polymer chains based on the N- and C- of proteins (CPC→N/C-P) was used as a key of the proteins which was captured trace amounts of heavy metals such as cadmium in the presence of innocuous ions in contaminated water sample. Protein-cross-linked hydrogels introduced for sequestration of heavy metal ions in water samples. As Figure 7, the Pea metallothioneins (PMTs) can capture toxic metal ions by condensing to form binding pockets. The synthetic route to access these materials involves the introduction of ketones on both protein termini. These groups are then used to cross-link alkoxyamine-substituted polymers through oxime formation [159]. Shirkhanloo et al used NH_2-UVM_7 based on US-D-μ-SPE method for speciation of manganese in water samples. The batch adsorption
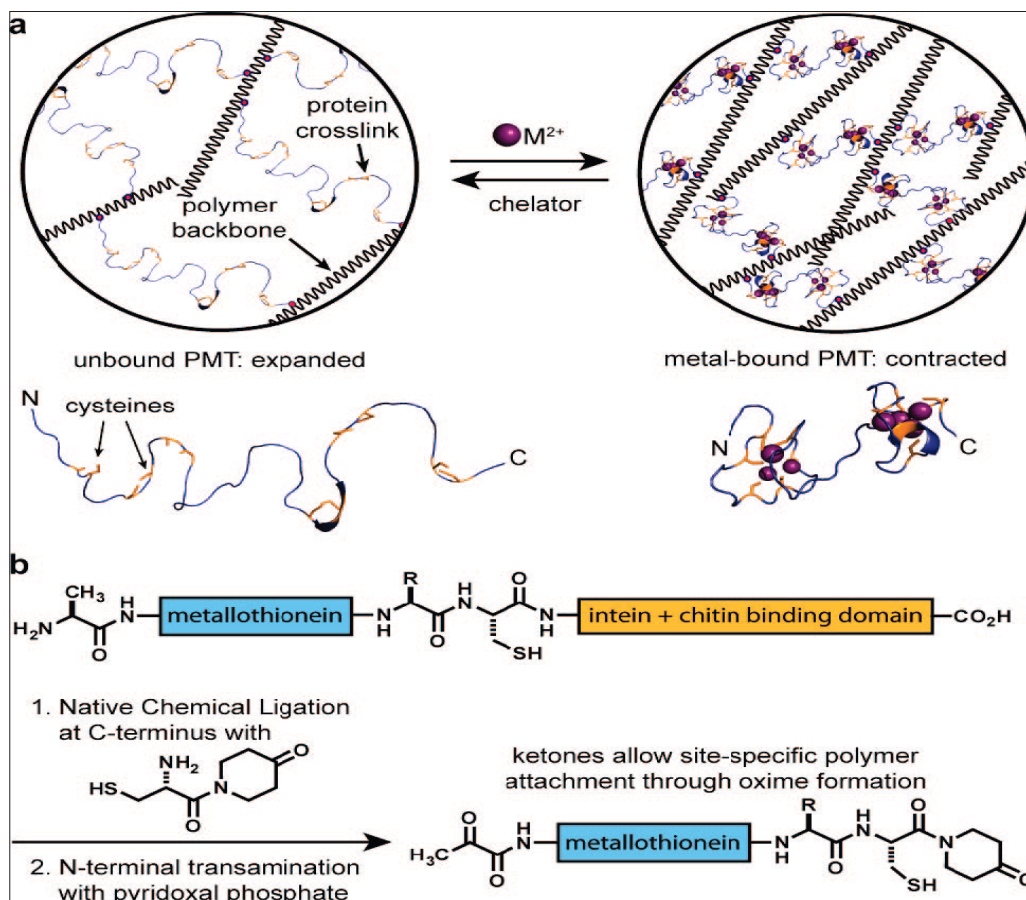

Fig. 7. Pea metallothioneins (PMTs) can capture toxic metal ions a) Condensing to form binding pockets b) Ketones used to cross-link alkoxyamine-substituted polymers [159]

capacity of NH_2-UVM_7 for Mn(II) and Mn(VII) ions was found to be 1733 μmol g^{-1} and 570 μmol g^{-1}, respectively. In optimized parameters, LOD (3Sb/m), and LOQ (10Sb/m) were 0.007 μg L^{-1} and 0.03 μg L^{-1} for Mn(II). The mean preconcentration factors for Mn(II) and Mn(VII) were calculated as 102.3 and 98.8 with RSD about 2.8%, respectively (Fig. 8). The regression equations for the calibration curves of Mn(II) and Mn(VII) were A=9.8438 C+0.0053 (R2=0.9997), and A=9.6922 C+0.0045 (R2=0.9995), respectively [160]. In addition, Shirkhanloo et al used NG-COOH for speciation of trace mercury in waters by US-D-IL- μ-SPE. Under optimized conditions, the linear range, LOD and PF/EF were obtained 0.03–6.3 μg L^{-1}, 0.0098 μg $L^{-1}$and 10.4 for caprine blood samples, respectively. The developed method was successfully applied to natural water and human/caprine blood samples. In order to validate the method described, two certified standard reference materials, NIST-SRM 995c (mercury species in caprine blood) and NIST-SRM1641e (total mercury inwater), were analyzed by US-D-IL- μ-SPE [161]. They used NH2-UVM7 based on USA-DSLMPME for speciation of trace amounts arsenic (III and V) in waters and human urine samples. The linear range, LOQ (3σ), RSD% and EF for As(V)were obtained 0.02–1.65 μg L^{-1}, 11 ng L^{-1}, 4.3% and 100.5. The recoveries (95–102%) was achieved by certified reference material in urine (NIST-SRM). The mean of LOD

was obtained 3.3 ng L^{-1} and 2.7 ng L^{-1} for human urine and standard samples, respectively (intra-day, Mean of LOD = 3)[162].

3.1. Chemistry techniques for heavy metals

Also, many chemistry techniques were reported in published papers for separation, extraction, preconcentration and speciation metals in different matrixes (Table 2). Recently, the liquid-liquid extraction methods (LLE) were used for separation and determination heavy metals from water and human biological samples. Some of LLE techniques such as, ultrasonic-thermostatic-assisted cloud point extraction procedure (UTA-CPE-FAAS), aqueous solvent-based dispersive liquid-liquid microextraction (AS-DLLME), cloud point extraction - slotted quartz tube-flame atomic absorption spectrometry (CPE-SQT-FAAS), surfactant-assisted dispersive liquid–liquid micro-extraction (SA-DLLME-FAAS), switchable liquid-liquid microextraction (SLLME-SQT-FAAS), surfactant-Based Dispersive Liquid-Liquid Microextraction based on FAAS(SB-DLLME-FAAS), vortex-assisted DLLME based on voltammetric (VA-DLLME-VM), microwave-assisted extraction - inductively coupled plasma-optical emission spectrometry (MAE-ICP-OES), Ionic liquid-based microwave-assisted dispersive liquid-liquid microextraction (IL-based MA-DLLME), Ionic liquid-based dispersive liquid-liquid microextraction (IL-DLLME), Ionic liquid
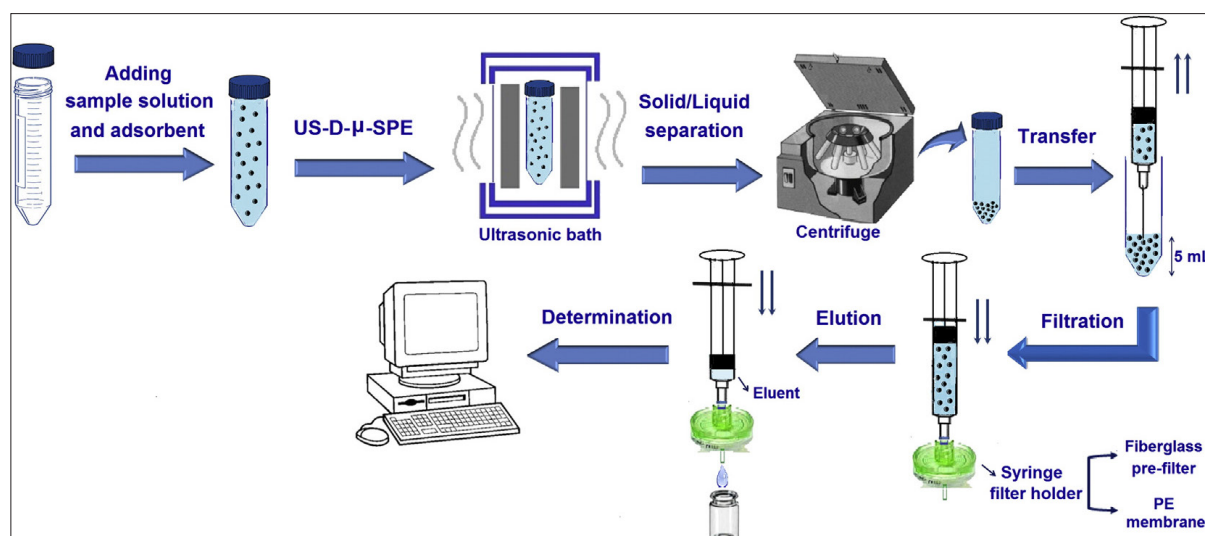

Fig. 8. Procedure of Mn speciation based on NH_2-UVM_7 by US-D-μ-SPE procedure [160].

Table 2. Solvent extraction for determination and separation of heavy metals in different matrix [173-197]

Sample	Metals	Method	Solvent /Ragent	EF/PF	LOD µg L^{-1}	Ref.
Wastewater	Cd	DLLME/SQT-FAAS	DPC	93.3	0.5	[173]
Milk	V(V) and Mo(VI)	UTA-CPE-FAAS	Nile blue A - PONPE	145 and 115	0.86 and 1.55	[174]
Vegetables						
Foodstuffs						
Parsley	Cd	CPE-SQT-FAAS	DPC	60	0.0007	[175]
Tap	Zn	SA-DLLME-FAAS	PAR	-----	0.5	[176]
River						
Well water						
Wastewater	Co	DLLME/SQT-FAAS	DPC	86.56	0.97	[177]
Tea	Co	SLLME-SQT-FAAS	Schiff base ligand	107.7	3.1	[178]
vitamin B12						
Food	Cu(II)	SB-DLLME-FAAS	Triton X-114	50	1.61	[179]
Water Samples						
Milk	Cd(II), Cu(II), Pb(II)	DLLME/FAAS	TDES	----	0.38–0.42	[180]
Chocolate	Ni	PV-IS-DLLME	APDC	17	100.0	[181]
Urine	Hg	VA-DLLME-VM	AuNPS-PE	---	1.1 - 1.3	[182]
human blood	Cr(III and VI)	CP-DILLME-ET-AAS	IICDET	25.2	0.0054	[183]
Human serum	Cd	DLLME-ETAAS	TSILs	10.2	0.005	[184]
Human blood	Cr(III and VI)	IL-DLLBME-ETAAS	NAC	10	0.005	[185]
Biodiesel	Na, K, Ca and Mg	RP-DLLME/FAAS	Iisopropanol,HNO$_3$,	----	0.006- 0.026	]186]
Water	Ta (I), Ta (III)	IL DLLME-ET-AAS	[C6MIm][PF6]	100	3.3 ng L^{-1}	[187]
Cosmetic	Hg (II), MeHg+ ,EtHg+	HPLC-ICPMS	[C6MIm][PF6]	760, 115, 235	1.3 ng L^{-1}	[188]
Wines	As (III)	DLLME-ETAAS	[C8MIm][PF6]	----	5.0 ng L^{-1}	[189]
Water	Cu(II)	DLLME-FAAS	[C4MIm][PF6] or [C16C4Im][Br]	54	3 300 ng L^{-1}	[190]
Water and leaves	Rh (III)	US-IL DLLME-FAAS	[C8MIm][NTf2]	----	0.37	[191]
Water	V (IV) and V (V)	TC-IL DLLME-ETAAS	[C4MIm][PF6]	----	0.0049	[192]
Tea, Soda	Se (IV)	USA-IL-DLLME-ETAAS	[C6MIm][NTf2]	150	12	[193]
Beer						
Milk						
Water	Au, Ag	MRTILs- DLLME-ETAAS	[C$_5$(MIM)$_2$][NTf$_2$]$_2$	245 and 240	3.2 and 3.7	[194]
Food	Zn, P, Cd, Pb, Fe, Mn, Mg, Cu, Ca, Al, Na, K	MAE -ICP-OES	MAE	----	0.01 mg kg^{-1} -7.8 mg kg^{-1}	[195]
Water	Pd and Pt	CPE-ICP OES	MBT	---	0.525 and 0.752	[196]
Water serum	Cu(II)	IL-mE-DLLME-CPE-ETAAS	Oxine-IL	70	0.132	[197]

EF: Enrichment Factor

UTA-CPE-FAAS: ultrasonic-thermostatic-assisted cloud point extraction procedure

AS-DLLME: Aqueous solvent-based dispersive liquid-liquid microextraction

DPC: Diphenylcarbazone

Nile blue A: 9-(diethylamino)benzo[a]phenoxazin-5-ylidene]azanium; sulfate-PONPE (polyoxyethylene-nonylphenyl ether

ETAAS: Electrothermal atomic absorption spectrometry

FAAS: Flame atomic absorption spectrometry

SQT-FAAS: Slotted quartz tube-flame atomic absorption spectrometry

CPE-SQT-FAAS: Cloud point extraction - slotted quartz tube-flame atomic absorption spectrometry

DPC: Diphenylcarbazone

SA-DLLME-FAAS : Surfactant-assisted dispersive liquid–liquid micro-extraction

PAR: 4-(2-pyridylazo) resorcinol

SLLME-SQT-FAAS: Switchable liquid-liquid microextraction

SB-DLLME-FAAS: Surfactant-Based Dispersive Liquid-Liquid Microextraction/FAAS

Triton X-114: Surfactant

TDES: Ternary deep eutectic solvent

APDC: ammonium pyrrolidine dithiocarbamate

VA-DLLME-VM: Vortex-assisted DLLME/ voltammetric

AuNPS-PE: gold nanoparticle-modified screen-printed electrodes

MAE-ICP-OES: microwave-assisted extraction - inductively coupled plasma-optical emission spectrometry

MBT: 2-mercaptobenzothiazole

Oxine-IL: 8-hydroxyquinoline-IL

UA-DLLME: Ultrasound-assisted dispersive liquid-liquid microextraction

UAE- IL-DLLME: Ultrasonic-assisted ionic liquid based dispersive liquid–liquid microextraction

USA-DLLME: Ultrasound-assisted dispersive liquid-liquid microextraction

USA-IL-DLLME: Ultrasound assisted ionic liquid dispersive liquid-liquid microextraction

ultrasound assisted dispersive liquid-liquid micro-extraction (IL-UA-DLLME), In-situ ionic liquid dispersive liquid-liquid microextraction(*in-situ* IL-DLLME), microwave-assisted extraction and dispersive liquid–liquid microextraction (MAE–DLLME), magnetic ionic liquid-based dispersive liquid-liquid microextraction) MIL-based DLLME), magnetic stirring-assisted dispersive liq-

uid-liquid microextraction (MSA-DLLME), magnetic stirrer induced dispersive ionic-liquid micro-extraction (MS-IL-DLLME), microwave-assisted dispersive liquid-liquid microextraction(MWA-DLLME), ionic liquid dispersive microextraction (IL-DLLME), surfactant assisted dispersive liquid-liquid microextraction (SA-DLLME), switchable solvent-based dispersive liquid-liquid microex-

Table 3. Different sorbents for extraction of heavy metals in human and environmental samples [198- 218]

Sample	Method	Sorbent	Heavy metals	LOD (ng L^{-1})	EF/PF	AC(mg g^{-1})	Ref.
Serum Blood	USA-D-µSPE-ETAAS	NH$_2$-UVM$_7$	Cd	2.0	25	108.6	[198]
Waters	MCD-µSPE-ETAAS	GSH	Pb, Cd, Cr	8.9, 4.0, 10	17, 18,17	146.3, 132.5, 125.8	[199]
Waters River	USA-CP-MSPE	AFSA	Pb	10.0	102	---	[200]
Urine Water	USA-DSL-MPME	NH$_2$-UVM$_7$	As $_{III}$, As$_V$	1.1	100.5	---	[201]
Blood Water	US-D-IL- µSPE-AT-FAAS	NG-COOH	Hg, MHg, EHg	9.8	10.4	153.7, 125.8, 125.8	[202]
Water Tap W	US-D- µSPE	NH$_2$-UVM$_7$	Mn $_{II}$, Mn $_{VII}$	7.0, 8.0	102.3, 98.8	1733 and 570 µmol.g^{-1}	[203]
Serum Blood	USA-D- µSPE	GONPs	Al	20.0	25	187.5	[204]
Water Drinking	SPE-FAAS	CdSNPs	Pb, Cu	---	---	200, 166.7	[205]
Wastewater	FTIR	G+MGO	Pb^{2+}, d^{2+} ,Cu^{2+}	---	---	358.96, 388.4, 169.8	[206]
Waters	SPE-FAAS	GO	Pb, Ni	1400–2100	95-102.5	195, 178	[207]
Waters	ET-AAS	GO-NH$_2$	Pb (II)	9.4	100	479	[208]
serum urine	H-US-D-µ-SPE	G-COOH	As species	2.1	53	125.4	[209]
River water	CHD-µSPE	GO	Pb, Cd, Cr	110, 15, 38	15	----	[210]
Waters	SPE-ETAAS	MnO$_2$/ CNT	PB, Cd	4.4, 1.5	100	----	[211]
Waters Urine	DµSPE-TRXRFS	MWCNT	Cr $_{(VI)}$	3000	66	154.3	[212]
Soils Waters	SPE-ICPMS	Ti- MSN	Cu	3.9	10	----	[213]
Blood	M-SPµE-FAAS	Modified carbon cloth	Cd	150	10	----	[214]
FOOD	SPE-FAAS	Dowex Marathon C	Pb	130	250	----	[215]
Agricultur	SPE-FAAS	F-MOF	Zn	200	238	----	[216]
Foods	SPE-FAAS	B2O3/TiO2	Cd	1440	50	172.5	[217]
Waters	D-µSPE-ETAAS	NH$_2$-SiO$_2$-GO	Pb	9.4	100	----	[218]

AC: Absorption Capacity
EF/PF: Enrichment factor/preconcentration factor
ET-AAS: Electro-thermal atomic absorption spectrometry
FAAS: Flame atomic absorption spectrometry
GSH: Graphene-silica hybrid
USA-D-µSPE: Ultrasound assisted-dispersive-micro solid phase extraction
MCD-µSPE: Moderate centrifugation-assisted dispersive micro solid phase extraction
USA-CP-MSPE: Ultrasound-assisted cloud point-micro solid phase extraction
AFSA: Amine functionalized silica aerogel
USA-DSL-MPME: Ultrasound assisted-dispersive solid-liquid multiple phase

microextraction
US-D-IL-µ-SPE: ultrasound assisted-dispersive-ionic liquid-micro-solid phase extraction
NG: Nanographene
CHD-µSPE: Coagulating homogenous dispersive micro-solid phase extraction
CdSPNs: Cadmium Sulfide Nanoparticles
TRXRFS: Total reflection X-ray fluorescence
GONPs: Graphene oxide nano-particles
M-SPµE: Miniaturized solid phase microextraction
SPE-FAAS: Solid phase extraction-flame atomic absorption spectrometry
GO-NH$_2$: Aminosilanized graphene oxide

traction (S-DLLME), temperature-assisted ionic liquid-based dispersive liquid–liquid Microextraction (TA-IL-DLLME), ultrasound-assisted dispersive liquid-liquid microextraction (UA-DLLME), ultrasonic-assisted ionic liquid based dispersive liquid–liquid microextraction (UAE- IL-DLLME), ultrasound-assisted dispersive liquid-liquid microextraction (USA-DLLME), ultrasound assisted ionic liquid dispersive liquid-liquid microextraction (USA-IL-DLLME) was used for heavy metal extraction in different matrixes (Table 2) [173-197]. Many researchers were reported other nanomaterial or sorbents for extraction metals and heavy metals from water, wastewaters, air pollution and human biological matrix which were shown in Table 3.

3.2. Nano particles for extraction heavy metals

The affinity of Hg towards Au was generally achieved by AuHg, AuHg3, and Au3Hg [219]. Lisha et al. reported the removal of Hg (II) with nanoparticles of Au (AuNPs) coated on aluminum [220]. NaBH4 helped to reduce Hg (II) to Hg (0) and removed by AuNPs with capacity of 4.0 g g $^{-1}$. Also, Jiménez et al. was used citrate-coated AuNPs for extraction mercury in water [221]. Absorption mercury with AuNPs was shown in Figure 9.

Magnetite (Fe_3O_4) as nanoadsorbent was used for heavy metal removal as environmental friendliness. Fe_3O_4 could be easily separated from liquid phase. Fe_3O_4 was used for heavy metals treatment in waters [222-224]. Giraldo et al. synthesized magnetite nanoparticles by using a co-precipitation method and were used for extracting of Pb (II) and Mn (II) in different samples [225]. In Figure 10, the removal of chromium was shown by chitosan–magnetite nanocomposite.
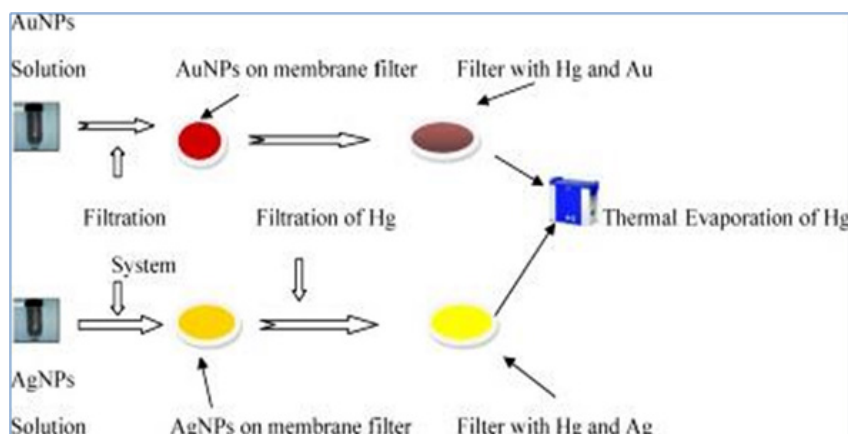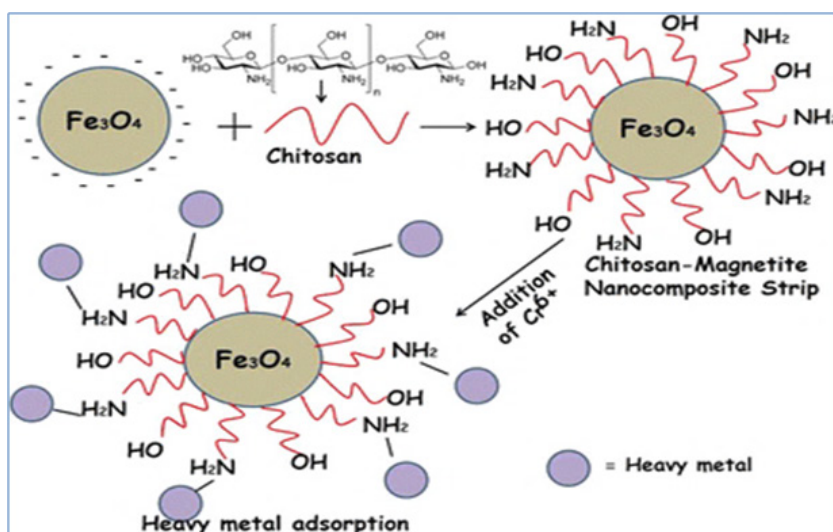

Fig. 9. The absorption mercury by AuNPs

Fig. 10. The removal of chromium by chitosan–magnetite nanocomposite strip

Magnetite particles are modified with groups such as, MPs-NH2 [226], MPs–COOH [227], MPs–SH [228]. The core-shell structure of PI-b-PEG diblock copolymer encapsulated with iron oxide nanoparticles [229]. PI-b-PEG diblock copolymer was used for removal heavy metals from waters [230]. The nanostructures of amphiphilic diblock copolymers due to the inherent curvature of the polymer were shown in Figure 11 which was used for extraction lead and other heavy metals from different matrixes.

Zero valent iron as nanoparticles of is a Fe (0) and ferric oxide coating (nZVI) which was used for extraction heavy metals from different matrix

(Figure 3) [231]. Also, nZVI as a novel adsorbent can be removed heavy metals (Fig. 12), such as mercury, chromium, copper, nickel, and cadmium from waters. [232-235]

The silica nanoparticles based on ligand of β-ketoenol–pyridine–furan (as a selective adsorbent was used for metal removal from waters (Pb,Cd,Zn,Cu) (Scheme 4). The engineered sorbent had high adsorption capacity for capturing toxic heavy metal in environmental samples [236-239].

4. Conclusions

In this review paper, constructive issues from novel published papers were selected for studying
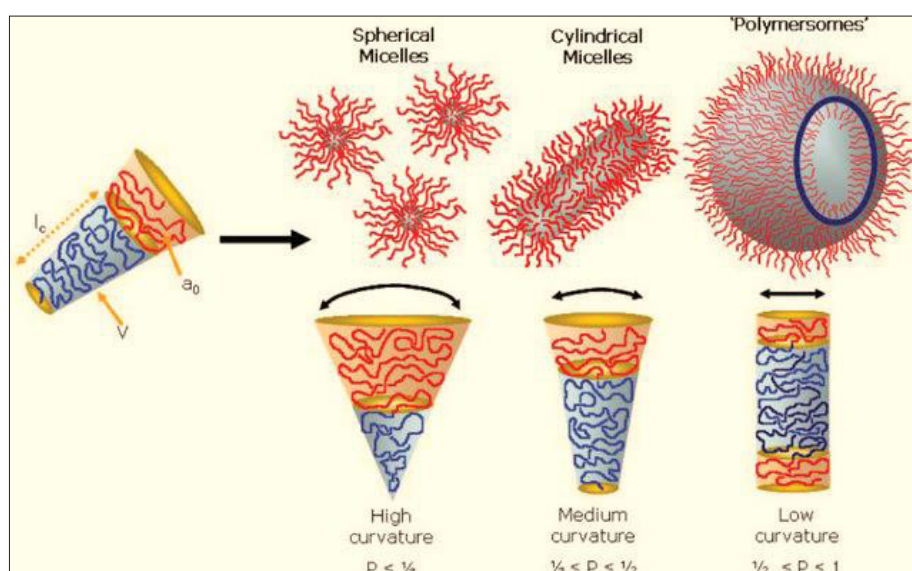

Fig. 11. The nanostructures of amphiphilic diblock copolymers for extraction lead ions
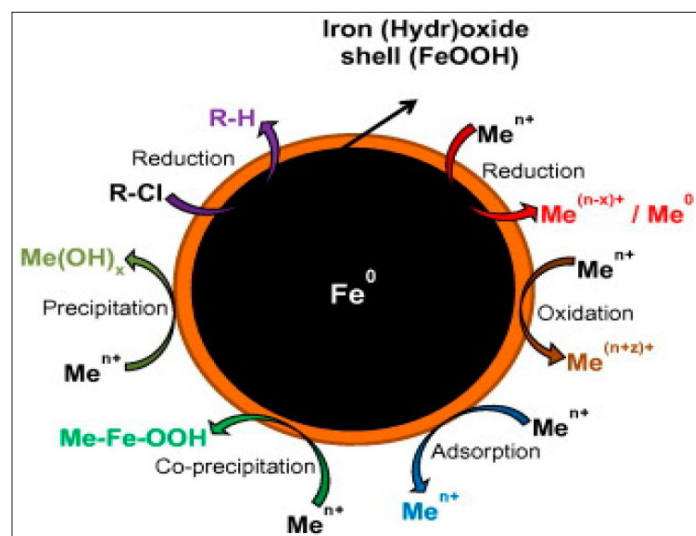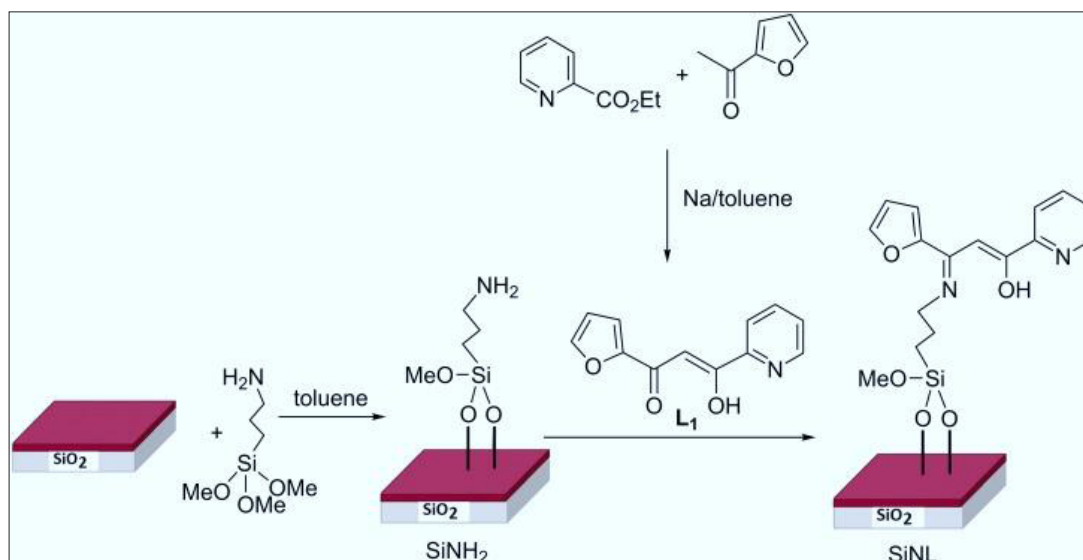

Fig. 12. The core-shell structure of nZVI used for extraction of metals [231]

Scheme 4. The Silica nanoparticles based on β-ketoenol–pyridine–furan as chelating agent for extraction heavy metals in liquid phase

of separation, preconcentration, and extraction of heavy metals from water, waste water, vegetable and human biologic samples. Recently, the SPE methods were coupled with spectrometry techniques such as atomic absorption spectrometry (AAS) based on various adsorbents included graphene, graphene oxide, activated carbon, carbon nanotubes (CNTs), zeolites, MOF, magnetic nanoparticles, carbon quantum dots (CQDs)a nd MSN which was used for ultra-trace determination of heavy metals in different matrixes. In addition, the liquid-liquid micro extraction techniques coupled with ET-AAS, F-AAS, ATF-AAS, SQT-FAAS, ICP-XRF, CV-AAS, ICP,ICP-AES, ICP-MS, ICP-OES, HPLC, voltammetry, UV-VIS, and FTIR were presented in this study by a lot of researchers. The proposed review showed us, the novel techniques based on nanotechnology had been developed in SPE and LLE methods since 2010 by authors. Also, SPE and solvent extraction based on different adsorbents and instrumental techniques were extended in various sciences such as, bio chemistry, nanotechnology, environmental analytical chemistry and human analysis during last decade.

5. References

[1] M.H. Dehghani, B. Heibati, A. Asadi, I. Tyagi, S. Agarwal, V.K. Gupta, Reduction of noxious Cr(VI) ion to Cr(III) ion in aqueous solutions using H_2O_2 and UV/H_2O_2 systems, J. Ind. Eng. Chem., 33 (2016) 197–200.

[2] Cárdenas Valdivia, M. M. López Guerrero, E. I. Vereda Alonso, J. M. Cano Pavón, A. García de Torres, Determination of As, Sb, and Hg in water samples by flow injection coupled HR CS ET-AAS with an in situ hydride generator, Microchem. J., 138 (2018) 109-115.

[3] S. Carballo, J. Terán, R. M. Soto, A. Carlosena, D. Prada, Green approaches to determine metals in lubricating oils by electrothermal atomic absorption spectrometry (ET-AAS), Microchem. J., 108 (2013) 74-80.

[4] M. Felipe-Sotelo, A. Carlosena, J. M. Andrade, M. J. Cal-Prieto, D. Prada, Slurry-based procedures to determine chromium, nickel and vanadium in complex matrices by ET-AAS, Microchem. J., 81 (2005) 217-224.

[5] G. Carrone, E. Morzan, M. Tudino , R. Etcheniqu, Determination of cadmium in commercial tobacco by ET-AAS, **J. Anal. At. Spectrom.**, **33** (2018) 1970-1973.

[6] H. Ashkenani, M. A. Taher, Use of ionic liquid in simultaneous microextraction procedure for determination of gold and silver by ET-AAS, Microchem. J., 103 (2012) 185-190.

[7] I. Mohammadpourfard , N. Shariatifar, G. R. Jahed-Khaniki, E. Ebadi-Fathabad, Determination of Heavy Metals in Apricot and Almond Oils, Iran. J. Health Sci., 3 (2015) 18-24.

[8] A. Prkić, I. Mitar , J. Giljanović, V. Sokol, P. Bošković,

I. Dolanc, T. Vukušić, Comparison of Potentiometric and ETAAS Determination of Copper and Iron in Herbal Samples, Int. J. Electrochem. Sci., 13 (2018) 9551 – 9560.

[9] G. M. dos Santos, D. Pozebon, C. Cerveira, D. P. de Moraes, Inorganic arsenic speciation in rice products using selective hydride generation and atomic absorption spectrometry (AAS), Microchem. J., 133 (2017) 265-271.

[10] M. Balali-Mood, B. Riahi-Zanjani, A. Mahdizadeh, V. Moradi, R. FazeliBakhtiyari, Arsenic and lead contaminations in commercial fruit juices of markets in mashhad, Iran, Iran. J. Toxicol., 12 (2018) 15-20.

[11] S. Deniz, A. Kasa, S. Sel, Ç. Büyükpınar. S. Bakırdere, Sensitive and Accurate Determination of Cobalt at Trace Levels by Slotted Quartz Tube-Flame Atomic Absorption Spectrometry Following Preconcentration with Dispersive Liquid–Liquid Microextraction, Anal. Lett., 52 (2019) 745-753

[12] P. Pohl, M. Kalinka, M. Pieprz, Development of a very simple and fast analytical methodology for FAAS/FAES measurements of Ca, K, Mg and Na in red beetroot juices along with chemical fractionation of Ca and Mg by solid phase extraction, Microchem. J., 147 (2019) 538-544.

[13] T. Daşbaşi, H. Muğlu, C. Soykan. A. Ülgen, Using a new synthesized polymer resin in various water and dried vegetables amples, J. Macromolecul. Sci., Part A, 55 (2018) 288-295

[14] E. Rossi, M. I. Errea, M. M. F. de Cortalezzi, J. Stripeikis, Selective determination of Cr (VI) by on-line solid phase extraction FI-SPE-FAAS using an ion exchanger resin as sorbent: An improvement treatment of the analytical signal, Microchem. J., 130 (2017) 88-92.

[15] P. Pohl, A. Dzimitrowicz, P. Jamroz, K. Greda, HR-CS FAAS based method for direct determination of total concentrations of Ca, Fe, Mg and Mn in functional apple beverages and evaluation of contributions of the bioaccessible fraction of these elements by in vitro gastrointestinal digestion and chemical fractionation, Microchem. J., 140 (2018) 248-255.

[16] N. Bader, H. Hasan, A. EL-Denali, Determination of Cu, Co, and Pb in selected frozen fish tissues collected from Benghazi markets in Libya, Chem. Methodol., 2 (2018) 56-63

[17] A. Turek, K. Wieczorek, W.M. Wolf, Digestion Procedure and Determination of Heavy Metals in Sewage Sludge—An Analytical Problem, Sustainability, 11 (2019) 1753.

[18] L. A. Meira, F. S. Dias, Application of constrained mixture design and Doehlert matrix in the optimization of dispersive liquid-liquid microextraction assisted by ultrasound for preconcentration and determination of cadmium in sediment and water samples by FAAS, Microchem. J., 130 (2017) 56-63.

[19] E. Mohammed, T. Mohammed, A. Mohammed, Optimization of instrument conditions for the analysis for mercury, arsenic, antimony and selenium by atomic absorption spectroscopy, Method. X, 5 (2018) 824–833.

[20] X. Yu, C.Liu, Y. Guo , T. Deng, Speciation Analysis of Trace Arsenic, Mercury, Selenium and Antimony in Environmental and Biological Samples Based on Hyphenated Techniques, Molecul., 24 (2019) 926.

[21] O. Syta, L. Kępa, A. Mistewicz, C. Wesołowska, B. Wagner, In situ study of Limoges painted enamels by portable X-ray *fluorescence* supported by laser ablation inductively coupled plasma mass *spectrometry* analysis of micro-samples, Microchem. J., 137 (2018) 37-44.

[22] P. R. Aranda, S. Moyano, L. D. Martinez, I. E. De Vito, Determination of trace chromium(VI) in drinking water using X-ray fluorescence spectrometry after solid-phase extraction, Anal. Bioanal. Chem., 398 (2010)1043–104

[23] P. Chauhan, R. P. Chauhan, M. Gupta, Estimation of naturally occurring radionuclides in fertilizers using gamma *spectrometry* and elemental analysis by *XRF* and XRD techniques, Microchem. J., 106 (2013) 73-78.

[24] L. M. Smieska, J. Twilley, A. R. Woll, M. Schafer, A. M. DeGalan, Energy-optimized synchrotron *XRF* mapping of an obscured painting beneath Exit from the Theater, attributed to Honoré Daumier, Microchem. J., 146 (2019) 679-691.

[25] J. Barek, A. Berka, V. Borek, The use of redox reactions in the analysis of dyes and dye intermediates: XIV. Direct current polarography of 4,4′-disubstituted azobenzenes in acetonitrile, Microchem. J., 30 (1984) 404-417.

[26] O. Meena, A. Garg, Y. Kumar, R. Pandey, Electro analytical Procedure for determination of Heavy Metals in Brassica oleraceae ver. Botrytis, Int. J. Chem. Tech. Res. 3 (2011)1596-1603

[27] J. C. García-Mesa, P. Montoro Leal, M. M López Guerrero, E. I. Vereda Alonso, Simultaneous determination of noble metals, Sb and Hg by

magnetic solid phase extraction on line ICP-OES based on a new functionalized magnetic graphene oxide, Microchem. J., 150 (2019) 104-141.

[28] Y. Yamini, M. Safari, Modified magnetic nanoparticles with catechol as a selective sorbent for magnetic solid phase extraction of ultra-trace amounts of heavy metals in water and fruit samples followed by flow injection ICP-OES, Microchem. J., 145 (2018) 503-511.

[29] J. Pérez-Arantegui, M. Resano, E. García-Ruiz, F. Vanhaecke, J. Coll, Characterization of cobalt pigments found in traditional Valencian ceramics by means of laser ablation-inductively coupled plasma mass spectrometry and portable X-ray fluorescence spectrometry, Talanta, 74 (2008) 1271-1280.

[30] P. Krystek, P. Favaro, P. Bode, R. Ritsema, Methyl mercury in nail clippings in relation to fish consumption analysis with gas chromatography coupled to inductively coupled plasma mass spectrometry: A first orientation, Talanta, 97 (2012) 83-86.

[31] B. N. Kumar, S. Kanchi, M.I. Sabela, K. Bisetty, N.V.V. Jyothi, Spectrophotometric determination of nickel (II) in waters and soils: Novel chelating agents and their biological applications supported by DFT method (UV-VIS), Karbala Int. J. Modern Sci., 2 (2016) 239-250

[32] W. Maher, M. Ellwood, S. Foster, G. Raber, Overview of hyphenated techniques using an ICP-MS detector with an emphasis on extraction techniques for measurement of metalloids by HPLC–ICPMS, Microchem. J., 105 (2012) 15-31.

[33] V. Majidi, Capillary electrophoresis inductively coupled plasma mass spectrometry, Microchem. J., 66 (2000) 3-16.

[34] Z. Stojanović, Z. Koudelkova, E. Sedlackova, D. Hynek, L. Richtera , V. Adam, Determination of chromium(vi) by anodic stripping voltammetry using a silver-plated glassy carbon electrode, **Anal. Method.**, **10** (2018) 2917-2923.

[35] N. Mouhamed, K. Cheikhou, G. Elhadji Momar Rokhy, D. M. Bagha, M. D. C. Guèye, T. Tzedakis, Determination of lead in water by linear sweep anodic stripping voltammetry (LSASV) at unmodified carbon paste electrode: Optimization of operating parameters, Am. J. Anal. Chem., 9 (2018) 171-186.

[36] M. Alrobaian, H. Arida, Assessment of Heavy and Toxic Metals in the Blood and Hair of Saudi Arabia Smokers Using Modern Analytical Techniques, Inter. J. Anal. Chem., 8 (2019) 1-8.

[37] A. J. Zimmerman, C. D. Weindorf, Heavy Metal and Trace Metal Analysis in Soil by Sequential Extraction: A Review of Procedures, Inter. J. Anal. Chem., 9 (2010) 1-7.

[38] A. S. Zahidqureshi, N. Mahboob, N. Khuram, Determination of Heavy Metal Toxicity in Blood and Health Effect by AAS (Detection of Heavy Metals and its Toxicity in Human Blood) Madiha Batool, Arch. Nano. Op. Acc. J., 1 (2018) 22-28.

[39] Y. Fu, Adsorption of Heavy Metal Sewage on Nano-materials such as Titanate/TiO2Added Lignin, Results in Physics, 7 (2018) 5-17.

[40] Y. Zhang, W. Bing, X. Hui, L. Hui, M. Wang, Y. He, B. Pan, Nanomaterials-enabled water and wastewater treatment, Nanoimpact., 3 (2016) 22–39.

[41] M. Tuzen, M. Soylak, Multiwalled carbon nanotubes for speciation of chromium in environmental samples, J. Hazard. Mater., 147 (2007) 219–225.

[42] M. Zendehdel, B. Shoshtari-Yeganeh, G. Cruciani, Removal of heavy metals and bacteria from aqueous solution by novel hydroxyapatite/zeolite nanocomposite, preparation, and characterization, J. Iran. Chem. Soc., 13 (2016) 1915–1930.

[43] Y. Ren, N. Yan, Q. Wen, Z. Fan, T. Wei, M. Zhang, J. Ma, Graphene/δ-MnO2 composite as adsorbent for the removal of nickel ions from wastewater, Chem. Eng. J., 175 (2011) 1-7.

[44] I. Ojea-Jiménez, X. López, J. Arbiol, V. Puntes, Citrate-coated gold nanoparticles as smart scavengers for mercury (II) removal from polluted waters, ACS Nano, 6 (2012) 2253-2259.

[45] D. S. K. Peker, O. Turkoglu, M. Soylak, Dysprosium (III) hydroxide coprecipitation system for the separation and preconcentration of heavy metal contents of table salts and natural waters, J. Hazard. Mater., 143 (2007) 555-560.

[46] M. Hiraide, T. Ito, M. Baba, H. Kawaguchi, A. Mizuike, Multielement preconcentration of trace heavy metals in water by coprecipitation and flotation with indium hydroxide for inductively coupled plasma-atomic emission spectrometry, Anal. Chem., 52 (1980) 804-807.

[47] M. Soylak, Column preconcentration/separation and atomic absorption spectrometric determinations of some heavy metals in table salt samples using amberlite XAD-1180, Turkish J. Chem., 7 (2003)

235-42.

[48] M. A. Akl, I. M. Kenawy, R. R. Lasheen, Organically modified silica gel and flame atomic absorption spectrometry: employment for separation and preconcentration of nine trace heavy metals for their determination in natural aqueous systems, Microchem. J., 78 (2004) 143-56.

[49] M. A. A. Akl, I. M. M. Kenawy, R. R. Lasheen, Organically modified silica gel and flame atomic absorption spectrometry: employment for separation and preconcentration of nine trace heavy metals for their determination in natural aqueous systems, Microchem. J., 78 (2004) 143-156.

[50] M. Tuzen, M. Soylak, Multi-element coprecipitation for separation and enrichment of heavy metal ions for their flame atomic absorption spectrometric determinations, J. Hazard. Mater., 162 (2009) 724-729.

[51] M. Soylak, N. D. Erdogan, Copper (II)–rubeanic acid coprecipitation system for separation–preconcentration of trace metal ions in environmental samples for their flame atomic absorption spectrometric determinations, J. hazard. Mater., 137 (2016) 1035-1041.

[52] G. Li, Z. Zhao, J. Liu, G. Jiang, Effective heavy metal removal from aqueous systems by thiol functionalized magnetic mesoporous silica, J. Hazard. Mater., 192 (2011) 277-283.

[53] G. Li, K.H. Row, Utilization of deep eutectic solvents in dispersive liquid-liquid micro-extraction, TrAC Trends in Anal. Chem., 7 (2019) 115651.

[54] M. A. Hashim, S. Mukhopadhyay, J. N. Sahu, B. Sengupta, Remediation technologies for heavy metal contaminated groundwater, J. Environ. Manag., 92 (2011) 2355-2388.

[55] H. Kim, K. Baek, J. Lee, J. Iqbal, J. W. Yang, Comparison of separation methods of heavy metal from surfactant micellar solutions for the recovery of surfactant, Desalination, 191 (2006) 186-192.

[56] Y. Sang, F. Li, Q. Gu, C. Liang, J. Chen, Heavy metal-contaminated groundwater treatment by a novel nanofiber membrane, Desalination, 223 (2008) 349-360.

[57] P. A. Kobielska, A. J. Howarth, O. K. Farha, S. Nayak, Metal–organic frameworks for heavy metal removal from water, Coordination Chem. Reviews, 358 (2018) 92-107.

[58] E. Alonso, A. Santos, M. Callejón, J. C. Jiménez, Speciation as a screening tool for the determination of heavy metal surface water pollution in the Guadiamar river basin, Chemosphere, 56 (2004) 561-570.

[59] S. Obiri, Determination of heavy metals in water from boreholes in Dumasi in the Wassa West District of western region of Republic of Ghana, Environ. Monitor. Assess., 130 (2007) 455-463.

[60] C. Riccardi, P. Di Filippo, D. Pomata, F. Incoronato, M. Di Basilio, M. P. Papini, S. Spicaglia, Characterization and distribution of petroleum hydrocarbons and heavy metals in groundwater from three Italian tank farms, Sci. Total Environ., 393 (2008) 50-63.

[61] M. A. Momodu, C. A. Anyakora, Heavy metal contamination of ground water: The Surulere case study, Res. J. Environ. Earth Sci., 2 (2010) 39-43.

[62] A. Rudnitskaya, A. Ehlert, A. Legin, Y. Vlasov, S. Büttgenbach, S. Multisensor, System on the basis of an array of non-specific chemical sensors and artificial neural networks for determination of inorganic pollutants in a model groundwater, Talanta, 55 (2001) 425-431.

[63] P. Kurup, C. Sullivan, R. Hannagan, S. Yu, H. Azimi, S. Robertson, D. Ryan, R. Nagarajan, T. Ponrathnam, G. Howe, A review of technologies for characterization of heavy metal contaminants, Indian Geotech. J., 47 (2017) 421-436.

[64] K.S. Yun, J. Gil, J. Kim, H.J. Kim, K.H. Kim, D. Park, J.Y. Kwak, H. Shin, K. Lee, J. Kwak, E.Yoon, A miniaturized low-power wireless remote environmental monitoring system using microfabricated electrochemical sensing electrodes, 12th international conference on solid-state sensors, actuators and microsystems, Cat. No. 03TH8664, IEEE, 2003.

[65] B. Bansod, T. Kumar, R. Thakur, S. Rana, I. Singh, A review on various electrochemical techniques for heavy metal ions detection with different sensing platforms, Biosen. Bioelectron., 94 (2017) 443-455.

[66] N. M. Isa, A. Z. Aris, W. Y. Lim, W. N. A. W. Sulaiman, S. M. Praveena, Evaluation of heavy metal contamination in groundwater samples from Kapas Island, Terengganu, Malaysia, Arab. J. Geosci., 7 (2014) 1087-1100.

[67] M. Afzal, G. Shabir, S. Iqbal, T. Mustafa, Q. M. Khan, Z. M.Khalid, Assessment of heavy metal contamination in soil and groundwater at leather industrial area of Kasur, Pakistan, CLEAN–Soil Air Water, 42 (2014) 1133-1139.

[68] A. Joshi, T. C. Nagaiah, Nitrogen-doped carbon nanotubes for sensitive and selective determination

of heavy metals, RSC Adv., 5 (2015) 105119-105127.

[69] H. X. Zhao, W. Cai, D. Ha, H. Wan, P. Wang, The study on novel microelectrode array chips for the detection of heavy metals in water pollution, J. Innovative Optic. Health Sci., 5 (2012), 1150002.

[70] C.S. Chapman, C.M. Van Den Berg, University of Liverpool, Electrochemical cell. U.S. Patent 8,277,618, 2012.

[71] J. Holmes, P. Pathirathna, P. Hashemi, Novel frontiers in voltammetric trace metal analysis: Towards real time, on-site, in situ measurements, TrAC Trends in Anal. Chem., 5 (2018) 5-11.

[72] M. Liu, G. Zhao, Y. Tang, Z. Yu, Y. Lei, M. Li, Y. Zhang, D. Li, A simple, stable and picomole level lead sensor fabricated on DNA-based carbon hybridized TiO_2 nanotube arrays, Environ. Sci. Tech., 44 (2010) 4241-4246.

[73] M. Gutiérrez-Capitán, A. Baldi, C. Jimenez-Jorquera, C. Fernández-Sánchez, R. Gomez, V. García, Stripping voltammetric detection of trace heavy metals using gold ultramicroelectrode arrays, IEEE, 9th IberoAmerican congress on sensors, 1-4, 2014.

[74] W. G. Yelton, M. P. Siegal, National Technology and Engineering Solutions of Sandia LLC, Nanoelectrode array for electrochemical analysis, U.S. Patent 7 (2009) 469.

[75] A. Sarı, M. Tuzen, D. Cıtak, M. Soylak, Adsorption characteristics of Cu (II) and Pb (II) onto expanded perlite from aqueous solution, J. Hazard. Mater., 148 (2007) 387-394.

[76] A. Sarı, M. Tuzen, Ö. D. Uluözlü, M. Soylak, Biosorption of Pb (II) and Ni (II) from aqueous solution by lichen (Cladonia furcata) biomass, Biochem. Eng. J., 37 (2007) 151-158.

[77] O. D. Uluozlu, M. Tuzen, D. Mendil, M. Soylak, Trace metal content in nine species of fish from the Black and Aegean Seas, Turkey, Food chemistry, 104 (2007) 835-840.

[78] A. Sarı, M. Tuzen, M. Soylak, Adsorption of Pb (II) and Cr (III) from aqueous solution on Celtek clay, J. Hazard. Mater., 144 (2007) 41-46.

[79] M. Tuzen, K. O. Saygi, Usta C., Soylak M., Pseudomonas aeruginosa immobilized multiwalled carbon nanotubes as biosorbent for heavy metal ions, Biores. Tech., 99 (2008) 1563-1570.

[80] İ. Narin, M. Soylak, L. Elçi, M. Doğan, Determination of trace metal ions by AAS in natural water samples after preconcentration of pyrocatechol violet complexes on an activated carbon column, Talanta, 52 (2000) 1041-1046.

[81] M. Tuzen, M. Soylak, L. Elci, Multi-element pre-concentration of heavy metal ions by solid phase extraction on Chromosorb 108, Analytica Chimica Acta, 548 (2005)101-108.

[82] U. Divrikli, N. Horzum, M. Soylak, L. Elci, Trace heavy metal contents of some spices and herbal plants from western Anatolia, Turkey, Int. J. food Sci. Tech., 41 (2006) 712-716.

[83] C. Duran, A. Gundogdu, V. N. Bulut, M. Soylak, L. Elci, H. B. Sentürk, M. Tüfekci, Solid-phase extraction of Mn (II), Co (II), Ni (II), Cu (II), Cd (II) and Pb (II) ions from environmental samples by flame atomic absorption spectrometry (FAAS), J. Hazard. Mater., 146 (2007) 347-355.

[84] A. Sari, D. Mendil, M. Tuzen, M. Soylak, Biosorption of palladium (II) from aqueous solution by moss (Racomitrium lanuginosum) biomass: Equilibrium, kinetic and thermodynamic studies, J. Hazard. Mater., 162 (2009) 874-879.

[85] D. Mendil, Ö. F. Ünal, M. Tüzen, M. Soylak, Determination of trace metals in different fish species and sediments from the River Yeşilırmak in Tokat, Turkey, Food Chem. Toxicol., 48 (2010) 1383-1392.

[86] A. Gundogdu, D. Ozdes, C. Duran, V. N. Bulut, M. Soylak, H. B. Senturk, Biosorption of Pb (II) ions from aqueous solution by pine bark (Pinus brutia Ten.), Chem. Eng. J., 153 (2009) 62-69.

[87] F. A. Aydin, M. Soylak, A novel multi-element coprecipitation technique for separation and enrichment of metal ions in environmental samples, Talanta, 73 (2007) 134-141.

[88] M. Tuzen, I. Karaman, D. Citak, M. Soylak, Mercury (II) and methyl mercury determinations in water and fish samples by using solid phase extraction and cold vapour atomic absorption spectrometry combination, Food Chem. Toxicol., 47 (2009) 1648-1652.

[89] M. Tuzen, D. Çıtak, D. Mendil, M. Soylak, Arsenic speciation in natural water samples by coprecipitation-hydride generation atomic absorption spectrometry combination, Talanta, 78 (2009) 52-56.

[90] M. Tuzen, K. O. Saygi, M. Soylak, Novel solid phase extraction procedure for gold (III) on Dowex M 4195 prior to its flame atomic absorption spectrometric determination, J. Hazard. Mater., 156 (2008) 591-595.

[91] M. Tuzen, A. Sarı, D. Mendil, O. D. Uluozlu, M. Soylak, M. Dogan, Characterization of biosorption process of As (III) on green algae Ulothrix cylindricum, J. Hazard. Mater., 165 (2009) 566-572.

[92] M. Soylak, O. Ercan, Selective separation and preconcentration of copper (II) in environmental samples by the solid phase extraction on multi-walled carbon nanotubes, J. Hazard. Mater., 168 (2009) 1527-1531.

[93] S. Saracoglu, M. Soylak, L. Elci, Separation/preconcentration of trace heavy metals in urine, sediment and dialysis concentrates by coprecipitation with samarium hydroxide for atomic absorption spectrometry, Talanta, 59 (2003) 287-293.

[94] T. W. Speir, A. P. Van Schaik, H. J. Percival, M. E. Close, L. Pang, Heavy metals in soil, plants, and groundwater following high-rate sewage sludge application to land, J. Water, Air, Soil Poll., 150 (2003) 319-358.

[95] P. J. H. Scheeren, R. O. Koch, C. J. N. Buisman, L. J. Barnes, J. H. Versteegh, New biological treatment plant for heavy metal contaminated groundwater, In EMC'91:Non-merrous metallurgy, Springer, 9 (2007) 403-416.

[96] H. Malassa, F. Al-Rimawi, M. Al-Khatib, M. Al-Qutob, Determination of trace heavy metals in harvested rainwater used for drinking in Hebron (south West Bank, Palestine) by ICP-MS, Environ. Monitor. Assess., 186 (2014) 6985-6992.

[97] M. G. Yalcin, I. Narin, M. Soylak, Heavy metal contents of the Karasu creek sediments, Nigde, Turkey, Environ. Monitor. Assess., 128 (2007) 351-357.

[98] O. D. Uluozlu, M. Tuzen, D. Mendil, M. Soylak, Determination of As (III) and As (V) species in some natural water and food samples by solid-phase extraction on Streptococcus pyogenes immobilized on Sepabeads SP 70 and hydride generation atomic absorption spectrometry, Food Chem. Toxicol., 48 (2010) 1393-1398.

[99] D. Mendil, F. Celik, M. Tuzen, M. Soylak, Assessment of trace metal levels in some moss and lichen samples collected from near the motorway in Turkey, J. Hazard. Mater., 166 (2009) 1344-1350.

[100] M. Tuzen, M. Soylak, K. Parlar, Cadmium and lead contamination in tap water samples from Tokat, Turkey, Bull. Environ. Conta. Toxicol., 75 (2005) 284-289.

[101] M. Tuzen and M. Soylak, Evaluation of Metal Levels of Drinking Waters from the Tokat-Black Sea Region of Turkey, Polish J. Environ. Studies, 15 (2006) 1-6.

[102] B. Naeemullaha, M. Tuzena, A new portable switchable hydrophilicity microextraction method for determination of vanadium in microsampling micropipette tip syringe system couple with ETAAS, Talanta, 5 (2018) 1-8.

[103] P. G. Jessop, L. Phan, A. Carrier, S. Robinson, C. J. Dürr, J. R. Harjani, A solvent having switchable hydrophilicity, Green Chem., 12 (2010) 809-814.

[104] E. Kazemi, S. Dadfarnia, A. M. Haji Shabani, P. Sadat Hashemi, Synthesis of 2-mercaptobenzothiazole/magnetic nanoparticles modified multi-walled carbon nanotubes for simultaneous solid-phase microextraction of cadmium and lead, Int. J. Environ. Anal. Chem., 97 (2017) 743-755.

[105] H. Heidari, A. Moghimi, H. R. Shahbazi, Solid phase extraction of trace cobalt (II) in industrial wastewaters by modified nanotube carbon carboxyl and its determination with flame atomic spectroscopy, Int. J. Bio-Inorg., 7 (2018) 43–57.

[106] Feist B., Selective dispersive micro solid-phase extraction using oxidized multiwalled carbon nanotubes modified with 1,10-phenanthroline for preconcentration of lead ions, Food Chem., 209 (2016) 37–42.

107] E. Zolfonoun, Solid phase extraction and determination of indium using multi-walled carbon nanotubes modified with magnetic nanoparticles, Anal. Meth. Environ. Chem. J., 1 (2018) 5-10.

[108] H. Shirkhanloo, A. Khaligh, H. Z. Mousavi, A. Rashidi, Ultrasound assisted-dispersive-ionic liquid-micro-solid phase extraction based on carboxyl-functionalized nanoporous graphene for speciation and determination of trace inorganic and organic mercury species in water and caprine blood samples, Microchem. J., 130 (2017) 245-254.

[109] H. Shirkhanloo, M. Ghazaghi, A. Rashidi, A. Vahid, Arsenic speciation based on amine-functionalized bimodal mesoporous silica nanoparticles by ultrasound assisted-dispersive solid-liquid multiple phase microextraction, Microchem. J., 130 (2017) 137–146.

110] M. Tuzen, A new robust, deep eutectic-based floating organic droplets microextraction method for determination of lead in a portable syringe

system directly couple with FAAS, Talanta, 196 (2019) 71-77.

[111] R. A. Zounr, M. Tuzen, N. Deligonul, M.Y. Khuhawar, A highly selective and sensitive ultrasonic assisted dispersive liquid phase microextraction based on deep eutectic solvent for determination of cadmium in food and water samples prior to electrothermal atomic absorption spectrometry, Food Chem., 253 (2018) 277-283.

[112] M. Tuzen, O.D. Uluozlu, D. Mendil, M. Soylak, L.O.R. Machado, W.N.L. DosSantos, S.L.C. Ferreira, A simple, rapid and green ultrasound assisted and ionic liquid dispersive microextraction procedure for the determination of tin in foods employing ETAAS, Food Chem., 254 (2018) 380-384.

[113] S. Moyano, G. Polla, P. Smichowski, J.A. Gásquez, L.D. Martinez, On-line preconcentration and determination of vanadium in tap and river water samples by flow injection-inductively coupled plasma-optical emission spectrometry (FI-ICP-OES), J. Anal. At. Spectrom., 21 (2006) 422-426.

[114] T. Stefanova-Bahchevanska, N. Milcheva, S. Zaruba, V. Andruch, V. Delchev, K. Simitchiev, Gavazov K. A., green cloud-point extraction-chromogenic system for vanadium determination, J. Mol. Liq., 248 (2017) 135-142.

[115] I. López-García, J.M.H. Juan, H.C. Manuel, Graphite furnace atomic absorption spectrometric determination of vanadium after cloud point extraction in the presence of graphene oxide, Spectrochim. Acta Part B, 143 (2018) 42-47.

[116] S. Khan, T.G. Kazi, J.A. Baig, N.F. Kolachi, H.I. Afridi, S.K. Wadhwa, F. Shah, Cloudpoint extraction of vanadium in pharmaceutical formulations, dialysate and parenteral solutions using 8-hydroxyquinoline and nonionic surfactant, J. Hazard. Mater., 182 (2010) 371-376.

[117] T. Asadollahi, S. Dadfarnia, A. M. H. Shabani, Separation/preconcentration and determination of vanadium with dispersive liquid–liquid microextraction based on solidification of floating organic drop (DLLME-SFO) and electrothermal atomic absorption spectrometry, Talanta, 82 (2010) 208-212.

[118] L. Chen, H. Xin, Y. Fang, Application of metal oxide heterostructures in arsenic removal from contaminated water, J. Nanomater., 2 (2014) 1–10.

[119] M.K. Ghosh, G.E.J. Poinern, T.B. Issa, 'Arsenic adsorption on goethite nanoparticles produced through hydrazine sulfate assisted synthesis method', Korean J. Chem. Eng., 29 (2012) 95–102.

[120] L. Feng, M. Cao, X. Ma, Superparamagnetic high-surface-area Fe_3O_4 nanoparticles as adsorbents for arsenic removal, J. Hazard. Mater., 217 (2012) 439–446.

[121] W. Tang, Y. Su, Q. Li, Mg-doping: a facile approach to impart enhanced arsenic adsorption performance and easy magnetic separation capability to alpha-Fe2O3 nanoadsorbents, J. Mater. Chem. A, 1 (2013) 830–836.

[122] D. Nabi, I. Aslam, I. A. Qazie, Evaluation of the adsorption potential of titanium dioxide nanoparticles for arsenic removal, J. Environ. Sci., 21 (2009) 402–408.

[123] M. I. Danish, I. A. Qazi, A. Zeb, Arsenic removal from aqueous solution using pure and metal-doped titania nanoparticles coated on glass beads: adsorption and column studies, J. Nanomater., 69 (2013) 1–17.

[124] C.A. Martinson, K.J. Reddy, 'Adsorption of arsenic(III) and arsenic(V) by cupric oxide nanoparticles', J. Colloid Interf. Sci., 336 (2009) 406– 411.

[125] R. Li, Q. Li, S. Gao, Exceptional arsenic adsorption performance of hydrous cerium oxide nanoparticles: Part A. Adsorption capacity and mechanism, Chem. Eng. J., 185 (2012) 127–135.

[126] Y. Liu, Q. Li, S. Gao, Exceptional As(III) sorption capacity by highly porous magnesium oxide nanoflakes made from hydrothermal synthesis, J. Am. Ceram. Soc., 94 (2011) 217–223.

[127] A. Goswami, P. K. Raul, M. K. Purkait, Arsenic adsorption using copper (II) oxide nanoparticles, Chem. Eng. Res. Des., 90 (2012) 1387–1396.

[128] H. Cui, Q. Li, S. Gao, Strong adsorption of arsenic species by amorphous zirconium oxide nanoparticles', J. Ind. Eng. Chem., 18 (2012) 1418–1427.

[129] S. A. Ntim, S. Mitra, Adsorption of arsenic on multiwall carbon nanotubezirconia nanohybrid for potential drinking water purification, J. Colloid Interf. Sci., 375 (2012) 154–159.

[130] R. Chen, C. Zhi, H. Yang, Arsenic(V) adsorption on Fe_3O_4 nanoparticle-coated boron nitride nanotubes', J. Colloid Interf. Sci., 359 (2011) 261–268.

[131] W. Yang, P. Ding, L. Zhou, Preparation of diamine modified mesoporous silica on multi-walled carbon nanotubes for the adsorption of heavy metals in aqueous solution, Appl. Surf. Sci., 23 (2013) 38–45.

[132] Y. M. Hao, C. Man, Z. B. Hu, Effective removal of Cu^{2+} ions from aqueous solution by amino-functionalized magnetic nanoparticles, J. Hazard. Mater., 184 (2014) 392–399.

[133] Y. T. Zhou, H. L. Nie, C. B. White, Removal of Cu^{2+} from aqueous solution by chitosan-coated magnetic nanoparticles modified with αketoglutaric acid, J. Colloid Interf. Sci., 330 (2009) 29–37.

[134] M. A. Salam, M. S. I. Makki, M. Y. A. Abdelaal, Preparation and characterization of multi-walled carbon nanotubes/chitosan nanocomposite and its application for the removal of heavy metals from aqueous solution', J. Alloy. Compd., 509 (2009) 2582–2587.

[135] O. Hakami, Y. Zhang, Banks C. J., Thiol-functionalised mesoporous silicacoated magnetite nanoparticles for high efficiency removal and recovery of Hg from water, Water Res., 46 (2012) 3913–3922.

[136] A. Farrukh, A. Akram, A. Ghaffar, Design of polymer-brush-grafted magnetic nanoparticles for highly efficient water remediation, ACS Appl. Mater. Interf., 5 (2013) 3784–3793.

[137] B. Tawabini, S. Al-Khaldi, M. Atieh, Removal of mercury from water by multi-walled carbon nanotubes, Water Sci. Technol., 61 (2010) 591–598.

[138] F. A. Al-Khaldi, B. Abu-Sharkh, A. M. Abulkibash, Cadmium removal by activated carbon, carbon nanotubes, carbon nanofibers, and carbon fly ash: a comparative study, Desalination Water Treat., 53 (2015) 1417–1429.

[139] F. P. Fato, D. W. Li, L. Zhao, K. Qiu, Simultaneous Removal of Multiple Heavy Metal Ions from River Water Using Ultrafine Mesoporous Magnetite Nanoparticles, ACS Omega, 44 (2019) 7543-7549.

[140] G. Gollavelli, C. C. Chang, Y. C. Ling, Facile Synthesis of Smart Magnetic Graphene for Safe Drinking Water: Heavy Metal Removal and Disinfection Control, ACS Sustainable Chem. Eng., 1 (2013) 462−472.

[141] X. Luo, J. Zeng, S. Liu, L. Zhang, An effective and recyclable adsorbent for the removal of heavy metal ions from aqueous system: magnetic chitosan/cellulose microspheres, Bioresour. Technol., 8 (2015) 135-142.

[142] M. Mahmoudi, S. Sant, B. Wang, S. Laurent, T. Sen, Superparamagnetic iron oxide nanoparticles (SPIONs): development, surface modification and applications in chemotherapy, Adv. Drug. Delivery Rev., 63 (2011) 24−46.

[143] N. Neyaz, W. Siddiqui, K. Nair, Application of surface functionalized iron oxide nanomaterials as a nanosorbents in extraction of toxic heavy metals from ground water: A review, Int. J. Environ. Sci., 4 (2013) 472−483.

[144] F. H. Chen, Q. Gao, J. Z. Ni, The grafting and release behavior of doxorubincin from Fe_3O_4 at SiO2 core-shell structure nanoparticles via an acid cleaving amide bond: the potential for magnetic targeting drug delivery, Nanotechnol., 19 (2008) 165103.

[145] X. Luo, X. Lei, N. Cai, X. Xie, Y. Xue, F. Yu, Removal of Heavy Metal Ions from Water by Magnetic Cellulose-Based Beads with Embedded Chemically Modified Magnetite Nanoparticles and Activated Carbon, ACS Sustainable Chem. Eng., 47 (2016) 3960-3969.

[146] M. A. Shannon, Science and technology for water purification in the coming decades, Nanosci. Technol., 452 (2008) 301−310.

[147] X. Luo, L. Zhang, Immobilization of Penicillin G Acylase in Epoxy-Activated Magnetic Cellulose Microspheres for Improvement of Biocatalytic Stability and Activities. Biomacromolecules, 11 (2010) 2896−2903.

[148] M. Gericke, J. Trygg, P. Fardim, Functional Cellulose Beads: Preparation, Characterization, and Applications, Chem. Rev., 113 (2013) 4812−4836.

[149] H. Karami, Heavy metal removal from water by magnetite nanorods, Chem. Eng. J., 219 (2013) 209−216.

[150] Y. Zhao, H. Chen, J. Li, C. Chen, Hierarchical $MWCNTs/Fe_3O_4/PANI$ magnetic composite as adsorbent for methyl orange removal, J. Colloid Interface Sci., 450 (2015) 189−195.

[151] C. Santhosh, R. Nivetha, P. Kollu, V. Srivastava, M. Sillanpää, A. Nirmala Grace, A. Bhatnagar, Removal of cationic and anionic heavy metals from water by 1D and 2D-carbon structures decorated with magnetic nanoparticles, Sci. Rep., 7 (2017) 14100-14107.

[152] S. Singh, K. C. Barick, D. Bahadur, Functional Oxide Nanomaterials and Nanocomposites for the Removal of Heavy Metals and Dyes Invited Review Article, Nanomater. nanotechnol., 3 (2013) 1-18.

[153] P. Z. Ray, H. J. Shipley, Inorganic nano-adsorbents for the removal of heavy metals and arsenic: a review, RSC Adv., 5 (2015) 29885−29907.

[154] G. Vilardi, T. Mpouras, D. Dermatas, N. Verdone, A. Polydera, L. Di, Palma Nanomaterials application

for heavy metals recovery from polluted water: the combination of nano zero-valent iron and carbon nanotubes. Competitive adsorption non-linear modeling, Chemosphere, 201 (2018) 716-729.

[155] M. Alrobaian and H. Arida, Assessment of Heavy and Toxic Metals in the Blood and Hair of Saudi Arabia Smokers Using Modern Analytical Techniques, Int. J. Anal. Chem.,14 (2019) 1-8.

[156] K. Liu, H. Qi, R. Dong, R. Shivhare, M. Addicoat, T. Zhang, H. Sahabudeen, T. Heine, S. Mannsfeld, U. Aiser, Z. Zheng, X. Feng, On-water surface synthesis of crystalline, few-layer two-dimensional polymers assisted by surfactant monolayers, Nature Chem., 11 (2019) 994–1000

[157] M. Rosillo-Lopez, C. G. Salzmann, Highly efficient heavy-metal extraction from water with carboxylated graphene nanoflakes, **RSC Adv., 8** (2018) 11043-11050.

[158] J. Zhao, X. Yan, T. Zhou, J. Wang, H. Li, P. Zhang, H. Ding, L. Ding, Multi-throughput dynamic microwave-assisted leaching coupled with inductively coupled plasma atomic emission spectrometry for heavy metal analysis in soil, **J. Anal. At. Spectrom., 30 (2015)** 1920-1926

[159] A. P. Esser-Kahn, A. T. Iavarone, Matthew B. Francis, Metallothionein-Cross-Linked Hydrogels for the Selective Removal of Heavy Metals from Water, J. American Chem. Society, 130 (2008) 15820–15822.

[160] H. Shirkhanloo, A. Khaligh, H. Zavvar Mousavi, A. Rashidi, Ultrasound assisted-dispersive-micro-solid phase extraction based on bulky amino bimodal mesoporous silica nanoparticles for speciation of trace manganese (II)/(VII) ions in water samples, Microchem. J., 124 (2016) 637–645.

[161] H. Shirkhanloo, A. Khaligh, H. Zavvar Mousavi, A. Rashidi, Ultrasound assisted-dispersive-ionic liquid-micro-solid phase extraction based on carboxyl-functionalized nanoporous graphene for speciation and determination of trace inorganic and organic mercury species in water and caprine blood samples, Microchem. J., 130 (2017) 245–254

[162] H. Shirkhanloo, M. Ghazaghi, A. Rashidi, A. Vahid, Arsenic speciation based on amine-functionalized bimodal mesoporous silica nanoparticles by ultrasound assisted-dispersive solid-liquid multiple phase microextraction, Microchem. J., 130 (2017) 137–146.

[163] H. Shirkhanloo, M. Ghazaghi, H. Z. Mousavi, Chromium speciation in human blood samples based on acetylcysteine by dispersive liquid–liquid bio microextraction and in-vitro evaluation of acetyl cysteine/cysteine for decreasing of hexavalent chromium concentration, J. Pharmac. Biomed. Anal., 118 (2016) 1–8.

[164] H. Shirkhanloo, A. Khaligh, F. Golbabaei, Z. Sadeghi, A. Vahid, A. Rashidi, On-line micro column preconcentration system based on amino bimodal mesoporous silica nanoparticles as a novel adsorbent for removal and speciation of chromium (III, VI) in environmental samples, J. Environ. Health Sci. Eng., 13 (2015) 13-47.

[165] C. S. A. Felix, D. L. F. da Silva, A. V. B. Chagas, A green on-line digestion system using 70% hydrogen peroxide and UV radiation for the determination of chromium in beer employing ETAAS, Microchem. J., 146 (2019) 1204-1208.

[166] E. G. Barrera, D. Bazanella, P. W. Castro, W. Boschetti, M. B. Dessuy, Alternative method for chromium determination in pharmaceutical drugs by HR-CS GF AAS and direct analysis of solid samples, Microchem. J., 132 (2017) 365-370.

[167] L. Boutorabi, M. Rajabi, M. Barzegar, A. Asghari, Selective determination of chromium(VI) ions using in-tube electro-membrane extraction followed by flame atomic absorption spectrometry, Microchem. J., 132 (2017) 378-384.

[168] M. Shirani, F. Salari, S. Habibollahi, A. Akbari, Needle hub in-syringe solid phase extraction based a novel functionalized biopolyamide for simultaneous green separation/preconcentration and determination of cobalt, nickel, and chromium (III) in food and environmental samples with micro sampling flame atomic absorption spectrometry, Microchem. J., 132 (2019) 104332-104340.

[169] M. Felipe-Sotelo, A. Carlosena, J. M. Andrade, M. J. Cal-Prieto, D. Prada, Slurry-based procedures to determine chromium, nickel and vanadium in complex matrices by ETAAS, Microchem. J., 81 (2005) 217-224.

[170] R. Pechancová, T. Pluháček, J. Gallo, D. Milde, Study of chromium species release from metal implants in blood and joint effusion: Utilization of HPLC-ICP-MS, Talanta, 185 (2018) 370-377.

[171] E. Jorge, M. M. Rocha, I. T. E. Fonseca, M. M. Neto, Studies on the strippingvoltammetric determination and speciation of chromium at a rotating-discbismuth film electrode, Talanta, 81 (2010) 556–564.

[172] D. Verma, S. K. Verma, M. K. Deb, Single-drop micro-extraction and diffuse reflectance Fourier transform infrared spectroscopic determination of chromium in biological fluids, Talanta, 78 (2009) 270–277.

[173] M. Fırat, S. Bakırdere, M. Selin Fındıkoğlu, E. Betül Kafa, E. Yazıcı, M. Yolcu, Ç. Büyükpınar, D. S. Chormey, S. Sel, F. Turak, Determination of trace amount of cadmium using dispersive liquid-liquid microextraction-slotted quartz tube-flame atomic absorption spectrometry, Spectrochim. Acta Part B At. Spectrosc., 129 (2017) 37-41.

[174] R. Gürkan, S. Korkmaz, N. Altunay, Preconcentration and determination of vanadium and molybdenum in milk, vegetables and foodstuffs by ultrasonic-thermostatic-assisted cloud point extraction coupled to flame atomic absorption spectrometry, Talanta, 155 (2016) 38-46.

[175] N. A. Kasa, S. Sel, D. S. Chormey, S. Bakırdere, Determination of cadmium at trace levels in parsley samples by slotted quartz tube-flame atomic absorption spectrometry after preconcentration with cloud point extraction, Measurement, 147 (2019) 106841.

[176] K. Shrivas, K. Dewangan, A. Ahmed, Surfactant-based dispersive liquid–liquid microextraction for the determination of zinc in environmental water samples using flame atomic absorption spectrometry, **Anal. Meth.**, **8** (2016) 5519-5525.

[177] S. Deniz, A. Kasa, S. Sel, Ç. Büyükpınar, S. Bakırdere, Sensitive and accurate determination of cobalt at trace levels by slotted quartz tube-flame atomic absorption spectrometry following preconcentration with dispersive liquid–liquid microextraction, Anal. Lett.,17 (2019) 745-753.

[178] E. Yazıcı, M. Fırat, S. Chormey, E. G. Bakırdere, S. Bakırdere, An accurate determination method for cobalt in sage tea and cobalamin: Slotted quartz tube-flame atomic absorption spectrometry after preconcentration with switchable liquid-liquid microextraction using a Schiff base, Food Chem., 302 (2019) 125330-125336.

[179] A.T. Bisgin, Surfactant-Assisted Emulsification and Surfactant-Based Dispersive Liquid-Liquid Microextraction Method for Determination of Cu(II) in Food and Water Samples by Flame Atomic Absorption Spectrometry, J. AOAC Inter., 102 (2019) 1516-1522.

[180] A. M. Farajzadeh, H. Dastoori, S. M. Sorouraddin, Development of a dispersive liquid-liquid microextraction method based on a ternary deep eutectic solvent as chelating agent and extraction solvent for preconcentration of heavy metals from milk samples, Talanta, 193 (2019) 120485.

[181] J. A. Barreto, R Santos de Assis, R. J. Cassella, V. Azevedo lemos, A novel strategy based on in-syringe dispersive liquid-liquid microextraction for the determination of nickel in chocolate samples, Author links open overlay panel, Talanta, 193 (2019) 23-28.

[182] E. Fernández, L. Vidal, A. C. García, A. Cana, Mercury determination in urine samples by gold nanostructured screen-printed carbon electrodes after vortex-assisted ionic liquid dispersive liquid–liquid microextraction, Analytica. Chimica. Acta., 915 (2016) 49-55.

[183] H. Shirkhanloo, M. Ghazaghi, M. M. Eskandari, Cloud point assisted dispersive ionic liquid -liquid microextraction for chromium speciation in human blood samples based on isopropyl 2-[(isopropoxycarbothiolyl)disulfanyl] ethane thioate, Anal. Chem. Res., 10 (2016) 18-27.

[184] H. Shirkhanloo, M. Ghazaghi, H. ZavvarMousavi, Cadmium determination in human biological samples based on trioctylmethyl ammonium thiosalicylate as a task-specific ionic liquid by dispersive liquid–liquid microextraction method, J. Molec. Liqu., 218 (2016) 478–483.

[185] H. Z. Mousavi, H. Shirkhanloo, M. Ghazaghi, Chromium speciation in human blood samples based on acetylcysteine by dispersive liquid–liquid biomicroextraction and in-vitro evaluation of acetyl cysteine/cysteine for decreasing of hexavalent chromium concentration, J. Pharmac. Biomed. Anal., 118 (2016) 1–8.

[186] E. C. Lourenço, E. Eyng, P. R. S. Bittencourt, Fabio A. Duarte, Rochele S. Picoloto, É. L. M. Flores, A simple, rapid and low cost reversed-phase dispersive liquid-liquid microextraction for the determination of Na, K, Ca and Mg in biodiesel, Talanta, 199 (2019) 1-7.

[187] L. B. Escudero, P. Berton, E. M. Martinis, R. A. Olsina, R. G. Wuilloud, Dispersive liquid-liquid microextraction and preconcentration of thallium species in water samples by two ionic liquids applied as ion-pairing reagent and extractant phase, Talanta, 88 (2012) 277–283.

[188] X. Jia, Y. Han, C. Wei, T. Duan, H. Chen, Speciation of mercury in liquid cosmetic samples by ionic liquid based dispersive liquid-liquid

microextraction combined with high-performance liquid chromatography inductively coupled plasma mass spectrometry, J. Anal. Atom. Spectrom., 26 (2011) 1380–1386.

[189] L. B. Escudero, E. M. Martinis, R. A. Olsina, R. G. Wuilloud, Arsenic speciation analysis in monovarietal wines by on-line ionic liquid-based dispersive liquid-liquid microextraction, Food Chem., 138 (2013) 484–490.

[190] J. F. Ayala-Cabrera, M. J. Trujillo-Rodríguez, V. Pino, Ó. M. Hernández-Torres, A. M. Afonso, J. Sirieix-Plénet, Ionic liquids versus ionic liquid-based surfactants in dispersive liquid–liquid microextraction for determining copper in water by flame atomic absorption spectrometry, Inter. J. Environ. Anal. Chem., 96 (2016) 101–118.

[191] E. Molaakbari, A. Mostafavi, D. Afzali, Ionic liquid ultrasound assisted dispersive liquid-liquid microextraction method for preconcentration of trace amounts of rhodium prior to flame atomic absorption spectrometry determination, J. Hazard. Mater., 185 (2011) 647–652.

[192] P. Berton, E.M. Martinis, L.D. Martinez, R.G. Wuilloud, Room temperature ionic liquid-based microextraction for vanadium species separation and determination in water samples by electrothermal atomic absorption spectrometry, Anal. Chim. Acta., 640 (2009) 40–46.

[193] M. Tuzen, O. Z. Pekiner, Ultrasound-assisted ionic liquid dispersive liquid–liquid microextraction combined with graphite furnace atomic absorption spectrometric for selenium speciation in foods and beverages, Food Chem., 188 (2015) 619–624.

[194] A. Beiraghi, M. Shokri, S. Seidi, B. M. Godajdar, Magnetomotive room temperature dicationic ionic liquid: A new concept toward centrifuge-less dispersive liquid– liquid microextraction, J. Chromatogr. A, 76 (2015) 1–8.

[195] V. Balarama, K. Mullapudi, K. Chandrasekaran, G. Venkateswarlu, D. Karunasagar, Development of a simple and rapid microwave-assisted extraction method using very dilute solutions of perchloric acid and hydrogen peroxide for the multi-elemental analysis of food materials by ICP-OES: A green analytical method, Microchem. J., 146 (2019) 807-817.

[196] E. J. Santos, S. Clarice, D. B. Amaral, N. Nagata, M. T. Grassi, Cloud point extractors for simultaneous determination of Pd and Pt in water samples by ICP OES with multivariate optimization, Microchem.

J., 152 (2020) 104300-104309.

[197] S. A. Arain, T. G. Kazi, H. I. Afridi, M. Shahzadi Arain, A. H. Panhwar, N. Khan, J. A. Baig, F. Shah, A new dispersive liquid–liquid microextraction using ionic liquid based microemulsion coupled with cloud point extraction for determination of copper in serum and water samples, Ecotoxicol. Environ. Safety, 126 (2016) 186–192.

[198] H. Shirkhanloo, M. Falahnejad, H. Zavvar Mousavi, On-line ultrasound-assisted dispersive micro-solid-phase extraction based on amino bimodal mesoporous silica nanoparticles for the preconcentration and determination of cadmium in human biological samples, Microchem. J., 124 (2016) 637-645.

[199] M. Ghazaghi, H. Zavvar Mousavi, A. M. Rashidi, H. Shirkhanloo, R. Rahighi, Graphene-silica hybrid inefficient preconcentration of heavy metal ions via novel single-step method of moderate centrifugation-assisted dispersive micro solid phase extraction, Talanta, 150 (2016) 476–484.

[200] M. Falahnejad, H. Zavvar Mousavi, H. Shirkhanloo, A.M. Rashidi, Preconcentration and separation of ultra-trace amounts of lead using ultrasound-assisted cloud point-micro solid phase extraction based on amine functionalized silica aerogel nano-adsorbent, 125 (2016) 236–241.

[201] H. Shirkhanloo, M. Ghazaghi, A. Rashidi, A. Vahid, Arsenic speciation based on amine-functionalized bimodal mesoporous silica nanoparticles by ultrasound assisted-dispersive solid-liquid multiple phase microextraction, Microchem. J., 130 (2017) 137–146.

[202] H. Shirkhanloo, A. Khaligh, H. Zavvar Mousavi, A. Rashidi, Ultrasound assisted-dispersive-ionic liquid-micro-solid phase extraction based on carboxyl-functionalized nanoporous graphene for speciation and determination of trace inorganic and organic mercury species in water and caprine blood samples, Microchem. J., 130 (2017) 245–254.

[203] H. Shirkhanloo, A. Khaligh, H. Zavvar Mousavi, A. Rashidi, Ultrasound assisted-dispersive-micro-solid phase extraction based on bulky amino bimodal mesoporous silica nanoparticles for speciation of trace manganese (II)/(VII) ions in water samples, Microchem. Journal 124 (2016) 637–645.

[204] F. Hosseini, H. Shirkhanloo, N. Motakef Kazemi, Nano analysis in biochemistry: in vitro separation and determination of aluminum in blood of dialysis patients based on graphene oxide nanoparticles

dispersed to ionic liquid, J. Nanoanal., 4 (2017) 99-109.

[205] S. Golkhah, H. Zavvar Mousavi, H. Shirkhanloo, A. Khaligh, Removal of Pb(II) and Cu(II) Ions from Aqueous Solutions by Cadmium Sulfide Nanoparticles, Int. J. Nanosci. Nanotechnol., 13 (2017) 105-117.

[206] Z. Ying, L. Chun-yan, Y. Jin-gang, J. Xin-yu, Adsorption properties of a novel 3D graphene/MgO composite for heavy metal ions, J. Cent. South Univ., 26 (2019) 813−823.

[207] H. Shirkhanlooa, A. Khaligh, H. Zavvar Mousavi, Al. Rashidi, Graphene oxide-packed micro-column solid-phase extraction combined with flame atomic absorption spectrometry for determination of lead (II) and nickel (II) in water samples, Int. J. Environ. Anal. Chem., 95 (2014) 1-17.

[208] R. Sitko, P. Janik, B. Feist, E. Talik, A. Gagor, Suspended aminosilanized graphene oxide nanosheets for selective preconcentration of lead ions and ultrasensitive determination by electrothermal atomic absorption spectrometry, ACS Appl. Mater. Iinterfaces, 6 (2014) 20144-20153.

[209] A. Khaligh, H. Zavvar Mousavi, H. Shirkhanloo, A. Rashidi, Speciation and determination of inorganic arsenic species in water and biological samples by ultrasound assisted-dispersive-micro-solid phase extraction on carboxylated nanoporous graphene coupled with flow injection-hydride generation atomic absorption spectrometry, RSC Adv., 5 (2015) 93347–93359.

[210] M. Ghazaghi, H. Zavvar Mousavia, A. Rashidi, H. Shirkhanloo, R. Rahighi, Innovative separation and preconcentration technique of coagulating homogenous dispersive microsolid phase extraction exploiting graphene oxide nanosheets, Anal. Chim. Acta, 902 (2016) 33–42.

[211] B. Yang, Q. Gong, L. Zhao, H. Sun, N. Ren, J. Qin, J. Xu, H. Yang, Preconcentration and determination of lead and cadmium in water samples with MnO2 coated carbon nanotubes by using ET-AAS, Desalination, 278 (2011) 65.

[212] Z. Bahadir, V. Bulut, M. Hidalgo, M. Soylak, E. Marguí, Determination of trace amounts of hexavalent chromium in drinking waters by dispersive micro-solid phase extraction using modified multiwalled carbon nanotubes combined with total reflection X-ray fluorescence spectrometry, Spectrochim. Acta Part B, 107 (2015) 170–177.

[213] C. Cui, H. Peng, Y. Zhang, K. Nan, M. He, B. Chen, B. Hu, Ti-containing meso- porous silica packed micro-column separation/preconcentration combined with inductively coupled plasma-mass spectrometry for the determination of trace Cr, Cu, Cd and Pb, in environmental samples, J. Anal. At. Spectrom., 30 (2015) 1386–1394.

[214] A.H. Panhwar, T.G. Kazi, H.I. Afridi, S.A. Arain, K.D. Brahman, M.S. Arain, A new solid phase microextraction method using organic ligand in micro-pipette tip syringe system packed with modified carbon cloth for preconcentration of cadmium in drinking water and blood samples of kidney failure patients, Spec-trochim. Acta Part A, 138 (2015) 296–302.

[215] T. Da, S. Saçmacı, A. Ülgen, S. Kartal, A solid phase extraction procedure for the determination of Cd(II) and Pb(II) ions in food and water samples by flame atomic absorption spectrometry, Food Chem., 174 (2015) 591–596.

[216] M. Babazadeh, R. Hosseinzadeh-Khanmiri, J. Abolhasani, E. Ghorbani-Kalhor, A. Hassanpour, Solid phase extraction of heavy metal ions from agricultureal samples with the aid of a novel functionalized magneticmetal–organicframe-work, RSC Adv., 5 (2015) 19884–19892.

[217] O.M. Kalfa, Ö. Yalçınkaya, A.R. Türker, Synthesis of nano B2O3/TiO2 composite material as a new solid phase extractor and its application top reconcentration and separation of cadmium, J. Hazard. Mater., 166 (2009) 455–461.

[218] R. Sitko, P. Janik, B. Feist, E. Talik, A. Gagor, Suspended aminosilanized graphene oxide nanosheets for selective preconcentration of lead ions and ultrasensitive determination by electrothermal atomic absorption spectrometry, ACS Appl. Mater., 6 (2014) 20144–20153.

[219] M.C. Sneed, R.C. Brasted, C.V. King, Comprehensive inorganic chemistry, J. Electrochem. Soc., 103 (1956) 83.

[220] K.P. Lisha, T. Pradeep, Towards a practical solution for removing inorganic mercury from drinking water using gold nanoparticles, Gold Bull., 42 (2009) 144–152.

[221] I. Ojea-Jiménez, X. López, J. Arbiol, V. Puntes, Citrate-coated gold nanoparticles as smart scavengers for mercury(II) removal from polluted waters, ACS Nano, 6 (2012) 2253.

[222] M.P. Watts, V.S. Coker, S.A. Parry, R.A.D. Pattrick, R.A.P. Thomas, R. Kalin, J.R. Lloyd,

Biogenic nano-magnetite and nano-zero valent iron treatment of alkaline Cr(VI) leachate and chromite ore processing residue, Appl. Geochem., 54 (2015) 27–42.

[223] C. Shan, Z. Ma, M. Tong, J. Ni, Removal of Hg(II) by poly(1-vinylimidazole)-grafted Fe_3O_4 @SiO2 magnetic nanoparticles, Water Res., 69 (2015) 252–260.

[224] M.E. Mahmoud, M.S. Abdelwahab, A.E.H. Abdou, Enhanced removal of lead and cadmium from water by Fe_3O_4-cross linked-O-phenylenediamine nano-composite, Sep. Sci. Technol., 51 (2016) 237–247.

[225] L. Giraldo, A. Erto, J.C. Moreno-Piraján, Magnetite nanoparticles for removal of heavy metals from aqueous solutions: Synthesis and characterization, Adsorp., 19 (2013) 465–474.

[226] Y.Q. Tan, M. Chen, Y.M. Hao, High efficient removal of Pb(II) by amino-functionalized Fe_3O_4 magnetic nano-particles, Chem. Eng. J., 191 (2012) 104–111.

[227] J. Shi, H.Y. Li, H.G. Lu, Zhao, X.W. Use of Carboxyl Functional Magnetite Nanoparticles as Potential Sorbents for the Removal of Heavy Metal Ions from Aqueous Solution. J. Chem. Eng. Data 2015, 60, 2035–2041.

[228] S.D. Pan, H.Y. Shen, Q.H. Xu, J. Luo, M.Q. Hu, Surface mercapto engineered magnetic Fe_3O_4 nano-adsorbent for the removal of mercury from aqueous solutions, J. Colloid Interface Sci., 365 (2012) 204–212.

[229] S. Christian, E. Robin, Z. Robert, F. Artur, K. Hauke, W. Christopher, O. Johannes, M. Jan-Philip, S. Theo, N. Kornelius, Polymer-assisted self-assembly of superparamagnetic iron oxide nanoparticles into well-defined clusters: Controlling the collective magnetic properties, Langmuir ACS J. Surf. Colloids, 30 (2014) 11190–11196.

[230] J. Yang, B. Hou, J. Wang, X. Huang, Nanomaterials for the Removal of Heavy Metals from Wastewater, Nanomaterials, 9 (2019) 424.

[231] O'Carroll D., Sleep B., Krol M., Boparai H., Kocur C. Nanoscale zero valent iron and bimetallic particles for contaminated site remediation, Adv. Water Resour., 51 (2013) 104–122.

[232] T. Liu, Z.L. Wang, Y. Sun, Manipulating the morphology of nanoscale zero-valent iron on pumice for removal of heavy metals from wastewater, Chem. Eng. J., 263 (2015) 55–61.

[233] Z. Zhen, H.Z. Wei, L.W. Li, X.X. Hua, Synchronous Treatment of Heavy Metal Ions and Nitrate by Zero-valent Iron, Huan Jing Ke Xue, 30 (2009) 775–779.

[234] S.M. Seyedi, H. Rabiee, S.M.S. Shahabadi, S.M. Borghei, Synthesis of Zero-valent Iron Nanoparticles via Electrical Wire Explosion for Efficient Removal of Heavy Metals: Water, Clean—Soil Air Water, 45 (2016) 1600139.

[235] W. Wei, Y. Hua, S. Li, W. Yan, W.X. Zhang, Removal of Pb(II) and Zn(II) using lime and nanoscale zero-valent iron (nZVI): A comparative study, Chem. Eng. J., 304 (2016) 79–88.

[236] S. Tighadouini, S. Radi, M. Bacquet, S. Degoutin, M. Zaghrioui, S. Jodeh, I Warad, Removal efficiency of Pb (II), Zn (II), Cd (II) and Cu (II) from aqueous solution and natural water by ketoenol–pyrazole receptor functionalized silica hybrid adsorbent, Sep. Sci. Technol., 52 (2017) 608–621.

[237] S. Radi, S. Tighadouini, M. Bacquet, S. Degoutin, Y. Garcia, New hybrid material based on a silica-immobilised conjugated β-ketoenol-bipyridine receptor and its excellent Cu (II) adsorption capacity, Anal. Method., 8 (2016) 6923–6931.

[238] S. Radi, S. Tighadouini, M. Bacquet, S. Degoutin, J-P Dacquin, D. Eddike, M. Tillard, Y. Mabkhot, β-Keto-enol tethered pyridine and thiophene: synthesis, crystal structure determination and its organic immobilization on silica for efficient solid-liquid extraction of heavy metals, Molecul., 21(2016) 888–900. doi: 10.3390/molecules21070888.

[239] S. Radi, S. Tighadouini, M. Bacquet, S. Degoutin, B. Revel, M. Zaghrioui, Quantitative removal of Zn(II) from aqueous solution and natural water using new silica-immobilized ketoenol–pyridine receptor, J. Environ. Chem. Eng., 3 (2015)1769–1778.